Biodegradation of Phenolic and Petroleum Wastewater by Isolated *Bacillus cereus*

A Thesis

Submitted in Partial Fulfillment of the
Requirements for the Degree of

DOCTOR OF PHILOSOPHY

by

ADITI BANERJEE

Centre for the Environment
Indian Institute of Technology Guwahati
Assam, India

September 2011

Dedicated
to

Chhoto Maasi and Dadu
&
P'moni and P'moshai

INDIAN INSTITUTE OF TECHNOLOGY GUWAHATI

CENTRE FOR THE ENVIRONMENT

CERTIFICATE

It is certified that the work described in this thesis entitled ***"Biodegradation of Phenolic and Petroleum Wastewater by Isolated Bacillus cereus"*** by **Aditi Banerjee** for the award of the degree of **Doctor of Philosophy** is an authentic record of the results obtained from the research work carried out under my supervision in the Centre for the Environment, Indian Institute of Technology Guwahati, India. The contents of this thesis have not been submitted to any other University or Institute for the award of any degree or diploma.

Prof. Aloke Kumar Ghoshal
Professor
Department of Chemical Engineering
Indian Institute of Technology Guwahati
Guwahati - 781039

Acknowledgement

I would like to express my foremost acknowledgement to my thesis supervisor, Prof. Aloke Kumar Ghoshal for his continuous support and encouragement throughout my research work. I am obliged for the ample freedom he allowed me in conducting my research. Any sort of appreciation or acknowledgement will, in fact, only demean his deeds towards my thesis work. Appreciation is expressed to the members of my doctoral committee, Dr. P. Saha, Dr. A. Ramesh and Dr. B. Mandal for their precious suggestions in completing this work. I owe my gratitude to the Centre for the Environment, Dept. of Chemical Engineering and CIF, IIT Guwahati for providing me all the supports and necessary facilities and thanks to all present and ex-staff members in the Centre for their help during my PhD studies. I sincerely acknowledge the financial support from MHRD and CSIR.

I owe my gratitude to the Heads of the Center, Prof. M. Roy and Prof. C. Mahanta, for allowing me to use the Center facilities in their respective tenures. I express my sincere thanks to all my colleague and technical assistants of the Center for their constant help. I am lucky to have wonderful juniors like Samarpita, Shrabonti, Kamal and Mriganka. I take this opportunity to express my sincere gratitude to all my hostel friends who always encouraged me in my academic and non-academic endeavors. I cherish my close association with *Su*, *Sandy*, *Nipa*, *Souvika*, *Kasturi*, *Deeplina*, *Priyanka, Atreyi, Biju, Bharti, Sumitra, Adreeja, Natasha, Mamta, Tejasha, Sangeetha,* …… and many other friendly faces always abound in my memories.

I would like to express my deep sense of gratitude to Pallab…….I don't know how I could acknowledge his unconditional Love and support! Lastly, and also most importantly, I would like to thank my whole family and my brothers and sisters for their endless love and affection. I appreciate their understanding and dedicated support at many testing times. Without them, none of my achievements would have been possible.

Aditi Banerjee

ABSTRACT

The thesis mainly focuses on the isolation of phenol-degrading bacteria from oil-contaminated sites and their application in the biodegradation of phenolic and petroleum wastewaters. Firstly, two potential phenol-degrading bacterial strains were isolated from two different site specific petroleum wastewaters and identified as *Bacillus cereus* MTCC 9817 strain AKG1 and *Bacillus cereus* MTCC 9818 strain AKG2, based on the 16S rDNA gene sequencing. In addition to the various morphological and biochemical characterizations, the optimum growth conditions and growth kinetics for both AKG1 and AKG2 were investigated. Next, biodegradation of phenol at various initial concentrations by isolated *B. cereus* strains were studied at their optimum physiological condition. The degradation kinetics revealed that the Haldane model fitted the experimental data fairly well. The phenol degradation mechanism in the isolated strains was also elucidated. Treatment of real petroleum wastewater samples, studied in batch mode by free cultures, demonstrated that co-culture of the free cells (AKG1 and AKG2) was most efficient in removing COD, TOC and ammonium nitrogen. Probable identification of bio-degradation products was performed by liquid chromatography and mass spectroscopy. Also, an attempt has been made to probe the structural changes of bacterial cell membrane as a result of the bacterial adaptation to the toxic environment of the petroleum wastewater.

The investigation with Ca-alginate immobilized AKG1 and AKG2 demonstrated enhanced tolerance of the immobilized cells to higher phenol concentrations (~ 2000 mg L^{-1}). The storage stability of the immobilized strains and their potential application in repeated batch biodegradation has also been evaluated. Degradation kinetics indicated that phenol degradation by immobilized strains could well be fitted by Haldane model. Moreover, biodegradation of petroleum wastewater samples by alginate immobilized strains have been investigated and the reduction in COD, TOC and ammonium nitrogen level evaluated. The immobilized cells were found to be less effective than the free cell systems in treating petroleum wastewater.

Finally, the fabrication and initial optimization of lab scale bioreactors for degrading phenolic and petroleum wastewater Ca-alginate immobilized *Bacillus cereus* (AKG1 and AKG2) were investigated. The performance of immobilized strains in phenol degradation in a packed bed reactor was studied and the combined effect of

external mass transfer with biochemical reaction on the mass transfer correlation was determined in terms of Colburn factor (J_D) and Reynolds number (N_{Re}). Continuous biodegradation of the petroleum wastewater was carried out in re-circulated packed bed reactors by the isolated strains immobilized in either Ca-alginate beads or polyurethane foam (PUF) cubes. The biodegradation performances of both the immobilized systems demonstrated the excellent efficacy of the immobilized AKG1 and AKG2 strains in treating petroleum wastewater in continuous mode of operation. Continuous bio-degradation of petroleum refinery wastewater in re-circulated fluidized bed reactors also demonstrated that the microbial treatment reduced the initial COD level and concentration of phenolic compounds efficiently.

CONTENTS

ABBREVIATIONS AND SYMBOLS

BOD	Biological oxygen demands (mg L^{-1})
bp	Base pair
cfu	Colony Forming unit
COD	Chemical oxygen demands (mg L^{-1})
DO	Dissolved oxygen (mg L^{-1})
DOC	Dissolved organic carbon (mg L^{-1})
EL_{50}	Half maximal effective loading rate
FBB	Fluidized bed bioreactor
HFMBR	Hollow fiber membrane bioreactor
HMSA	2-hydroxymuconic semialdehyde
HMSD	2-hydroxymuconic semialdehyde dehydrogenase
HODH	2-hydroxy-6-oxohepta-2,4dienoate hydrolase
ILALB	Internal loop airlift bioreactor
LL_{50}	Half maximal lethal loading rate
MFC	Microbial fuel cell
MSM	Mineral salt medium
OD	Optical density
O & G	Oil and grease
ORP	Oxidation reduction potential
PAH	Polycyclic aromatic hydrocarbons
PBR	Packed bed reactor
PBS	Phosphate buffered saline
PUF	Polyurethane foam
RBC	Rotating biological contactor
SBR	Sequencing batch reactor
SS	Suspended solids
TDS	Total dissolve solid
TOC	Total organic carbon (mg L^{-1})
USEPA	United States Environmental Protection Agency
WHO	World Health Organization
A	Column cross sectional area (cm^2)
A_m	Surface area per unit weight of dried cells for mass transfer (cm^2 g^{-1})
C	Outlet phenol concentration (mg L^{-1})
C_0	Inlet phenol concentration (mg L^{-1})

C_S	Phenol concentration at cell surface (mg L^{-1})
D_f	Phenol diffusivity (cm s^{-1})
d_p	Immobilized bead diameter (cm)
dz	Change in height of column (cm)
G	Mass flux of phenol solution (g cm^{-2} h^{-1})
h	Height of the reactor bed (cm)
J_D	Colburn factor
k	Intrinsic first-order degradation rate constant (L g^{-1} h^{-1})
K	Constant in Eq. (5.1.11) in **Chapter 5**
K_I	Substrate-inhibition constant (mg L^{-1})
k_m	Mass transfer coefficient (cm h^{-1})
k_p	Observed first-order biodegradation rate constant (L g^{-1} h^{-1})
K_S	Substrate-affinity constant (mg L^{-1})
N	Parameter given by Eq. (5.1.13) in **Chapter 5**
N_{Re}	Reynolds number
q	Specific degradation rate (h^{-1})
Q	Volumetric flow rate (mL min^{-1})
q_{max}	Maximum degradation rate (h^{-1})
r	Phenol removal rate (mg g^{-1} h^{-1})
r_m	Mass transfer rate (mg g^{-1} h^{-1})
S	Substrate concentration (mg L^{-1})
S_0	Initial Substrate Concentration (mg L^{-1})
W	Dry weight of biomass (g)
ε	Void fraction in packed bed
μ	Specific growth rate of cell (h^{-1}) in **Chapter 2**
	Feed viscosity (g cm^{-1} s^{-1}) in **Chapter 5**
μ_{max}	Maximum growth rate (h^{-1})
ρ	Feed density (g cm^{-3})
ρ_p	Bead density (g cm^{-3})

LIST OF TABLES

LIST OF FIGURES

CHAPTER 1

Introduction and Literature Review

This chapter gives a brief introduction on the toxicity of phenolic compounds commonly present in the petroleum wastewater and their environmental effect. The biodegradation studies of phenolic compounds and refinery wastewater have been discussed in detail. The chapter also presents the importance of different bioreactors in microbial treatment with particular emphasis on the wastewater. An outline of the principal objectives of the present work and the organization of the thesis has also been included at the end of the chapter.

Chapter 1

INTRODUCTION AND LITERATURE REVIEW

1.1. Introduction

Energy, since the dawn of the human civilization, has been playing a fundamental role in transforming the human life. As people's need for energy is essential for survival, some of the most important engagements of human life have been the production, conversion and consumption of that energy. Indeed, energy is arguably the key to the advancement of human civilization as the evolution of human societies has been heavily dependent on the conversion of energy for human use (Oswald, 1907; Barbour et al., 1982).

Presently, the global energy demand is met by various kinds of energy sources including oil, coal, natural gas, nuclear energy, biofuel, hydrothermal energy, geothermal energy, wind, solar, ocean (tidal) power, etc. Although concerted efforts have been made to substitute fossil fuels, especially with the renewable energy sources, crude oil remains the most important raw material for the generation of energy in the global context (Figure 1.1a). India, in this regard, is not far behind from the global scenario of oil consumption (Figure 1.1b). In 2009, India was the fourth largest consumer of oil in the world with an estimated consumption of approximately 3 million barrels per day (bpd), which is expected to grow at 100 bpd annual consumption through 2011 (Lalwani and Singh, 2010). Also, India became the sixth largest net importer of oil in the world in 2009, importing nearly 2.1 million bpd. According to the Energy Information Administration (EIA), India is expected to become the fourth largest net importer of oil in the world by 2025, only behind the United States, China, and Japan. In 2009, India produced nearly 880 thousand bpd of total oil (Lalwani and Singh, 2010), and had around 5.6 billion barrels of proven oil reserves as of January 2010, the second-largest amount in the Asia-Pacific region after China.

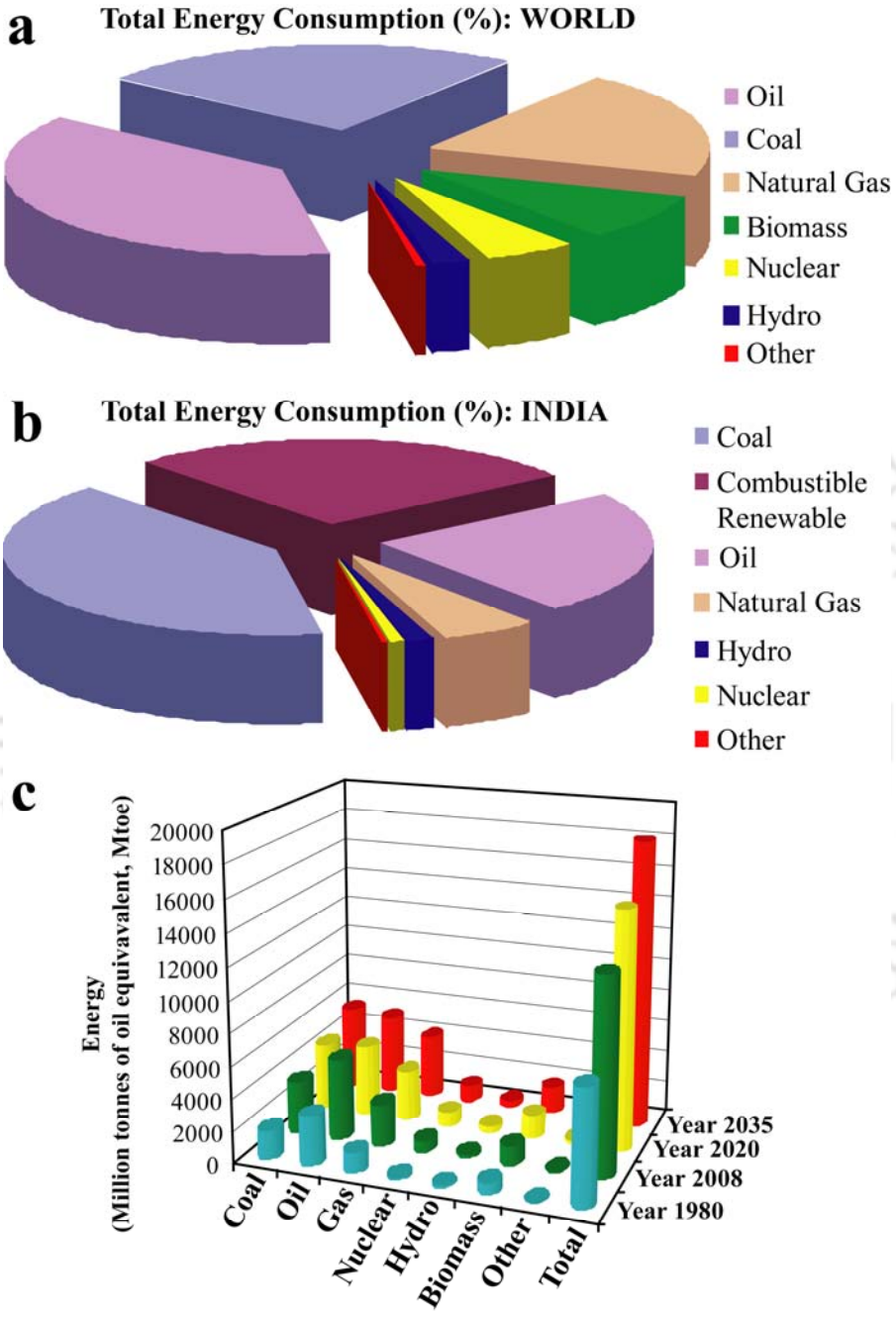

Figure 1.1. Total energy consumption (a) worldwide (based on *World Energy Outlook 2010*, International Energy Agency) and (b) in India in the Year 2008 (adapted from Lalwani and Singh, 2010, *Canad. J. Electri. Electron. Eng.* 1, 122-140). (c) World energy demand (based on *World Energy Outlook 2010*, International Energy Agency).

In order to meet the ever-increasing global energy demand (Figure 1.1c), which is expected to increase by a staggering 44% over the next two decades (Doggett and Rascoe, 2009), the exploration and processing of crude oil, followed by the generation of petroleum refinery effluents, will remain a globally important issue. In a broader sense, generation of gaseous, liquid, and solid wastes is an unavoidable consequence of industrial, agricultural and domestic activities. However, the adverse effect of these activities on the environmental must be minimized to ensure sustainability of human life. Reduced generation, improved treatment strategies and proper utilization of wastes, along with conservation and appropriate utilization of natural resources, hold the key of a successful strategy for maintaining the environment and, in turn, the very existence of human civilization.

1.2. Petroleum Wastewater

Petroleum and refinery wastewater, hereafter termed as 'petroleum wastewater', originates from the effluents of industries primarily involved in exploration of crude oil, refining crude oil and manufacturing fuels, lubricants and other petrochemical intermediates (Harry, 1995). During the refining process of crude oil, a large amount of water is consumed and, consequently, considerable volumes of wastewater are generated from the petroleum industries (Coelho et al., 2006). It has been estimated that the volume of the petroleum refinery effluent generated during processing of crude oil is 0.4–1.6 times the amount of the crude oil processed (Coelho et al., 2006). Hence, a total of 33.6 million barrels per day (bpd) of effluent is produced worldwide, based on the present yield of 84 million bpd of crude oil (Doggett and Rascoe, 2009). Furthermore, the global oil demand is expected to reach up to 107 million bpd over the next two decades. In this regard, it has been projected that oil would supply 32% of the world's energy demand by 2030. On the other hand, biofuels including ethanol, biodiesel, etc. are expected to account for 5.9 and million bpd by 2030, while contributions from renewable energy sources like wind, solar power, etc. are estimated to be 4–15% (Doggett and Rascoe, 2009; Marcilly, 2003). Consequently, the effluents from the oil industry will continually be produced and discharged into the world's main water bodies.

The petroleum refinery effluents are composed of oil and grease along with many other toxic organic compounds. Petroleum is essentially a complex mixture of hundreds

of hydrocarbons that can be divided into several classes based on related structures. The petroleum mixture can be fractionated by silica gel chromatography into a saturated or aliphatic fraction, an aromatic fraction, and an asphaltic or polar fraction (Brown et al., 1969). The saturated fraction of hydrocarbons includes *n*-alkanes, branched alkanes, and cyclo-alkanes (naphthenes). However, the *n*-alkanes do not pose serious environmental risk as they are generally considered the most readily degraded components in a petroleum mixture (McKenna and Kallio, 1964; Treccani, 1964; Kator et al., 1971). In this regard, the biodegradation of *n*-alkanes with molecular weight as high as *n*-C_{44} has been reported (Haines and Alexander, 1974). On the other hand, the aromatic fraction contains phenols and other polycyclic aromatic hydrocarbons (PAHs) that are relatively stable constituents of petroleum and are potential or proven carcinogens from the environmental aspects (Simpson et al., 1995). Pavlova and Ivanova (2003), in this regard, analyzed the composition of sludge from the petroleum wastewater treatment basin in order to get insight into the components of the petroleum wastewater. The authors reported the presence of isoprenoids (2,6,10-trimethyldodecane, 2,6,10-trimethyltridecane, norpristane, pristane and phytane), *n*-alkanes, unresolved complex mixture of aliphatics originating from degraded oil, significant amount of PAHs (naphthalene, acenaphthalene, phenanthrene, fluorene, pyrene, benzo[a]anthracene, chrysene, Table 1.1) and small quantities of oxygen containing compounds (phthalates, aldehydes, ketones, aromatic acids).

Table 1.1. Typical members of PAHs present in the sludge of the petroleum wastewater treatment basin (Adapted from A. Pavlova and R. Ivanova, 2003. *J. Environ. Monit.* 5, 319–323).

Compounds	Spiked concentration (μg kg^{-1})
Naphthalene	38
Acenaphthene	30
Acenaphthylene	27
Fluorene	37
Phenanthrene	44
Anthracene	40
Pyrene	42
Benz[a]anthracene	50
Benzo[k]fluoranthene	50
Fluoranthene	60
Chrysene	50
Benzo[a]pyrene	100

1.3. Environmental Impact of Petroleum Wastewater

Petroleum wastewaters are regarded as priority pollutants primarily due to the presence of high level of PAHs which are toxic and tend to persist in the environment (Mrayyana and Battikhi, 2005; Wake, 2005). Petroleum wastewater contains a wide variety of harmful toxic compounds at varied concentrations. The petroleum refinery effluents containing high level of organic matter, when discharged into water bodies, promote excess bacterial oxidation leading to the depletion of dissolved oxygen (DO) (Attiogbe et al., 2007). This greatly affects the minimum level of DO (~ 2 mg L^{-1}) necessary for maintaining normal aquatic life (Attiogbe et al., 2007). Inhibition in algae proliferation has been observed in the water bodies where petroleum and oil refinery effluents were discharged (El-Naas et al., 2009b; Pardeshi and Patil, 2008). Some of the aquatic toxicological signatures of the petroleum wastewater are listed in Table 1.2. Moreover, the chemical and biochemical reactions in the oxygen depleted anaerobic condition, due to the discharge of petroleum wastewaters, often result in malicious colours, tastes and odours in water (Attiogbe et al., 2007).

Phenol and other phenolic compounds, in this regard, pose the most serious threat to the environment because of their extreme toxicity (Kavitha and Palanivelu, 2004), stability, bioaccumulation and ability to persist in the environment for long periods. They, generally, are carcinogenic, causing considerable damage to the eco-system in water bodies along with human health (Abdelwahab et al., 2009; Lathasree et al., 2004; Pardeshi and Patil, 2008). Toxicity of phenols and their possible bioremediation have been discussed in detail in subsequent sections.

The nitrogen– and sulphur– containing compounds present in the form of ammonia and hydrogen sulphide, respectively, in the refinery effluents are highly toxic (Altas and Büyükgüngör, 2008). Hydrogen sulphide, in aqueous medium, exists in equilibrium with bisulphide (HS^-) and the most reduced form sulphide (S_2^-) which has a high oxygen demand (2 mol O_2 per liter per mol of S_2^-) thus greatly contributing to oxygen depletion (Poulton et al., 2002). This has been shown to result in fish mortality when the maximum limit exceeds 0.5 mg L^{-1} for freshwater and saltwater fish (Altas and Büyükgüngör, 2008). In order to maintain the water quality, various regulatory bodies have set maximum limit of discharge for each component of the waste (Table 1.3).

Table 1.2. Aquatic toxicity of residual fuel oils (adapted from Category Assessment Document for Reclaimed Petroleum Hydrocarbons: Residual Hydrocarbon Wastes from Petroleum Refining, Petroleum HPV Testing Group, American Petroleum Institute. 2010).

Species	Test Material [#]	Effect	Concentration (mg L^{-1})	References
Rainbow trout (*Oncorhynchus mykiss*)	Light residual fuel oil	96 h, LL_{50}	>1000	Shell, 1997a
Rainbow trout (*Oncorhynchus mykiss*)	Heavy residual fuel oil	96 h, LL_{50}	100 – 1000	Shell, 1997b
Daphnia magna	Light residual fuel oil	48 h, EL_{50}	>1000	Shell, 1997c
Daphnia magna	Heavy residual fuel oil	48 h, EL_{50}	220 – 469	Shell, 1997d
Raphidocelis subcapitata	Light residual fuel oil	72 h, EL_{50} (based on growth rate)	100 – 300	Shell, 1997e
		72 h, EL_{50} (based on biomass yield)	3 – 10	
Raphidocelis subcapitata	Heavy residual fuel oil	72 h, EL_{50} (based on growth rate)	30 – 100	Shell, 1997f
		72 h, EL_{50} (based on biomass yield)	30 – 100	

[#] Test material was a water accommodated fraction (WAF), a water sample equilibrated with the oily test material of interest.
LL_{50}: Half maximal Lethal Loading rate, EL_{50}: Half maximal Effective Loading rate [toxicological end points used to express the loading rate of the product lethal (LL) to or produce a specific effect (EL) in 50% of the test organisms]

Table 1.3. Regulatory standards of various parameters in petroleum refinery effluent for discharging into water-body (adapted from Diya'uddeen et al., 2011. *Process Safety Environ. Prot.* 89, 95–105).

pH	Composition (mg L^{-1})								Reference
	COD	BOD	DOC	O & G	SS	Ammonia	Phenols	Sulphides	
6–9	100	10–15	–	10	70	15	–	–	Ma et al. (2009)
–	100	40	–	–	–	–	–	–	Hami et al. (2007)
6.7	200	–	20	23	–	70	3.7	–	Santos et al. (2006)
6–9	150	30	–	10	30	–	–	10	Environmental Health Safety Guidelines (2009)

COD: Chemical Oxygen Demand, BOD: Biological Oxygen Demand, DOC: Dissolved Organic Carbon, O & G: Oil and Grease, SS: Suspended Solids

1.4. Phenol: A Major Constituent of Petroleum Wastewater

Phenol is one of the major constituent aromatic pollutants that are usually found in wastewaters from petroleum industries and oil refineries. Besides, phenol is also present in many other industrial effluents such as wastewaters from coal processing plants, pulp and paper manufacturing plants, resin and coke manufacturing, steel plants, pharmaceutical industries, plastic and varnish industries, textile units, pesticide plants, smelting and related metallurgical operations (Kumar et al., 2005; Edalatmanesh et al., 2008).

Phenol, commonly known as carbolic acid, is a white crystalline solid having a strong odour and generally used in liquid form. It is an aromatic compound containing a hydroxyl group (OH) attached to the benzene ring. Phenol is mildly acidic, but requires careful handling as it can cause burns. It is soluble in most organic solvents and also fairly soluble in water with a solubility of about 83 g L^{-1} at 20 °C (Lide, 2004). Phenols can be found either as natural or artificial mono-aromatic compounds in the environment as major pollutants. Phenol, in nature, can be generated from forest and rangeland fires and natural decay of lignocellulosic material (Wang et al., 2007; Agarry et al., 2008). The chemical structure of phenol, other phenolic compounds and polyaromatic compounds commonly found in petroleum refinery effluents are shown in Figure 1.2.

1.4.1. Toxicity of Phenol

Phenol and its derivatives (phenolics) are considered to be among the most recalcitrant and hazardous contaminants due to their high toxicity for human life, aquatic life and others (El-Naas et al., 2009; Shourian et al., 2009). Phenol and other phenolic compounds pose serious environmental threat as they can easily contaminate nearby water courses due to their water solubility and high toxicity (Mollaei et al., 2010).

Phenol can quickly penetrate the skin and may cause severe irritation to the eyes, mucous membranes and the respiratory tract. Hence, human exposure to phenol through ingestion, contact or inhalation may lead to critical health hazards and possible carcinogenesis (El-Naas et al., 2009). Furthermore, exposure to phenol by oral route may result in severe liver and kidney damage, and acute cardiac toxicity including weak pulse, cardiac depression, and reduced blood pressure. Ingestion of 1 g of phenol is reported to be lethal to human (Nuhoglu and Yalcin, 2005).

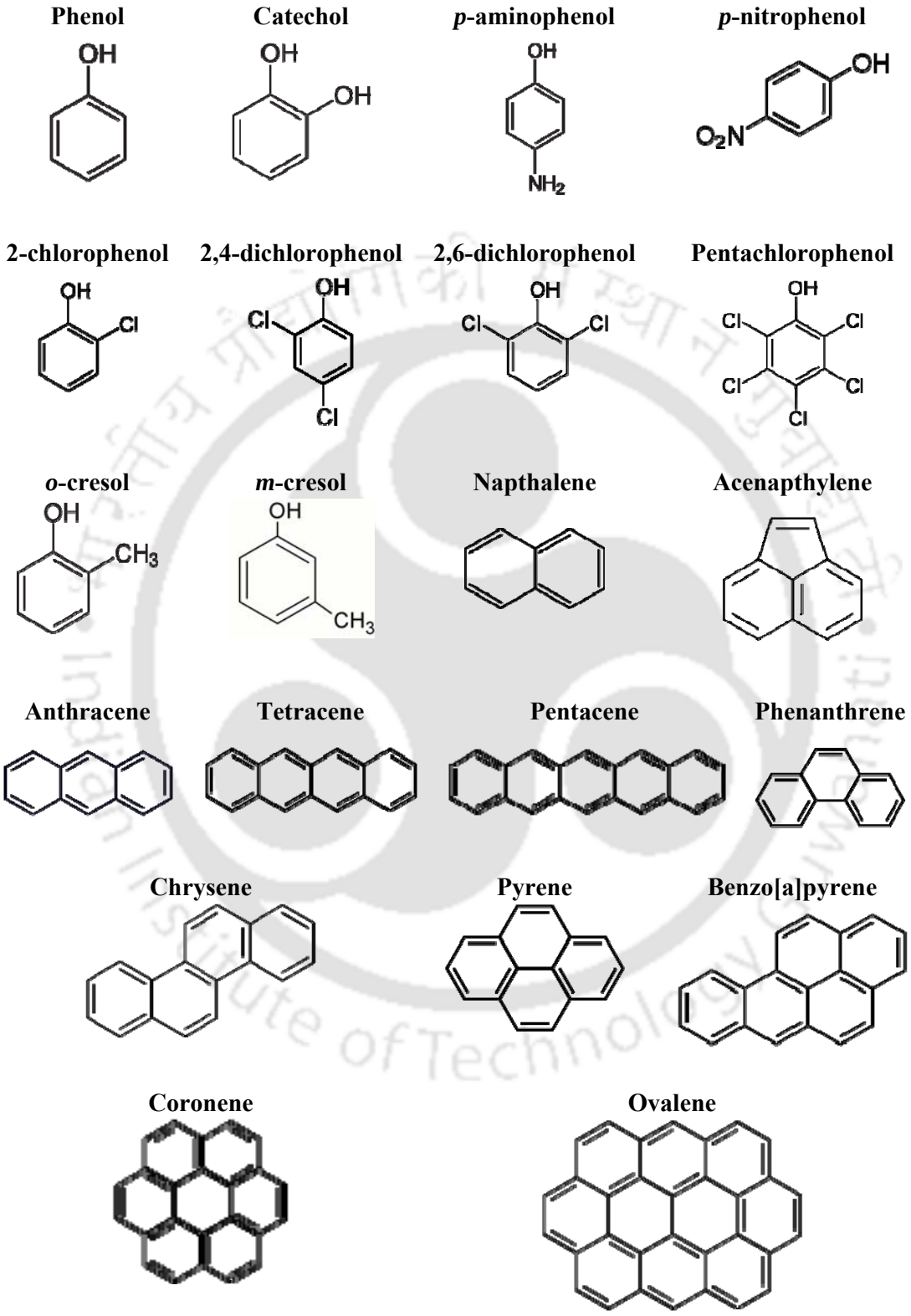

Figure 1.2. Chemical structure of phenol, other phenolic compounds and polyaromatic compounds commonly found in petroleum refinery effluents (Lide, 2004).

Phenol and other phenolic compounds have detrimental effects on the aquatic micro– flora and fauna at a very low concentration of 5 mg L^{-1} (Santos et al., 2009). Although, the concentration of phenol in wastewater generally varies from 10 mg L^{-1} to 300 mg L^{-1}, it can occasionally reach as high as 4.5 g L^{-1} in highly contaminated wastewater. Phenol may either exert its toxic effect by reducing enzyme activity or even be lethal to fish at relatively low levels of 5–25 mg L^{-1}, depending on the temperature and state of maturity of rainbow trout (Brown et al., 1967). Moreover, phenol contaminated wastewater, when chlorinated for disinfection, produces highly toxic polychlorinated phenols. Phenol, even at a very low concentration of 2 μg L^{-1}, imparts objectionable taste and odor to drinking water (Chung et al., 2003). Also, phenol and its homologues can adversely affect the performance of the wastewater treatment plants by inhibiting the microbial growth (Ren and Frymier, 2003).

Due to their potential toxicity, the United States Environmental Protection Agency (USEPA) has defined phenol and other phenolic compounds as priority pollutants and set a water purification level of phenol concentration less than 1 μg L^{-1} in surface waters (Keith and Telliand, 1979). The World Health Organization (WHO) has set their guideline of 1 μg L^{-1} to regulate the phenol concentration in drinking waters (Environmental Health Criteria-EHC 161, 1994). Also, a limit of 0.5 μg L^{-1} has been directed by the European Council Directive for regulating phenol concentration in the drinking waters (Tziotzios et al., 2005). Whereas, 0.35 mg L^{-1} is kept for effluent phenol concentration for petroleum oil refineries by Central Pollution Control Board, India (Ministry of Environment and Forest, Govt. of India).

1.4.2. Removal of Phenol

In order to protect the soil and the aquatic ecosystem from being contaminated with phenol and other phenolic compounds, it is necessary to treat the industrial effluents prior to disposal in the environment. A number of physico-chemical methods such as adsorption, ion-exchange, liquid-liquid extraction and chemical oxidation have been reported in the literatures for efficient removal of phenol from industrial wastewater.

Adsorption technology has been widely applied for the removal of organic and inorganic micro-pollutants such as phenol from aqueous solutions (Ahmaruzzaman, 2008). To this end, activated carbons are the most extensively investigated adsorbents having excellent adsorption capabilities for phenolic compounds due to their high

surface-area, pore volume, and porosity (Hsieh and Teng 2000; Salame and Bandosz, 2006; Ozkaya, 2006; Kumar et al., 2007; Martínez et al., 2009). However, the cost associated with regeneration and the production of carbons dust due to the brittle nature of carbons used for phenol removal (Terzyk, 2003; Namane and Hellal, 2006) has led the researchers to find other economic and environment-friendly alternatives. In this regard a wide variety of material such as clay (Yapar and Yilmaz, 2005), silica beads (Phan, 2000), zeolite (Kozhevnikov et al., 1985; Kuleyin, 2007), chitosan (Rhee et al., 1998), dead biomass (Rao and Viraraghavan, 2002), sawdust (Jadhav and Vanjara, 2004), rice husk (Ahmaruzzaman and Sharma, 2005), fly ash (Gupta et al., 2000), red mud (Tor et al., 2006), etc. have been explored for efficient adsorption of phenol.

Polymeric adsorbents have also emerged as a viable alternative for efficient removal of phenol (Oh et al., 2003; Kujawski et al., 2004). Although adsorption by uncharged polymeric resins has been extensively investigated for removing hydrocarbons from wastewater (Ku and Lee, 2000; Xu et al., 2008), they have demonstrated a lower capacity of phenol removal than that of the activated carbon (Lee et al., 2004; Carmona et al., 2006). The overall phenol removal from wastewater can be improved by using anionic resins which can uptake phenol via ion-exchange mechanism in addition to adsorption (Carmona et al., 2006). The removal of phenol from aqueous solution by ion-exchange, in fact, can be traced back as early as 1949 when Kunin and McGarvey (1949) reported that phenol could be removed from solution by using anion exchange resin. Subsequently, they also demonstrated the successful removal of phenol form typical industrial wastewater by commercially available ion-exchange resins, Amberlite IRA-400 (Chasanov et al., 1956). A lot of studies on the efficient phenol removal by ion-exchange method have been reported since then (Ku and Lee, 2000; Carmona et al., 2006; Caetano et al., 2009).

In recent years, catalytic oxidation has gained much attention in converting organic pollutants into inorganic carbon or into products that can be eliminated by the biological residual treatment (Britto et al., 2008). The method of catalytic oxidation by different oxidizing agent such as ozone, oxygen, hydrogen peroxide, sulfite-oxygen or the combination of them has been demonstrated to be extremely effective in the removal of phenols from industrial wastewater (Kulkarni and Dixit, 1991; Trabelsi et al., 1996; Hamoudi et al., 2000; Shukla et al., 2011). Besides, the method of solvent

extraction has also been investigated to separate phenol from contaminated water (Wang and Hu, 1994; Xu et al., 2006; Juang et al., 2009).

However, most of these physico-chemical methods do not actually degrade phenol. Instead, they transfer it from one phase to another and, thereby, produce hazardous secondary pollutants. Moreover, these techniques suffer from additional disadvantage of high cost. In this regard, biodegradation has emerged as a more environment-friendly and cost effective alternative for phenol removal in recent years.

1.5. Biodegradation of Phenol

The process of biodegradation exploits the ability of microorganisms (such as bacteria, fungi and algae) to convert organic pollutants to water, carbon dioxide and biomass under aerobic or anaerobic condition in an environmentally benign way. The biodegradation method of phenol removal draws universal preference due to the possibility of complete mineralization of phenol (El-Naas et al., 2009; Liu et al., 2009), avoiding undesirable by-products or secondary pollutants produced as a result of pheysico-chemical treatment of phenol containing wastewater.

1.5.1. Phenol-Degrading Microorganism

The hazardous and toxic xenobiotics, being structurally different from naturally occurring compounds, are difficult to degrade. However, due to rapid advancement in the field of biotechnological research in recent years, a wide range of microorganisms have been identified which can utilize toxic xenobiotics to meet their metabolic requirement. In this regard, a large number of microorganisms including bacteria, fungi and algae have been demonstrated to degrade phenol and other phenolic compounds. Phenol can be degraded either aerobically (Ruiz-Ordaz et al., 2001; Melo et al., 2005; Ucun et al., 2010) or anaerobically (Levénet al., 2006; Azbar et al., 2009; Bajaj et al., 2009; Hussain et al., 2010), depending on the specific growth conditions required by the microorganisms.

1.5.1.1. Bacteria

In recent years, the biodegradation of phenol and other phenolic compounds by bacteria has been the subject of extensive research in the field of biochemical as well as environmental engineering. This has led to the isolation and characterization, at both

the physiological and genetic level, of a wide variety of bacteria that are capable of phenol biodegradation. Undoubtedly, *Pseudomonas putida* and other members of *Pseudomonas* genus are the most widely investigated bacteria in this regard due to their high phenol removal efficiency (Hsieh et al., 2008; El-Naas et al., 2010). Several other bacteria which have been studied for phenol biodegradation include *Acinetubacter sp.*, *Sphingomonas sp.*, *Ewingella sp.*, *Alcaligenes sp.*, *Ochrobactrum sp.*, *Ralstonia sp.*, and *Bacillus sp.*. A detailed list of phenol degrading bacteria with specific degradation characteristics is presented in Table 1.4.

1.5.1.2. Fungi

Fungi are stout microorganisms in a sense that they can tolerate the presence of high concentration of various toxic materials, even at a low bioavailability exploiting their powerful extracellular oxidative enzymatic system (Agarry et al., 2008). Fungi also play their part in the biodegradation of phenol. Yeasts are the commonly found fungi in the contaminated environments and some of them such as *Candida tropicalis*, *Fusarium flocciferium* and *Trichosporon cutaneum* are capable of utilizing phenol as the major carbon and energy source (Stoilova et al., 2007; Agarry et al., 2008). Also, strains from *Penicillium*, *Aspergillus*, *Graphium* and *Phanerochate* genera have been reported to disintegrate phenol and other aromatic pollutants. Various fungi that are capable of phenol biodegradation are listed in Table 1.5.

1.5.1.3. Algae

Recently, much interest is being drawn to the investigation of degrading phenol by using algae. Although most of the algae have low tolerance to the acute toxicity of phenols, some cyanobacteria and eukaryotic microalge (Table 1.5) such as *Chlorella sp., Scenedesmus sp., Selenastrum capricornutum, Tetraselmis marina, Nostoc punctiforme and Oscillatoria animalis* have been reported to be capable of bio-transforming phenolic compounds (Lika and Papadakis, 2009).

Table 1.4. Various phenol-degrading bacteria with their degradation characteristics.

Bacteria	Pollutant	Concentration (mg L^{-1})	pH	Temp. (^{0}C)	Phenol Removal (%)	Degradation Time (h)	Study
Free Pseudomonas putida MTCC 1194	Synthetic phenol	100-1000	7.0 *	30 #	> 95 (for C_0 = 250 mg L^{-1})	24	Bandyopadhyay et al., 1998
Immobilized *Pseudomonas putida* ATCC 11172	Synthetic phenol	100	5.5-6.0	25-30	97.5		Mordocco et al., 1999
Free *Pseudomonas putida* DSM 548	Synthetic phenol	1-100	6.8	26 ±0.5	100 (for C_0 = 23.4 mg L^{-1})	14	Monteiro et al., 2000
Immobilized *Pseudomonas putida* ATCC 17484	Phenol and non-phenolics in raw wastewater	200-1000 (batch); 250-2500 (fluidized)	6.6	30	100 > 98	260 (batch, C_0 = 1000 mg L^{-1})	González et al., 2001
Free and immobilized *Pseudomonas putida* ATCC 17484	Synthetic phenol	1000	6.6	30	> 98		Gonzalez et al., 2001
Free *Halomonas campisalis*	Synthetic phenol	130	8-11	30	100	~ 50 (C_0 = 100 mg L^{-1}, pH 9.5)	Alva and Peyton, 2003
Free *Pseudomonas putida* MTCC 1194	Synthetic phenol Synthetic catechol	1000 500	7.1	29.9	100	162 94	Kumar et al., 2005
Free *Bacillus brevis*	Synthetic phenol	750-1750	8.0 *	34 ±0.1	> 95	144 (for C_0 = 1750 mg L^{-1})	Arutchelvan et al., 2006
Free *Ewingella americana*	Synthetic phenol	0-1000	7.5	37	100 (for C_0 = 300 mg L^{-1})	24	Khleifat, 2006
Free *Alcaligenes faecalis*	Synthetic phenol	0-1800	7.2	30	100 (for C_0 = 1600 mg L^{-1})	76	Jiang et al., 2007
Free and immobilized *Acinetubacter sp*. strain PD 12	Synthetic phenol	100-1100	7.2 *	30 #	99 (for C_0 = 500 mg L^{-1}; free cell)	9	Wang et al., 2007
Immobilized *Ralstonia eutropha*	Synthetic phenol	25-500	7.0	30	68 (for C_0 = 100 mg L^{-1})		Tepe and Dursun, 2008
Rhizobium sp. CCNWTB 701	Synthetic phenol	100-1000	6.8±0.2	28	100	72 (for C_0 = 1000 mg L^{-1})	Wei et al., 2008

Bacteria	Pollutant	Concentration (mg L^{-1})	pH	Temp. (^{0}C)	Phenol Removal (%)	Degradation Time (h)	Study
Free Pseudomonas sp. SA01	Synthetic phenol	300-1000	7.0	30	100	20-85	Shourian et al., 2009
Immobilized *Pseudomonas putida*	Synthetic phenol	5-150	7.0	30	100	0.3-5	El-Naas et al., 2009
Mixed (1:1) culture of *Acinetubacter sp.*XA05 and *Sphingomonas sp.* FG03; free and immobilized	Synthetic phenol	200-1000	7.2 *	30 #	> 95 (for C_0 = 800 mg L^{-1})	35	Liu et al., 2009
Corynebacterium sp. DJ1	Synthetic phenol	500-2500	7.5 *	30 #	100 (for $C_0 \leq$ 2000 mg L^{-1})	~ 60 (for C_0 = 1500 mg L^{-1})	Ho et al., 2009
Free mixed bacterial consortium	Synthetic phenol	23.5- 658	7.2	25 ± 2	90-100	1-10	Bajaj et al., 2009
Free mixed aerobic activated sludge and anaerobic sludge	Synthetic phenol	400, 1000	7.0	30	> 95	< 60	Luo et al., 2009
Free *Cupriavidus metallidurans*	Synthetic mixture of phenol and humate potassium	400-1400	6.6	23.5	100 (for C_0 = 400 mg L^{-1})	~ 45	Stehlickova et al., 2009
Free *Ochrobactrum sp.*	Synthetic phenol	50-400	8 *	30	~ 45 (for C_0 = 62 mg L^{-1})	96	Kılıç, 2009
Immobilized *Pseudomonas putida*	Synthetic phenol	40-190	7.0	30	74-100	0.8-1.8	El-Naas et al., 2010
Free *Corynebacterium glutamicum*	Phenol in contaminated soil	199.5-1995.1		30	~ 95 (for C_0 = 798.05 mg L^{-1})	72	Lee et al., 2010
Immobilized *Pseudomonas putida*	Synthetic phenol	10-150	7.0	30	88-97	0.67-2.55	El-Naas et al., 2010
Free culture of *Pseudomonas aeruginosa* and *Pseudomas fluorescence*	Synthetic phenol	100-500		30	100	24-96	Agarry et al., 2010
Free *Pseudomonas putida* LY1	Synthetic phenol	0-800	7.1-7.3	25 #	100	~ 55 (for C_0 = 310 mg L^{-1})	Yi et al., 2010

* denotes optimum pH; # denotes optimum temperature

Table 1.5. Various phenol-degrading fungi and algae with their degradation characteristics.

Fungi/Algae	Pollutant	Concentration (mg L^{-1})	pH	Temp. (^{0}C)	Phenol Removal (%)	Degradation Time (h)	Study
Immobilized *Trichosporon cutaneum* R57	Synthetic phenol	1000		28	100	45 (PAN membrane) 51 (PA membrane)	Godjevargova et al., 2006
Fusarium sp.	Synthetic phenol	420	6 *	30 #	100	480 (without sucrose) 360 (in presence of 3 g L^{-1} sucrose)	Cai et al., 2007
Aspergillus awamori NRRL 3112	Synthetic mixture of phenol, catechol, 2,4-DCP and 2,6-DMP	1000 (total)		30	25-100 (phenol)	168	Stoilova et al., 2007
Mutant strain of *Candida tropicalis*, CTM 2	Synthetic mixture of phenol and 4-CP	4 CP: 400 (in presence of 0-800 phenol) Phenol: 2500 (in presence of 0-30 4-CP)		30	100 (mixture of 300 phenol 400 4-CP)	50.5	Jiang et al., 2008
Resting *Candida tropicalis* NCIM 3556	Synthetic phenol	2000-10000		28	100	24	Varma and Gaikwad, 2008
Recycled resting *Candida tropicalis* NCIM 3556	Synthetic phenol	2000		28	70	24	Varma and Gaikwad, 2009
Paecilomyces variotii JH6	Synthetic phenol	100-1800	5 *	37 #	100	100 (without glucose) 70 (with glucose)	Wang et al., 2010
Ochromonas danica	Synthetic phenol and *p*-cresol	10-100	6.6	25	100 (phenol)	120	Semple and Cain, 1996
Scenedesmus quadricauda *Ankistrodesmus braunii*	Synthetic catechol and tyrosol	400	6.2	25	95 (catechol) 50 (tyrosol) 85 (catechol) 5 (tyrosol)	600	Pinto et al., 2002

* denotes optimum pH; # denotes optimum temperature;
PAN: polyacrylonitrile; PA: polyamide; 2,4-DCP: 2,4-dichlorophenol; 2,6-DMP: 2,6-dimethoxyphenol; 4-CP: 4-chlorophenol

1.5.2. Parameters Affecting Microbial Degradation of Phenols

Various biotic and abiotic parameters such as substrate concentration, temperature, pH, oxygen content, bioavailability and physico-chemical properties of the pollutant can influence the multifaceted process of phenol biodegradation by either enhancing or retarding the microbial metabolism (Agarry et al., 2008; El-Naas et al., 2009; Trigo et al., 2009). Therefore, in order to achieve the maximum phenol degradation, each of these parameters needs to be optimized for a specific microorganism.

1.5.2.1. pH

The pH of the culture medium is an important parameter in phenol biodegradation as the extreme pH values (≤ 3 or ≥ 9) can exert detrimental effect on the microbial growth. Bandyopadhyay et al. (1998) studied the phenol biodegradation by *Pseudomonas putida* MTCC 1194 with varying medium pH ranging from pH 4 to pH 9; and demonstrated that the highest phenol degradation occurred at the neutral condition of pH 7. In their study of phenol degradation by free and immobilized *Acinetobacter sp.* strain PD12, Wang et al. (2007) showed that the degradation rate constant was almost invariable in the pH range of 7.2–10 for both the free and immobilized cells. However, it started to decrease below pH 7.2 for both free and immobilized system, ultimately resulting in the complete inhibition of the degrading activity at pH 5.5 in case of free cells. The effect of media pH on phenol degradation by *Ochrobactrum sp.* was studied by Kilic (2009) and the highest phenol degradation was observed at pH 8 in the investigated pH range of 6–9. Liu et al. (2009) investigated the degradation of phenol by mixed culture of *Acinetobacter sp.* XA05 and *Sphingomonas sp.* FG03; and found that the media pH did not have any significant effect on the phenol degradation, by free as well as immobilized cells, in the range of pH 7 – pH 9. However, the degradation by free cells gradually decreased in the acidic pH and reached almost complete inhibition at pH 6. On the other hand, the immobilized cells followed the same trend but still maintained an acceptable degradation rate at the same pH of 6.

1.5.2.2. Temperature

Change in temperature can influence the process of phenol biodegradation as different microorganisms have different temperature range for their optimal growth. Although most of the phenol biodegradation studies had been performed in the temperature range

25–35 °C as shown in Table 1.4, successful phenol degradation has been reported at temperatures as low as 10 °C and as high as 50 °C by *Pseudomonas putida* and *Bacillus stearothermo-philes*, respectively (Agarry et al., 2008). The effect of temperature on the phenol degradation by *Pseudomonas sp.* SA01 was investigated by Shourian et al. (2009) at three different temperatures of 25 °C, 30 °C and 37 °C. They found that the maximum phenol biodegradation occurred at 30 °C. Liu et al. (2009) also showed that the mixed culture of *Acinetobacter sp.* XA05 and *Sphingomonas sp.* FG03 degraded maximum phenol at 30 °C. In this regard, El-Naas et al. (2009) proposed that exposure to temperatures higher than 35 °C could affect the bacterial enzymes responsible for the benzene ring cleavage, the critical step in the biodegradation of phenols.

1.5.2.3. Substrate Concentration

The substrate concentration is an important parameter in the phenol biodegradation as phenol itself is well known to inhibit microbial growth, especially at higher concentrations. This phenomenon is commonly known as 'substrate inhibition'. Adjei and Ohta (2000) reported that phenol was completely inhibitory for cyanide utilization by the bacteria *Burkholderia cepacia* strain C-3. *Bacillus brevis* was shown to degrade phenol completely at an initial phenol concentration as high as 1750 mg L^{-1}, although it took about 120 h as compared to that of 24 h and 48 h for 750 and 1000 mg L^{-1} phenol, respectively (Arutchelvan et al., 2006). In their study of phenol biodegradation by *Rhizobium sp.* CCNWTB 701 isolated from mining tailing region, Wei et al. (2008) investigated the effect of substrate concentration on the biodegradation efficiency by varying initial phenol concentration from 100 mg L^{-1} to 1000 mg L^{-1}. It was observed that the time for phenol degradation increased in high phenol concentration with ~99.5% and ~78.3% phenol degradation within 62 and 66 h, starting with an initial concentration of 900 and 1000 mg L^{-1}, respectively. Also, the specific phenol degradation rate first increased and then decreased with increasing phenol concentration, while the maximum value was found at 400 mg L^{-1}. Similar results were also reported for the phenol degradation by *Pseudomonas sp.* SA01 (Shourian et al., 2009) where degradation time increased from 20 h to 85 h with increasing concentration of initial phenol concentration from 500 to 1000 mg L^{-1}, while complete inhibition of degradation capabilities was observed at 1200 mg L^{-1}.

1.5.2.4. Culture System

The biodegradation of phenol can be carried out either by suspended microbial culture or immobilized microbial cells. It has been observed that immobilization of microbial cells onto solid supports such as alginate, poly-acrylamide or chitosan particles, diatomaceous earth, activated carbon, sintered glass, polyvinyl alcohol and polymeric membrane could result in enhanced degradation efficiency as compared to that of the free (suspension) cell system (El-Naas et al., 2009; Liu et al., 2009; Shourian et al., 2009). Moreover, the systems with immobilized cultures are more stable to shock loading than the suspended cultures with free cells (Gerrard et al., 2006). Kim et al. (2006) showed that calcium alginate immobilization of microbial cells effectively increased the tolerance of *Pseudomonas putida* MK1 to phenol and improved the degradation of pyridine in a binary mixture of the two compounds. In a study of phenol degradation by *Pseudomonas putida* entrapped within the beads prepared by chitosan crosslinked with sodium tri-polyphosphate, Hsieh et al. (2008) demonstrated that the entrapped cells were superior to the free suspended ones in terms of tolerance to the environmental loadings and repeating usage. Also, the entrapped cells degraded influent phenol completely in the packed column mode of operation with the addition of hydrogen peroxide in order to increase the dissolved oxygen level for cell metabolism.

1.5.2.5. Chemical Structure of Phenols

The chemical structure of a particular pollutant determines, to a significant extent, the biodegradability and hence, the toxicity of that compound. The difference in chemical structure can be substantiated by the degree of branching and the number, type or position of the substituents. As the number of substituents in the structure increases, in most cases, the degradability deceases and the toxicity of the pollutant increases. For example, substituted phenols such as mono, di-, tri- and penta- chlorophenol are less degradable than unsubstituted phenol. In addition, *ortho*- and *para* substituted phenols are more degradable than *meta* substituted phenols (Agarry et al., 2008).

1.5.2.6. Other Factors

The presence of naturally occurring carbon sources such as glucose, yeast extract, etc. can greatly affect the efficiency of microbial degradation of toxic pollutants. In this

regard, the co-metabolism process, which can be described as the degradation of a compound only in the presence of another organic material that serves as the primary growth substrate, is an ideal example of the substrate interaction during the biodegradation of pollutants (Annadurai et al., 2008). Co-metabolism has been attributed to the production of broad-specificity enzymes, where both the primary substrate and the other compound compete for the same enzyme (Bhatt et al., 2007). The biodegradation of phenol and phenolic compounds has been reported to increase with increasing concentrations of inorganic nutrients (such as phosphate and nitrate), whereas high concentrations of organic nutrients (such as glucose, yeast extract, etc.) could affect it adversely (Gladyshev et al. 1998). Also, the presence of metabolic inhibitors or competing substrates has significant impact on the bio-degradation system (Mordocco et al., 1999; Tsai and Juang, 2006).

1.5.3. Pathway of Phenol Biodegradation

Microbial metabolism of a particular metabolite is essentially a process of energy conversion maintained by a series of biochemical reactions, catalyzed with a specific set of enzymes, producing the ultimate source of energy (Bailey and Ollis, 1987). A number of mesophilic bacteria are capable of utilizing aromatic compounds such as phenols as carbon and energy sources. During phenol biodegradation, cleavage of the aromatic ring is typically achieved via the *ortho* (intradiol) or *meta* (extradiol) pathways (Yang and Humphrey, 1975), as shown in Figure 1.3. The latter is generally observed in case of mesophilic and thermophilic bacilli (Ali et al., 1998). The most well known key dihydroxy-aromatic intermediates resulting from the biodegradation of aromatic compounds are catechol, protocatechuic acid and gentisic acid. These intermediates further undergo ring fission following the Krebs cycle to yield other metabolites, such as pyruvic acid, acetic acid, succinic acid and acetyl-Coenzyme A (acetyl-Co A) (Loh and Chua, 2002).

Among the three dihydroxy-aromatic intermediates, the most frequently encountered metabolite before ring cleavage is catechol. The formation of catechol proceeds via the incorporation of molecular oxygen into its aromatic precursor (Kwon and Yeom, 2009). The primary substrates that can be funneled into catechol range from single ring benzene to three-ring phenanthrene (Cao and Loh, 2008).

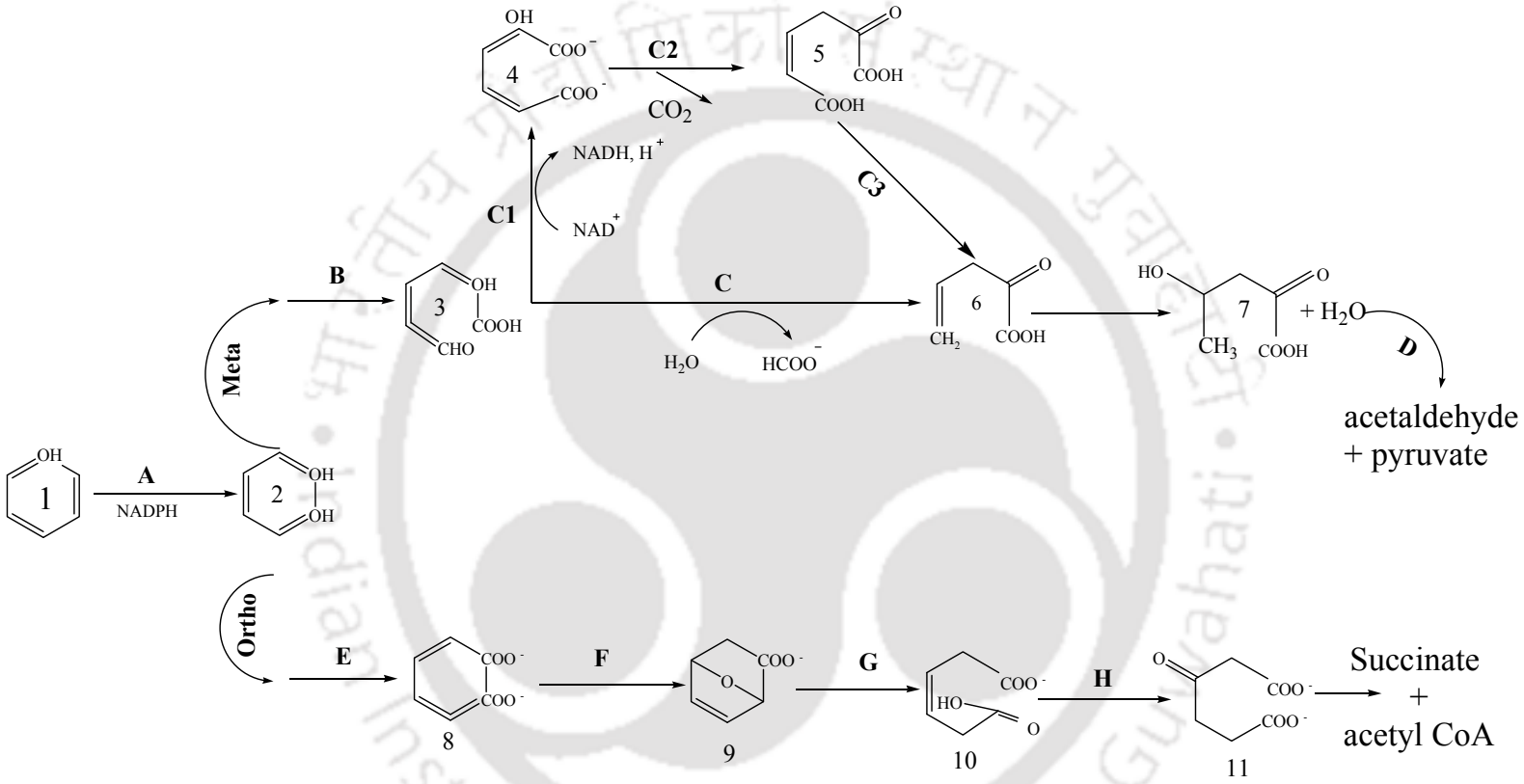

Figure 1.3. Phenol degradation pathway.
1: phenol; 2: catechol; 3: 2-hydroxymuconic semialdehyde; 4: 4-oxalocrotonic acid (enol form); 5: 4-oxalocrotonic acid (keto form); 6: 2-oxopent-4-enoic acid; 7: 4-hydroxy-2-oxovalerate; 8: *cis, cis*- muconate; 9: muconolactone; 10: β-ketoadipate enol lactone; 11:β-ketoadipate
A: Phenol hydroxylase; B: Catechol 2,3 oxygenase; C: 2-hydroxy-6-oxohepta-2,4-dienote hydrolase; C1: 2-hydroxymuconic semialdehyde dehydrogenase; C2: 4-oxalocrotonate tautomerase; C3: 4-oxalocrotonate decarboxylase; D: aldolase; E: Catechol 1,2 oxygenase; F: lactonizing enzyme; G: isomerase; H: hydrolase

So, in short, biodegradation of phenol follows a sequence of

(a) hydroxylation by phenol hydroxylase to form catechol,

(b) ring cleavage by catechol-2,3-dioxygenase to produce 2-hydroxymuconic semialdehyde (HMSA) in *meta*-pathway,

or

ring cleavage by catechol-1,2-dioxygenase to produce *cis, cis*-muconate in *ortho* -pathway,

(c) HMSA is either oxidized to 4-oxalocrotonate or hydrolyzed to 2-oxopent-4-enoate in case of *meta*-pathway

or

cis, cis-muconate gets converted into muconolactone in *ortho* -pathway.

Wang et al. (2007) reported that the biodegradation of phenol by the bacterial strain *Acinetobactor sp.* PD12 followed the *ortho*-pathway as they detected C120 activity. Jiang et al. (2007) also showed the involvement of the *ortho*-pathway in the phenol biodegradation by the bacterial strain *Alcaligenes faecalis*. However, the activity of the C230 involved in the catechol ring fission via the *meta*-pathway was demonstrated in the degradation of phenol by the bacterium *Ewingella americana* (Khleifat, 2006). Although very little is known about phenol metabolism by fungi, previous studies showed that phenol was metabolized by the *β*-ketoadipate pathway through the *ortho*-fission of catechol (Stoilova et al., 2006).

1.5.4. Strategies for Improved Phenol Biodegradation

Although much research has been carried out on the biodegradation of phenol, investigation for efficient phenol degradation by microorganism, especially at high phenol concentration which exerts substrate inhibition on microbial growth, is far from being exhausted. Described below, are some strategies that have been employed for improved phenol biodegradation.

1.5.4.1. Immobilization

Immobilization of microbial biomass for the degradation of phenol is a promising and effective technique that has drawn considerable interest in recent years. Immobilization serves several purposes such as protection of the bacteria against high phenol

concentrations, ease of separation and re-use the biomass (El-Naas et al., 2009). The superior performance of the immobilized biomass compared to free cells in biodegradation of phenol has been well reported. In this regard, whole cell immobilization in which microorganisms are physically entrapment inside a polymeric matrix has been extensively investigated (Aksu and Bulbul, 1998; Annadurai et al., 2008). In one of the early studies, Keweloh et al. (1989) demonstrated that the immobilization of microorganisms (*Escherichia coli*, *Pseudomonas putida* and *Staphylococcus aureus*) in calcium alginate beads reduced the growth inhibition caused by bacteriostatic concentrations of phenol. The increase in phenol tolerance was reported to occur at different culture conditions and growth rates of the cells. El-Naas et al. (2009) evaluated the biodegradation of phenol by *Pseudomonas putida* immobilized in polyvinyl alcohol (PVA) gel pellets in a bubble column bioreactor at different conditions.

The biodegradation of phenol in continuous mode at an influent concentration of 100 mg L^{-1} by immobilized *Pseudomonas putida* was investigated by Mordocco et al. (1999) and they reported, by comparing the performance of the immobilized cells in calcium alginate beads to that of free cells, that the superiority of the immobilized cell system was more pronounced. The significance of this low level of concentrations was substantiated by the authors in light of the potential toxicity of phenol at concentrations as low as 5 mg L^{-1}. Wang et al (2007) investigated the immobilization of *Acinetobacter sp.* strain PD12 in PVA carrier and demonstrated that the immobilized cells could tolerate higher phenol levels and wider changes in temperature and pH. The authors also reported the improved thermal stability, better storage stability and excellent reusability for at least fifty cycles in case of immobilized cells.

1.5.4.2. Hyper-Phenol Tolerant Bacteria

Although several microorganisms have been identified that can degrade phenols, little information is available on bacteria with a high phenol-tolerance and high metabolizing activity (Wang et al., 2007). Hence, there still exists the scope of further investigation in this regard to isolate new hyper-phenol tolerant bacteria that can grow at elevated concentration of phenol. A novel phenol degrading bacterium *Acinetobacter sp.* strain PD12 was isolated from sludge by Wang et al., (2007) that can remove 99.6% of 500 mg L^{-1} phenol within 9 h and metabolize phenol at concentrations up to 1100 mg L^{-1}.

In recent years, aerobic granules, a self immobilized biomass, has emerged as an effective alternative to decontaminate highly contaminated wastewater (Adav et al., 2007; 2008; Liu et al., 2009). Aerobic granules can yield a biomass concentration as high as 15 g L^{-1} and have an ability to degrade high strength wastewater up to 15 kg COD m^{-3} day^{-1} (Adav et al., 2007). Ho et al. (2009) used aerobic granules to degrade high strength phenol, upto 5000 mg L^{-1}, at an acceptable rate, even after acid or alkaline pre-treatment. Microscopic observation revealed that live cells are principally distributed throughout the surface layer of the granule, with an extracellular polymeric layer covering them and protecting from phenol toxicity (Adav et al., 2007; 2008).

1.5.4.3. Implication of Mixed Culture

A mixed microbial culture, sometimes, is more efficient in complete mineralization of phenols. However, literature reports of using mixed cultures of microorganisms in phenol degradation are not adequate as compared to the extensively reported pure culture (Saravanan et al., 2008). In this regard, a mixed culture of *Acinetobacter sp.* XA05 and *Sphingomonas sp.* FG03 strains was investigated for phenol degradation and demonstrated better degradation efficiencies as compared to the individual pure cultures (Liu et al., 2009). The improved degradation efficiency could be due to the fact that the strains of XA05 and FG03, being isolated from different environments, have different enzyme system and, hence, different phenol degradation pathway. In mixed culture, they can act synergistically to overcome the substrate inhibition of phenol. Similar synergistic effects were also reported by Monteiro et al. (2000) while investigating the biodegradation of organic chemicals by mixed culture.

1.5.4.4. New Strains of Bacteria

The members of *Pseudomonas* genus have been mostly studied bacteria for the biodegradation of phenol. More concerted efforts are needed to explore newer bacterial strains for efficient treatment of phenol contaminated wastewater. Recently, growing attention has been directed towards new and more efficient microorganisms for this purpose. In this regard, Tepe and Dursun (2008) reported the phenol biodegradation in a packed bed reactor by immobilized *Ralstonia eutropha*. *Ralstonia pickettii* strain LD1 can metabolize mono-chlorophenols which represent an important challenge as they are formed during the chlorination of the water (Ryan et al., 2007).

1.5.5. Kinetics and Modeling of Phenol Biodegradation

The information of the kinetics of a particular biodegradation process, which provides an idea about the effectiveness of the microbial system (Agarry et al., 2008), is crucial for improving the process control and the removal efficiency of the corresponding pollutant (Monteiro et al., 2000; Agarry et al., 2008). The kinetic models generally relate the specific growth rate of the biomass to the utilization rate of the substrate (contaminant) (El-Naas et al., 2009). The rate of biomass growth (in mg L^{-1} h^{-1}), based on material balance, can be represented as:

$$\frac{dX}{dt} = \mu X - k_d X \qquad (1.1)$$

where X is the biomass concentration (mg L^{-1}); μ is the specific growth rate (h^{-1}); and k_d is the decay coefficient (h^{-1}) (Kumar et al., 2005; Tsai and Juang, 2006). On the other hand, the rate of substrate consumption (in mg L^{-1} h^{-1}) can be represented as:

$$\frac{dS}{dt} = -\frac{\mu X}{Y} \qquad (1.2)$$

where S is the substrate concentration (mg L^{-1}) and Y is the biomass yield ($=\frac{dX}{dS}$, g g^{-1}).

A number of kinetic models, as shown in Table 1.6, have been proposed to describe the dynamics of microbial growth on phenol. The Monod (Table 1.6, Eq 1.4) and the Haldane model (Table 1.6, Eq 1.5) are the two most extensively studied kinetic models to investigate the biodegradation of phenol. Although these models primarily describe the dependence of the specific growth rate on the substrate concentration, they can also be employed to predict the biodegradation rate with respect to initial phenol concentration using Eq. 1.2. While the Monod model does not considers the inhibitory effect of phenol, the Webb model (Table 1.6, Eq. 1.6) and Haldane model take the inhibitory effect into consideration by incorporating the substrate inhibition constant K_I in the equation (El-Naas et al., 2009). Due to its mathematical simplicity for describing the growth kinetics taking account of the inhibitory substrate and applicability in case of continuous bioreactors, the Haldane model has been widely used (Kumar et al., 2005; Tsai and Juang, 2006). However, all these models assume that Y is constant over the concentration range, which is only valid when the phenol concentration is much higher than the substrate–affinity constant, K_S ($S >> K_S$) (El-Naas et al., 2009).

In the Haldane equation, a large K_I value indicates the lower sensitivity of the microorganism toward substrate inhibition. The Haldane equation, for very large K_I values, actually simplifies to the Monod equation (Juang and Tsai, 2006). On the other hand, at high substrate concentrations when $S >> K_S$, the Haldane equation reduces to the following equation,

$$\mu = \frac{\mu_{max} S}{S + \left(S^2 / K_I\right)} \tag{1.3}$$

which ultimately results in the linearized Haldane's equation (Table 1.6, Eq 1.7) (Kumar et al., 2005; Marrot, 2006). Haldane's growth kinetics is a three-parameter model, whereas Monod's and linearized Haldane's model are two-parameter models. The estimated parameters by Monod and the linearized Haldane model were used by Kumar et al. (2005) to provide the initial guess values for Haldane model parameters in the study of phenol degradation by *P. putida* MTCC 1194. Other models of inhibitory kinetics were proposed by Yano et al. (1966) (Table 1.6, Eq 1.8) and Aiba et al. (1968) (Table 1.6, Eq 1.9), respectively. Aiba model was later modified by Edwards (1970) (Table 1.6, Eq 1.10). Aiba model and its adapted form by Edwards are, in fact, the modified versions of Monod equation which describe the Haldane-type growth kinetics.

Saravanan et al. (2008) reported that an extended Monod-type model originally proposed by Han-Levenspiel (Table 1.6, Eq 1.11) was efficient in explaining the growth of a microbial consortium at different substrate concentrations. According to Bajaj et al. (2009), the Han-Livenspiel model is based on the inhibitory effect of a product formed during the degradation, while the Haldane model accounts for the effect of the substrate itself on the microbial growth. Although the Haldane model could predict the specific growth rates with respect to initial substrate concentrations fairly well, the inadequacy of this model in correlating the phenol degradation for high initial phenol concentrations was reported by Wang and Loh (1999). The authors predicted that the Haldane model would model the substrate consumption anomalously, especially for $S_0 \approx \sqrt{K_S K_I}$ which is the critical substrate concentration S^*. Furthermore, the basic assumption of constant yield coefficient Y used in the Haldane model is not always true, especially at the extremes of specific growth rate. Wang and Loh (1999), hence, proposed a new model of phenol degradation (Table 1.6, Eq 1.12) by incorporating the inhibitory effect of the metabolic intermediates as well as accounting for a variable yield of biomass.

Table 1.6. Various models for phenol biodegradation kinetics.

Model		Eq. No	Description of Parameters
Monod model (Monod, 1949)	$\mu = \frac{\mu_{max} S_0}{K_S + S_0}$	1.4	μ: Specific growth rate (h^{-1});
Haldane (Andrews) model (Haldane, 1965)	$\mu = \frac{\mu_{max} S_0}{K_S + S_0 + \frac{S_0^2}{K_I}}$	1.5	μ_{max}: Maximum specific growth rate (h^{-1});
Webb model: (Webb, 1963)	$\mu = \frac{\mu_{max} S_0 \left(1 + \frac{S_0}{K}\right)}{S_0 + K_S + \frac{S_0^2}{K_I}}$	1.6	S_0: Initial Substrate concentration (mg L^{-1}); S: Substrate concentration (mg L^{-1});
Linearized Haldane model	$\frac{1}{\mu} = \frac{1}{\mu_{max}} + \frac{S_0}{\mu_{max} K_I}$	1.7	S_m: Critical substrate concentration above which the growth stops (mg L^{-1});
Yano model (Yano et al, 1966)	$\mu = \frac{\mu_{max} S_0}{K_S + S_0 + \frac{S_0^2}{K_I}\left(1 + \frac{S_0}{K}\right)}$	1.8	K_S: substrate-affinity constant (mg L^{-1});
Aiba model (Aiba et al, 1968)	$\mu = \frac{\mu_{max} S_0}{K_S + S_0} \exp\left(\frac{-S_0}{K_I}\right)$	1.9	K_I: Substrate-inhibition constant (mg L^{-1});
Edward model (Edwards, 1970)	$\mu = \mu_{max} S_0 \left[\exp\left(\frac{-S_0}{K_I}\right) - \exp\left(\frac{-S_0}{K_S}\right)\right]$	1.10	K: the constant in Yano and Webb models (mg L^{-1}); K_P:Proportionality constant (mg L^{-1});
Han-Levenspiel model (Han and Levenspiel, 1988)	$\mu = \frac{\mu_{max}\left(1 - \frac{S_0}{S_m}\right)^n}{K_S + S_0 - \left(1 - \frac{S_0}{S_m}\right)^m}$	1.11	k_s: Saturation constant for substrate consumption (mg L^{-1}); R_m: Maximum specific consumption rate of substrate (h^{-1});
Wang-Loh model (Wang and Loh, 1999)	$-\frac{dS}{Xdt} = \frac{R_m S}{k_s + S + f(i)}, f(i) = \frac{(S_0 - S)^2}{K_P}$ $X = X_0 e^{\mu t}, \mu = \frac{\mu_{max} S_0}{K_S + S_0 + \frac{S_0^2}{K_I}}$,	1.12	X: Biomass concentration (mg L^{-1}); X_0: Initial biomass concentration (mg L^{-1}); m, n: Empirical constants.

1.6. Bioreactor for Treating Phenolic and Petroleum Wastewater

In last few decades, biological treatment of toxic pollutants and industrial wastewater has gained tremendous attention in the scientific community as well as in the industrial arena. Consequently, various kinds of reactor configuration for biodegradation process, starting from the more conventional activated sludge system to highly advanced microbial fuel cell (MFC) or hollow fiber membrane bioreactor, have been reported in the literature. Batch or semi-batch reactors are mainly used for laboratory studies, anaerobic digestion and manufacture of pharmaceuticals; while continuous reactors are often employed for aerobic treatment of municipal and industrial wastes (Sundstrom and Klei, 1979). Two extreme mixing regimes are represented by well stirred tank reactor and plug flow reactors. Intermediate degrees of mixing can be achieved by employing well-stirred reactors in series or by designing plug flow reactors with axial dispersion. The overall model of the reactor can be developed by combining the equations for the hydraulic regime and the kinetics of the reactions (Sundstrom and Klei, 1979). As compared to the suspended culture of free microbial cells, the immobilization process affects the bioreactor performance by providing the retention of active biomass on support particles, flexibility of reactor design and the improved thermal and operational stability (Aksu and Bülbül, 1998).

A brief account of major types of bioreactors with their successful applications in the biodegradation of wastewaters, especially the phenolic pollutants and effluents of petroleum/oil based industries, is presented in the following sections.

1.6.1. Sequencing Batch Reactor (SBR)

Sequencing batch reactor (SBR) represents a periodic discontinuous system accompanied by a robust microbial population capable of persisting and metabolizing in extremely adverse conditions. In SBR, the microorganisms can be periodically exposed to defined process conditions easily by setting the exposure time, frequency of exposure and amplitude of the respective concentration irrespective of influent conditions (Wilderer et al., 2001). The main advantages of the SBR are the inherent flexibility of cyclic phasing providing different operating modes and cost effectiveness. SBR processes have been reported to save more than 60% of expenses required for conventional activated sludge process in operating cost (Chang et al., 2000). Main disadvantages of SBR include sludge disposal and high specific energy consumption.

This type of reactor was used by Silva et al. (2002) to remove phenol and NH_3-nitrogen with ~ 95% and 99% removal efficiency of the pollutants, respectively. Rao et al. (2005) investigated the performance of granular activated carbon-biofilm configured sequencing batch reactor (SBGR) for treating composite chemical wastewater in aerobic environment. The authors reported the excellent performance of the reactor with respect to substrate degradation rate, maintaining its performance even at high operating organic loading rate (OLR) of 5.5 kg COD m^{-3} day^{-1}.

1.6.2. Biofilm-Based Reactor

In biofilm based reactors, biomass is attached on a solid surface as a layer and substrates as well as oxygen diffuse into the layer to form products by biochemical reaction, with concurrent formation of additional biomass. The main advantages of this type of bioreactors are the high removal rate, greater stability of the system and quick recovery from shock load and washout. However, biofilm reactors suffer from limited mass transfer, clogging, formation of preferential paths or channeling, etc. (Jou et al., 2003; Shetty et al., 2007; Stehlickova et al., 2009; Ucun et al., 2010). Biofilm based reactors can be modified in a variety of configurations including the most common trickling filter, rotating biological contactor (Sundstrom and Klei, 1979), fluidized beds, packed beds, rotating fiber discs and microporous membranes. All these systems, irrespective of their configuration, demonstrate operational advantages compared to more conventional suspended growth reactors such as activated sludge systems.

Bajaj et al. (2008) investigated the aerobic degradation of a synthetic wastewater with high phenol content (up to 5170 mg L^{-1}) by an immobilized mixed consortium in a continuous fixed bed reactor. In order to achieve improved biodegradation efficiency compared to the conventional techniques, a new fixed-film bioreactor system was constructed by Jou et al. (2003) with highly porous polyurethane foam providing huge surface area that allowed the attachment and growth of microorganism at a concentration of as high as 8000 mg L^{-1}. With a hydraulic retention time (HRT) of 8 h, a consistent COD removal efficiency of more than 85% and nearly complete degradation of phenol from industrial oil refinery wastewater was reported by the authors. Li et al. (2011) investigated the bioremediation of coal gasification wastewater in a laboratory-scale moving bed biofilm reactor (MBBR) with COD, phenols, SCN^- and NH_4^+–nitrogen removal efficiency of 81%, 89%, 94% and 93%, respectively.

1.6.3. Packed Bed Reactor (PBR)

The packed bed reactor (PBR) is arguably the most convenient configuration among the various kinds of reactor designs used for continuous operation with immobilized cells (Livingston and Chase, 1991; Quail and Hill, 1991). In this type of reactor, the bed column is packed with suitable packing material and the biomass is either immobilized in the packing materials or grown onto the surface of the packing material as a layer. A PBR has various process–engineering advantages including high-yield operation, ease of scaling-up, possible automation of separation process leading to high degrees of purification, opportunity of treating large volume of wastewater continuously by a specified quantity of immobilized cells, and reuse of biomass (Karel et al., 1985; Aksu and Bulbul, 1998; Tepe and Dursun, 2008).

Biodegradation of phenol was investigated by Aksu and Bulbul (1998) in this type of reactor in continuous mode using Ca-alginate immobilized *Pseudomonas putida*. It was shown that phenol removal in the packed column system was strongly affected by the solute diffusion into the pores of Ca-alginate gels. Waul et al. (2008) studied a dynamic modeling approach in order to estimate *in-situ* model parameters to describe the degradation of methyl *tert*-butyl ether (MTBE) in a laboratory packed bed reactor. In another study, the immobilized bacteria *Ralstonia eutropha* was studied by Tepe and Dursun (2008); while Tziotzios et al. (2005) investigated the ability of bacterial populations isolated from olive pulp to degrade phenol in a pilot-scale packed bed reactor with gravel as support material. The microbial reduction of perchlorate by pure as well as mixed culture in a packed bed bioreactor was investigated by Kim and Logan (2001). Gerrard et al. (2006) proposed a simple, plug-flow model to represent continuous biodegradation in a packed bed reactor. In order to minimize the impact of formaldehyde discharged into the environment, Oliveira et al. (2004) investigated the microbial degradation of formaldehyde in a horizontal-flow anaerobic reactor packed with immobilized sludge. The authors successfully demonstrated 99.7% formaldehyde and 92% COD removal efficiency, respectively. The Monod kinetic model was found to fit the experimental data well.

A two-stage up-flow packed bed reactor system was studied by Venkataraman et al. (1992) for the treatment of dairy wastewater using nylon pads as supporting media for the biomass. This system demonstrated excellent biodegradation efficiency with maximum COD removal efficiency being observed in the range of 93.8–98.5% and

72.5–84% in the first and second stage of the system, respectively. In another study, Chen et al. (2007) used a packed bed biofilm reactor (PBBR) with self-floating biocarriers to treat highly concentrated aniline wastewater with a COD value as high as 24,000 mg L^{-1}. The authors demonstrated that the PBBR could treat the aniline wastewater effectively with 94% COD removal efficiency at a OLR of 0.9 kg COD m^{-3} day^{-1}. Moreover, the system was able to maintain a COD removal efficiency of 75% when subjected to a high OLR of 12.27 kg COD m^{-3} day^{-1} corresponding to a HRT of 1 day. Nardi et al. (2005) investigated the biodegradability of gasoline contaminated wastewater in bench-scale horizontal-flow anaerobic immobilized biomass (HAIB) reactors. The concentration of benzene, toluene, and *m*-xylene were gradually increased to 15 mg L^{-1} and the HAIB reactor was found to remove 95% of these pollutants at a HRT exceeding 12 h. Also, a COD removal efficiency of 99% was reported by the authors.

1.6.4. Fluidized Bed Bioreactors (FBR)

Recently, the application of fluidized bed reactors for the biodegradation of pollutants and wastewater has gained much interest due to their superior performance and some inherent advantages. As the transport of substrate, oxygen and other nutrients takes place from bulk solution to the surface of the biofilm in the fluidized bed reactors, the knowledge of mass transfer coefficient of a particular pollutant, from bulk solution to the surface of the biomass, is essential for the successful design and operation of the fluidized bed reactors (Vinod and Reddy, 2006). High volumetric degradation rates can be achieved in fluidized bed reactors because of high specific biofilm surface area available for mass transfer. Moreover, the prevailing turbulence can actually release part of the biomass that covers the solid particles resulting in the steady mass transfer rate through the microbial film. However, attention must be paid to prevent the excessive detachment and washouts of the microbial biofilm adhered to solid particles in order to maintain the optimum volumetric reaction rate. This can be achieved by using porous particles such as granular activated carbon as carriers and maintaining a non-turbulent regime in the fluidized bed reactor.

The aerobic biodegradation of diesel fuel (DF)-contaminated wastewater was investigated by Lohi et al. (2008) in a three-phase fluidized bed reactor using solid lava rock particles as the support for the biomass. The results showed that the reactor, under

unsteady state operation, removed 100% DF and 97% COD from wastewater loaded with 0.43–1.03 kg m^{-3} day^{-1} of DF and 547–4025 mg L^{-1} of COD, respectively. For influent COD concentrations up to 1345 mg L^{-1}, the removal is greater than 90%. On the other hand, steady state operation removed 100% of the 200 mg L^{-1} DF and ~ 96% of the 1237 mg L^{-1} COD from the wastewater. Gonzalez et al. (2001) found that best results for biodegradation of phenol with *P. putida* were obtained when a continuous FBR with immobilized cells was operated. In their study on the anaerobic treatment of a real cotton textile wastewater in a fluidized bed reactor using pumice as the support material, Sen and Demirer (2003) demonstrated that around 82% COD, 94% BOD_5 and 59% color were removed, respectively, for HRT of ~ 24 h and OLR of 3 kg COD m^{-3} day^{-1}. However, an external carbon source in the form of glucose (about 2000 mg L^{-1}) was required for efficient treatment of textile wastewater in the study. In their study, Mayer et al. (2008) used *Candida tropicalis* immobilized onto granular activated carbon in the continuous FBR for efficient removal of phenol at volumetric loading rates as high as 60 mg L^{-1} h^{-1}, feeding phenol as the sole carbon source. When fed with a mixture of phenol and 4-chlorophenol, the FBR was able to remove more than 98% of 4-chlorophenol at the volumetric loading rate of 4.1 mg 4-chlorophenol L^{-1} h^{-1} and 55 mg phenol L^{-1} h^{-1} without any apparent deterioration of bioreactor performance.

1.6.5. Trickling Filter

In trickling filter, the wastewater is distributed over the top of the bed packed with rocks or plastic structures to trickle through the bed. Kornaros and Lyberatos (2006) investigated the effectiveness of the biological treatment of wastewaters from a dye manufacturing company using a trickling filter. The microbial population developed in the trickling filter was reported to efficiently remove COD levels up to 36,000 mg L^{-1} under aerobic conditions. The phenol removal efficiency of *Pseudomonas putida* DSM 548 in a trickling bed biofilm reactor packed with PORAVER particles was evaluated by Sa and Boaventura (2001). The average residence time t_r, in the trickling bed reactor was found (as a function of the hydraulic loading rate, L and the column depth, D) to be $t_r = 0.034\ D / (L^{0.85})$. Recently, Akker et al. (2008) has investigated the effectiveness of high rate, plastic-packed trickling filters as a pre-treatment process to remove low level of ammonia from polluted surface water in order to eliminate the interference of ammonia with chlorination in water treatment plants.

1.6.6. Rotating Biological Contactor (RBC)

A rotating biological contractor is essentially consisted of several plastic discs attached to a central drive shaft. The discs, placed parallel to each other with intermediate spacing to allow fluid flow between them, are partially submerged in the liquid so that they are exposed alternately to substrate in the wastewater and oxygen in the air during rotation (Sundstorm and Klei, 1979; Melo et al., 2005). These devices are easier to operate under varying load conditions than trickling filters (Masters, 1998). In a laboratory scale study, Tyagi et al. (1993) investigated the effectiveness of a modified rotating biological contactor (RBC), with polyurethane foam attached to the discs as porous support media, in the biodegradation of a petroleum wastewater. The removal efficiency of the total COD and oil, for the hydraulic loadings studied, were above 87 and 80%, respectively. Also, more than 99% and 85% removal were observed for ammonia-nitrogen and phenol, respectively.

1.6.7. Internal Loop Airlift Bioreactor (ILALB)

Airlift bioreactors are pneumatically agitated reactors where fluid circulation takes place in a defined cyclic pattern. They are known for mechanical simplicity, good mixing behavior, high capacity, absence of mechanical agitators and low cost (Saravanan et al., 2009). Unlike the conventional reactors such as stirred-tank or bubble columns, shear stress in ILALB is almost constant and mild throughout the reactor, which favors the microbial growth (Kanai et al., 1996). Some of the inherent problems of most internal airlift reactors are gas entrainment in the downcomer, and some cellular damage caused by the adherence of the light particles to the bubbles and subsequent disengagement and bursting of the bubbles (Loh and Liu, 2001).

An ILALB was employed by Feng et al. (2007) for the phenol degradation by the yeast *Candida tropicalis* with a maximum phenol concentration of 1200 mg L^{-1}. Quan et al. (2004) constructed an ILALB packed with honeycomb-like ceramic as the carrier to immobilize microorganism for simultaneous degradation of phenol and 2,4-dichlorophenol under fed-batch and continuous operations. Biodegradation of phenolic wastewaters by *Pseudomonas sp.* SP-1 in an ILALB was studied by Vinod and Reddy (2005), and complete degradation of phenol was observed with a feed concentration of phenol as high as 1034 mg L^{-1}.

1.6.8. Hollow Fiber Membrane Bioreactor (HFMBR)

In the hollow fiber membrane bioreactor, the membrane protects the microbial cells from the adverse effects of high concentrations of toxicants and/or salt (which can significantly affect the microbial growth), by physically separating the wastewater from the biological medium where degradation actually occurs (Junag and Wu, 2007; Li and Loh, 2007). The advantages of using HFMBR against conventional activated sludge processes include the significant reduction of the plant volume, the possibility of using higher biomass concentrations (5–17 g L^{-1}), the reduction of the waste sludge volume and the possibility of continuous operations (Gander et al., 2000).

Microporous polypropylene hollow fibers were investigated by Junag and Wu (2007) for the biodegradation of phenol by *Pseudomonas putida* BCRC 14365 at varying salt concentrations (0-1.78 M NaCl). The same module bioreactor was operated in a dynamic mode by Chung et al. (2005) for the degradation of high concentration of phenol (up to 2800 mg L^{-1}) by *Pseudomonas putida* under various operating conditions. In a study by Alberti et al. (2007), microfiltration hollow-fiber membranes were employed in the bioreactor for treating the wastewater coming from the washing of mineral oil storage tanks. The biomass used the hydrocarbon as a substrate and the reactor demonstrated hydrocarbon removal efficiencies ranging between 93% and 97%, even at high concentrations of hydrocarbon.

1.6.9. Microbial Fuel Cells (MFC)

In recent years microbial fuel cell (MFC) technology has generated considerable interests among researchers (Du et al., 2007). In MFC, the energy stored in chemical bonds in organic compounds is converted to electrical energy through the catalytic reactions by microorganisms (Gil et al., 2003; Moon et al., 2006; Choi et al., 2003). MFCs essentially provide the benefit of power generation while biodegrading organic pollutants such as phenol. Organic pollutants found in municipal wastewater can effectively fuel MFCs. Wastewater from food processing units, sanitary wastes, swine wastewater and corn stover have been used as biomass sources for MFCs due to the abundance of organic matters in these sources (Suzuki et al., 1978; Liu et al., 2004; Oh and Logan, 2005; Min et al., 2005; Zuo et al., 2006). In MFC meditated wastewater treatment, COD removal efficiency up to 80% has been reported (Liu et al., 2004; Min et al., 2005).

1.7. Scope and Objective of the Present Work

Detailed literature review on the biodegradation of phenolic and petroleum wastewater reveals that, among many other petroleum hydrocarbons, individual degradation of phenol, benzene, hexadecane, xylene, toluene, etc. by microbial communities is well documented. However, reports on the microbial treatment of raw petroleum wastewater are scant. Hence, our objective in the present study is to isolate bacterial strain(s), from oil contaminated sites, that are able to degrade petroleum hydrocarbon and to study their capability to degrade raw petroleum wastewater. To begin with, phenol has been chosen phenol as the model pollutant due to the abundance of phenolic compounds in the petroleum wastewater and their significant toxicity. In view of that, the present research work was undertaken with the following principal objectives:

- Isolation, identification and characterization of site specific bacteria based on phenol degradation
- Growth kinetics for the isolated bacteria
- Phenol degradation kinetics by the isolated bacteria
- Investigation on bacterial degradation of petroleum wastewater as a whole
- Study of the performance of bacterial degradation in laboratory scale reactor

1.8. Organization of the Thesis

The present thesis has been organized into six chapters as described below:

Chapter 1: Introduction and Literature Review

Chapter 1 briefly discusses the source of the pollution due to oil spills and their environmental impacts elaborating the background of the present research work. In addition to the different theoretical aspects of petroleum wastewater, this part also emphasize on various physical, chemical and especially the biological remedial methods of petroleum wastewater along with a detailed literature review. The scope and objectives of the present work have also been stated in this chapter

Chapter 2: Isolation, Characterization and Growth Optimization of Hyper Phenol Tolerant Bacteria

This chapter describes the isolation of two potential phenol-degrading bacterial strains from two different site specific petroleum wastewaters. The isolated strains were identified as *Bacillus cereus* MTCC 9817 strain AKG1 and *Bacillus cereus* MTCC

9818 strain AKG2 using a method based on the 16S rDNA gene sequencing. The optimum growth temperature for both AKG1 and AKG2 was 37 °C, but the optimum pH was found to be 7.0 and 7.5, respectively. Their growth kinetics was also investigated in addition to the various morphological and biochemical characterization.

Chapter 3: Batch Biodegradation Studies using Free Cell Culture of Isolated Bacillus cereus

Chapter 3 is divided into two sections. In the first section, biodegradation of phenol at various initial concentrations by isolated *B. cereus* strains were studied at their optimum physiological condition. Analyses of the degradation kinetics demonstrated that the Haldane model predicted the experimental degradation data for both the strains fairly well. The investigation of the phenol degradation mechanism in the isolated strains was also elucidated.

In the second section, treatment of real wastewater (Sample I and II) was studied in a batch mode system by free cultures. Based on the performance in treating the petroleum wastewater samples, the co-culture of the free cells (AKG1 and AKG2) was found to be most efficient in overall removal of chemical oxygen demand (COD), total organic carbon (TOC) and ammonium nitrogen (NH_4^+–N). Liquid chromatography and mass spectroscopic analysis were carried out for identification of the bio-degradation products. FT-IR study was also performed to investigate the structural changes of bacterial cell membrane as a result of the bacterial adaptation to the toxic environment of the petroleum wastewater.

Chapter 4: Batch Biodegradation Studies with Calcium-Alginate Immobilized Cells of Isolated B. cereus

There are two sections in Chapter 4. First section describes the establishment of Ca-alginate immobilized system of AKG1 and AKG2, and the study of the optimum conditions for phenol degradation by the immobilized strains in batch mode demonstrating the enhanced tolerance of the immobilized cells to higher phenol concentrations (as high as 2000 mg L^{-1}). The excellent storage stability of the immobilized strains and their potential application in repeated batch biodegradation has also been shown. The study on degradation kinetics indicated that the phenol degradation by the immobilized strains could well be fitted by the Haldane model as well as Yano model.

In the second section, the biodegradation of two different site specific petroleum wastewater samples (Sample I and II) by immobilized AKG1 and AKG2 have been investigated and the concurrent changes in COD, TOC and NH_4^+–N contents have been evaluated. The effect of external nitrogen source on biodegradation efficiencies was also studied. The immobilized cells, however, were found to be less effective than the free cell systems in treating the petroleum wastewater samples.

Chapter 5: Continuous Degradation Study using Immobilized Cell Cultures

The fabrication and initial optimization of lab scale bioreactors for degrading phenol as well as petroleum wastewater are described in Chapter 5 which is further divided into three sections. The first section presents the biodegradation of phenol by Ca-alginate immobilized *Bacillus cereus* (AKG1 and AKG2) in a packed bed reactor with continuous mode of operation. The biodegradation rate of phenol was found to be dependent on the flow rate as well as the initial phenol concentration. Combining the effect of external mass transfer with biochemical reaction, the mass transfer correlation was developed in terms Colburn factor (J_D) and Reynolds number (N_{Re}).

The second section describes the continuous biodegradation of the petroleum wastewater in re-circulated packed bed reactors by the isolated strains of AKG1 and AKG2 immobilized in either Ca-alginate beads or polyurethane foam (PUF) cubes. The biodegradation performances of both the immobilized systems, evaluated by determining the reduction in the COD, TOC, phenolic compounds, NH_4^+–N and PO_4^{3-}–P level, demonstrated the excellent efficacy of the immobilized AKG1 and AKG2 strains in treating petroleum wastewater in continuous mode of operation.

Continuous biodegradation of petroleum wastewater in re-circulated fluidized bed reactors is described in the third section. Biodegradation performance was evaluated by determining the reduction in the COD and phenolic compounds in the wastewater sample. The microbial treatment reduced the initial COD level and concentration of phenolic compounds by 95% or more demonstrating the excellent efficacy of the immobilized AKG1 and AKG2 strains in treating petroleum wastewater in continuous mode of operation in fluidized bed bioreactors.

Chapter 6: Conclusions and Scope for Future Work

This chapter presents major inferences drawn from the present work and scopes for future studies.

CHAPTER 2

Isolation, Characterization and Growth Optimization of Hyper Phenol Tolerant Bacteria

Isolation and characterization of two phenol degrading bacteria showing high phenol-tolerance from oil-contaminated sites has been reported in this chapter. Optimization of growth parameters and growth kinetics of the isolated bacteria has also been investigated. This part of the work has been published in ***Journal of Hazardous Materials*** *176* ***(2010)*** *85-91.*

Chapter 2

ISOLATION, CHARACTERIZATION AND GROWTH OPTIMIZATION OF HYPER PHENOL TOLERANT BACTERIA

2.1. Introduction

Phenols and phenolic compounds, prevalent in petroleum waste, are potentially toxic causing critical health hazards. Hence, it is of utmost importance to reduce the phenol level in industrial effluents to tolerant limits prior to being released into the environment (Gianfreda et al, 2006). Conventional physical and chemical methods, such as granular or biological activated carbon filtration, ozonation, chlorination, H_2O_2/UV process, solvent extraction and membrane separation, used to eliminate waste organic compounds from industrial wastewater are costly and have inherent drawbacks of producing secondary hazardous products (Cardoso et al, 2009). On the other hand, biodegradation that exploits the ability of microorganism (generally bacteria) to convert organic pollutants to water, carbon dioxide and biomass under aerobic or anaerobic condition appears to be the most environmentally benign method of removal of oil pollutants avoiding undesirable by-products or secondary pollutants like in chemical scrubbing or thermal waste gas treatment (Devinny et al, 1999).

Phenol-degrading microorganism has been observed to display substrate inhibition at high phenol concentrations. The maximum specific cell growth rate, μ_{max}; substrate-affinity constant, K_S; and substrate-inhibition constant, K_I vary over a wide range depending on cell type and culture environments. Thus, isolation of bacteria with high phenol degrading capability and investigation of their detailed growth as well as degradation kinetics in presence of phenolic substrates merit immense environmental importance.

2.2. Literature Review

Recent studies on the biodegradation of mono-aromatic hydrocarbons such as benzene, toluene and phenol using mixed-substrate system revealed a number of substrate interactions during hydrocarbon degradation (Goldsmith and Balderson, 1988). Meyer et al. (1984) observed diauxic degradation of benzene in the presence of phenol while Reardon et al. (2000) observed that benzene and toluene were better growth substrates for *Pseudomonas putida* F1 than phenol, resulting in faster growth and higher yield coefficients. Therefore, microorganisms with high biodegrading capability for phenols and phenolic compounds have been subjects of recent research (Juang and Tsai, 2006).

In order to obtain high phenol tolerance, microorganisms have also been isolated from phenol-rich wastes (Rigo and Alegre, 2004; Vijayagopal and Viruthagiri, 2005; Tsai et al, 2005; Santos and Linardi, 2004). In this regard, *Pseudomonas* is the most widely reported bacteria for the biodegradation of phenolic compounds (Chitra et al, 1995; Bandhyopadhyay et al, 1999) and the inhibitory effect of phenol became predominant at the concentration of 500 mg L^{-1} or above. On the other hand, very little is known for the degradation of phenol derivatives by *Bacillus sp.* The thermophilic phenol degrading *Bacillus theroleovorans* strain A2 was found to be able to degrade phenol at temperature as high as 70 °C (Rosvita et al, 1999). The studies on phenol degradation by *Bacillus stearothermophilus* were mainly focused on the enzymatic pathways involved during such degradation (Gurujeyalakshmi and Oriel, 1989; Dong et al, 1992). Information on degradation behavior of species like *Bacillus cereus* for phenol and its derivatives in the literature are scant.

In the microbial degradation of phenol, the specific phenol degradation rate is often modeled using the Haldane equation by coupling substrate removal rate to cell growth rate with a constant yield coefficient (Pawlowsky and Howell, 1973), which is valid only within a very narrow range of initial phenol concentrations. Variations in cell mass yield are expected when cells grow very slowly during substrate inhibition (Pawlowsky and Howell, 1973; Allsop et al, 1993). Hence, the assumption of a constant cell yield coefficient should be used with caution when the specific substrate degradation rate is modeled as it is directly related to the specific cell growth rate.

2.3. Outline of the Research Work

1) Two hyper-phenol tolerant bacterial strains, AKG1 and AKG2, which can grow in presence of phenol as the sole carbon and energy sources were isolated from oil refinery and oil exploration sites, respectively.
2) The isolated strains were identified as *Bacillus cereus* MTCC9817 (AKG1) and *Bacillus cereus* MTCC9818 (AKG2) by determining the phylogenetic positions based on the 16S rDNA sequence analysis.
3) The optimum growth conditions for the isolates *B. cereus* AKG1 MTCC9817 and *B. cereus* AKG2 MTCC9818 were investigated during the degradation of phenol in a batch system.
4) The batch growth kinetics of the isolates in presence of phenol as the sole substrate was studied using wide range of substrate concentration (viz. 100–2000 mg L^{-1}).

2.4. Experimental Section

2.4.1. Chemicals and Culture Medium

A basic mineral salt medium (MSM) containing 4.0 g L^{-1} sodium nitrate ($NaNO_3$), 3.61 g L^{-1} disodium hydrogen phosphate (Na_2HPO_4), 1.75 g L^{-1} potassium dihydrogen phosphate (KH_2PO_4), 0.2 g L^{-1} magnesium sulfate ($MgSO_4.7H_2O$), 0.05 g L^{-1} calcium chloride ($CaCl_2.2H_2O$), 1.0 mg L^{-1} ferrous sulfate ($FeSO_4.5H_2O$), 50 µg L^{-1} copper sulfate ($CuSO_4.5H_2O$), 10 µg L^{-1} sodium molybdate (Na_2MoO_3), 10 µg L^{-1} manganese sulfate ($MnSO_4$) and 3 g L^{-1} Yeast extract was used for the growth of the microorganisms. Solid media was prepared by the addition of 15 g L^{-1} (1.5 %) agar to the medium. Prior to use, the media were sterilized in an autoclave at 121 °C for 15 min. All inorganic chemicals were of analytical grade unless specified otherwise and were obtained from E-Merck India. The growth media were prepared by adding phenol of required concentration (100–2000 mg L^{-1}) to the MSM. Initially for isolation process, the pH of the medium was maintained at 6.5 and the working volume was 100 mL in all experiments.

2.4.2. Isolation and Culture Conditions

For the isolation of phenol degrading bacteria, wastewater samples were obtained from two different origins namely the refinery site (Sample I) and the exploration site

(Sample II). 1 mL of each sample was added separately to 250 mL Erlenmeyer flask containing 100 mL of carbon free MSM and phenol at initial concentration of 500 mg L^{-1}. The pH of the media was adjusted to 6.5 with 1 *N* NaOH and 1 *N* HCl solution. The flasks were incubated at 37 °C in a rotary shaker at 120 rpm. When the cultures became turbid, 1 mL of each culture was transferred to 100 mL of fresh medium for next 48 h. The above procedure was repeated three times. At the end of the incubation process, the enriched culture was suitably diluted and plated on solid media. Each separated colony appearing on the agar plates was re-streaked on fresh agar plate (containing high concentration of phenol than previous) until pure colony was obtained. The isolated bacteria from the refinery site and the exploration site were named AKG1 and AKG2, respectively. After acclimatization for two months, one colony from each sample was isolated on the basis of their ability of growing at high phenol concentration (1800 mg L^{-1} and 1650 mg L^{-1}) as a sole carbon source.

2.4.3. Characterization and Identification of Strain

The isolated pure bacteria cultures were sent to Microbial Type Culture Collection (MTCC) & Gene Bank Chandigarh, India for biochemical characterization and 16S rDNA sequence determination (Table 1). The sequencing results were submitted to Gene Bank database to carry out similarity search for nucleotides by online BLAST tool (http://www.ncbi.nlm.nih.gov). The thermodynamic properties of the isolated cultures were also determined by using the online tool BIOTOOL (http://www.unc.edu/~cail/biotool/oligo/index.html). Pure cultures were stored in 50 mM KH_2PO_4:K_2HPO_4 buffer (at pH 7.0 and 7.5, respectively, for strain AKG1 and AKG2) containing 30 % (v/v) glycerol at −20 °C. Working cultures were maintained by subculturing every six weeks on phenol-agar plates.

2.4.4. Analysis of Cell Concentration

Cell concentrations in the samples were analyzed by measuring the optical density (OD) at 600 nm using UV-vis spectrophotometer (Perkin Elmer, lamda 35, USA) with the culture medium as reference.

2.4.5. Effects of pH, Temperature and Initial Phenol Concentration on Growth of the Isolate

Optimum temperature, pH and phenol concentration for the growth of the microorganisms were determined. Each experiment was carried out in batch mode in 250 mL Erlenmeyer flask containing 100 mL mineral media along with Yeast extract (3 g L^{-1}) at 120 rpm. First, the experiments were carried out at various temperatures ranging from 31 to 39 °C, keeping initial phenol concentration at 1000 mg L^{-1} and pH 6.5 under shaking condition to find out the optimum temperature for the growth of the microbes. At this optimum temperature further experiments were also carried out at various pH values ranging from 6 to 8 with initial phenol concentration of 1000 mg L^{-1} to find out the optimum pH for the growth of the microbes. In order to find out the optimum initial phenol concentration for the growth of the isolated microbes and analyze their growth kinetics, additional experiments were carried out with various initial phenol concentrations ranging from 100–2000 mg L^{-1} at optimum temperature and pH. The optimum value of a parameter corresponds to the maximum specific growth rate of cell, μ_{max} (h^{-1}) as observed from the experiments. Calculation procedure of μ is discussed in the subsequent section.

2.4.6. Growth Kinetics of Isolated Microorganisms

Each 250 mL shake flask containing phenol as a carbon source, 100 mL of MSM media, and 1 mL of cell suspension (OD_{600} 0.017~0.023) was incubated in a shaker (120 rpm) at 37 °C. The initial concentration of phenol in culture was maintained in the range of 100 mg L^{-1} to 2000 mg L^{-1}. Samples were collected at designated intervals for cell concentration measurement.

Growth kinetics is an essential and mandatory input for the design of any biological reactor where microbial degradation is carried out. Since microbial growth kinetics is highly sensitive to the microbes of concern and other physicochemical conditions of the reactor, it is extremely important to have suitable growth kinetics for a microbial process. In order to represent the growth kinetics of inhibitory compound in the present study, several available kinetics models were fitted to the experimental data for selecting the best model(s) (Table 2). The specific growth rate of cells in a batch system, μ (h^{-1}), is defined as $\mu = \frac{\mu_{max} S[1+(S/K)]}{S + K_S + (S^2/K_I)}$ (2.1)

where S is the substrate concentration (mg L^{-1}), μ_{max} is the maximum growth rate (h^{-1}), K_S is the substrate-affinity constant (mg L^{-1}) and K_I is the substrate-inhibition constant (mg L^{-1}). A larger K_I value indicates that the culture is less sensitive to substrate inhibition (Onysko et al, 2000). The value of μ is determined at the exponential phase of the growth curve. From the linear plot of X vs. ln (S/S_0), after a short lag phase, the value of μ for an initial phenol concentration (S_0) is obtained. Where, X is the cell concentration in either g L^{-1} (dry basis) or in absorbance unit at 600 nm (OD). Such plot indicates that the phenol was the limiting substrate in this region and the cultures were growing exponentially (Yang and Humphrey, 1975). From the values of μ vs. S_0, the values of μ_{max}, K_S and K_I are obtained using regression analysis in MATLAB 7.0 ©.

2.5. Results and Discussion

2.5.1. Isolation and Identification of Bacteria

Both strains AKG1 and AKG2 were characterized as rod-shaped, gram positive, oxidase and catalse positive bacteria (Table 1). When examined using scanning electron microscopy (SEM), after 12 h growth, cells measured 1.24 µm in width and 3.38 µm in length for strain AKG1 and 1.41 µm in width and 3.6 µm in length for strain AKG2 (Figure 2.1). The complete details of the biochemical and physiological characteristics of both strains are given in Table 1.

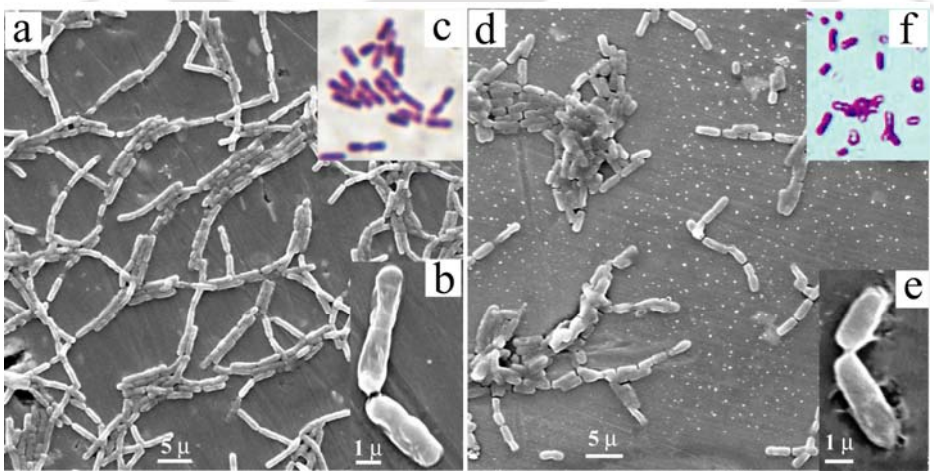

Figure 2.1. (a) and (d) represents SEM images of AKG1 and AKG2, respectively, with 1.01 K× magnification. (b) and (e) SEM images of AKG1 and AKG2, respectively, with 7.0 K× magnification. Snaps (c) and (f) represent Gram staining pictures of AKG1 and AKG2, respectively, at 100×.

Table 2.1. Biochemical and physiological characteristics of isolated AKG1 and AKG2 identified as *Bacillus cereus* MTCC9817 and *Bacillus cereus* MTCC9818, respectively. (+: positive; −: negative; (+): weak growth).

Colony Morphology			***Physiological Tests***		
	AKG-1	**AKG-2**		**AKG-1**	**AKG-2**
Configuration	Round	Round	Growth at temperature	>10°C to 55 °C	4°C to 55°C
Margin	Entire	Entire	Growth at pH	>5 to < 9	>5 to < 9
Elevation	Raised	Raised	Growth on NaCl (%)	2.0% to < 10.0 %	2.0% to < 10.0 %
Surface	Flat	Flat			
Opacity	Opaque	Opaque	***Acid production from***		
Gram's Reaction	+ve	+ve			
Cell shape	Rods	Rods	Salicin	(+)	(+)
Size (µm)	2-4	2-4	Xylose	−	−
Spore	+	+	Mannitol	−	−
Motility	+	+	Dextrose	+	+
			Biochemical tests		
Indole test	−	−	Growth on MacConkey agar	N.G.	N.G.
Methyl red test	(+)	(+)	Esculin hydrolysis	+	+
Voges proskauer	−	−	Gelatin hydrolysis	+	+
Citrate utilization	(+)	(+)	Starch hydrolysis	+	+
H_2S production	−	−	Catalase test	+	+
Gas production	−	−	Tween 20 hydrolysis	+	+
Oxidase test	+	+	Tween 40 hydrolysis	(+)	(+)
Urea hydrolysis	+	+	Tween 80 hydrolysis (Lipase test)	−	−
Nitrate reduction	−	−	Arginine dihydrolase	+	+

Partial 16S rDNA sequencing results obtained from MTCC, Chandigarh, India, showed that AKG1 and AKG2 had 1369 and 1444 base pairs (bp), respectively. Gene analysis by online BLAST tool indicates that both the strains were equally similar with *Bacillus cereus*, *Bacillus thuringiensis* and *Bacillus subtilis*. But, their morphological and biochemical characteristics were more similar to *Bacillus cereus*. On the basis of these reports, MTCC, Chandigarh, India, characterized them as *Bacillus cereus* and was designated as strain AKG1 *Bacillus cereus* MTCC 9817 (gb FJ841975) and AKG2 *Bacillus cereus* MTCC 9818 (gb FJ841976). The high bootstrap support of the tree shown in Figure 2.2a derived from the 16S rDNA analysis (Dereeper et al, 2008) demonstrated that strains AKG1 and AKG2 are typical members of the genus *Bacillus*. The 16S rDNA sequence of strain AKG1 showed the closest relation to *Bacillus cereus* 99.63% and *Bacillus coagulans* 99.63% followed by 99.34% homology with *Bacillus thuringiensis* strain 2PR56-10. AKG2 was related to *Bacillus thuringiensis* strain CMG 861 with 99.37% homology. The similarity search between AKG1 and AKG2 gave the lowest similarity 99.19% among all. Eight gaps and three mismatches were found in total similarity search among AKG1 and AKG2. The three gaps lies in between 1320 bp to 1369 bp of AKG1 with 1383 bp to 1431 bp of AKG2 (Fig 2.2b). The thermodynamic properties as obtained by the online tool, BIOTOOL indicated that strain AKG1 has 54% GC content with −2275.9 kcal mol^{-1} Gibbs free energy (ΔG), −12074.5 kcal mol^{-1} enthalpy (ΔH) and 31576.1 cal mol^{-1} K^{-1} entropy (ΔS). Strain AKG2 shows entropy ΔS = 33253.8 cal mol^{-1} K^{-1}, Gibbs energy ΔG = 2396.8 kcal mol^{-1} and enthalpy ΔH = 12715.8 kcal mol^{-1} with lower GC content (53%) than AKG1 (54%).

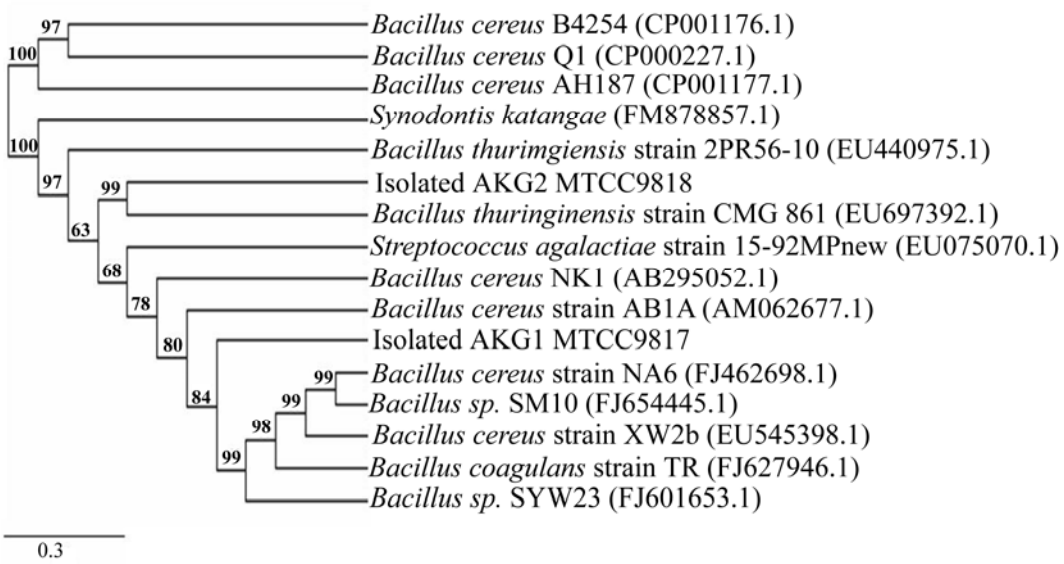

Figure 2.2a. The neighbor-joining Phylogenetic tree was constructed and bootstrapped (1000 iterations) using Robust Phylogenetic Analysis for the Non-Specialist (Dereeper et al, 2008) to represent the relationship between the phenol-degrading strain AKG1 and AKG2 and representative species of the genus *Bacillus* and related genera. Bootstrap values are noted on the branch and the scale bar (=0.3) represents nucleotide substitution per 100 nucleotide.

```
Query1320 AGTTTGTAACACCCGAAGTCGGTGGGGTAACCTTTTTGGA-GCCAGCCGCC  1369
          ||||||||||||||||||||||||||||||||||||||| ||| |||| |||||
Sbjct1383 AGTTTGTAACACCCGAAGTCGGTGGGGTAACCTTTT-GGAAGCCA-CCGCC  1431
```

Figure 2.2b. A part of the similarity search shows the mismatch between isolated two strains AKG1 and AKG2. Here, query represents the strain AKG1 MTCC 9817 where sbjct represent the second strain AKG2 MTCC 9818

2.5.2. Effect of Incubation Temperature on Bacterial Growth on Phenol

Figure 2.3 shows the growth rate profiles of isolated bacteria at initial pH 6.5 and at varying temperatures. It can be noticed from the figure that the growth rate was increasing with temperature till 37 °C for both cases. At temperature higher than 37 °C growth rate decreased. This is attributed to the fact that at higher temperature microbe may not survive, therefore, shows lower rate of growth. For both isolates, the optimum growth temperature of 37 °C indicates that isolated strains are mesophilic by nature.

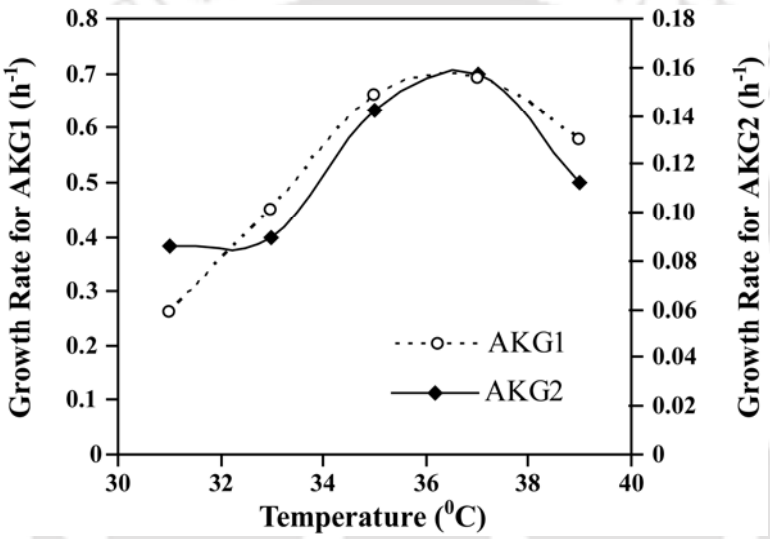

Figure 2.3. Specific growth rates of AKG1 and AKG2 for various temperatures at pH 6.5 and initial substrate (phenol) concentration of 1000 mg L^{-1}.

2.5.3. Effect of Initial pH on Bacterial Growth

Figure 2.4 shows the growth profile of the phenol degrading bacteria at various pH values. It can be seen that the microbes grew efficiently at almost neutral medium. Enzymes produced by microbes are affected by the change in pH because it is an important factor in the stability of the enzymes and pH change affects the solubility of enzymatic compounds. Extremely high or low pH values generally results in complete loss of activity for most of the enzymes. Thus, for each enzyme there is also a region of optimal pH. Therefore, the optimum pH is the most favorable pH value where the enzyme is most active and the microbes are stable. Irrespective of temperature, strains AKG1 and AKG2 showed maximum growth rate at pH 7.0 and 7.5 respectively using phenol as a sole carbon source.

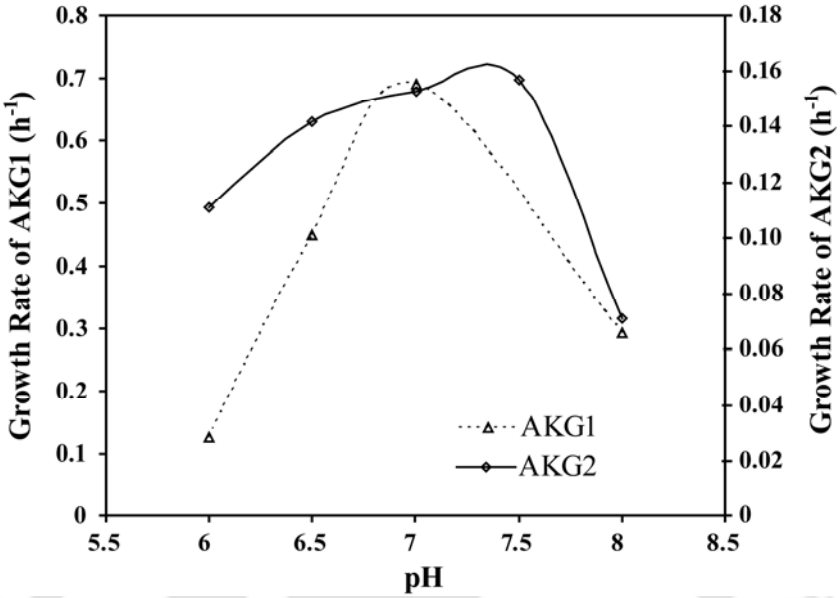

Figure 2.4. Specific growth rates of AKG1 and AKG2 for various pH at optimum temperature (37°C) and initial substrate (phenol) concentration of 1000 mg L^{-1}.

2.5.4. Effect of Initial Substrate (Phenol) Concentration on Bacterial Growth

For AKG1, a maximum growth rate was observed at 600 mg L^{-1}, while, for AKG2, it was observed at 1000 mg L^{-1} of initial phenol concentration (Figure 2.5). Phenol has been shown to have a significant inhibitory effect on growth of microorganism at higher concentration (>1000 mg L^{-1}). No significant growth was observed for initial phenol concentration of 2000 mg L^{-1} and beyond. This suggests that the microbe is inefficient for phenol concentration beyond 2000 mg L^{-1}. Yeast extract was added in the growth medium as inducer to increase the biomass in short period of time. A typical biomass concentration profile (as OD_{600}) of AKG1 *Bacillus cereus* MTCC 9817 and AKG2 *Bacillus cereus* MTCC 9818 at 1000 mg L^{-1} is shown in Figure 2.6. The figure does not show idealized curve, but that curve obtained when the experimental points are joined up, thus avoiding an arbitrary interpretation of the results. After the highest growth peak, it is observed that absorbance at 600 nm is decreasing. It is due to the cell death because of cell lyses. Similar phenomenon is already reported in the literatures (Gurujeyalakshmi and Oriel, 1989; Jiang et al, 2006; Schmauder, 2004). For strain AKG2, a prominent late growth phase was observed.

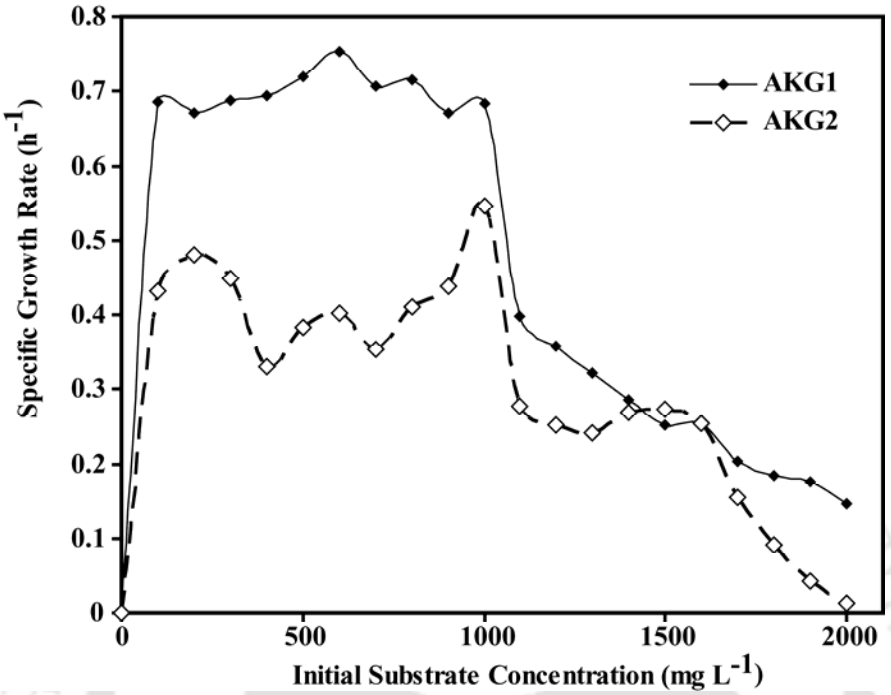

Figure 2.5. Growth rate curves for AKG1 and AKG2 for various initial substrate (phenol) concentrations at optimum temperature and pH.

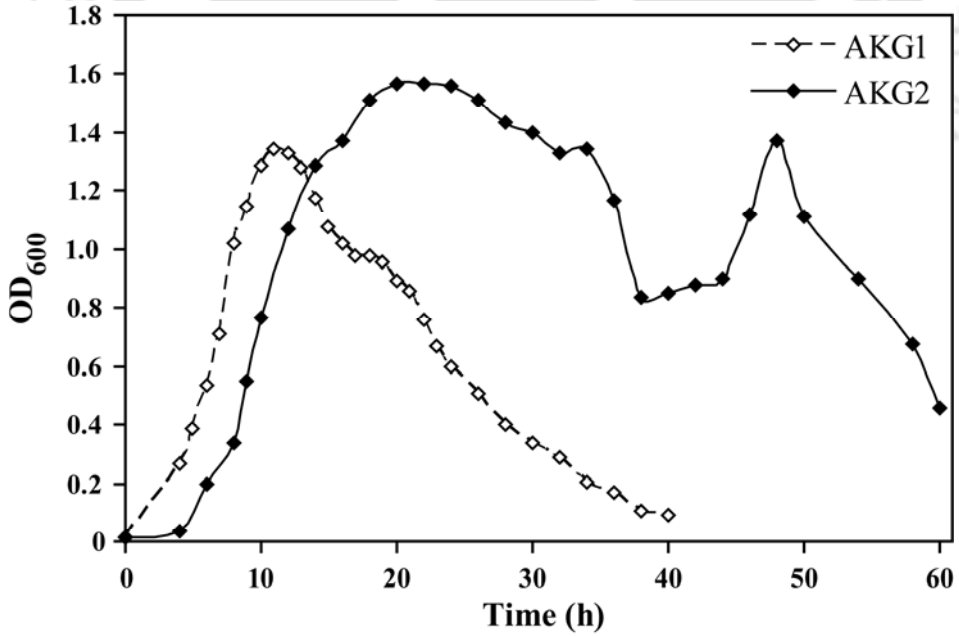

Figure 2.6. Typical growth curves of AKG1 and AKG2 with 1000 mg L^{-1} phenol as a carbon source at optimum temperature and pH.

2.5.5. Growth Kinetics Studies for Bacillus cereus AKG1 and AKG2

Figure 2.7 shows the prediction of the experimental specific growth rate by various kinetic models (Table 2.2) for various initial phenol concentrations. All the models used in this study have been generally used to describe substrate inhibition model. From the figure, it was observed that, between the five different models, Yano model for the strain AKG1 and Edward model for the strain AKG2 fit the data well with respect to their kinetic parameters. Table 2.2 represents their kinetic parameters along with their R^2 (coefficient of determination) values. Table 2.3 showed a comparison of the present experimental biokinetic parameters when calculated using Haldane model with those previously reported in literature, although, Haldane model is not our best fitted model. The biokinetic parameters thus estimated were found to be higher than the literature data.

The simulated growth profiles of isolated strains for various initial phenol concentrations were obtained using the estimated biokinetic parameters as input. These biokinetic parameters are highly sensitive to their initial guess values, which in turn may change the accuracy of prediction of experimental growth profiles. Therefore, in this study, sensitivity analysis for parametric estimation have carried out. Here, four different sets (Table 2.4) of biokinetic parameters (μ, K_S and K_I) values were used as initial guesses. Table 2.4 presents the R^2 obtained by various initial changes considered. The table clearly indicates that, Haldane model has the most repeatability for both the cases, but, Yano model and Edward model provided the best fit for entire data sets for each of them respectively. The latter two models also repeatedly identified the similar biokinetic parameters with negligible deviation except the *Case 1* (μ<1, K_S <1, K_I <1) (Table 2.4).

The values of inhibition constants (K_I) using Haldane model, the most widely used model, for both the strains in the present case are higher than the reported literature data (Table 2.3) for pure cultures. This reflects that the isolated strains can tolerate higher phenol concentration than the reported values (Table 2.3). This high phenol tolerance characteristic of the isolated strains in the present case could be due to their genetic modifications because of long time exposure in phenol contaminated wastes. Our best fitted models (Yano and Edward models for strains AKG1 and AKG2, respectively) predicted higher growth rate (1.024 h^{-1}) for strain AKG1 and little lower growth rate (0.5969 h^{-1}) for strain AKG2, than Haldane model with higher inhibition constants for

both cases (Table 2.4). Webb model and Aiba model fitted very poorly to all data sets for both the strains.

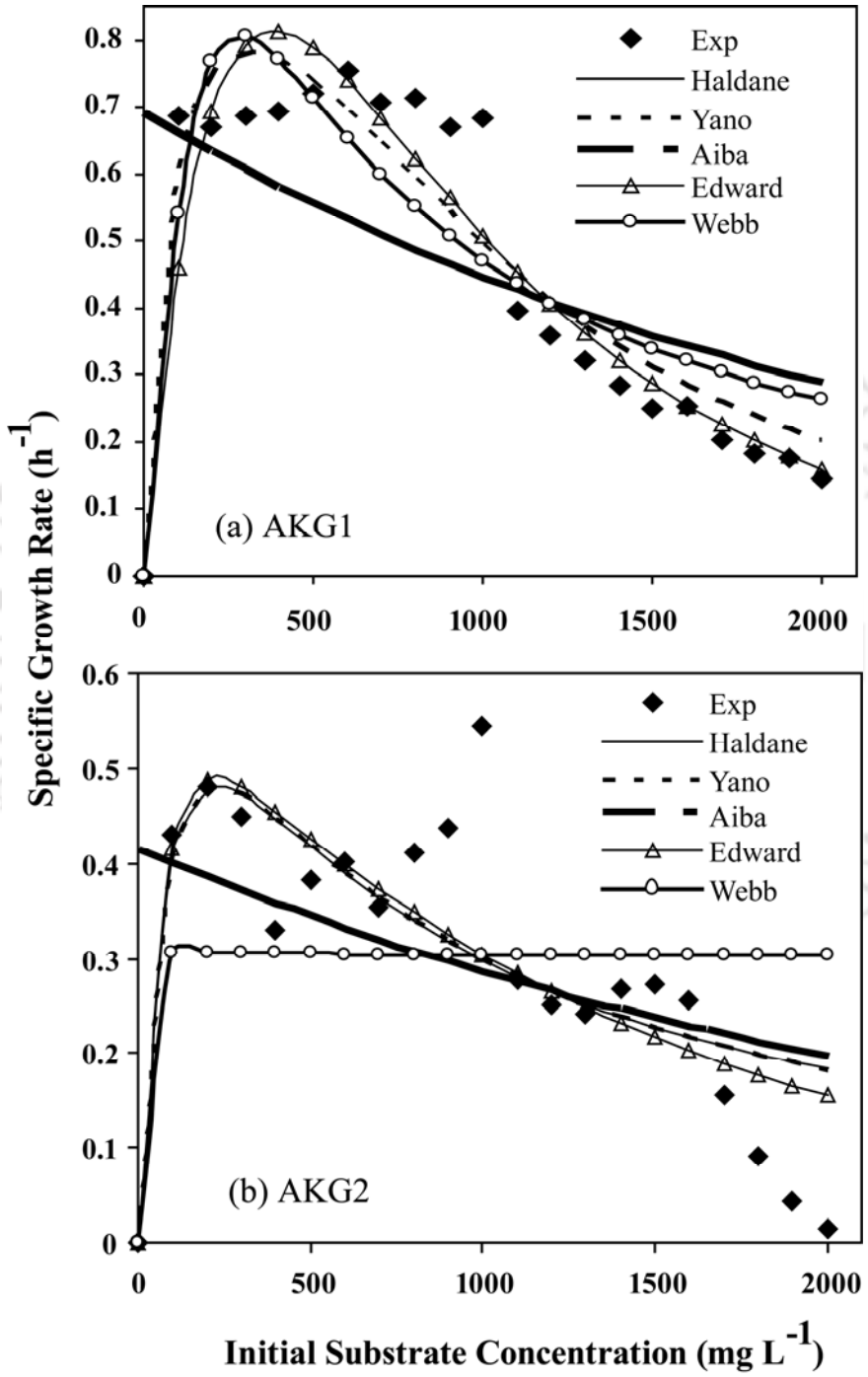

Figure 2.7. Model prediction of experimental specific growth rates of AKG1 and AKG2 in phenol.

Table 2.2. Kinetic parameters obtained by different models.

Strain	Model	μ_{max} (h^{-1})	K_s (mg L^{-1})	K_I (mg L^{-1})	K (mg L^{-1})	R^2	SD_{avg}
AKG1	Haldane Model $\mu = \frac{\mu_{max} S}{K_S + S + \frac{S^2}{K_I}}$ (Haldane, 1965)	0.4396	129.4	637.8	–	0.8094	0.067
	Yano Model $\mu = \frac{\mu_{max} S}{K_S + S + \frac{S^2}{K_I}\left(1 + \frac{S}{K}\right)}$ (Yano et al, 1966)	1.024	66.68	1.718×10^5	5.863	0.899	0.048
	Aiba Model $\mu = \frac{\mu_{max} S}{K_S + S} \exp\left(\frac{-S}{K_I}\right)$ (Aiba et at, 1968)	31420	4.548×10^4	2390	–	0.3095	0.106
	Edward Model $\mu = \mu_{max} S \left[e^{\left(\frac{-S}{K_I}\right)} - e^{\left(\frac{-S}{K_S}\right)} \right]$ (Edwards, 1970)	0.1702	208	845.1	–	0.8864	0.041
	Webb Model $\mu = \frac{\mu_{max} S \left(1 + \frac{S}{K}\right)}{S + K_S + \frac{S^2}{K_I}}$ (Webb, 1963)	4.208	602	135.5	4.259×10^5	0.8089	0.067
AKG2	Haldane Model	0.9332	110.5	494.4	–	0.6623	0.043
	Yano Model	0.9246	108.4	503.4	2.727×10^5	0.663	0.043
	Aiba Model	9231	2.226×10^4	3014	–	0.2404	0.066
	Edward Model	0.5969	69.93	1483	–	0.7076	0.041
	Webb Model	0.412	8.542	3.054	4.136	0.1812	0.079

Table 2.3. Comparison of the growth kinetics parameter of microbial culture.

	Bacterial Strain	System	Concentration (mg L^{-1})	Haldane's Model			Temperature/ pH	Reference
				μ_{max} (h^{-1})	K_s (mg L^{-1})	K_I (mg L^{-1})		
1	*P.putida* CCRC14365	Batch	0–4000	0.245	0.129	12.6	30/ 7.0	(Juang and Tsai, 2006)
2	Mixed culture I	Batch	0–900	0.260	25.4	173.0	28 ± 0.5 / 6.6	(Pawlowsky and Howell, 1973)
3	Mixed culture II (filamentous organism)	Batch	0–1000	0.223	5.86	934.5	28 ± 0.5 /6.6	(Pawlowsky and Howell, 1973)
4	*P.putida* DSM548	Batch	NA	0.57	2.4	106	30 /6.0	(Yang and Humphrey,1975)
5	*Pseudomonas putida* (ATCC 17514)	Continuous	0–500	0.567	2.39	106.0	30 /6.0	(Yang and Humphrey,1975)
6	*T. cutaneum*	Continuous	0–900	0.464	1.66	380.0	30 / 4.5	(Yang and Humphrey,1975)
7	*P.putida* CCRC14365	Batch	0–600	0.33	13.9	NA	30 / 6.8	(Chung et al, 2003)
8	*P.putida* DSM548	Batch	0–100	0.44	6.2	54.1	26 / 6.3~6.8	(Alvaro et al, 2000)
9	*P.putida* DSM50222	Batch		0.53	<1.0	470	30 / 6.2~6.7	(Hill and Robinson, 1975)
10	*Pseudomonas putida* (ATCC 17484)	Batch/ Continuous	0–700	0.534	0.015	470.0	30 /(6.2–6.7)	(Hill and Robinson, 1975)
11	*Alcaligenes faecalis*	Batch	10–1400	0.15	2.22	245.37	30 / 7.2	(Bai et al, 2007)
12	Mixed culture	Batch	0–800	0.309	44.92	525.00	27±1 / 7.0	(Saravanan et al, 2008)
13	*P. putida* (F1ATCC 700007)	Batch	750–1750	0.051	18.0	430	30 / 7.0	(Abuhamed et al, 2004)
14	*P. putida* (MTCC1194)	Batch	0–1000	0.305	36.33	129.79	29.9 ±0.5 / 7.1	(Abuhamed et al, 2004)
15	*P. putida*	Batch	5–150	NA	NA	NA	30 / 7.0	(Naas et al, 2009)
16	AKG1 *Bacillus cereus* MTCC 9817 (gb FJ841975)	Batch	0–2000	0.440	129.4	637.8	37 / 7.0	Present work
17	AKG2 *Bacillus cereus* MTCC 9818 (gb FJ841976)	Batch	0–2000	0.933	110.5	494.4	37 / 7.5	Present work

Table 2.4. Calculated coefficient of determination (R^2) values for initial guess changing for each model using non-linear regression method.

Initial Value	R^2									
	Haldane Model		**Yano Model**		**Aiba Model**		**Edward Model**		**Webb Model**	
	AKG1	*AKG2*	*AKG1*	*AKG2*	*AKG1*	*AKG2*	*AKG1*	*AKG2*	*AKG1*	*AKG2*
Case1: μ <1, K_S<1, K_I<1	0.8094	0.6623	−2.419	−2.514	−3.458	−3.561	−3.458	−3.561	0.1732	0.1812
Case 2: μ <1, K_S>1, K_I>1	0.8094	0.6623	0.8990	0.6630	0.3095	0.2400	0.8864	0.6876	0.8089	0.3114
Case 3: μ=1, K_S>1, K_I>1	0.8094	0.6623	0.8990	0.7354	0.3095	0.2401	0.8864	0.7076	0.8089	0.4580
Case 4: μ >1, K_S<1, K_I<1	0.8094	0.6623	0.8989	−2.132	0.3089	0.2397	0.8864	0.7076	0.348	0.2599

2.6. Conclusions

Two phenol-degrading bacteria were isolated from a phenol-enriched mixed culture from two different sites. Both strains were identified as *Bacillus cereus* MTCC 9817 strain AKG1 and *Bacillus cereus* MTCC 9818 strain AKG2 using a method based on the 16S rDNA gene sequencing. Both the strains have a great potential to grow at very high concentration of phenol. The optimum growth temperatures for *Bacillus cereus* AKG1 and AKG2 was 37 °C, utilizing phenol as the substrate. Though both strains belong to same genus, results show that, they have a characteristic growth difference. Strain AKG1 can easily grow on 1000 mg L^{-1} phenol without any inhibition effect but can not sustain in phenol media for more than 40 hours, whereas, AKG2 has a slow growth rate with inhibition effect on 1000 mg L^{-1} phenol concentration and long time sustainability. As all these properties have a direct or indirect relation on isolates characteristics, thus, this difference may lead them to act differently in the same environment. The above experimental parameters are invariably required for the design and simulation of batch and continuous bioreactors for treatment of phenolic wastewaters. This potential of the strains towards high phenol utilization for industrial effluent treatment and decontamination of natural polluted areas have been studied and described in subsequent chapters.

CHAPTER 3

Batch Biodegradation Studies using Free Cell Culture of the Isolated *Bacillus cereus*

Chapter 3 mainly describes the biodegradation behaviour of the isolated Bacillus cereus strains in batch culture mode and is divided into two parts. Section 3.1 discusses the phenol degradation kinetics of the isolated strains and the biochemical pathway of phenol degradation. This part of work has been published in ***Bioresource Technology*** *101****(2010)*** *5501-5507****.***

The biodegradation of real petroleum wastewater samples is reported in Section 3.2. Overall, the isolated bacteria have been found to be efficient in degrading phenol as well as treating raw petroleum wastewater. This part of work has been orally presented in the ***2010 AIChE Annual Meeting****, Salt Lake City, UT.*

Chapter 3

BATCH BIODEGRADATION STUDIES USING FREE CELL CULTURE OF THE ISOLATED *BACILLUS CEREUS*

3.1. PHENOL BIODEGRADATION: KINETICS AND PATHWAY

3.1.1. Introduction

The knowledge of the biodegradation kinetics of toxic substances is very important for both predicting their fate and the design of efficient remediation process. Moreover, the degradation kinetics is an essential and mandatory input for the design of any biological reactor where biodegradation is performed. Thus, investigating the kinetics of phenol biodegradation by the isolated *B. cereus* strains (AKG1 and AKG2) is crucial for the optimal design and operation of biological treatment of phenol contaminated wastewater by them.

Apart from the degradation kinetics, it is of fundamental importance to investigate the mechanism of phenol degradation by a particular microorganism. Some mesophillic bacteria can utilize aromatic compounds such as phenol as carbon and energy sources by cleaving the aromatic ring via either *ortho* or *meta* pathway (Yang and Humphrey, 1975). The pathway of microbial phenol degradation has already been discussed elaborately in **Chapter 1** (*Section 1.4.5*). Briefly, degradation of phenol follows a sequence of (a) hydroxylation to catechol, (b) ring cleavage via catechol-2,3-dioxygenase to 2-hydroxymuconic semialdehyde (HMSA) for meta pathway, and via catechol-1,2-dioxygenase to *cis, cis*-muconate for ortho pathway, (c) HMSA is either oxidized to 4-oxalocrotonate or hydrolyzed to 2-oxopent-4-enoate in case of *meta* and *cis, cis*-muconate gets converted into muconolactone for *ortho* cleavage. As the phenol concentration in the wastewater can affect the degradation pathway (Loh and Chua, 2002), it is important to investigate the phenol degradation mechanism in isolated AKG1 and AKG2 strains under realistic conditions especially in wastewater treatment where phenol concentration can vary widely (1–3000 mg L^{-1}) (El-Naas et al., 2010).

3.1.2. Literature Review

The inhibitory nature of phenol at its high concentration is well known, and a variety of substrate inhibition models have been used to describe the dynamics of growth of pure (Bandhyopadhyay et al., 2001; Ho et al., 2009) and mixed cultures (Marrot et al., 2006; Gonzalez et al., 2001; Alcocer et al., 2007) with phenol as substrate. The phenol degradation rate has often been modeled by the widely used Haldane equation (Ho et al., 2009; Alcocer et al., 2007). In some cases, the substrate degradation rate has been coupled to the cell growth rate with a constant yield coefficient (Wang et al., 2008). Variations in cell mass yield can also be expected when cells grow very slowly during substrate inhibition (Monteiro et al, 2000; Monsalvo et al., 2009; Wang et al., 1979). Besides substrate inhibition, variation in the cell mass yield can also be attributed to the accumulation of metabolic intermediates and their inhibition effect on substrate consumption (Gonzalez et al. 2001; Wang et al., 1979). Thus, suitability of a degradation kinetics model is strongly dependent on the combination of the substrate of concern, its concentration ranges and the microorganism to be used.

In most of the phenol degrading bacteria, the degradation of phenol follows either the *ortho* or the *meta* pathway (Yang and Humphrey, 1975). The latter is generally observed in case of mesophilic and thermophilic bacilli (Ali et al., 1998). However, till date, most of the studies on phenol degradation pathways by various strains have been carried out either for low concentration range of phenol (Monteiro et al., 2000) or for only single initial concentration of phenol (200 mg L^{-1}) (Alcocer et al., 2007). However, the degradation pathways might change with change in initial concentration of phenol in the wastewater (Loh and Chua, 2002). Furthermore, depending on the metabolic pathway undergone by the substrate and consequently the intermediate compounds produced, the state and composition of the wastewater can also vary.

3.1.3. Outline of the Research Work

1) Biodegradation of phenol by the isolated strains, *B. cereus* AKG1 MTCC 9817 and *B. cereus* AKG2 MTCC 9818 has been carried out for several initial concentrations of phenol ranging from 100 mg L^{-1} to 2000 mg L^{-1}.
2) Suitable degradation kinetics model(s) for both the strains in the whole range of initial phenol concentration (100-2000 mg L^{-1}) have been identified and the corresponding biokinetic parameters have been determined.

3) Finally, the phenol degradation pathways by two strains at various initial concentrations of phenol (100-2000 mg L^{-1}) have been investigated.

3.1.4. Experimental Section

3.1.4.1. Chemicals and Culture Medium

The details of chemicals and culture medium have been described in *Section 2.4.1* in **Chapter 2**.

3.1.4.2. Microorganism and Culture Conditions

The strains AKG1 and AKG2 were isolated from the wastewater samples from the refinery site (Site I) and from the exploration site (Site II) respectively. As discussed in **Chapter 2**, the strains were identified as *Bacillus cereus* by the Microbial Type Culture Collection unit (MTCC), New Delhi, India and named as *Bacillus cereus* AKG1 MTCC9817 and *Bacillus cereus* AKG2 MTCC9818. Phenol containing MSM medium as discussed in *Section 3.1.4.1*, was used for growth (at 37 °C and 120 rpm shaking) and maintenance of both the strains. The pH values in the culture media were initially adjusted to 7.0 and 7.5 using NaOH (1*N*) and HCl (1*N*) solutions for the strains AKG1 and AKG2 respectively; the optimum growth conditions for the respective strains as reported in **Chapter 2.**

3.1.4.3. Analysis of Cell and Substrate Concentration

Cell concentration in the sample was analyzed by measuring the optical density (OD) at 600 nm using UV-vis spectrophotometer (Perkin Elmer, lamda 35, USA) with the culture medium as reference. Samples were withdrawn at regular intervals and centrifuged at 8000 rpm for 15 min to remove the cell debris. The supernatants were filtered through a Millipore filter paper (0.2 µm). The filtrate was analyzed for residual phenol concentration at room temperature with a mobile phase of acetonitrile (80 %): water (20 %) at a flow rate of 0.8 mL min^{-1} by HPLC (High Performance Liquid Chromatography) (ProSTAR, Varian) equipped with a UV–vis detector and C18 column (particle size 7 µm, length 15 cm and diameter 6.4 mm). An aliquot of 20 µl of the filtrate was injected and analyzed using UV-vis detector at wave length of 280 nm for detection of phenol.

3.1.4.4. Batch Biodegradation Study

All the biodegradation experiments were carried out in batch mode in 250 mL Erlenmeyer flasks, containing 100 mL MSM media, 1 mL of cell suspension (OD_{600} 0.017~0.023), yeast extract (3 g L^{-1}) as inducer to increase the growth rate and appropriate amount of phenol as substrate. The culture medium was incubated at 37 °C under shaking condition (120 rpm). The initial concentration of phenol in the culture medium was varied from 100 to 2000 mg L^{-1} with an interval of 100 mg L^{-1}. The initial pH of the medium was adjusted to 7.0 for medium containing strain AKG1 and 7.5 for medium containing strain AKG2; the optimum growth conditions for the respective strains as determined in **Chapter 2**. Samples were withdrawn at regular intervals, centrifuged (8,000 rpm, 15 min) and filtered. The filtrates were analyzed for residual phenol concentration as discussed in *Section 3.1.4.3*.

The chemical oxygen demand (COD) of the supernatant sample, a measure of organic strength of wastewater, was determined by the dichromate method (closed reflux, titrimetric method) (APHA, 1998). 2.5 ml of the supernatant, after proper dilution, was added to the digestion solution (0.01667 M potassium dichromate) followed by sulfuric acid reagent. The whole mixture was digested at 150 °C for 2 h. Ferroin indicator (0.05 mL) was added to the digested mixture cooled at room temperature for titration with standardized 0.01 M ferrous ammonium sulfate (FAS). The end point is a sharp color change from blue-green to reddish brown. The COD value was calculated as mg O_2 L^{-1} using the equation, $COD = \frac{(A-B) \times M \times 8000}{mL\ sample}$, where, A is the FAS used for blank (mL), B the FAS used for sample (mL), M the molarity of FAS and the factor 8000 is the milli-equivalent weight of oxygen × 1000 mL L^{-1}. The data presented here are the arithmetic average of the results obtained from the two repeated degradation experiments under identical conditions.

3.1.4.5. Phenol Degradation Kinetics

In the present study, to represent the degradation kinetics of phenol, several available kinetics models, such as (Haldane model, Yano model, Aiba model, Edward model and Webb model) were fitted to the experimental data obtained from the batch degradation experiments (described in *Section 3.1.4.4*) in order to select the suitable model(s). The degradation rate, q (h^{-1}) for those models are represented in Table 3.1.1. Where, S_0 is

the initial substrate concentration (mg L^{-1}), q_{max} the maximum degradation rate (h^{-1}), K_S the substrate-affinity constant (mg L^{-1}), K the constant in Yano and Webb models (mg L^{-1}) and K_I is the substrate-inhibition constant (mg L^{-1}). A larger K_I value indicates that the culture is less sensitive to substrate inhibition (Webb, 1963). The degradation rate, q was determined from the gradient of a semi-logarithm plot of substrate concentration, S versus time for each initial substrate concentration, S_0 investigated. From the values of q vs. S_0, the values of the kinetic parameters for various models were obtained using non-linear regression analysis in MATLAB 7.0©.

Table 3.1.1. Various models for degradation kinetics.

Model	Equation	Reference
Haldane	$q = \frac{q_{max} S_0}{K_S + S_0 + \frac{S_0^2}{K_I}}$	(Haldane, 1965)
Yano	$q = \frac{q_{max} S_0}{K_S + S_0 + \frac{S_0^2}{K_I}\left(1 + \frac{S_0}{K}\right)}$	(Yano et al., 1966)
Aiba	$q = \frac{q_{max} S_0}{K_S + S_0} \exp\left(\frac{-S_0}{K_I}\right)$	(Aiba et al., 1968)
Edward	$q = q_{max} S_0 \left[\exp\left(\frac{-S_0}{K_I}\right) - \exp\left(\frac{-S_0}{K_S}\right)\right]$	(Edwards, 1970)
Webb	$q = \frac{q_{max} S_0 \left(1 + \frac{S_0}{K}\right)}{S_0 + K_S + \frac{S_0^2}{K_I}}$	(Webb, 1963)

3.1.4.6. Phenol Degradation Pathway

Degradation pathway study was carried out with the culture media containing various initial concentrations of phenol (100, 500, 1000, 1500, and 2000 mg L^{-1}). To determine the metabolic intermediates, the samples were taken at regular intervals and filtered through 0.20 µm Nylon 6, 6 membranes (Pall Corporation, India). The collected cells were washed with the buffer solution, KH_2PO_4:K_2HPO_4 (50 mM, pH 7.0), resuspended in the same buffer and sonically disrupted to prepare the crude extracts. The crude extracts thus obtained were separated from the cell debris by centrifugation at 10,000 rpm and 4 °C for 30 min. The reaction mixture (3 mL) containing KH_2PO_4:K_2HPO_4

buffer (50 mM, pH 7.0) and catechol (1 μmol) was equilibrated at 37 °C. Then the cell extract (100 μL) was added to it. To detect catechol-2,3-dioxygenase and catechol-1,2-oxygenase activities, the formation of the reaction products 2HMSA and *cis, cis*-muconate were measured spectrophotometrically (Perkin Elmer, lamda 35, USA) at 375 nm and 260 nm, respectively (Neumann et al., 2004).

3.1.5. Results and Discussion

3.1.5.1. Phenol Degradation Performances by the Isolated Strains

As mentioned in *Section 3.1.4.4*, phenol degradation experiments were carried out with both the strains for a wide range of its initial concentration (100–2000 mg L^{-1} with an interval of 100 mg L^{-1}). Figure 3.1.1 (a, b) shows the phenol degradation profile with time for some of its initial concentrations (100, 500, 1000, 1500, 2000 mg L^{-1}) covering the whole range. It is observed from the figure that in 40 h, strain *B. cereus* AKG1 MTCC9817 is able to degrade 99.1%, 100%, 94.81%, 44.33% and 10.42% phenol and strain *B. cereus* AKG2 MTCC 9818 is able to degrade 81%, 59.05%, 61.82%, 22.71% and 3.19% phenol when initial concentrations of phenol were 100, 500, 1000, 1500, 2000 mg L^{-1}, respectively. The strain AKG2 requires 60 h to degrade 100% phenol when its initial concentration is 500 mg L^{-1}. Thus, the strain AKG1 degrades phenol relatively faster than the strain AKG2. In fact, the time requirement for the complete degradation of phenol with its initial concentration up to 1000 mg L^{-1} in the culture medium remains the same for a specific strain. The difference in growth rates and phenol tolerance characteristics of the strains could be due to their genetic modifications in different environment and different time of exposure. However, the degradation efficiency drastically falls down for the initial phenol concentrations of 1500 and 2000 mg L^{-1}. This is because of the fact that the lag periods for such higher initial concentrations of phenol are much higher due to the inhibitory effect of phenol (Ho et al., 2009 and Wang et al., 2008).

Similar observations can be seen in Figure 3.1.2 indicating percentage COD removal with time for all these concentrations. After 48 h of treatment for initial phenol concentration of 500 mg L^{-1}, the COD removal by AKG1 is the highest (94.11%), whereas AKG2 is able to remove only 61.11%. Within this time period (i.e., 48 h) the highest COD removal by AKG2 is 64.70% when the initial phenol concentration is 1000 mg L^{-1}.

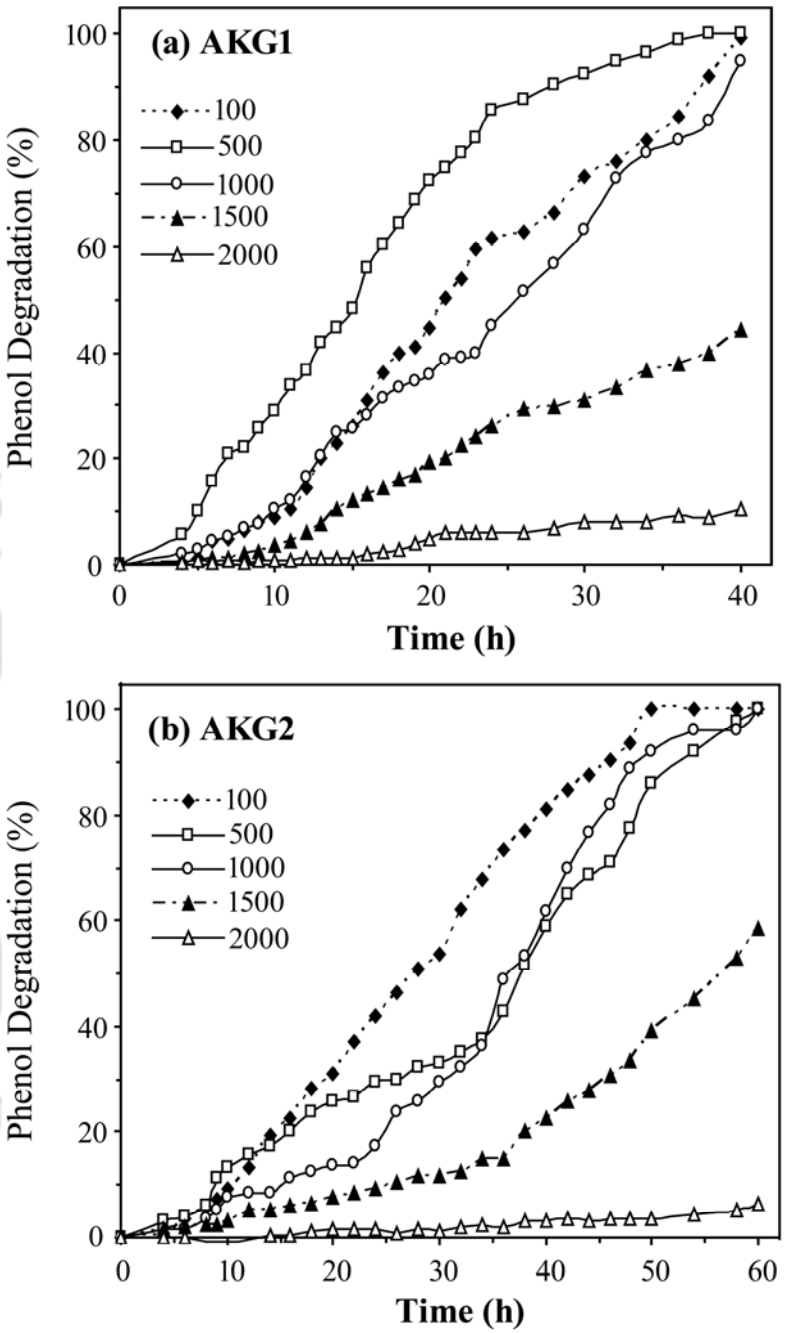

Figure 3.1.1. Phenol degradation profile of (a) AKG1 and (b) AKG2 at various initial phenol concentrations viz. 100, 500, 1000, 1500 and 2000 mg L^{-1}.

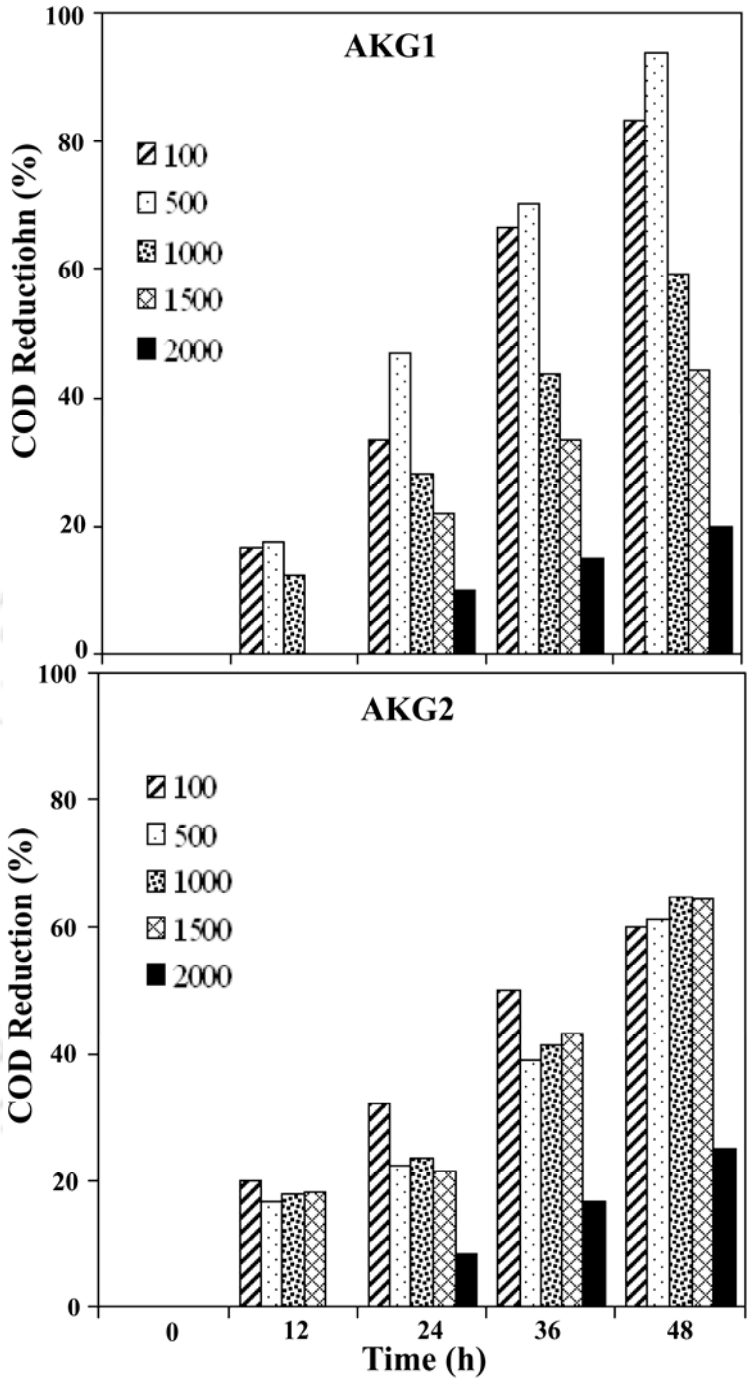

Figure 3.1.2. COD removal by AKG1 and AKG2 at various initial phenol concentrations (viz. 100, 500, 1000, 1500 and 2000 mg L^{-1}).

3.1.5.2. Kinetics of Phenol Degradation

The plot of the negative logarithm of S/S_0 vs. time is a straight line with a slope equal to q, the phenol degradation rate. A typical plot is shown in Figure 3.1.3. The straight line indicates that the degradation rate is first-order after a dead time of about 6-8 h for both the strains. The obtained q values suggest that the phenol degradation rate by AKG1 is almost double of that by AKG2. All the q values were calculated for the various values of S_0 used in the biodegradation study for both the strains. Figure 3.1.4 represents the variations of q with S_0 for both the strains. q_{max} is obtained at initial phenol concentrations of about 800 mg L^{-1} for AKG1 and about 200 mg L^{-1} for AKG2. The degradation rate gradually decreases thereafter with further increase in initial phenol concentration. This is due to the substrate inhibition effect. The values of q_{max} are 0.1075 and 0.0553 for strains AKG1 and AKG2, respectively, confirming the fact that phenol degradation rate by AKG1 is almost double of that by AKG2. In terms of COD removal efficiency at 48 h time period, AKG1 is 1.54 times (AKG1 : AKG2 = 94.11 : 61.11) more effective when initial phenol concentration is 500 mg L^{-1}, whereas, when initial phenol concentration is 1500 mg L^{-1}, AKG2 is 1.44 times more active. Thus from Figure 3.1.1 and 3.1.4, it can be concluded that AKG1 is faster degrading but effective for relatively lower range of initial phenol concentration, i.e. upto 500 mg L^{-1}. On the other hand, AKG2 is slower degrading but more effective for relatively higher initial phenol concentration, i.e. beyond 1000 mg L^{-1}. It may further be observed that for strain AKG1 the degradation rate is very fast when the initial concentration of phenol is 500 mg L^{-1}. About 80% of the degradation is reached pretty quickly and then the rate gradually decreases till about 100% consumption of phenol because of the depletion of phenol (Figure 3.1.1). This type of phenomena is observed because the experiment is carried out in batch mode. Contrarily, for initial concentration of phenol of 100 mg L^{-1} the degradation rate is not as fast as the case of 500 mg L^{-1} but the degradation is almost linear with time till almost complete consumption of phenol (Figure 3.1.1). The differences in the degradation rates can also be seen from the experimental points shown in Figure 3.1.4. The higher degradation rate for initial concentration of phenol of 500 mg L^{-1} than that of 100 mg L^{-1} is due to the higher growth rate for initial concentration of phenol of 500 mg L^{-1} than that of 100 mg L^{-1}, which has already been demonstrated in *Section 2.5.4* of **Chapter 2.**

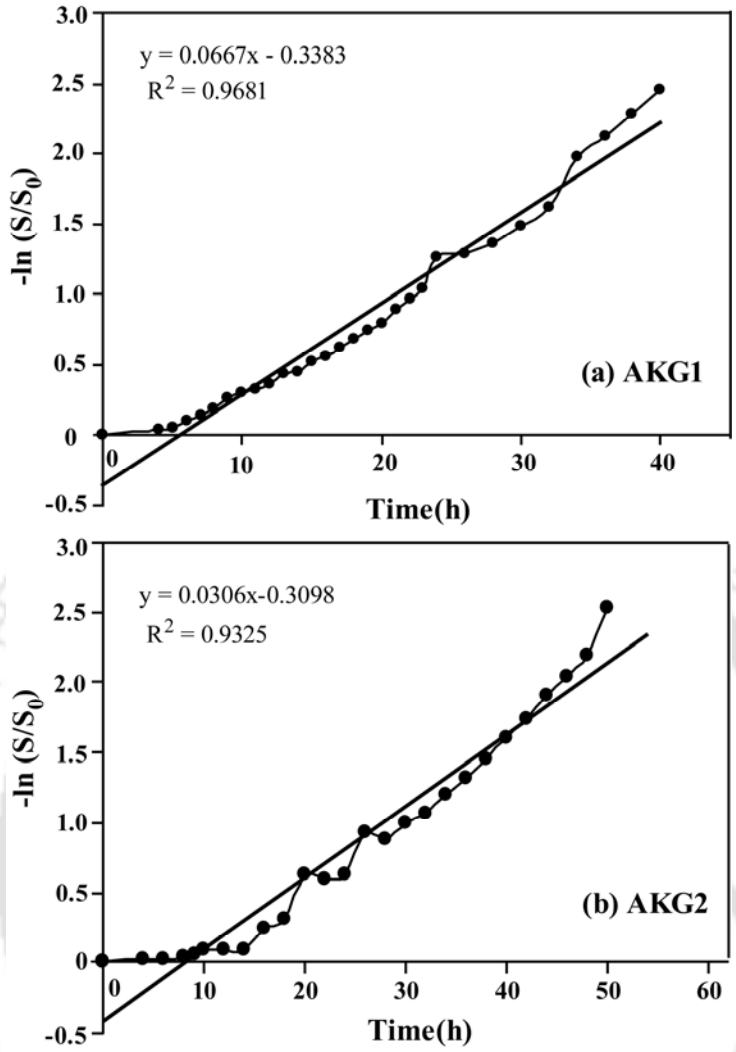

Figure 3.1.3. Typical plot of determining *q* at the initial phenol concentration of 1000 mg L^{-1}.

3.1.5.3. Degradation Modeling

The relation between the degradation rate and the initial substrate concentration is represented by a set of empirically derived rate equations referred to as theoretical models generated to describe the behaviors of a given system. Figure 3.1.4 shows the variations of the degradation rates of strain AKG1 and AKG2 at various initial concentration levels of phenol studied. The figure also shows the predictions of the experimental data by the five different models (Table 3.1.1) used in the work. The experimentally obtained substrate degradation rate values at various initial phenol concentrations were used to fit the above models for estimating the kinetic parameters using the nonlinear regression analysis in Matlab 7.0®.

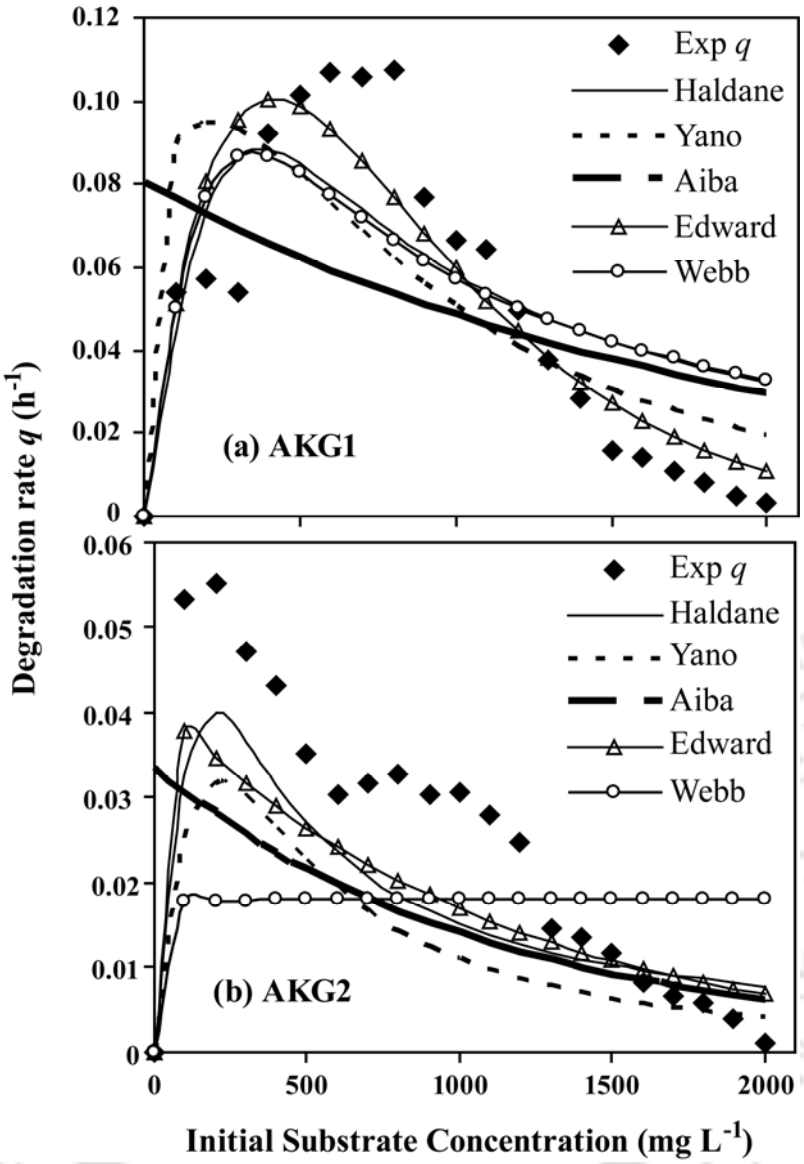

Figure 3.1.4. Experimental and predicted degradation rates at different initial phenol concentrations.

The values of the biokinetic parameters based on the fitting of the above models are reported in Table 3.1.2 for both the strains. The Haldane model predicts the experimental degradation data fairly well for both the strains. But Edward model gives the best fit for strain AKG1 with coefficient of determination, R^2 = 0.838 and SD_{avg} = 0.008 (Table 3.1.2). For strain AKG2, prediction by Yano model with R^2 = 0.865 and SD_{avg} = 0.170 is as good as Haldane model (Table 3.1.2). Similar phenomena of growth characteristics were observed for both the strains which have been discussed in **Chapter 2**.

Table 3.1.2. Degradation kinetics parameters for various models

Strain	Model	q_{max} (h^{-1})	K_S (mg L^{-1})	K_I (mg/L)	K (mg/L)	R^2	SD_{avg}
AKG1	Haldane	2.785×10	59150	2.411	–	0.644	0.013
	Yano	1.105×10^{-1}	22.28	26390	3.366×10	0.595	0.014
	Aiba	9.256×10^{2}	11530	2355	–	0.219	0.019
	Edward	4.701×10^{-1}	407	431.3	–	0.838	0.008
	Webb	5.917×10^{-1}	1002	119.7	1.398×10^{5}	0.616	0.014
AKG2	Haldane	1.635	9.706	3873	–	0.819	0.006
	Yano	1.279×10^{-1}	344.4	1272	2.762×10^{2}	0.865	0.170
	Aiba	1.534×10^{2}	1475	4559	–	0.304	0.009
	Edward	4.151×10^{-2}	125.88	1117	–	0.787	0.006
	Webb	5.900×10^{-3}	17.91	610.8	5.900×10^{-2}	0.103	0.010

The simulated degradation profiles (Figure 3.1.4) by the isolated strains for various initial phenol concentrations were obtained using the estimated biokinetic parameters as input. Estimation of these biokinetic parameters are highly sensitive to their initial guess values required as input during regression analysis. Improper initial guess values may result in inaccurate values of the biokinetic parameters, which in turn affect the accuracy of prediction of the experimental degradation profiles. Therefore, in the present work, sensitivity analysis for the estimation of these parameters have carried out. Here, four different sets of biokinetic parameters (q, K_S and K_I) values were used as initial guesses as indicated in Table 3.1.3. Degradation profiles were simulated applying all the five models using the estimated biokinetic parameters for the different sets of initial guess values. The coefficient of determination (R^2) for each case was determined. The R^2 values, thus obtained by various initial guess considered, are reported in Table 3.1.3. It can be observed from the R^2 values in the table that the Haldane model has the most consistency for both the strains. The Edward model provides a better fit for strain AKG1 as can be seen from Figure 3.1.4 as well as from the R^2 values in Table 3.1.3. The Edward model and the Yano model show the similar R^2 values for the various initial guess values with negligible deviations except the *Case 1*, where the initial guess values have been q <1, K_S <1 and K_I <1 (Table 3.1.3).

Table 3.1.3. Initial guess values and the corresponding coefficient of determination (R^2)

Initial Value	R^2									
	Haldane Model		**Yano Model**		**Aiba Model**		**Edward Model**		**Webb Model**	
	AKG1	*AKG2*	*AKG1*	*AKG2*	*AKG1*	*AKG2*	*AKG1*	*AKG2*	*AKG1*	*AKG2*
Case1: q <1, K_S<1, K_I<1	0.6426	0.8422	−1.551	−1.51	−1.885	−2.108	−1.885	−2.108	0.0951	0.1053
Case 2: q <1, K_S>1, K_I>1	0.6442	0.8193	0.3693	0.8646	0.2188	0.3041	0.8473	0.7872	0.6163	0.1031
Case 3: q =1, K_S>1, K_I>1	0.6436	0.8272	0.5951	0.865	0.215	0.3168	0.6462	0.7872	0.6157	0.2378
Case 4: q >1, K_S<1, K_I<1	0.6437	0.8173	0.5951	0.8639	0.2182	0.1949	0.8378	0.7872	0.192	0.1977

3.1.5.4. Degradation Mechanism

In order to understand the phenol degradation pathway, both *ortho*- and *meta*- cleavage pathways were investigated in the isolated AKG1 and AKG2 strains. Absence of characteristic absorbance of *cis, cis*-muconate at 260 nm indicated that the phenol biodegradation did not follow the *ortho*-cleavage pathway. However, absorbance at 375 nm, which is due to formation of 2-HMSA, confirmed the *meta*-cleavage activity for both the strains. The UV-visible spectrophotometric measurements were carried out for various initial phenol concentrations viz. 100, 500, 1000, 1500 and 2000 mg L^{-1} in order to confirm whether the cleavage pathway was irrespective of its initial concentration or not (Figure 3.1.5). Similar trend was observed for both the strains at various initial concentrations of phenol in the context of formation of 2-HMSA. From Figure 3.1.5, it can be observed that the absorbance at 375 nm first increased linearly with respect to time, then decreases and finally reached a steady state. During the first 10 h of incubation, low absorbance at 375 nm for both the stains implied that this time period was required for the formation of catechol from phenol and induction of adequate enzyme for further degradation. Once catechol was formed, degradation process was channeled exclusively via *meta*-pathway by both the strains.

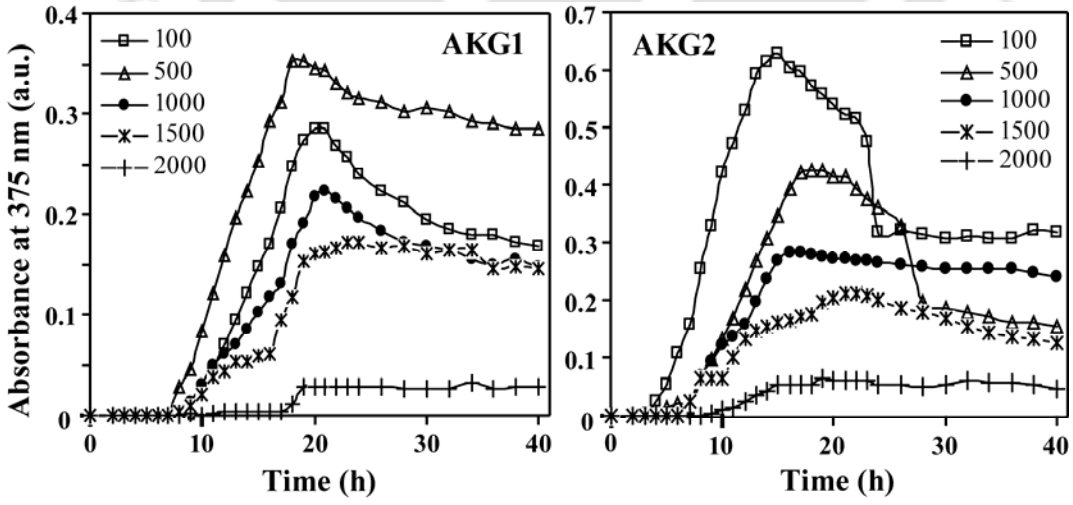

Figure 3.1.5. Absorbance of cell extract at 375 nm for various initial phenol concentrations (mg L^{-1}) in AKG1 and AKG2, respectively.

When the activities of the strains were compared at various phenol concentrations, AKG1 demonstrated maximum 2-HMSA accumulation at initial concentration of 500 mg L^{-1} (AKG1 showed highest degradation at ~800 mg L^{-1} phenol) whereas the same was observed at 100 mg L^{-1} in AKG2 (AKG2 showed highest degradation at ~200 mg L^{-1} phenol). Moreover, for a constant initial phenol concentration of 1000 mg L^{-1}, accumulation of 2-HMSA was low by strain AKG1 than AKG2 (Figure 3.1.6a); although AKG1 showed higher phenol degradation rate than AKG2. It could be an indirect evidence of stability of the active enzyme in the strains. There could be the presence of relatively stable catechol-2,3-oxygenase, along with relatively weak phenol hydroxylase, in AKG2. On the other hand, stable phenol hydroxylase could be present with weak catechol-2, 3-oxygenase in AKG1 (Ali et al., 1998).

Interestingly, an additional peak at 292 nm was observed in case of AKG1 during pathway detection (Figure 3.1.6b). This spectral characteristics are consistent with those reported for 4-oxalocrotonate (Adams and Ribbons, 1988). So, it is predictable that, in case of the strain AKG1, enzyme 2-hydroxymuconic semialdehyde dehydrogenase (HMSD), quantitatively converts HMSA into 4-oxalocrotonate. In case of the strain AKG2, absence of 4-oxalocrotonate, indirectly indicates the presence of enzyme 2-Hydroxy-6-oxohepta-2,4dienoate hydrolase (HODH), which converts 2-HMSA into 2-oxopent-4-enoate. Presence of toxic intermediate compound 4-oxalocrotonate may be the reason for low sustainability of the strain AKG1. The subsequent steady values of the absorbance possibly indicates that the rate of formation of 2-HMSA is equal to its rate of conversion into the next level of compounds.

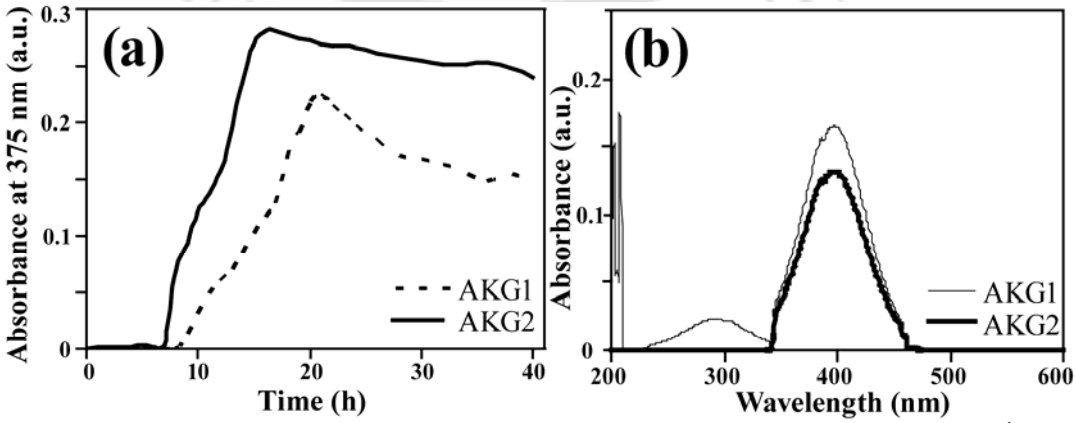

Figure 3.1.6. (a) Absorbance at 375 nm for initial substrate concentrations 1000 mg L^{-1}. (b) UV-spectral data at t = 18 hr when initial substrate concentration is 1000 mg L^{-1}

3.1.6. Conclusions

The two isolated strains AKG1 and AKG2 were able to degrade phenol efficiently at varying initial phenol concentration of 100–1000 mg L^{-1}; although the degradation efficiency was greatly affected at phenol concentrations of 1500 mg L^{-1} or more. The maximum degradation rate (q_{max}) was obtained at initial phenol concentrations of about 800 mg L^{-1} and 200 mg L^{-1} for AKG1 and AKG2, respectively. The Haldane model predicted the experimental degradation data for both the strains fairly well. The strains were found to follow the *meta*-cleavage pathway through formation of 2-HMSA as an intermediate product. The strain AKG1 showed lower accumulation of 2-HMSA than AKG2, which might be due to the fact that catechol-2,3-oxygenase enzyme was much weaker in strain AKG1 than phenol hydroxylase.

3.2. BIODEGRADATION OF PETROLEUM WASTEWATER

3.2.1. Introduction

Wastewater from the petroleum refining industries usually contains high concentrations of aliphatic and aromatic petroleum hydrocarbons, some of which being water soluble and highly mobile, can easily reach the drinking water sources downstream from discharges causing severe health hazards, in addition to the problem of malicious odor and taste, even at very low concentrations. In this regard, reduction of the pollutant level in the petroleum wastewater to environmentally tolerable limits, prior to being released into the environment, is a challenging issue.

Recently, biodegradation of industrial wastewater such as petroleum refinery effluents has emerged as a potential alternative to the conventional physicochemical methods. As the microbial degradation is a complicated process, development of superior bioremediation process needs proper understanding of chemical and bio-chemical processes involved in the transformation of the pollutants (Calvo et al., 1997; Algappan and Cowan, 2004). Hence, having the efficient phenol biodegradation capabilities of the isolated *B. cereus* AKG1 MTCC9817 and *B. cereus* AKG2 MTCC9818 been demonstrated (discussed in **Chapter 2**) and their phenol degradation pathway elucidated (discussed in **Section 3.1**), we were further interested to investigate the efficacy of these strains for the treatment of real petroleum wastewater.

3.2.2. Literature Review

The complex phenomenon of bioremediation becomes further complicated in case of a petroleum wastewater because a real petroleum wastewater consists of numerous components of varying toxicity levels. Among many petroleum hydrocarbons, biodegradation of individual components like phenol, benzene, hexadecane, xylene and toluene have been well documented in the literature (Singleton, 1994; WHO, 1994; Mahajan, 1989). However, unlike controlled laboratory experiments in which measurements can usually be interpreted easily, a 'cause-to-effect' relationship is often difficult to be established from real wastewater studies. Thus, laboratory treatments to remediate pollutants have been more efficient than that of a scaled-up real field situation, where critical parameters are more difficult to control (Tumbasa et. al., 2004).

Most of the present investigations in this area have focused on a restricted number of pollutants including polyaromatic hydrocarbons, polychlorinated biphenyls, dioxines, pesticides, organochlorine compounds, nitroaromatics, metals, and endocrine disrupting chemicals. Pour et al. (2005) reported the biodegradation of petroleum hydrocarbons in an immobilized cell airlift bioreactor by using soil contaminated with petroleum hydrocarbons as the source of naturally occurring microorganisms. Jin et al. (2006) identified *Zoogloea sp.* from crude oil contaminated sludge having strong ability to degrade lubricating oil. Lohi et al. (2008) treated diesel fuel contaminated wastewater aerobically in a three-phase fluidized bed reactor under unsteady and steady state; while Wang et al. (2007) studied degradation characteristics for pentyl amine and aniline by isolated *Pseudomonas sp.* PN1001. Gargouri et al (2011) studied the degradation of crude oil and hydrocarbon-contaminated wastewater by microbial consortium.

Availability of the state-of-art analytical instruments such as GC/MS or LC/MS-MS have now made it possible to detect the pollutants present in the wastewater, their metabolic fate (Tumbasa et. al., 2004) downstream after the microbial treatment and composition analysis (Hilpert et al., 1978) of various components present before and after treatment. However, till date, detailed information on the microbial degradation behavior of real petroleum wastewater, including the composition analysis of the wastewater before and after treatment, is not available in the literature. Even, such information available on the synthetic or simulated petroleum wastewater is also scant.

3.2.3. Outline of the Research Work

1) Biodegradation of petroleum wastewater collected from two origins, namely oil refinery site and oil exploration site, by the isolated strains *B. cereus* AKG1 MTCC9817 and *B. cereus* AKG2 MTCC9818 in batch culture have been investigated.
2) Degradation performances have been analyzed through the measurements of chemical oxygen demand (COD), total organic carbon (TOC), biological oxygen demand (BOD) and ammonium nitrogen.
3) Fate of the petroleum wastewater has been investigated through mass spectrometric (LC-MS-MS) analysis of the biodegradation products.
4) Finally, an attempt has been made to provide some insight on the bacterial membrane adaptation towards such wastewater samples.

3.2.4. Experimental Section

3.2.4.1. Chemicals and Culture Medium

The details of chemicals and culture medium have been described in *Section 2.4.1* in **Chapter 2**.

3.2.4.2. Microorganism and Culture Conditions

The isolated strains AKG1 and AKG2 were grown in phenol containing MSM medium as discussed in *Section 3.1.4.2* of **Chapter 3**.

3.2.4.3. Batch Biodegradation Study

To carry out the biodegradation of the petroleum wastewater, 100 mL of pre-autoclaved wastewater samples were incubated with the isolated strains (OD=0.8) in conical flasks at their optimum temperature 37 °C at 120 rpm for the desired period of time. Strains AKG1 and AKG2 were added in the ratio of 1:1 in the case of co-culture. To determine the effect of external nitrogen sources on microbial treatment, parallel batches of biodegradation were also performed by adding 3% yeast extract (organic nitrogen) or 0.3 % (w/v) ammonium sulfate (inorganic nitrogen) in the wastewater samples. During the experiment, 2 mL of samples were withdrawn at regular intervals and centrifuged (8000 rpm, 15 min) to remove cell debris. The supernatant was filtered through a 0.2 μm filter paper wherever necessary. Supernatant was analyzed to determine the COD, BOD, TOC and NH_4^+−N. The above mentioned parameters were measured according to standard methods (APHA, 1998). Multi parametric water quality analysis of the refinery wastewater before and after microbial treatment in packed bed has been made by Multi Parameter Water Quality Sonde**.**

3.2.4.4. Analysis of COD

The COD of the samples was measured as described in *Section 3.1.4.4* in **Chapter 3**.

3.2.4.5. Analysis of TOC

TOC content was measured by TOC analyzer (O.I. Analytical Aurora, Model 1030).

3.2.4.6. Analysis of BOD

Dissolved oxygen (DO) in the sample was measured (DO electrode, Cheminco, India) and BOD (mg L^{-1}) was calculated as, $BOD = [(D_1 - D_2) - SV_S]/P$; where D_1= initial DO of diluted sample, D_2= final DO of diluted sample, S= oxygen uptake of seed, V_S= volume of seed in the respective seed bottle and $1/P$ = dilution factor.

3.2.4.7. Analysis of Ammonia Nitrogen (NH_4^+−N)

NH_4^+−N was measured by the standard phenate method (APHA, 1998). Briefly, phenol (1 mL), sodium nitroprusside (1 mL) and oxidizing solution (4:1 alkaline citrate and sodium hypochlorite, 2.5 mL) were added to 25 mL sample. Intensely blue compound, indophenol, was formed during the reaction. The mixture was kept in dark at room temperature for 1 h for color development before recording absorbance at 640 nm.

3.2.4.8. Analysis of Phenolic Compounds and Biodegradation Products

Concentrations of phenolics were analyzed by High Performance Liquid Chromatograhy (HPLC, ProSTAR, Varian) equipped with a UV–visible detector and C18 column (particle size 7 µm, length 15 cm and diameter 6.4 mm). The filtrate from the supernatant of the sample was analyzed for its contents by LC-MS and MS-MS mode using LC–MS instrument of Waters Q-Tof Premier with a mobile phase of acetonitrile (80 %): methanol (20 %) at a flow rate of 0.8 equipped with a C18 reverse phase column (particle size 1.7 µm, 1×55 mm column). An aliquot of 25 µl of the filtered sample was injected and analyzed. The run was carried out using electrospray ionization (ESI) interfaces in negative ion modes. The MS spectra obtained were analyzed by NIST 08 MS (Demo).

3.2.4.9. Analysis of Bacterial Membrane Adaptation by Fourier Transform Infra Red (FT-IR) Spectroscopy

Bacterial strains AKG1 and AKG2, grown in presence of phenol or the wastewater samples, were harvested by centrifugation (8000 rpm for 10 min) and bacterial membrane was isolated following previously reported method (Bligh and Dyer, 1959). Briefly, bacterial pellet was re-suspended in phosphate buffer saline (PBS, pH 7.0). To 1 mL of bacterial suspension, 3.75 mL chloroform-methanol mixture (1:2, v/v) was added and vortexed. Then 1.25 mL chloroform was added to the mixture and mixed well. Finally, 1.25 mL MiliQ water was added and mixed well. The resulting solution was centrifuged at 2000 rpm for 5 min at room temperature to give a two-phase system (aqueous top, organic bottom). Bottom phase were recovered and dried by lyophilization for further FT-IR analysis. FT-IR spectra were recorded with FT-IR spectrometer (Perkin-Elmer, PE-RXI) from 4000 to 400 cm^{-1}. A background spectrum was measured for pure KBr.

3.2.5. Results and Discussion

3.2.5.1. Removal of COD from the Wastewater

COD, widely used to determine the level of pollutants present in a particular wastewater sample, is measured by the amount of a specified oxidant that reacts with the sample under controlled conditions and expressed in term of its oxygen equivalence. The COD level was measured to be 5920 mg L^{-1} and 6400 mg L^{-1} in the wastewater sample from oil refinery site (Sample I) and oil exploration site (Sample II), respectively. Figures 3.2.1 shows the percentage of COD removed by the isolated strains (AKG1 and AKG2) from influent wastewater samples in the absence of any external nitrogen source. It is worth mentioning here that during the degradation process, substrate can be used up for (i) the generation of a product of different structure (ii) the generation of volatile compounds and/or gases like CO_2, CH_4 etc, and (iii) the growth of microbes. The later two cases only can lead to the removal of COD.

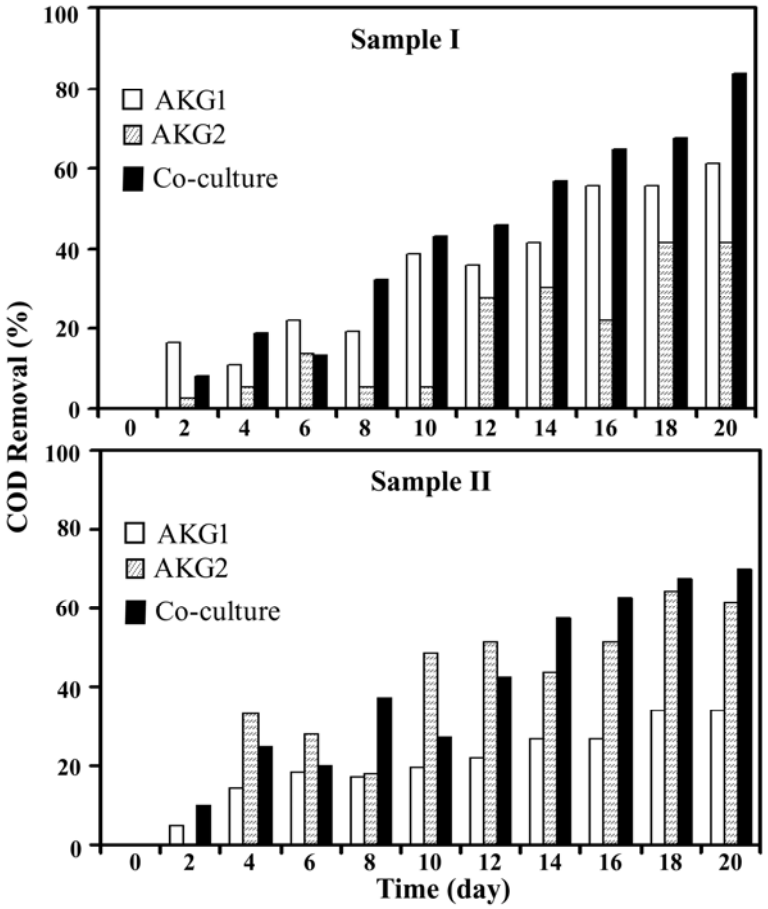

Figure 3.2.1. COD removal from wastewater samples (Sample I and II) by AKG1, AKG2 and co-culture in absence of external nitrogen source.

From the Figure 3.2.1, it can be observed that the COD removal fluctuated in the initial period (up to 10th day) of the treatment, especially in case of AKG2 and co-culture system. However, the COD was removed at a stable rate afterwards for all the three systems (AKG1, AKG2 and co-culture). It is important to mention here that the unstable nature of COD reduction has also been reported in earlier studies (Feng et al., 2008; Calheiros et al., 2009; Ji, 2009). As clear from the figure, co-culture system was the most efficient in removing the COD level from the wastewater samples. After 20 days of biodegradation, co-culture reduced the COD level by 83.78 % and 70% for Sample I and Sample II, respectively.

Further experiments were carried out in order to investigate the effect of external nitrogen sources on the COD removal efficiency by treating the wastewater sample in presence of yeast extract (organic nitrogen) or ammonium sulfate (inorganic nitrogen). The results for COD reduction after 20 days in various cases were compared and presented in Table 3.2.1. Table 3.2.1 shows that the maximum COD removal was achieved by co-culture system, both in absence and in presence of external nitrogen sources. Co-culture system removed 83.78% COD from Sample I in absence of external nitrogen source; whereas the value increased to 89.18% and 86.48% in presence of organic and inorganic nitrogen source, respectively. On the other hand, the COD removal by co-culture in Sample II increased to 79.5% and 72.5% in presence of organic and inorganic nitrogen source, respectively, as compared to that of 70% in absence of external nitrogen source. Among the pure cultures, AKG1 showed better COD removal from Sample I while AKG2 was better in COD reduction from Sample II. The lowest COD removal (34.14%) was observed in Sample II by AKG1 in absence of external nitrogen source; whereas the highest COD removal (89.18%) was obtained in Sample II by the co-culture in presence of yeast extract as external nitrogen source.

Table 3.2.1: Comparison of the COD removal (%) performance of the different systems.

	COD removal (%)					
	Without eternal N_2 supplement		**Organic N_2 supplement** (Yeast)		**Inorganic N_2 supplement** (Ammonium Sulfate)	
	Sample I	*Sample II*	*Sample I*	*Sample II*	*Sample I*	*Sample II*
Free AKG1	61.11	34.14	69.44	51.21	66.66	41.46
Free AKG2	41.66	61.53	55.55	69.23	47.22	64.10
Co-culture	83.78	70	89.18	79.5	86.48	72.5

3.2.5.2. Removal of TOC from the Wastewater

The initial TOC level before the treatment was measured to be 1550 mg L^{-1} and 1680 mg L^{-1} in the wastewater Sample I and Sample II, respectively. Figure 3.2.2 shows the TOC reduction in wastewater samples during the 20 days of treatment in absence of external nitrogen source. The TOC removal from the wastewater samples followed similar trend as that of COD removal and increased gradually with time. Among the three systems, co-culture was found to be most efficient in TOC reduction. The biodegradation of the wastewaters by AKG1, AKG2 and co-culture was also carried out in presence of external nitrogen sources and the TOC reduction in various cases are compared in Table 3.2.2. It can be seen from the Table 3.2.2 that the supply of external nitrogen source, overall, increased the TOC removal irrespective of the culture system; although a small reduction in TOC removal by co-culture was observed only in case of Sample I. The maximum reduction (84.54%) of TOC level in Sample I was obtained by co-culture system in presence of yeast extract, as compared to that of 77.28% and 83.45% in presence of ammonium sulfate and in absence of external nitrogen sources, respectively. On the other hand the highest TOC removal (75.95%) from Sample II was observed in case of the co-culture system in presence of yeast extract; while the value was 70% and 54% in presence of ammonium sulfate and in absence of external nitrogen sources, respectively.

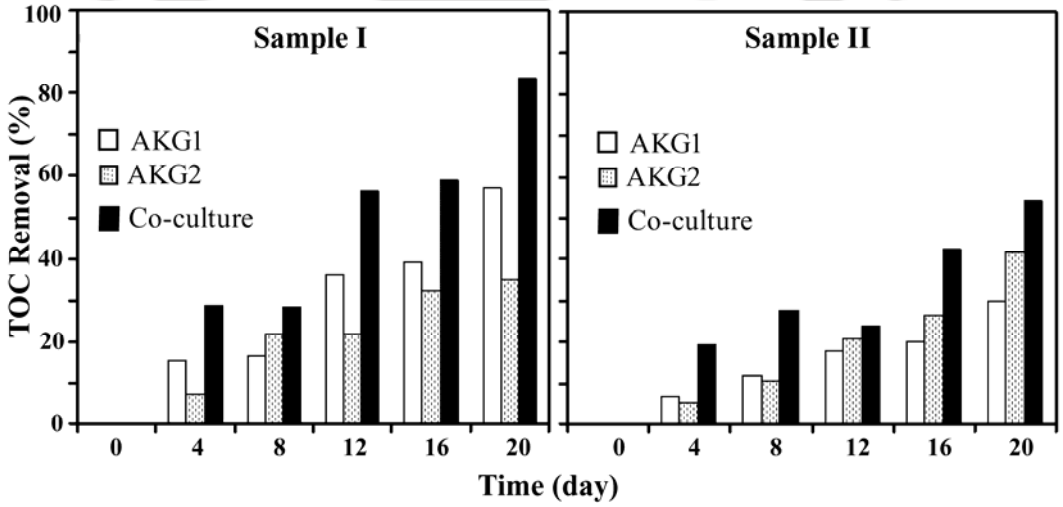

Figure 3.2.2. TOC removal from wastewater samples (Sample I and II) by AKG1, AKG2 and co-culture in absence of external nitrogen source.

Table 3.2.2: Comparison of the TOC removal (%) performance of the different systems.

	TOC removal (%)					
	Without eternal N_2 supplement		**Organic N_2 supplement** (Yeast)		**Inorganic N_2 supplement** (Ammonium Sulfate)	
	Sample I	*Sample II*	*Sample I*	*Sample II*	*Sample I*	*Sample II*
Free AKG1	57.12	30.00	65.45	48.00	63.51	35.00
Free AKG2	34.68	41.59	45.52	55.99	39.77	45.00
Co-culture	83.45	54.00	84.54	75.95	77.28	70.00

3.2.5.3. Analysis of BOD in the Wastewater

During the microbial treatment of the petroleum wastewater, the changes in the BOD level of the samples were also investigated and the results are sown in Figure 3.2.3. It was observed that, in addition to the COD removal, there was a prominent increase in BOD level of the wastewater. The initial BOD values of the petroleum wastewaters were 180 mg L^{-1} (Sample I) and 420 mg L^{-1} (Sample II), respectively. The BOD values increased to as high as 672 mg L^{-1}, 524 mg L^{-1} and 861 mg L^{-1} for sample I after 20 days of microbial treatment by AKG1, AKG2 and co-culture, respectively. On the other hand, the values reached to 997 mg L^{-1}, 1237 mg L^{-1} and 1532 mg L^{-1} for sample II after treatment with AKG1, AKG2 and co-culture, respectively.

It may be mentioned here that, according to Sun et al. (2008), the BOD/COD ratio is the index of biodegradability performance. A BOD/COD ratio of 0.9~1.0 is generally considered as the cut-off point for the biodegradable wastewater (Contreras et. al., 2003; Gaetano J.C. 1999). The extremely low initial BOD/COD ratio (0.030 in Sample I and 0.065 in Sample II) in the petroleum wastewater implied that petroleum wastewater was difficult to be degraded biologically. However, after microbial treatment by the co-culture of the isolated strains, the BOD/COD ratio increased to 0.89 in Sample I and to 0.79 in Sample II indicating a significant improvement of biodegradability of the wastewater samples. The increase in BOD/COD ratio could be due to the decomposition of the complex and more toxic molecules (difficult to be digested by the microbes) into simpler and less toxic ones (easily digestible by the microbes). As the isolated strains gradually acclimatize at high phenol concentration, bacterial cell membrane becomes more resistant and the survived cells starts to

synthesize enzymes required for metabolizing the wastewater contents (Yang and Humphrey, 1975).

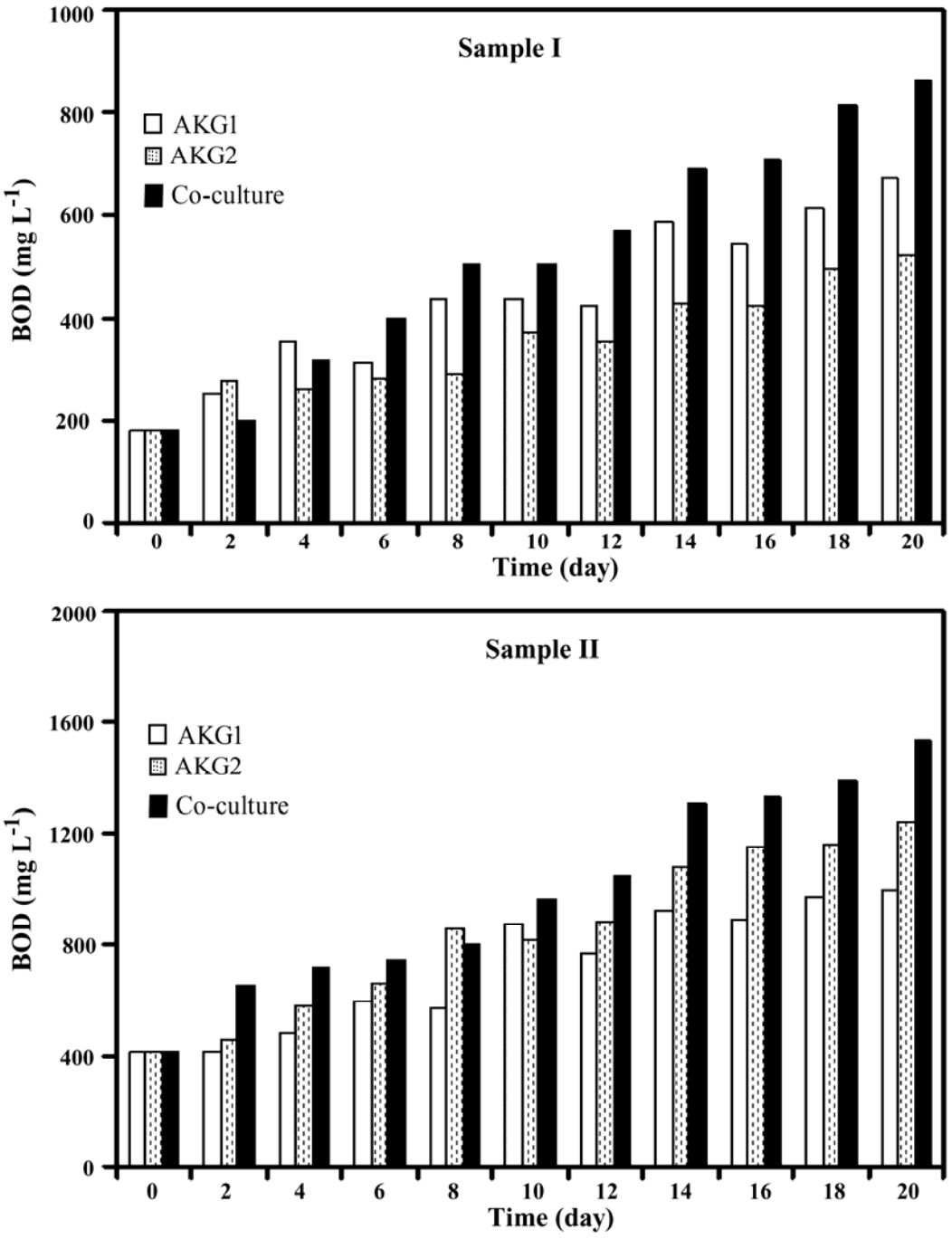

Figure 3.2.3. The BOD level in the wastewater samples during the microbial treatment by AKG1, AKG2 and the co-culture.

3.2.5.4. Removal of Ammonium Nitrogen (NH_4^+−N) from the Wastewater

Figure 3.2.4 shows the amount of NH_4^+−N in the wastewater samples I and II during the microbial treatment. It is clear from the figure that the treatment reduced the NH_4^+−N level in the wastewaters significantly. The amount of NH_4^+−N removal under various conditions is listed in Table 3.2.3. The maximum removal NH_4^+−N (68.12%) from Sample I was obtained by co-culture treatment; whereas that of Sample II (82.46%) was observed in case of AKG2 treatment. Strain AKG2 was isolated from sample II wastewater (exploration site) and it might have adapted itself better to the A-N environment than that by the strain AKG1. Therefore, AKG2 must have shown better performance than the co-culture which contains strain AKG1 also in it.

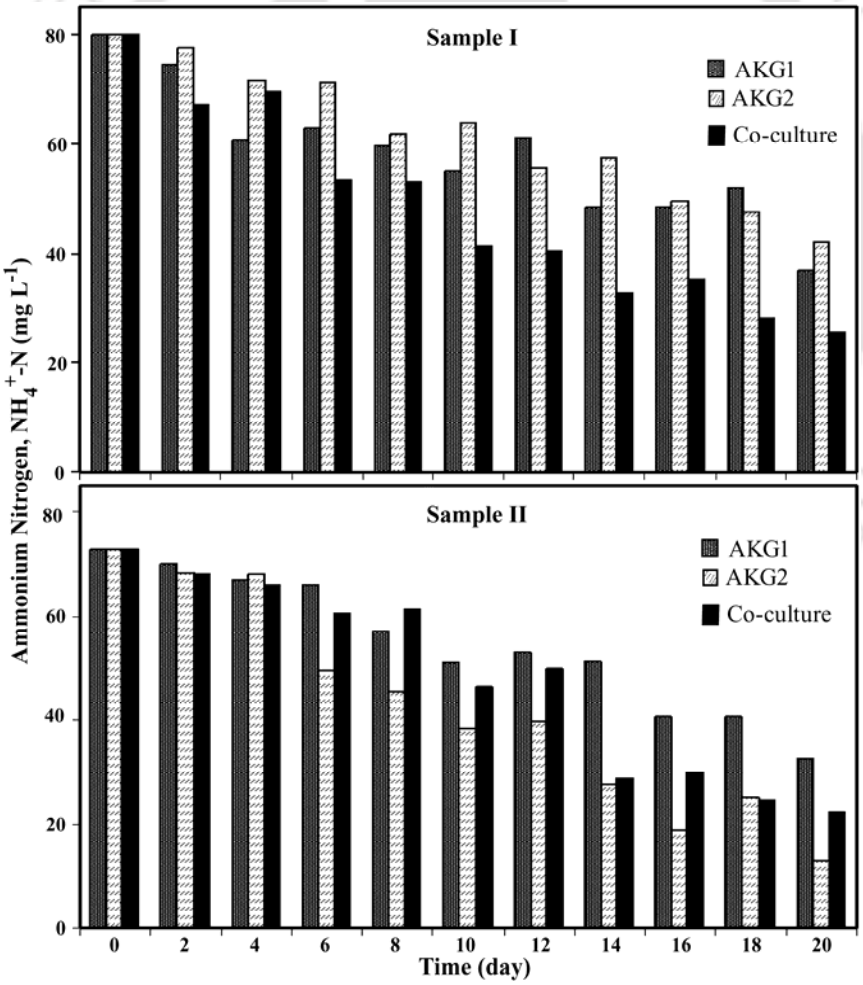

Figure 3.2.4. The ammonium nitrogen (NH_4^+–N) level in the wastewater samples during the microbial treatment by AKG1, AKG2 and the co-culture.

Table 3.2.3: Overall performance by various systems for NH_4^+−N removal

	Reduction of ammonium-nitrogen (%)		
	AKG1	*AKG2*	*Co-culture*
Sample I	54	47.5	68.12
Sample II	55.34	82.46	69.45

3.2.5.5. Removal of Phenolic Compounds from the Wastewater

Phenol and other phenolic derivatives are the major organic compounds usually present in petroleum refinery wastewater and have a direct contribution to the COD level of the wastewater. In the present study, the removal of the phenolic compounds was investigated by measuring their concentration at regular intervals during the microbial treatment of the wastewater samples by co-culture system. The initial concentrations of the phenolic compounds in the wastewater samples were 1543 mg L^{-1} (Sample I) and 1971 mg L^{-1} (Sample II), respectively. Figure 3.2.5 shows the removal of phenolics from Sample I and Sample II by the co-culture of AKG1 and AKG2. After the completion of the microbial treatment for 20 days, the concentrations of the phenolic compounds in Sample I and Sample II were reduced by 57.35% and 45.85%, respectively.

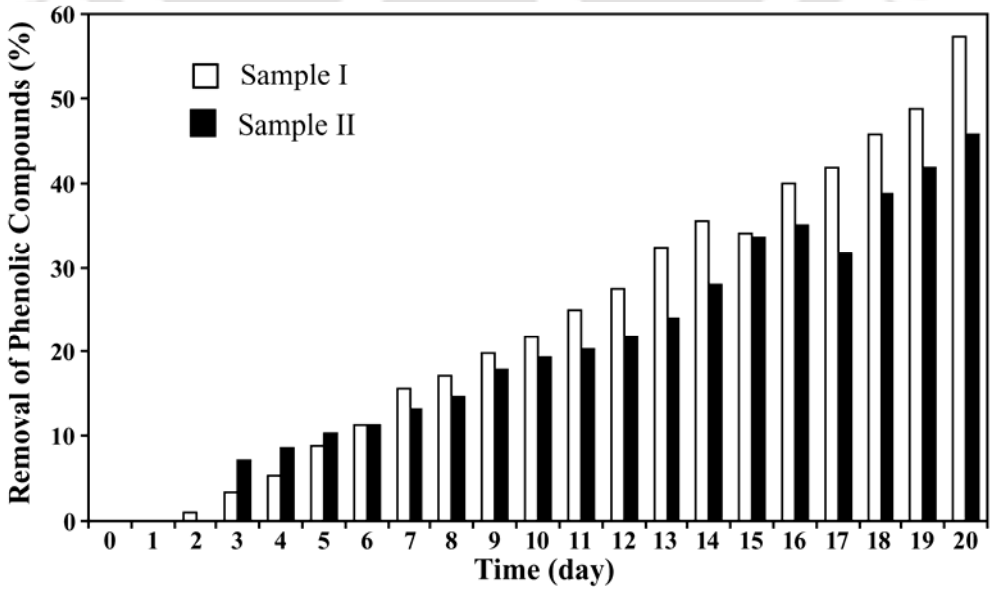

Figure 3.2.5. Phenolic compound removal by co-culture treatment of the wastewater samples.

3.2.5.6. Analysis of Water Quality by UV-absorption Spectroscopy

Both oils and oil products have certain characteristic absorbance in the UV range (Chen et al., 1985; Verner et al., 2000). In general, the aromatic compounds of the oil show the absorbance maxima at the wavelength of 250–260 nm, whereas the alkane components show absorbance in the 215–230 nm wavelength range (Verner et al., 2000). The oil components in the wastewater samples in the present study were assessed qualitatively by UV absorption spectroscopy (Zhao et al., 2006). Both the wastewater samples showed characteristics peaks at 206–215 nm (Figure 3.2.6) indicating the presence of alkanes in both the samples. On the other hand, Sample I also showed a prominent peak around 269 nm confirming the presence of phenolic compounds; although that of the Sample II was not as prominent. Most importantly, Figure 3.2.6 demonstrates that the microbial treatment significantly removed the oil components from both the wastewater samples.

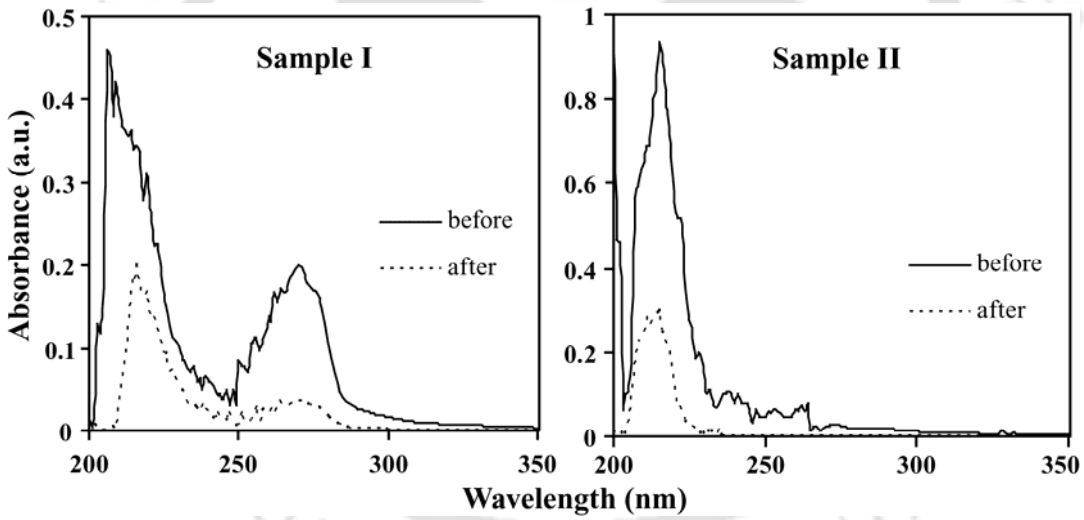

Figure 3.2.6. UV absorption spectra of the wastewater samples (I and II) before and after the microbial treatment.

3.2.5.7. Analysis of the Biodegradation Products

In order to investigate the products of the microbial biodegradation of the wastewaters, samples were collected at specified intervals and, after appropriate dilution ($\times 10^{35}$) and sample preparation, analyzed by liquid chromatography and mass spectroscopy (LC-MS and MS-MS, Waters Q-Tof Premier, US). Figure 3.2.7 represents the liquid chromatographic patterns of the wastewater samples (Sample I and Sample II) at

different stages of the biodegradation using the coculture of the isolated strains AKG1 and AKG2. The results show prominent changes in the chromatograms of both the samples with time. Each peak of chromatogram was further examined by mass spectroscopy (MS) and subsequently analyzed by NIST 08 MS software (Table 3.2.4).

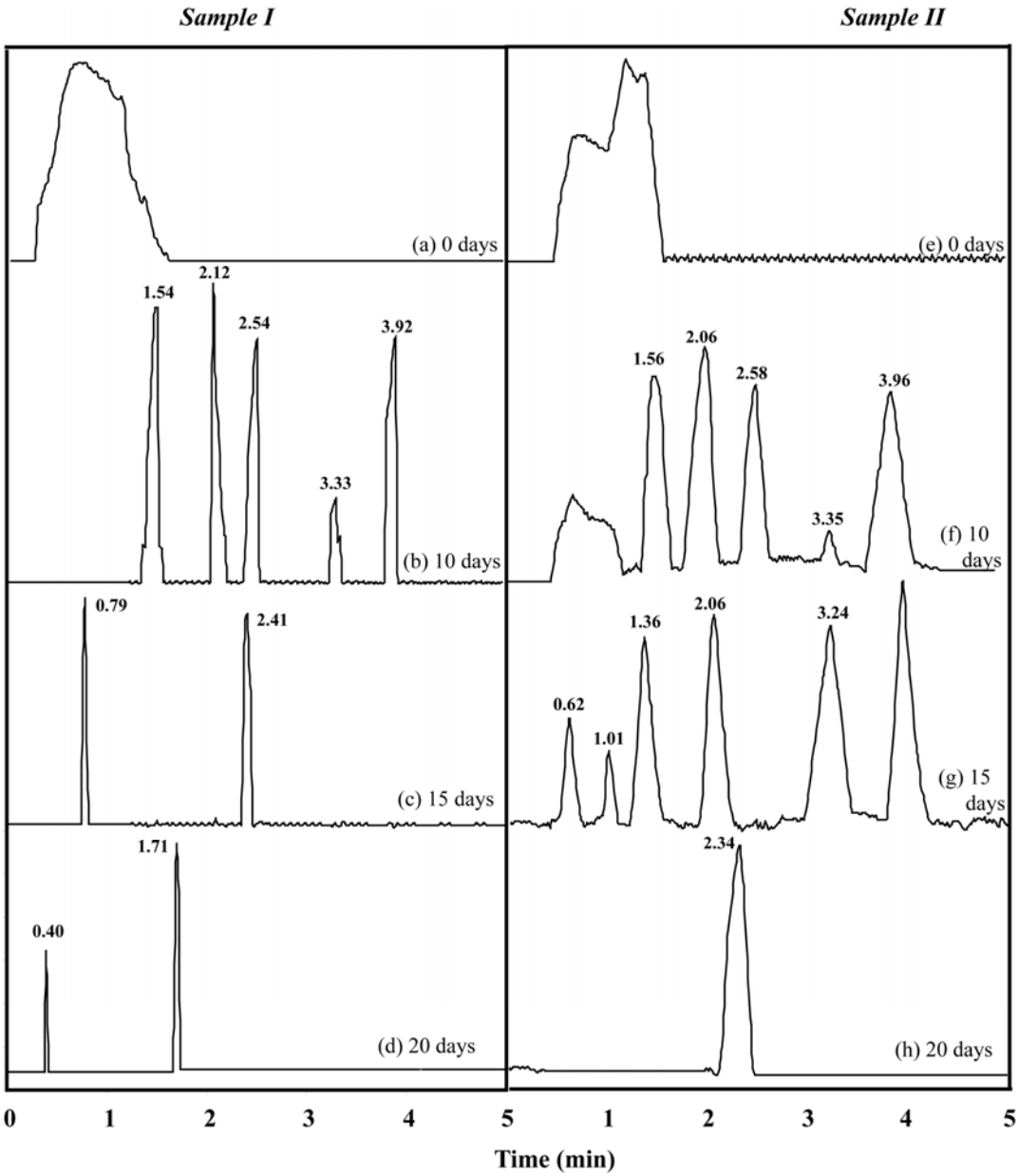

Figure 3.2.7. Liquid chromatographic (LC) patterns of the wastewater samples (I and II) at specified time points (0, 10, 15 and 20 days) during the biodegradation.

On day zero, i.e. at the start of the microbial treatment, both the wastewater samples showed broad liquid chromatographic peak (Figure 3.2.7a and e) indicating the

presence of complex mixture of several compounds in samples; which were further confirmed by the mass spectroscopic data (Figure 3.2.8). However, as the microbial biodegradation of the wastewater samples progressed, the numbers of compounds started to reduce as evident from the less number of peaks (Figure 3.2.7). It can also be observed from the liquid chromatograms after 15 or 20 days (Figure 3.2.7c, d and g, h) of treatment that, in addition to the number of peaks, the elution time of the compounds also decreased. The reduction in the number of peaks as well as the peak area was indicative of the reduction in COD level in the wastewater samples. Moreover, the decrease in the elution time indicated the formation of simpler molecules which could, actually, improve the biodegradability of the wastewater samples.

Overall, the liquid chromatogram of Sample I showed five different peaks (at 1.54, 2.12, 2.54, 3.33, and 3.92 min) on 10^{th} day, two different peaks (at 0.79 and 2.41 min) on 15^{th} day and two different peaks (at 0.40 and 1.71 min) on 20^{th} day of the treatment (Figure 3.2.7a–d). On the other hand, Sample II produced six different peaks (at 0.62, 1.56, 2.06, 2.58, 3.35 and 3.96 min) on day 10, six peaks (at 0.62, 1.01, 1.36, 2.06, 3.24 and 3.96 min) on day 15 and one peak at 2.34 min on day 20 (Figure 3.2.7e–h). The compounds corresponding to each peak in the liquid chromatograms of the wastewater samples, as separated based on the difference in elution time, were further investigated by mass spectroscopy (Figure A3.2.1–A3.2.17). The mass spectra of those compounds were subsequently analyzed by NIST 08 MS (Demo) software in order to predict the probable identification of the biodegradation products. The probable products of the microbial treatment of the wastewater samples are listed in Table 3.2.4. From the Table 3.2.4, it can be predicted that the major biodegradation products of the wastewater Sample I after 20 days of treatment were 4-(phenylamino)-phenol and 2,6-dichlorophenyl-1-acetonitrile. On the other hand, 2-hydroxy-3-(3-methyl-2-butenyl) 1,4-naphthalenedione was the principal biodegradation product of the wastewater Sample II.

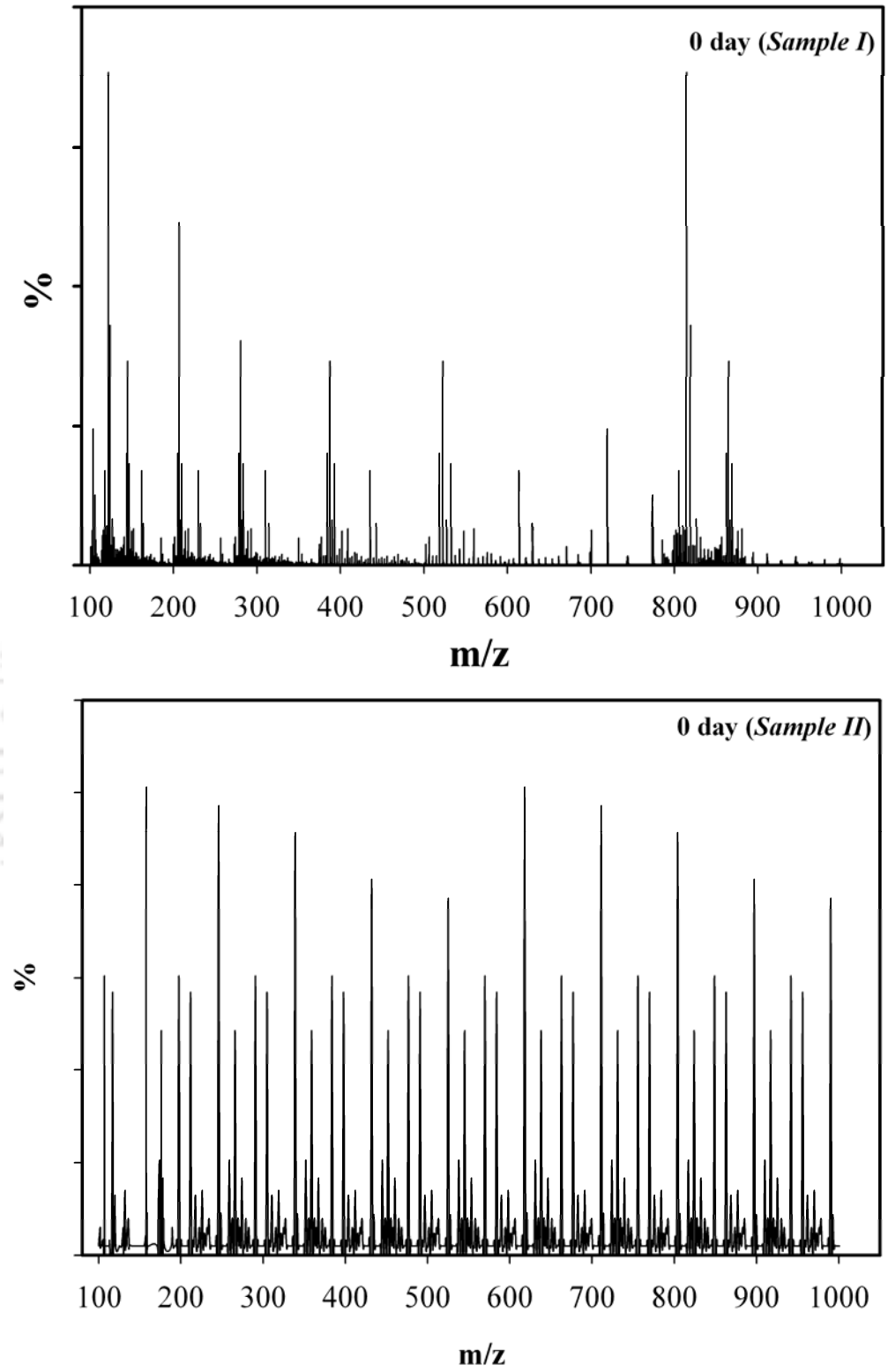

Figure 3.2.8. Mass spectra of the wastewater samples (I and II) at the start (Day 0) of the microbial treatment.

Table 3.2.4: Summary of the mass spectroscopic analysis of the biodegradation products from the wastewater samples.

Treat-ment time	Peak* (min)	*m/z* in mass spectra	Probable compound
Sample I			
10th Day	1.54	100,101,176,178,200,201, 202,203,249 (Figure A3.2.1)	9-(2-nitroethenyl)-anthracene
	2.12	130,141,143,235,237,239, 241,272,274 (Figure A3.2.2)	Hexachloro-cyclopentadiene
	2.54	100,113,126,134,149,163, 174,187,202,211,237,252.	Undetermined
	3.33	104,115,141,169,196,227 (Figure A3.2.3)	N,N-diphenyl-hydrazinecarboxamide
	3.92	115,128,129,217,218,273, 274,275 (Figure A3.2.4)	2,6-bis(phenylmethylene)-cyclohexanone
15th Day	0.79	114,124,141,150,184. (Figure A3.2.5)	2,4-dichloro-benzeneacetonitrile
	2.41	106,128,154 (Figure A3.2.6)	2-ethenyl-naphthalene
20th Day	0.40	185,152,112 (Figure A3.2.7)	4-(phenylamino)-phenol
	1.71	115,149,190 (Figure A3.2.8)	2,6-dichlorophenyl-1-acetonitrile
Sample II			
10th Day	1.56	252,250,254,143,145 (Figure A3.2.9)	2,4-dibromo-phenol
	2.06	139,154,195,230,231,232, 264,265,266,267 (Figure A3.2.10)	2-amino-2',5-dichloro-benzophenone
	2.58	114,170,210,226 (Figure A3.2.11)	3-methyl-N,N-bis(3-methylbutyl)-1-butanamine
	3.35	169,168,196,167,227,170, 197 (Figure A3.2.12)	N,N-diphenyl-hydrazinecarboxamide
	3.96	115,128,129,217,218,273, 274,275 (Figure A3.2.13)	2,6-bis(phenylmethylene)-cyclohexanone
15th Day	0.62	180,182,145,184,147,109,74, 73	Undetermined
	1.01	145,109,175,147,74,177,75,1 11	Undetermined
	1.36	112,152 (Figure A3.2.14)	acenaphthene
	2.06	115,144 (Figure A3.2.15)	naphthalenol
	3.24	130, 132, 131	Undetermined
	3.96	115,128,129,217,218,273, 274,275 (Figure A3.2.16)	2,6-bis phenylmethylene-cyclohexanone
20th Day	2.34	105,149,198,227,242 (Figure A3.2.17)	2-hydroxy-3-(3-methyl-2-butenyl)1,4-naphthalenedione

* Peak position in the liquid chromatogram based on elution time (min).

3.2.5.8. Adaptation of Bacterial Membrane to Wastewater

It is well established that the microorganisms are able to adapt to the presence of toxic organic compounds by using different kinds of adaptive mechanisms (Ramos, 1997). Among them, changes in the fatty acid composition of membrane lipids are the most important for their survival. Generally, to understand the effective membrane surveillance, exopolysaccharides (EPS) present in the cell surfaces are extracted and examined. Proteins and polysaccharides are the major components of EPS (Gao, 2008; Yu, 2007; Liu, 2007). In order to investigate the bacterial adaptation to the wastewater samples in the present study, the EPS from AKG1 and AKG2 grown in presence Sample II and sample I, respectively, was extracted (as described in *Section 3.2.4.8*) and subsequently analyzed by FT-IR. It is important to mention here that the bacterial strains grown in MSM supplemented with phenol as carbon source, thereby already adapted to the phenol environment, were used as the 'control' cells in the FT-IR analysis.

The FT-IR spectra of EPS component of the cell membrane from both the isolated strains, after being grown in presence of phenol or wastewater samples, are shown in Figure 3.2.9. A number of absorption peaks representing the presence of various functional groups on cell surface were observed in the FT-IR spectra. Close inspection of the FT-IR spectra revealed that the absorption peaks in wastewater-exposed bacteria showed shift of bands relative to those observed in case of phenol. The band at 3290 cm^{-1} in phenol treated strains (Figure 3.2.9c,d), which represent the stretching effect of O-H bond, shifted to 3166 cm^{-1} (AKG2 in Sample I, Figure 3.2.9b) and 3243 cm^{-1} (AKG1 in Sample II, Figure 3.2.9a) in presence of wastewater. The peak responsible for –COC– at 1078 cm^{-1} (Figure 3.2.9c,d) also shifted to 1052 cm^{-1} (Figure 3.2.9a,b). Both these band (3290 cm^{-1} and 1078 cm^{-1}) represent the functional groups present in membrane polysaccharides and proteins (Sheng, 2006). Moreover, the band at 1629 cm^{-1}, resulted from C=O and C-N (Amide I) stretching, shifted to 1517 cm^{-1} (Figure 3.2.9b) and 1542 cm^{-1} (Figure 3.2.9a). The band at 1544 cm^{-1}, which is a combination of N-H bending and C-N (Amide II) stretching, shifted to 1359 cm^{-1} (Figure 3.2.9b) and 1450 cm^{-1} (Figure 3.2.9a), respectively. Amide I and Amide II correspond to the functional groups in proteins (Sheng, 2006). The results of FT-IR analysis of bacterial membrane indicated that the polysaccharide and protein components were affected and evolved their structure in order to adapt the toxicity of the wastewater samples.

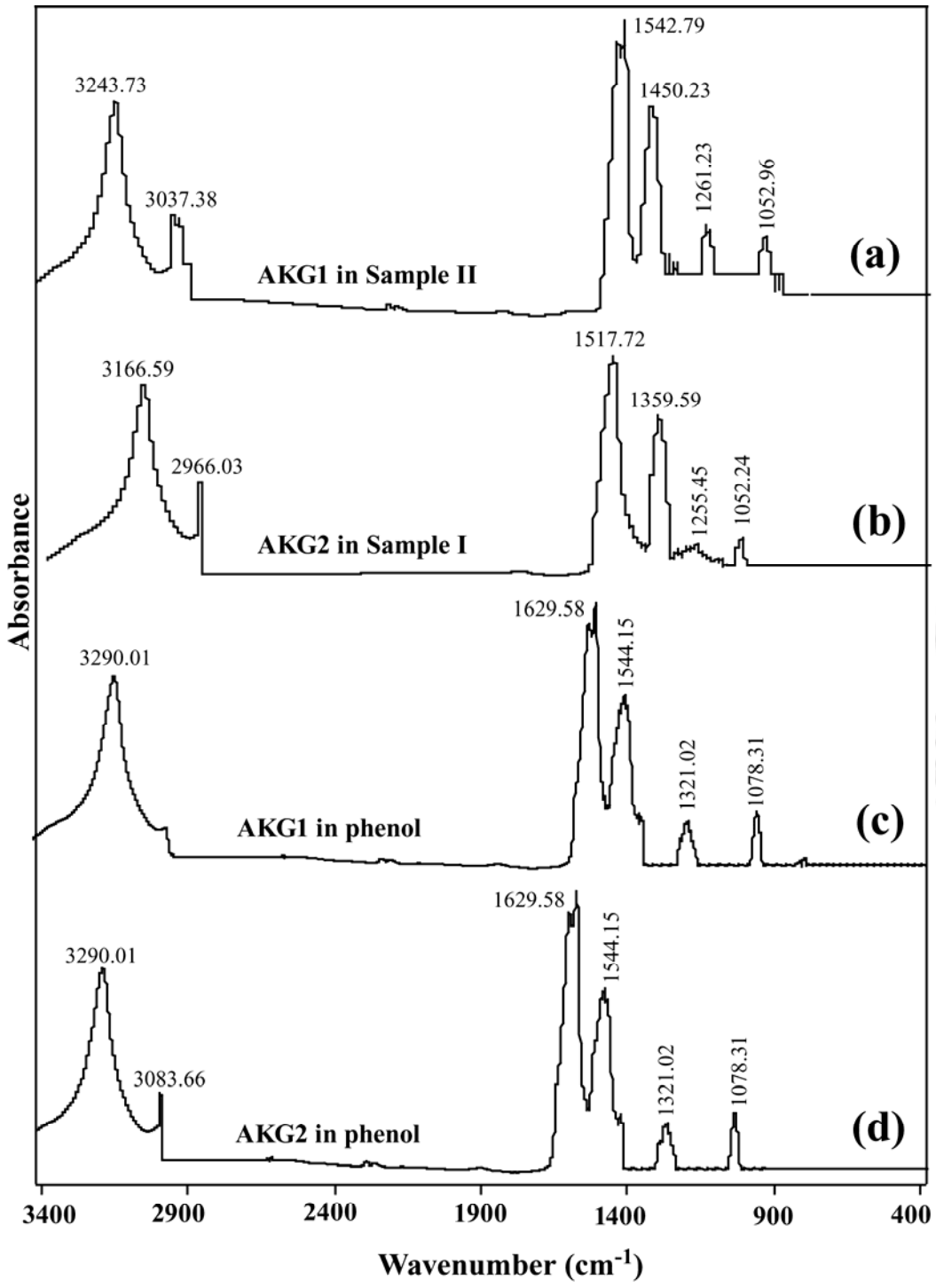

Figure 3.2.9. FT-IR spectra of bacterial membrane from (a) AKG1 grown in Sample II, (b) AKG2 grown in Sample I. Strains grown in presence of phenol (c, d) was used as 'control' cells.

3.2.6. Conclusions

Based on the performance in treating the petroleum wastewater samples, the co-culture of the free cells (*B. cereus*: AKG1 and AKG2) was found to be most efficient in overall removal of COD, TOC and NH_4^+–N as well as improving the BOD level of the wastewater samples. The liquid chromatography of the treated wastewater samples also indicated the reduction of COD level and increase in the biodegradability of the treated samples. Mass spectroscopic analysis of the biodegradation products demonstrated the probable presence of 2-hydroxy-3-(3-methyl-2-butenyl)1,4-naphthalenedione and a mixture of 4-(phenylamino)-phenol and 2,6-dichlorophenyl-1-acetonitrile as the end products of the microbial treatment of Sample II and sample I, respectively, for 20 days. Finally the FT-IR study revealed that the AKG1 and AKG2 strains adapted to the toxic environment of the petroleum wastewater through the structural changes of their cell membranes.

3.2.7. Appendix

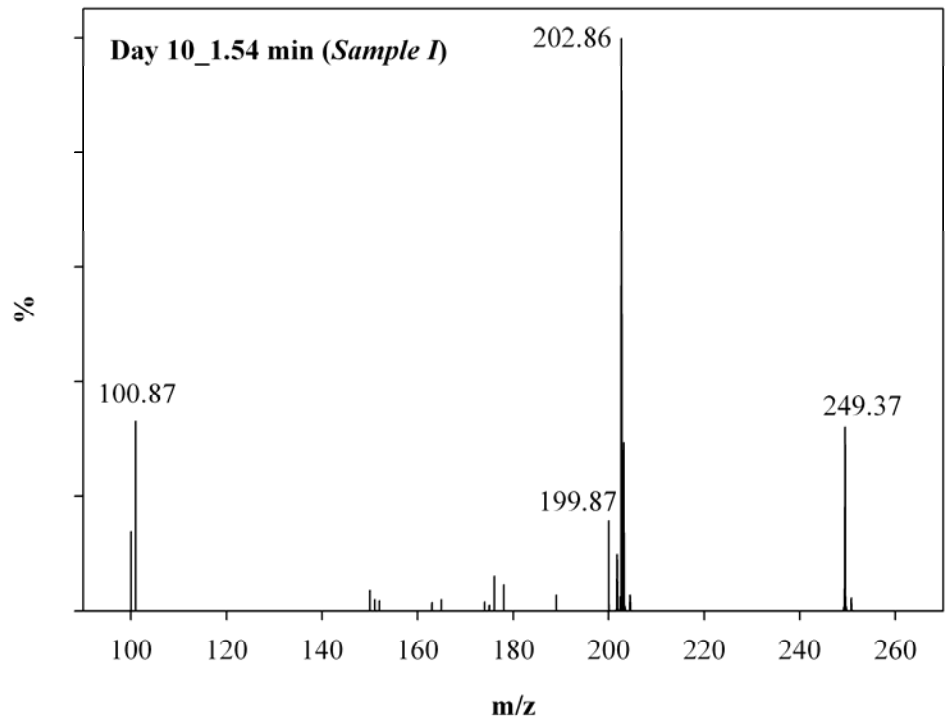

Figure A3.2.1. Mass spectrum of Sample I on Day 10 eluted at 1.54 min in the LC.

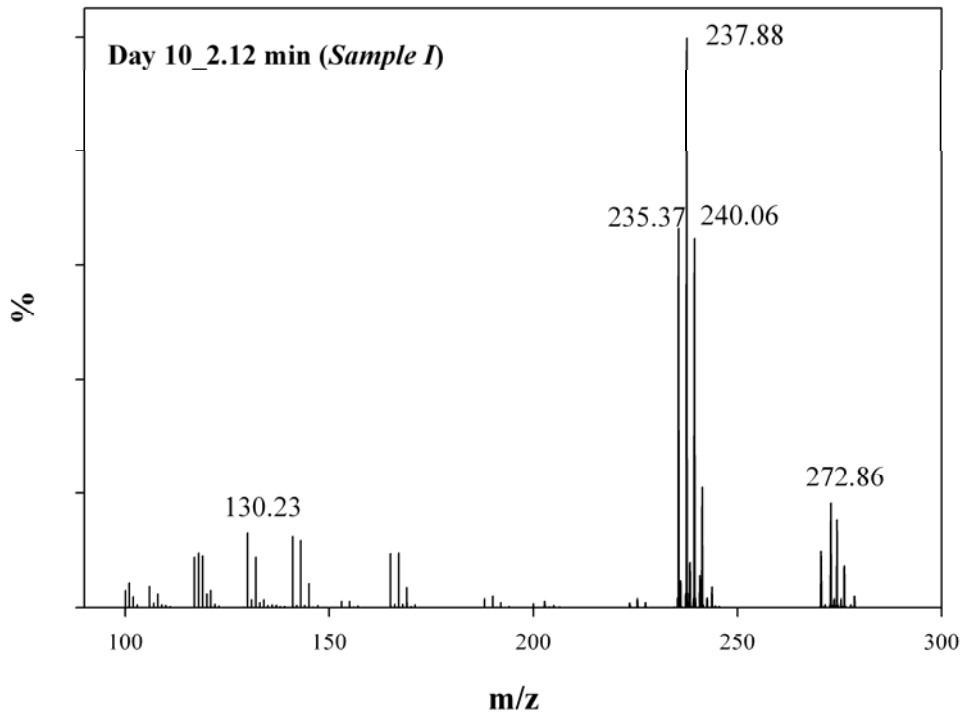

Figure A3.2.2. Mass spectrum of Sample I on Day 10 eluted at 2.12 min in the LC.

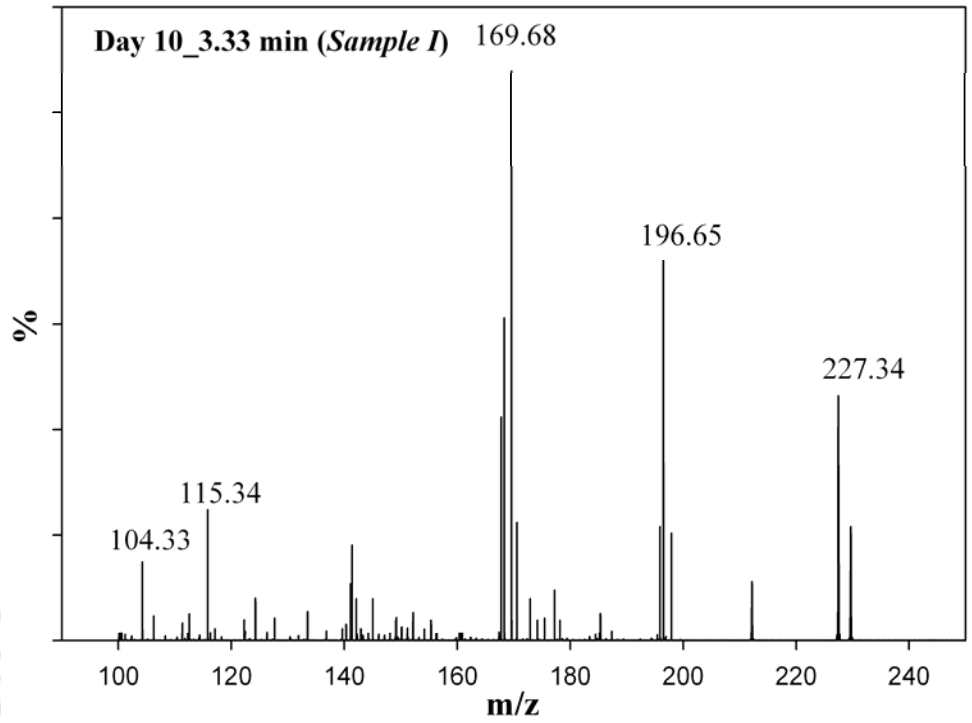

Figure A3.2.3. Mass spectrum of Sample I on Day 10 eluted at 3.33 min in the LC.

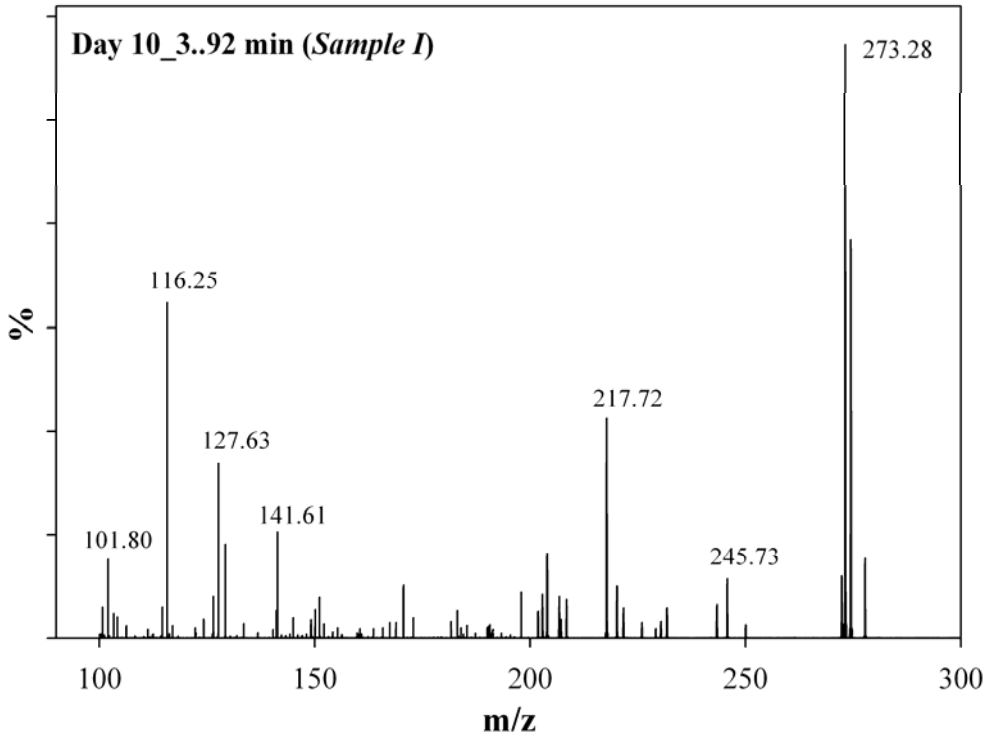

Figure A3.2.4. Mass spectrum of Sample I on Day 10 eluted at 3.92 min in the LC.

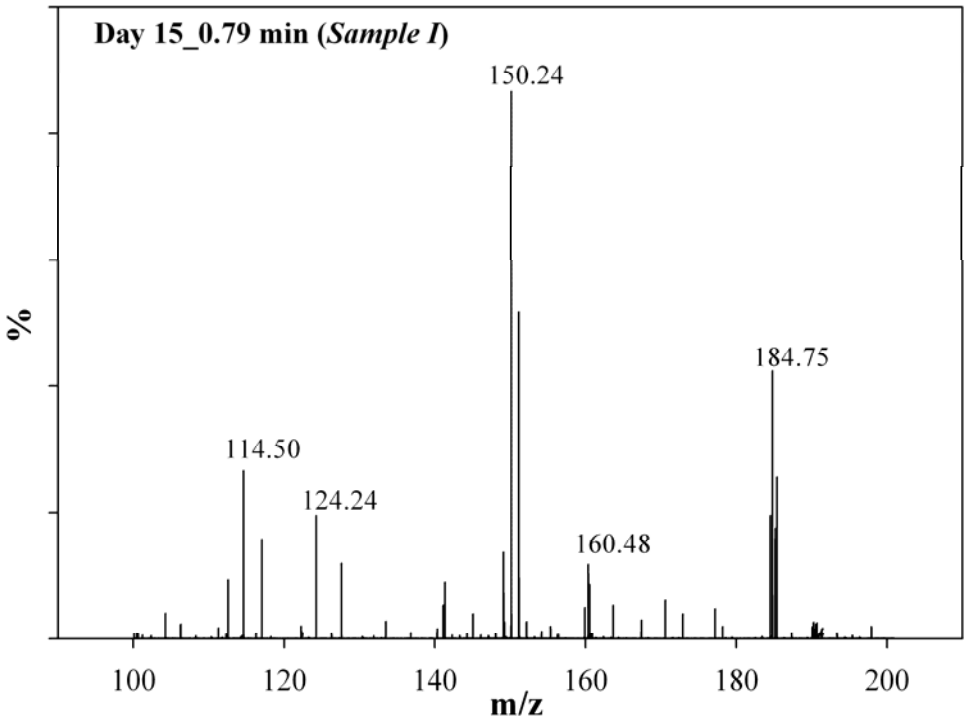

Figure A3.2.5. Mass spectrum of Sample I on Day 15 eluted at 0.79 min in the LC.

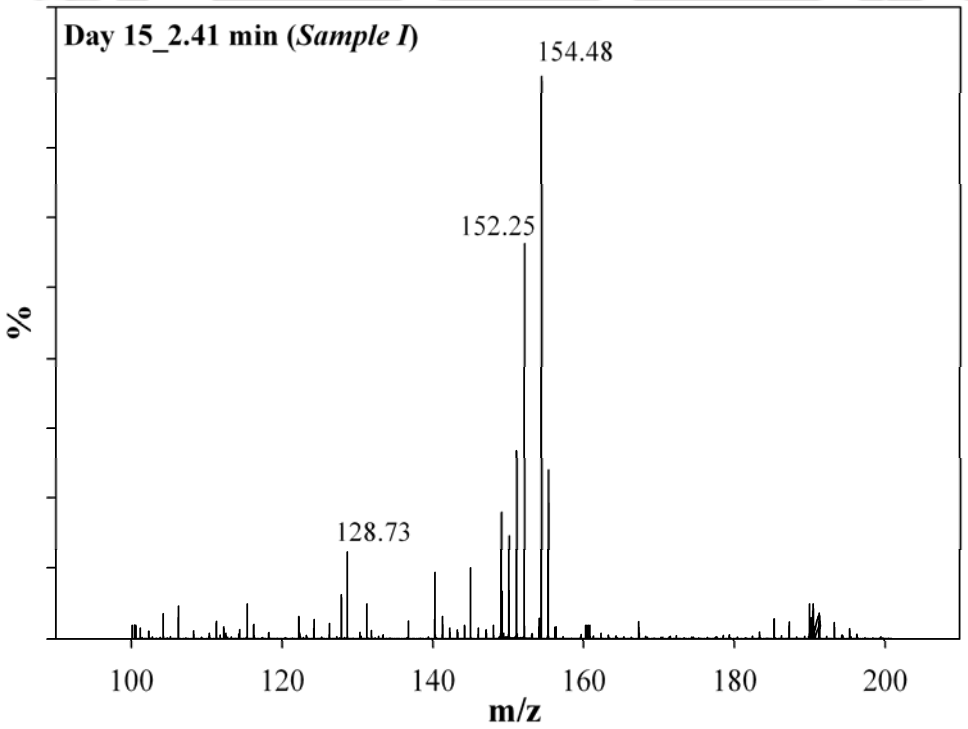

Figure A3.2.6. Mass spectrum of Sample I on Day 15 eluted at 2.41 min in the LC.

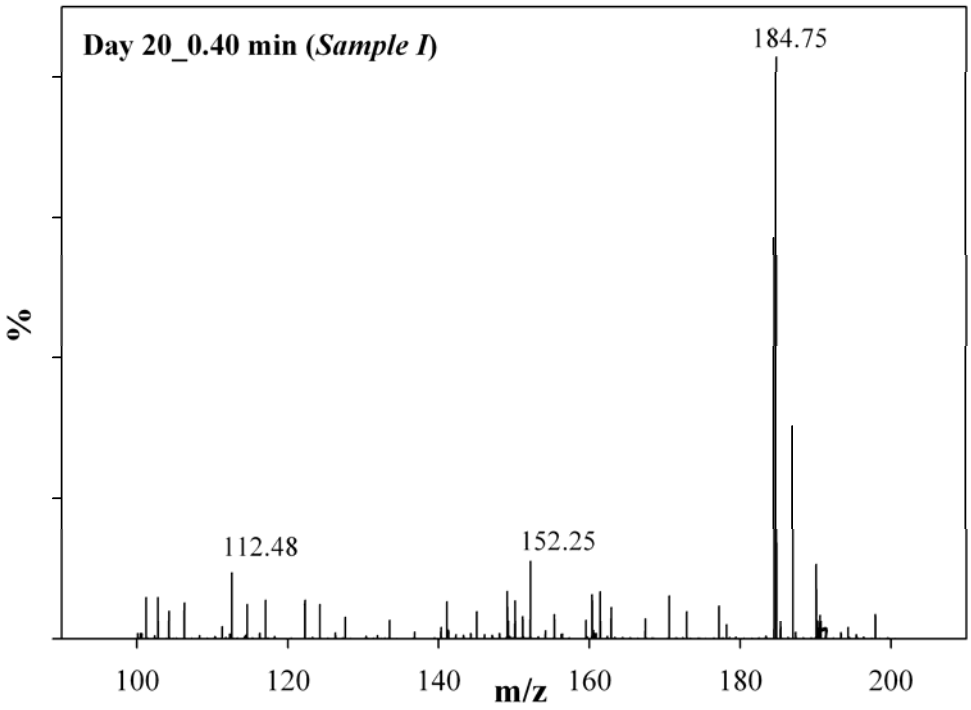

Figure A3.2.7. Mass spectrum of Sample I on Day 20 eluted at 0.40 min in the LC.

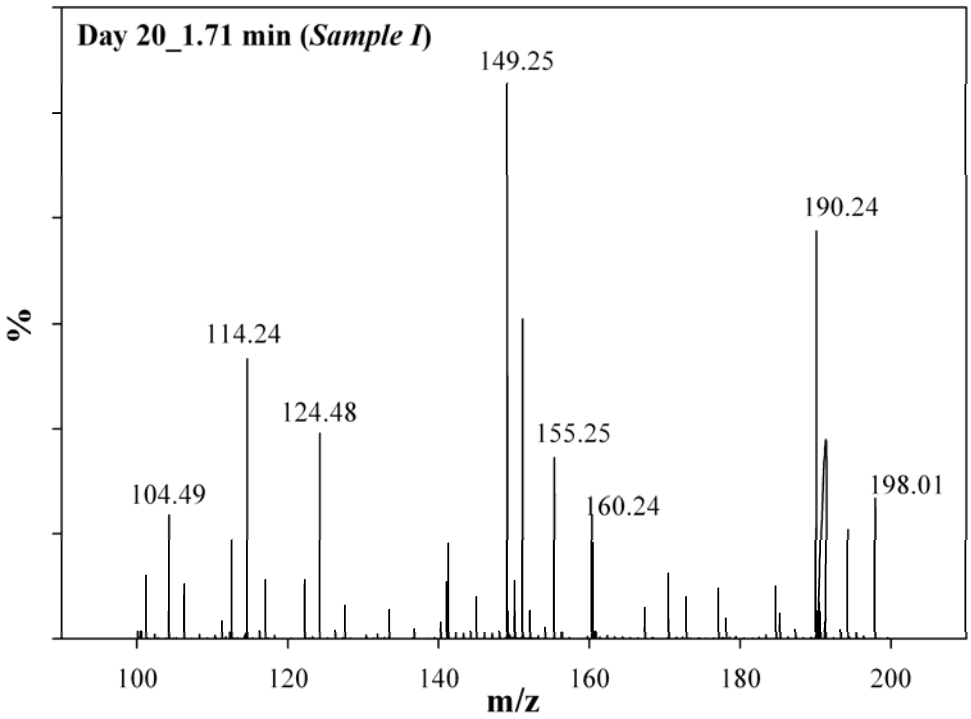

Figure A3.2.8. Mass spectrum of Sample I on Day 20 eluted at 1.71 min in the LC.

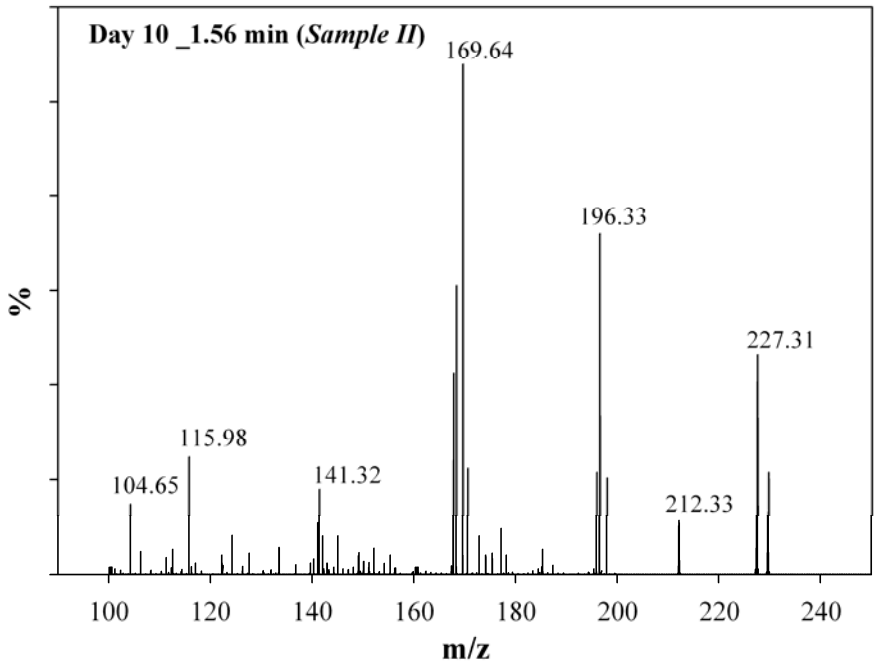

Figure A3.2.9. Mass spectrum of Sample II on Day 10 eluted at 1.56 min in the LC.

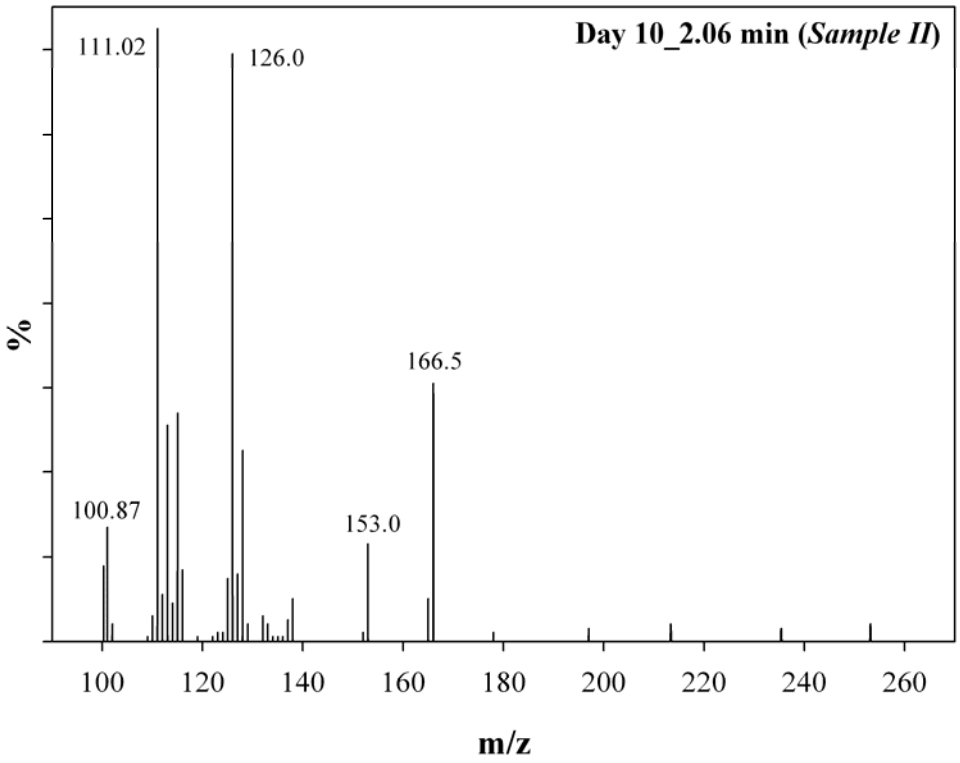

Figure A3.2.10. Mass spectrum of Sample II on Day 10 eluted at 2.06 min in the LC.

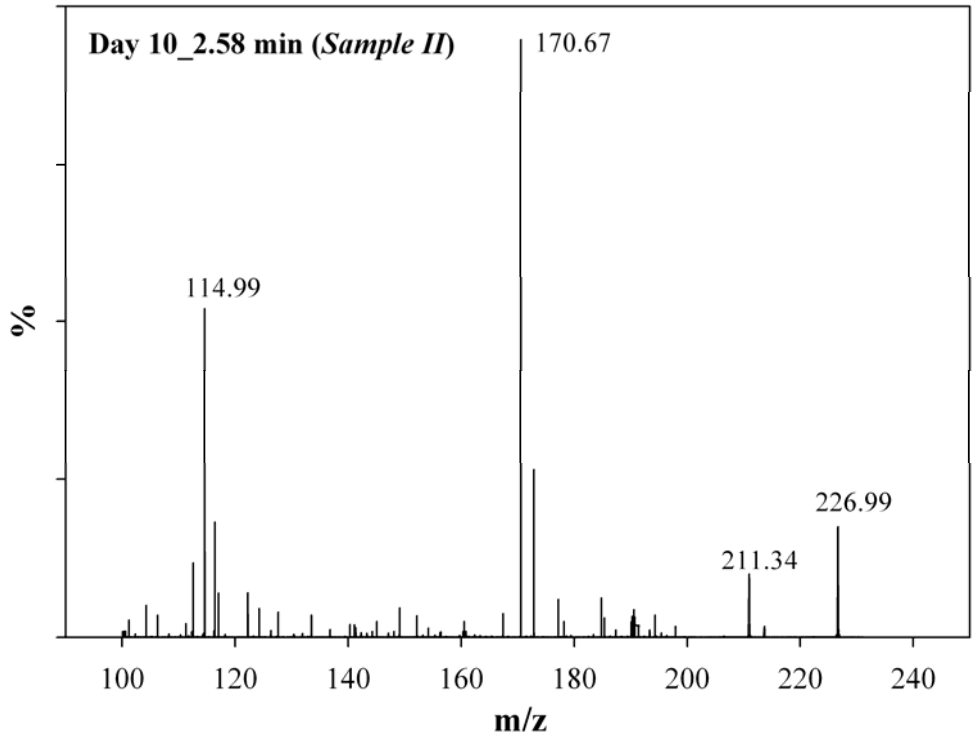

Figure A3.2.11. Mass spectrum of Sample II on Day 10 eluted at 2.58 min in the LC.

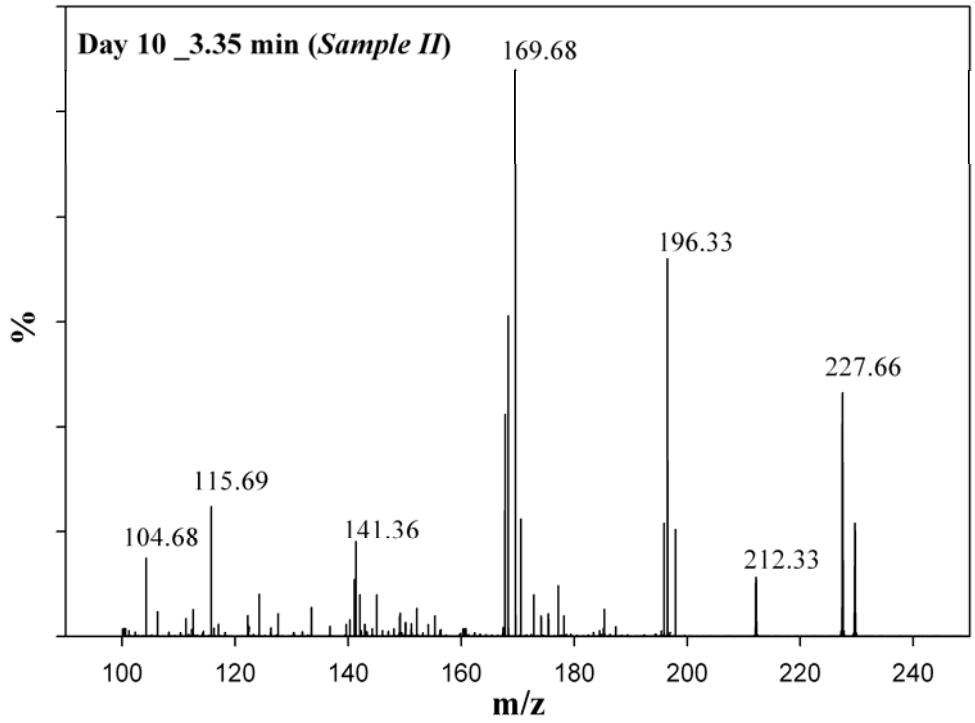

Figure A3.2.12. Mass spectrum of Sample II on Day 10 eluted at 3.35 min in the LC.

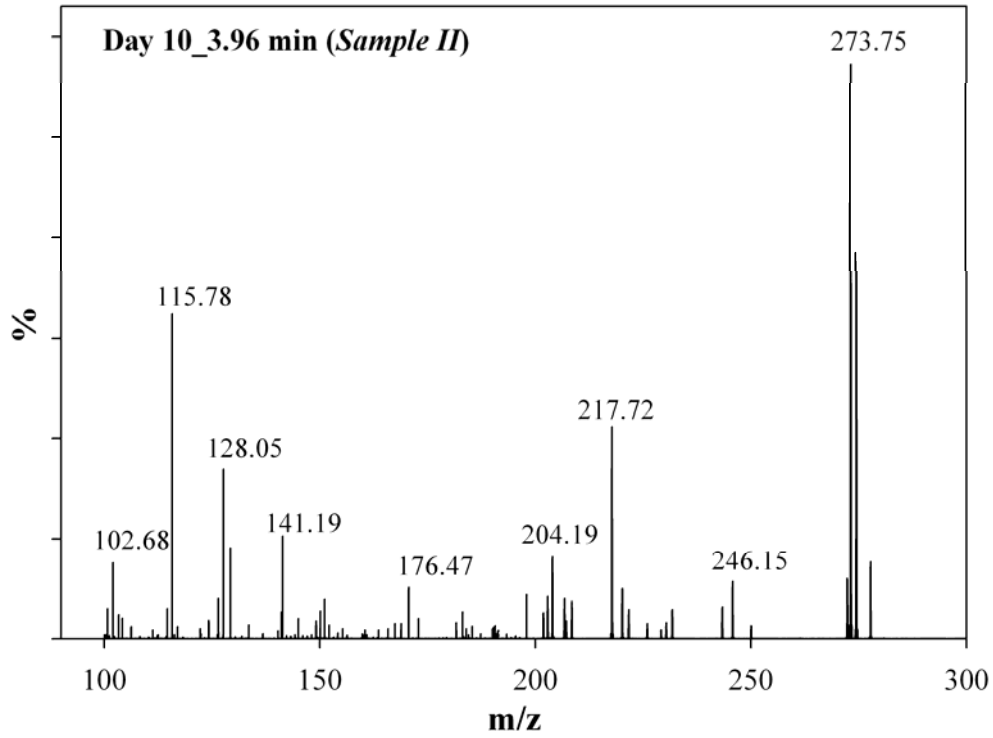

Figure A3.2.13. Mass spectrum of Sample II on Day 10 eluted at 3.96 min in the LC.

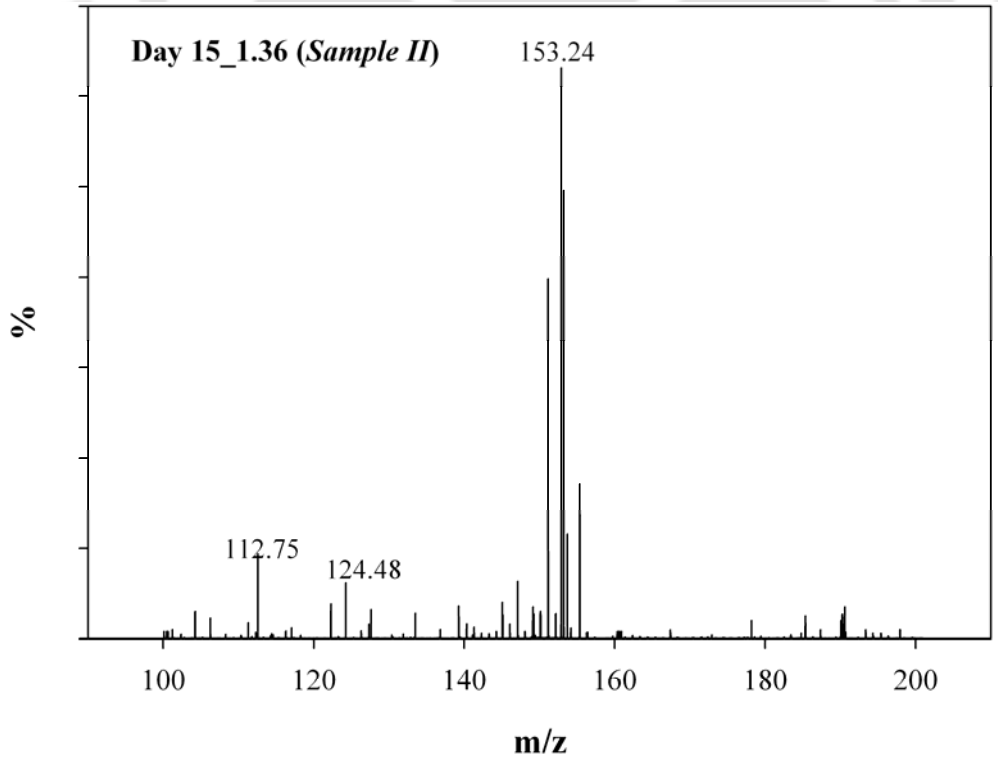

Figure A3.2.14. Mass spectrum of Sample II on Day 15 eluted at 1.36 min in the LC.

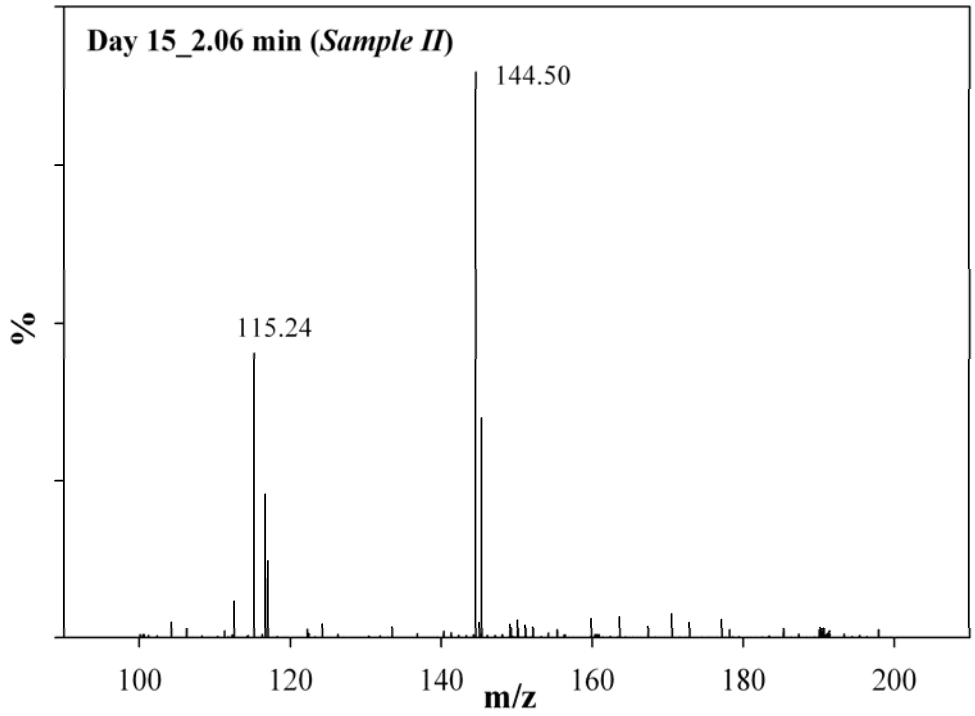

Figure A3.2.15. Mass spectrum of Sample II on Day 15 eluted at 2.06 min in the LC.

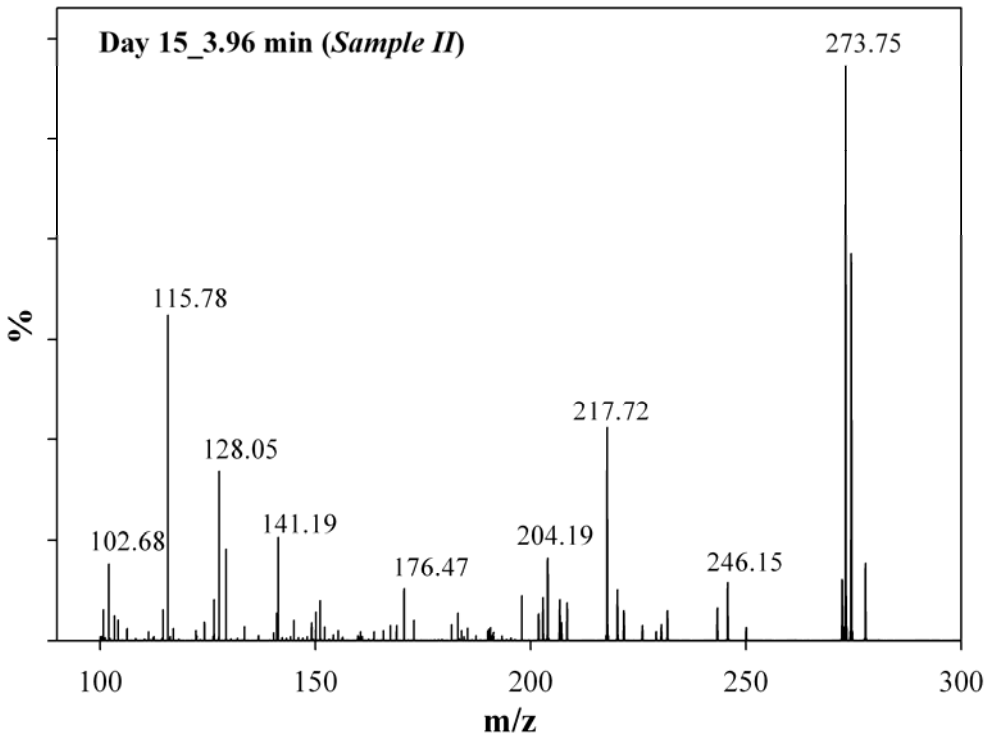

Figure A3.2.16. Mass spectrum of Sample II on Day 15 eluted at 3.96 min in the LC.

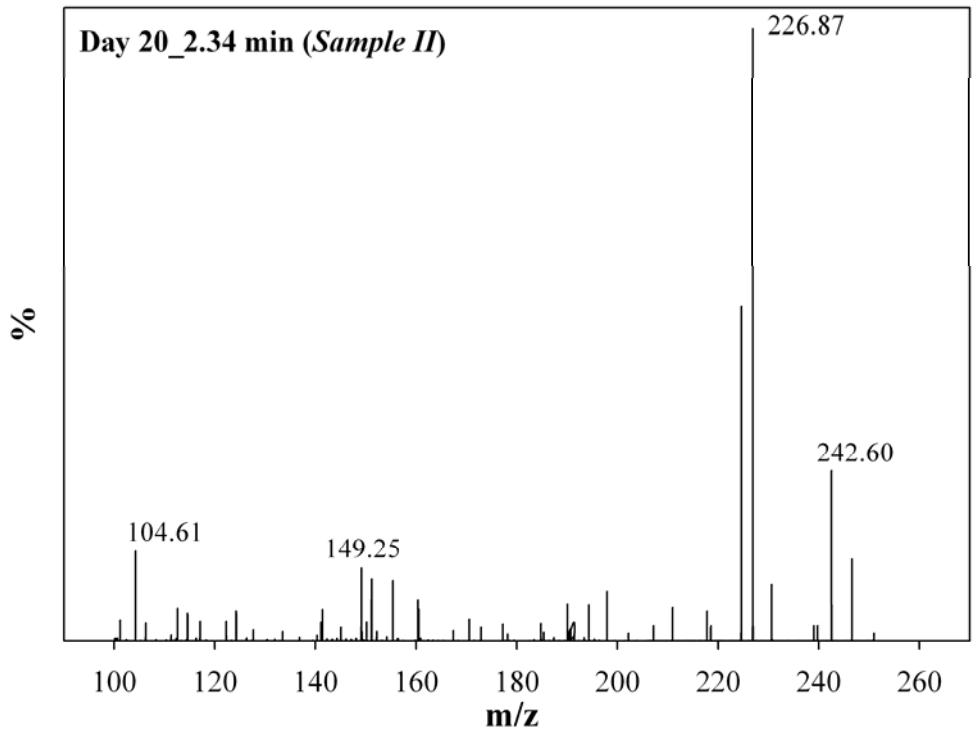

Figure A3.2.17. Mass spectrum of Sample II on Day 20 eluted at 2.34 min in the LC.

CHAPTER 4

Batch Biodegradation Studies using Calcium-Alginate Immobilized Cells of Isolated *B. cereus*

Development of Ca-alginate immobilized system for the isolated B. cereus strains and their biodegradation behaviour have been reported in Chapter 4 which is further divided into two parts. Section 4.1 discusses phenol biodegradation by immobilized B. cereus in batch culture with analysis of the degradation kinetics. The immobilized strains showed enhanced phenol tolerance and potential for repeated batch biodegradation. This part of the work has been accepted in ***International Biodeterioration and Biodegradation*** *(DOI: 10.1016/j.ibiod.2011.04.011).*

Successful biodegradation of two different site specific petroleum wastewater samples with concurrent changes in COD, TOC and ammonium nitrogen contents by immobilized B. cereus strains have been described in Section 4.2. This part of work has been orally presented in the ***2010 AIChE Annual Meeting****, Salt Lake City, UT.*

Chapter 4

BATCH BIODEGRADATION STUDIES USING CALCIUM-ALGINATE IMMOBILIZED CELLS OF ISOLATED *B. CEREUS*

4.1. PHENOL BIODEGRADATION: OPTIMIZATION AND KINETICS

4.1.1. Introduction

Phenols, polycyclic aromatic hydrocarbons (PAHs) and various heavy metals are the main toxic constituents of petroleum wastewater (Naas et al., 2009). Among these hazardous pollutants, phenol and other phenolic compounds pose serious environmental threat as they can easily contaminate nearby water courses due to their excellent water solubility and high toxicity (Santos et al., 2009; Mollaei et al., 2010). In order to remove the phenol and other phenolic compounds from industrial effluents including petroleum wastewater, biodegradation appears to be the most environmentally benign method. However, substrate inhibition of microbial growth at higher concentrations of toxic pollutants such as phenol poses a critical challenge in biodegradation of industrial wastewater (Wang and Loh, 1999).

In order to overcome the barrier of substrate inhibition, immobilization of microorganisms on various supports has gained much interest in last few years due to its potential for improvement of biodegradation efficiency in terms of sustainability as compared to free cells (Ehrhardt and Rehm, 1989; Patil et al., 2006). Though there have been several studies on immobilization on various strains, no such study is reported (to the best of our knowledge) with immobilization of strain *B. cereus*. In this context, the investigation to evaluate the phenol biodegradation capabilities of the immobilized strains of isolated *B. cereus* AKG1 MTCC9817 and *B. cereus* AKG2 MTCC9818 merits critical importance. Moreover, the knowledge of the phenol degradation kinetics by these immobilized strains is a necessary parameter for their successful application in the microbial treatment of real petroleum wastewater.

4.1.2. Literature Review

According to the U.S. Environmental Protection Agency (USEPA), phenol is a major pollutant (Keith and Telliand, 1979; Rodríguez et al., 2000) which can affect the aquatic micro–flora and fauna at a very low concentration of 0.005 mg mL^{-1} and is lethal to fish at concentration of 5–25 ppm (Santos et al., 2009). Also, phenol and its homologues can adversely affect the performance of the wastewater treatment plants by inhibiting the microbial growth (Ren and Frymier, 2003). Furthermore, human exposure to phenol through ingestion, contact or inhalation leads to critical health hazards and possible carcinogenesis (Nuhoglu and Yalcin, 2005; Naas et al., 2009).

Different approaches such as the genetically engineered microorganisms (Soda et al., 1998), adaptation of bacterial cell to higher substrate concentration (Masque et al., 1987) and immobilization of microbial cells have been reported to eliminate the substrate inhibition (Jianlong et al., 2001; Chen et al., 2010). Acclimatization, carried out by exposing microorganism to gradually increasing pollutant concentration, is a slow process and not always a viable option. On the other hand, the possibility of unpredicted effect on environment leaves the application of genetically modified microorganism in biodegradation debatable (Sayler and Ripp, 2000). Whole cell entrapment is one of the most well established methods of cell immobilization where microbial cells are entrapped in carriers made of bio-polymeric beads (Mattiasson, 1983). Immobilization of cells into polymeric matrix show improved cell viability and can tolerate higher concentrations of toxicants for longer duration (Patil et al., 2006; Ha et al., 2009). Immobilized cells, therefore, have the potential of degrading higher concentration of toxic pollutants such as phenol and phenolic compounds, which cannot be accomplished with free cells. The other advantages of using immobilized cells in biodegradation of toxic pollutants include improved operational stability, potential for scale-up and protection of the immobilized cells from environmental stresses including freezing/thawing (Leung et al., 1995), wet/dry cycles (Trevors et al., 1993), species-specific phases (Smith et al., 1996), etc. It is very difficult to develop a generalized method for successful immobilization of all microbial cells as the particular conditions and method greatly vary from one cell to another. Polymeric gel beads of calcium-alginate, in this respect, have been well studied by several researchers for efficient entrapment of microbial cells due to their low toxicity to cells, ease of use and low cost (Gonzalez et al., 2001; Takako et al., 2003; Munoz et al., 2005; Chen and Lin, 2007).

4.1.3. Outline of the Research Work

1) *B. cereus* AKG1 MTCC9817 and *B. cereus* AKG2 MTCC9818A strains have been immobilized into Ca-alginate beads and their phenol biodegradation has been investigated to determine the optimal pH and alginate concentration.
2) The phenol degradation performance of the immobilized strains, at optimal condition, has been compared with that of free cells.
3) The effects of storage time on the phenol degradation capabilities of the immobilized cells and the re-usability of the immobilized beads have also been investigated.
4) Finally, the phenol degradation kinetics of the immobilized cells have been investigated by fitting of various degradation models and compared with that of free cells.

4.1.4. Experimental Section

4.1.4.1. Microorganisms and Culture Medium

The details of chemicals and culture medium have already been described in *Section 2.4.1* in **Chapter 2**.

4.1.4.2. Immobilization of Bacterial Cell in Alginate Beads

The phenol degrading bacteria (AKG1 MTCC9817 and AKG2 MTCC9818) were harvested after 12 h of growth from 1 L of culture medium. The cell pellet (12 ± 1.2 g wet weight containing 2.1×10^{11} cfu) was obtained by centrifugation at 5,000 rpm for 10 min and subsequently re-suspended in 10 mL phosphate buffered saline (PBS). A stock of 5% (w/v) sodium alginate was prepared in the MSM medium and autoclaved at 121 °C for 15 min. 10 mL of bacterial cell suspension (2.1×10^{11} cfu) was added to 50 mL of sterilized alginate solution and mixed by stirring on a magnetic stirrer. This alginate–cell mixture was extruded drop by drop into a cold sterile 0.1 M calcium chloride solution ($CaCl_2$) using a peristaltic pump. The drops of alginate–cell solution were gelled to form uniform and defined-sized sphere upon contact with $CaCl_2$ solution. The immobilized beads were kept in 0.2 M $CaCl_2$ solution at room temperature for 1 h to complete the gel formation. The beads were then rinsed with MSM followed by distilled water to remove residual $CaCl_2$. Blank alginate beads without bacterial cells were also prepared in the same way for control experiments.

4.1.4.3. Effect of pH and Alginate Concentration on Phenol Degradation

Alginate was used as a gel matrix to immobilize strains AKG1 and AKG2. Factors such as alginate concentration, pH and initial phenol concentration which might have impact on degradation of phenol by the immobilized cells were investigated. Each experiment was carried out in batch mode in 250 mL Erlenmeyer flask containing 100 mL MSM media at 120 rpm. First, the experiments were carried out at various pH (6.5, 6.7, 6.9, 7.0 and 7.5), keeping initial phenol concentration at 1000 mg L^{-1} at 37 °C. At the optimum pH further experiments were carried out at various alginate concentrations (2.0%, 2.5%, 3.0% and 3.5% prepared from the stock solution) with initial phenol concentration of 1000 mg L^{-1} in order to find out the optimum alginate concentration for the degradation studies. In order to find out the effect of initial phenol concentration on the degradation studies and analyze the degradation kinetics, additional experiments, as discussed later in (*Section 4.1.4.4*), were carried out with various initial phenol concentrations ranging from 100–2000 mg L^{-1} at 37 °C, optimum pH and optimum alginate concentration.

4.1.4.4. Phenol Biodegradation by Free Cells and Immobilized Cells

All the biodegradation experiments were carried out in batch mode in 250 mL Erlenmeyer flasks containing 100 mL MSM media (without Yeast extract i.e. without any extranal nitrogen source) and the desired amount of phenol (100, 500, 1000, 1500 and 2000 mg L^{-1}). For free cells, 5 mL of cell suspension (2.13 x 10^{11} cfu) was added to the culture media (without Yeast extract) and incubated at 37 °C under shaking condition (120 rpm). The initial pH of the medium was adjusted to 7.0 for AKG1 and 7.5 for AKG2, the optimum pH for the growth of the respective strains as determined in **Chapter 2**. The experiments were carried out for 22 days and 30 days for the strains AKG1 and AKG2, respectively.

For immobilized cells, 25 g of wet alginate beads containing immobilized AKG1 and AKG2 as discussed under *Section 4.1.4.2* were added to culture media (without Yeast extract). The pH values of media were adjusted to the optimum one as obtained based on the experiments carried out as per *Section 4.1.4.3*. Control experiments were also carried out using only blank alginate beads without bacterial entrapment. The experiments were carried out for 26 days and 36 days for the strains AKG1 and AKG2, respectively. The amount of phenol degradation in the respective experiments was

determined by measuring the residual phenol concentration as discussed in *Section 4.1.4.6*.

4.1.4.5. Stability and Reusability Study

In order to investigate the effect of storage on the phenol degrading capability of the immobilized cells, the beads containing the entrapped cells were stored for varying duration of time (up to 60 days) at 4 °C. The immobilized cells were then used for phenol degradation to examine the reusability of the immobilized cell in repeated batch experiment degradation of phenol. The batch biodegradation was carried out as described in *Section 4.1.4.4*. After every 26 days (AKG1) or 36 days (AKG2), the immobilized cells were aseptically removed from the medium and washed 3 times with sterile distilled water. Then, the beads were used again separately for degradation together with fresh medium containing the required amount of phenol under same experimental conditions.

4.1.4.6. Analysis of Phenol Concentration

Samples were withdrawn at regular intervals of time and filtered through a Millipore filter paper (0.2 μm). The filtrate was analyzed for residual phenol concentration by HPLC (ProSTAR, Varian) equipped with a UV–visible detector and C18 column (particle size 7 μm, length 15 cm and diameter 6.4 mm) at room temperature with a mobile phase of acetonitrile (80%): water (20%) at a flow rate of 0.8 mL min^{-1}. An aliquot of 20 μL of the sample was injected and analyzed using UV-visible detector at wave length of 280 nm for detection of phenol.

4.1.4.7. Phenol Degradation Kinetics

Among several available kinetics models, the mostly used and suitable models (Chung et al., 2003) namely, Haldane model, Yano model and Edward model were fitted to the experimental data in order to select the best model(s) to represent the degradation kinetics of phenol by free and immobilized cells in the present study (Table 4.1.1). The details of analyses of phenol degradation kinetics have been described in *Section 3.1.4.5* (**Chapter 3**).

4.1.5. Results and Discussion

4.1.5.1. Effect of pH on Degradation of Phenol by Immobilized Cells

Figure 4.1.1 shows the phenol degradation by immobilized cells at various pH values. It is evident from the figure that the phenol can be degraded most efficiently by the immobilized cells almost at neutral pH. The phenol degradation rates by immobilized AKG1 and AKG2 were maximal at pH 6.7 and 6.9, respectively. It may be mentioned here that the pH is an important factor for the activity of the enzymes produced by microbes as pH change can affect the solubility and stability of enzymatic compounds (Banerjee and Ghoshal, 2010a). Extremely high or low pH values generally results in complete loss of activity for most of the enzymes. Furthermore, the degradation of phenol was much quicker for AKG1 than for AKG2 at respective pH values.

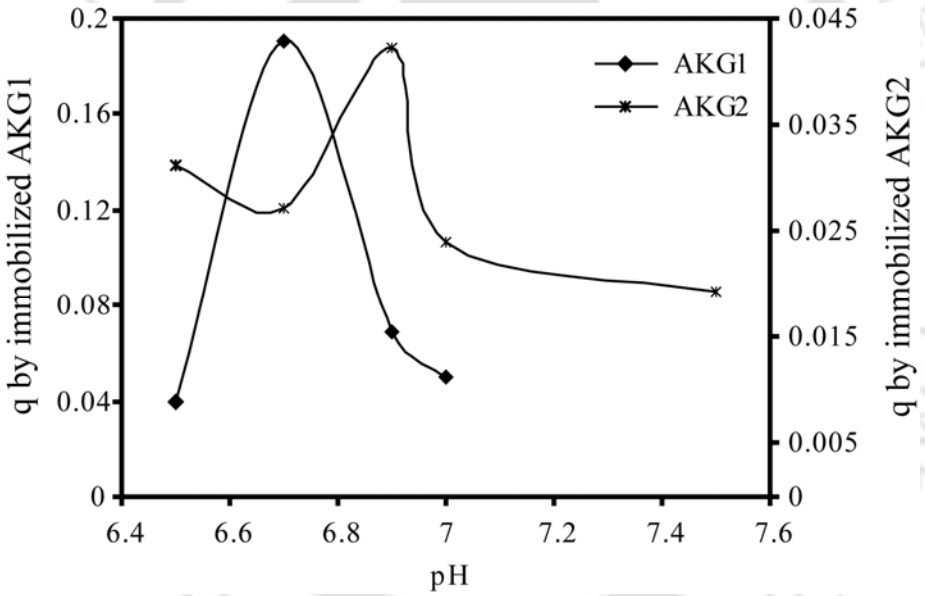

Figure 4.1.1. Degradation rate (q) of immobilized AKG1 and AKG2 at various pH values.

The range of study was maintained narrow as it had been already observed earlier the optimal pH for the maximum growth of free AKG1 and AKG2 strains to be 7.0 and 7.5, respectively, in **Chapter 2**. The optimal pH values for maximum phenol degradation by immobilized cells in the present study (6.7 for AKG1 and 6.9 for AKG2) are now shifted slightly towards acidic condition (Figure. 4.1.1). It is also reported in various literatures (Bandyopadhyay et al. 1998; Chakraborty et. al., 2010; Reda et. al., 2010) for various strains that phenol degradation rate is the highest near neutral pH of 7.0. Similar observation was also reported previously by Chung et al.

(2003) in a study of phenol degradation by *Pseudomonas putida* immobilized in Ca-alginate beads. This shift in the poly-anionic nature of the alginate matrix is due to the presence of numerous carboxylic groups which can decrease the effective H^+ concentration in media by attracting H^+ around the active parts of the immobilized cells. The pH of the medium for immobilized strains in the present study, hence, had to be decreased in order to maintain the optimum H^+ concentration required for the respective strains.

4.1.5.2. Effect of Alginate Concentration on Phenol Degradation by Immobilized Cells

The control experiments with alginate beads without bacterial cells demonstrated that no detectable loss in phenol concentration occurred due to evaporation/adsorption on the beads. The phenol degradation rate q, at various alginate concentrations is shown in Figure 4.1.2. The initial phenol concentration was fixed at 1000 mg L^{-1} to compare the performances. Figure 4.1.2 demonstrates that the rate of phenol degradation for both the strains initially increases with increasing alginate concentration and subsequently reaches the maximum value at an alginate concentration of 3%. However, further increase in alginate concentration results in decrease in q value. In spite of the higher degradation rate of phenol in AKG1 compared to AKG2, same alginate concentration (3%) is found to be optimum for both the strains.

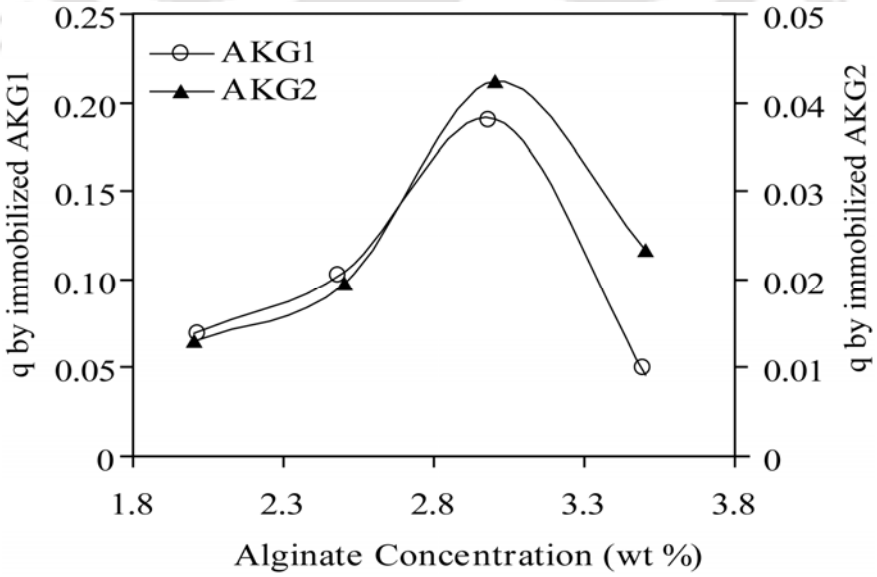

Figure 4.1.2. Degradation rate (q) of immobilized AKG1 and AKG2 at various alginate concentrations (wt %)

According to the literature, the effective diffusion coefficient of phenol in the alginate bead decreases significantly with increase in alginate concentration; it is reduced from 5.20×10^{-10} m^2s^{-1} (Aksu and Bulbul, 1999) to 2.60×10^{-10} m^2s^{-1} (Bandhyopadhyay et al., 2001) when the alginate concentration is increased from 2% to 3%. So, apparently, the phenol degradation rate is expected to be more for alginate concentration lower than 3%. However, an alginate concentration of 3% is found to be optimum for phenol degradation by the immobilized strains in the present work. The lower rate of phenol degradation below 3% alginate was because of the reduced stability of the beads at lower alginate concentration. The ruptured beads forced the cells to be in direct exposure to the phenol environment, which might have in turn reduced the growth as well as the degradation rates. On the other hand, the reduction in degradation rate observed at higher alginate concentrations (above 3%) was due to poor diffusion through the compact and rigid matrix of the beads produced at higher alginate concentrations (Chung et al., 2003). Previous report by Mollaei et al. (2010) also demonstrated that the time required for complete degradation of 1000 mg L^{-1} phenol by *Pseudomonas* sp. SA01 immobilized in 3% alginate beads was less than that of the 2% alginate beads, but almost same as that of the 4% alginate beads.

4.1.5.3. Phenol Degradation by Free Suspended Cells and Alginate-Immobilized Cells

Figures 4.1.3(a) and 4.1.3(b) depict the profile of phenol degradation with time by free AKG1 and AKG2 strains (without Yeast extract). The results show that free AKG1 can degrade the phenol completely up to an initial phenol concentration of 1000 mg L^{-1}, without any significant lag phase. The time required for complete degradation of phenol was 8.5, 9 and 11 days for 100 mg L^{-1}, 500 mg L^{-1} and 1000 mg L^{-1} of initial phenol concentration, respectively. However, only 70% and 32% phenol degradation were observed over 22 days of monitoring period when the initial phenol concentration was increased to 1500 mg L^{-1} and 2000 mg L^{-1}. On the other hand, free AKG2 can completely degrade phenol only up to 500 mg L^{-1} with complete degradation occurring within 13 and 16 days at 100 and 500 mg L^{-1} of initial phenol, respectively. Furthermore, free AKG2 was not able to fully degrade phenol at initial concentration of 1000 mg L^{-1} or above over 30 days of monitoring period. The phenol degradation by free AKG2 was 89%, 76% and 20% at 1000 mg L^{-1}, 1500 mg L^{-1} and 2000 mg L^{-1} phenol, respectively.

Phenol degradation by immobilized bacteria (AKG1 and AKG2) was investigated at various initial phenol concentrations (100–2000 mg L^{-1}) and the degradation profiles are shown in Figures 4.1.3(c) and 4.1.3(d). The figures show that immobilized AKG1 was able to degrade phenol completely within 14, 17 and 25 days at the initial phenol concentration of 100, 500 and 1000 mg L^{-1}, respectively. Furthermore, 89% and 54% of phenol was degraded by immobilized AKG1, within the experimental period (26 days), when initial concentration was 1500 mg L^{-1} and 2000 mg L^{-1}, respectively. On the other hand, complete phenol degradation by immobilized AKG2 at the initial concentration of 100, 500 and 1000 mg L^{-1} were observed within 20, 24 and 36 days, respectively. Within 36 days of monitoring period, immobilized AKG2 was able to degrade 64% and 53% phenol at the initial concentration of 1500 mg L^{-1} and 2000 mg L^{-1} respectively.

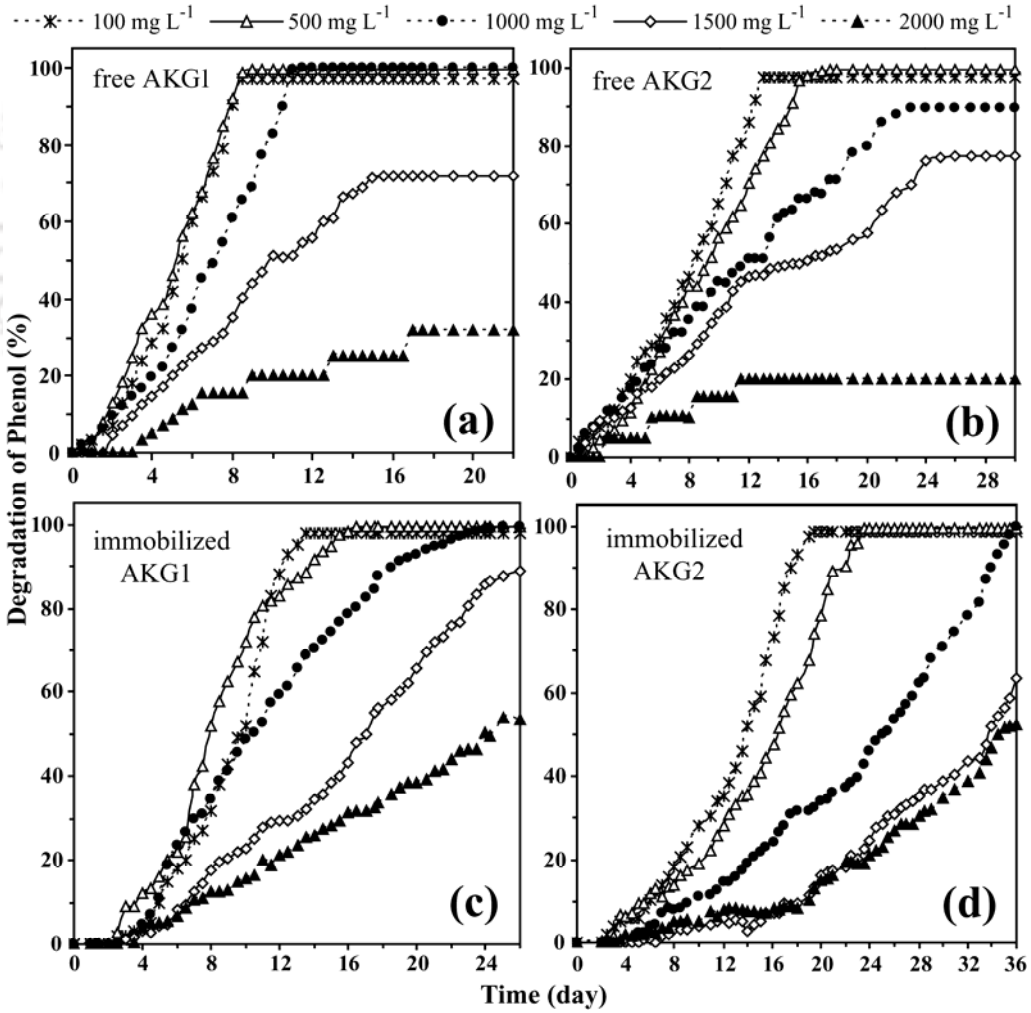

Figure 4.1.3. Phenol degradation profiles of (a) free AKG1, (b) free AKG2, (c) immobilized AKG1 and (d) immobilized AKG2 at various initial phenol concentrations.

The phenol degradation behavior by the free bacteria and their immobilized counterparts was investigated in the present study in order to asses the feasibility of using alginate beads containing AKG1 and AKG2 in bioreactors for degradation of phenol present in petroleum wastewater. Almost complete degradation of phenol was observed by freely suspended AKG1 and AKG2 at lower phenol concentration (100–1000 mg L^{-1}) and the degradation time was found to be directly proportional to the initial phenol concentration. However, at higher phenol concentrations (above 1500 mg L^{-1}) the phenol degradation was affected considerably, which was evident from the distinct lag phases observed during the degradation (Figure 4.1.3a,b). This could be due to the toxic effect of phenol at high concentrations inhibiting phenol biodegradation by culture death (Mollaei et al, 2010). Similar substrate inhibition was reported by Chung et al. (1998) for *P. putida* ATCC 49451 at phenol concentrations above 1000 mg L^{-1}.

In order to improve cell tolerance and achieve efficient biodegradation at high phenol concentrations, AKG1 and AKG2 in the present work were immobilized in alginate beads. Alginate is one of the most frequently used matrices for whole–cell immobilization because of its high porosity and biodegradability (Chen et al., 2010). The results in the present work (Figure 4.1.3c, d) demonstrate that the immobilization of both the bacterial strains (AKG1 and AKG2) into alginate beads resulted in improved substrate tolerance and efficient biodegradation of phenol at higher phenol concentrations (1500 mg L^{-1} or above), which are otherwise toxic to free bacteria. At the highest phenol concentration (2000 mg L^{-1}) tested in the present study, immobilized AKG1 and AKG2 showed 54.0% and 52.5% phenol degradation, respectively; which was 22% and 32.5% higher than that of the respective free strains. However, the phenol degradation by the immobilized cells was slower than that of the free cells, which could be due to two reasons. Firstly, the amount of biomass for free cell case is more due to its growth with time, which is not possible in the immobilized cells. Also, high initial dosage (about 2.7×10^8 cfu per bead) used during immobilization played a critical role. As pointed out by Pramanik et al. (2011), when higher initial cell concentrations are used during immobilization, cell growth is negligible due to less space to grow and more competition for substrate. Secondly, the additional barrier in the mass transfer processes presented by the immobilizing matrix, alginate (Chung et al., 2003). Previously, Chen et al. (2007) also reported the slower biodegradation of phenol and trichloroethene by *P. putida* immobilized in chitosan beads.

4.1.5.4. Effect of Storage on Phenol Degradation and Reusability of Immobilized Cells

Figure 4.1.4 shows the effect of the storage time of the alginate beads on the phenol degradation capabilities of the immobilized cells. It was observed that the phenol degradation rate was unaffected up to a storage time of 30 days for both the immobilized cells, AKG1 and AKG2. Only a little decrease in degradation efficiency was observed when the immobilized beads were stored for 60 days. The result essentially shows that the alginate beads with immobilized cells can be stored up to 30 days without any reduction in phenol degradation efficiency.

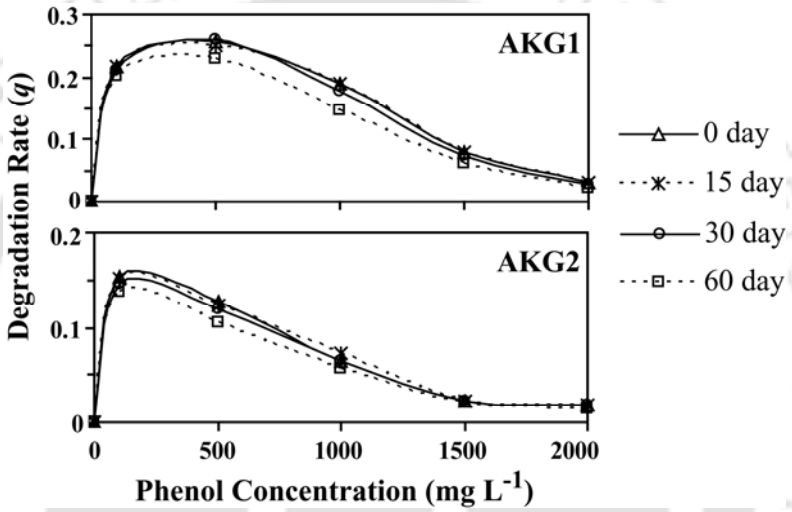

Figure 4.1.4. Degradation rate (q) of immobilized AKG1 and AKG2 at various initial phenol concentrations after 0, 15, 30 and 60 days of storage at 4 °C.

In order to investigate the stability and durability of the immobilized alginate beads containing AKG1 or AKG2, experiments were carried out to reuse the beads for repeated batch degradation of phenol. The results of repeated batch degradation are shown in Figure 4.1.5. The duration for each batch was 26 days for AKG1 and 36 days for AKG2. It was observed that the immobilized cells (both AKG1 and AKG2) could efficiently be reused for three consecutive batches without any significant decrease in phenol-degrading efficiency. However, an initial lag phase was observed in the third cycle of batch degradation and, hence, further batches of degradation were not carried out. It is evident from Figure 4.1.5 that the bioactivity of the immobilized AKG1 and AKG2 was stable over 80 days and 110 days, respectively, in repeated batch degradation of phenol. It may be mentioned here that the leakage of entrapped cells

from alginate beads and deformation or weakening of alginate matrix were not observed in the present experimental conditions.

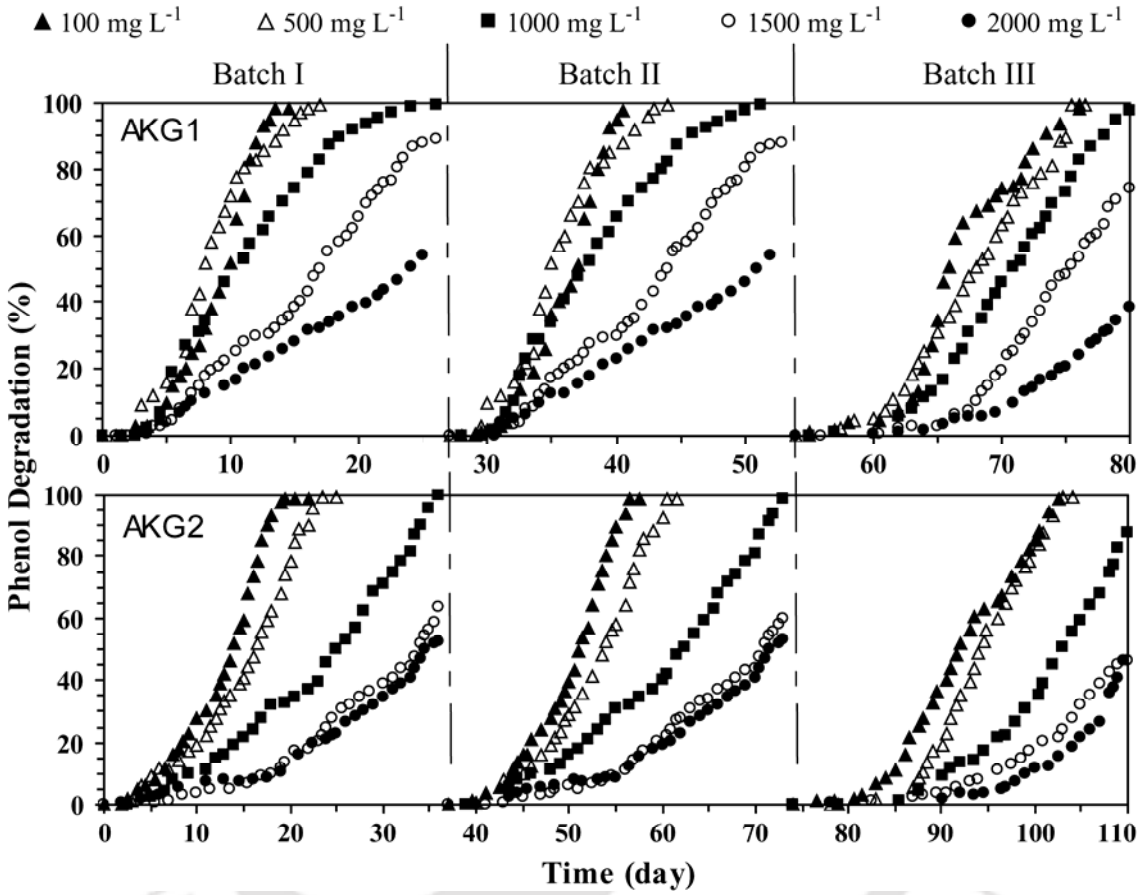

Figure 4.1.5. Phenol degradation by immobilized AKG1 and AKG2 at various initial phenol concentrations in repeated batch-biodegradation.

The storage and reusability of the cell-entrapped alginate beads constitute the important parameters for successful application of these immobilized cells for the biodegradation of phenol in practical field. Results in the present study (Figure 4.1.4) demonstrate that the immobilized cells can be stored for one month without compromising with their phenol-degrading capacity. Additionally, the immobilized beads can effectively be reused over a long period of time – 80 days for AKG1 and 110 days for AKG2 – for batch biodegradation applications without significant changes in phenol degradation (Figure 4.1.5). Previous report (Mollaei et al, 2010) demonstrated

that *Pseudomonas* sp. immobilized in alginate beads could be reused over 28 days for biodegradation of phenol. Furthermore, Ha et al. (2009) reported that the bacterial cells immobilized in alginate matrix could be used over a period of 36 h for repeated biodegradation of chlorferon and diethlythiophosphate, while alginate beads containing entrapped *Klebsiella oxytoca* were successfully recycled over a period of 8 days by Chen et al. (2010) for biodegradation of propionitrile. However, it is difficult to compare the results of individual reports due to the difference in experimental conditions and the microbial strain too. Nonetheless, it is apparent that the prepared beads are quite good in terms of reusability, stability, storage capability and phenol concentration. Moreover, strain AKG1 is better than AKG2 in performance

4.1.5.5. Kinetics and Modeling of Phenol Degradation

The phenol degradation rates (q) were calculated for various S_0 used in the biodegradation of phenol by free as well as immobilized strains and are shown in Figure 4.1.6. The results indicate that the phenol degradation rate (q) demonstrated by free suspended strain (without Yeast extract) is higher than immobilized strain (without Yeast extract). The experimental degradation rate was maximum at initial phenol concentrations of about 500 mg L^{-1} for both free and immobilized AKG1, whereas free and immobilized AKG2 demonstrated maximum q at 100 mg L^{-1}. The experimental phenol degradation rates demonstrated by free and immobilized AKG1 (0.44 h^{-1} and 0.26 h^{-1}, respectively) were found to be higher than those of AKG2 (0.24 h^{-1} and 0.15 h^{-1}, respectively) (Figure 4.1.6).

The relation between the degradation rate and the initial substrate concentration is described by a set of empirically derived rate equations referred to as theoretical models. Three different models namely Haldane, Yano and Edward (Table 4.1.1) were used in the present study to relate the degradation rate with the initial phenol concentration. The experimentally obtained values of substrate degradation rate at various S_0 were used to fit the above models (Figure 4.1.6) using the nonlinear regression analysis in Matlab 7.0® for estimating the kinetic parameters. The values of the biokinetic parameters obtained from the fitting of the above models are summarized in Table 4.1.1 for free as well as immobilized strains. Table 4.1.1 shows that the both Haldane and Yano models provide adequate fit for the entire set of experimental data.

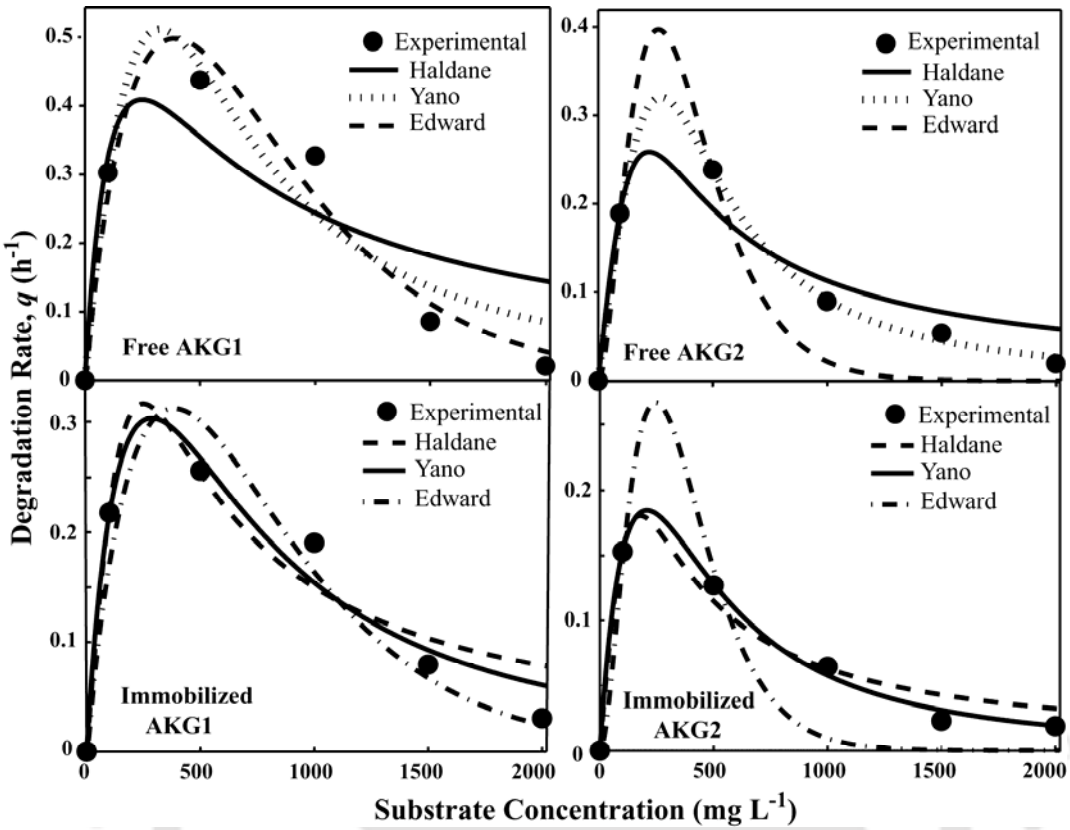

Figure 4.1.6. Model prediction of experimental degradation rates of phenol by free and immobilized AKG1 and AKG2.

Table 4.1.1: Kinetics parameters of phenol degradation obtained by various models

Model		AKG1		AKG2	
		Free	*Immo*	*Free*	*Immo*
Haldane (Haldane, 1965): $q = \frac{q_{max} S_0}{K_S + S_0 + (S_0^2 / K_I)}$	q_{max} (h^{-1})	21.48	12.73	11.69	6.95
	K_S (mg L^{-1})	2.43	5.14	12.02	20.11
	K_I (mg L^{-1})	5882	6210	7902	9108
	R^2	0.839	0.963	0.981	0.961
	SD_{avg}	0.015	0.044	0.012	0.052
Yano (Yano et al., 1966): $q = \frac{q_{max} S_0}{K_S + S_0 + \frac{S_0^2}{K_I}\left(1 + \frac{S_0}{K}\right)}$	q_{max} (h^{-1})	0.92	0.40	6.31	4.15
	K_S (mg L^{-1})	12.10	17.81	80.73	84.31
	K_I (mg L^{-1})	3248	4127	2972	3708
	K (mg L^{-1})	10.004	37.4	20.17	13.42
	R^2	0.932	0.941	0.992	0.995
	SD_{avg}	0.012	0.010	0.021	0.027
Edward (Edwards, 1970): $q = q_{max}\left[\exp\left(\frac{-S_0}{K_I}\right) - \exp\left(\frac{-S_0}{K_S}\right)\right]$	q_{max} (h^{-1})	0.33	0.12	0.25	0.19
	K_S (mg L^{-1})	10.10	22.29	55.19	80.61
	K_I (mg L^{-1})	2310	3412	2312	2728
	R^2	0.962	0.921	0.965	0.984
	SD_{avg}	0.280	0.115	0.521	0.195

The analysis of the degradation kinetics by model-fitting shows that the Yano model, among all the three models used in the present study, predicts the experimental data fairly well for all the cases (Table 4.1.1). The Haldane model also fits the experimental data reasonably well giving the best fit for immobilized AKG1 (R^2 =0.963, SD_{avg} =0.044) and second best for free AKG2 (R^2 =0.981, SD_{avg} =0.012) (Table 4.1.1). Edward model, on the other hand, shows high R^2 values but suffers from high standard deviation which is almost ten times higher than that of the Haldane and Yano model. As the evaluation of the biokinetic parameters are greatly sensitive to their initial guess values (used as input for regression analysis) and inappropriate initial guess values may lead to erroneous values of biokinetic parameters compromising the accuracy of predicted degradation profiles, sensitivity for estimating these parameters were further analyzed. Here, four different sets of biokinetic parameters (q, K_S and K_I) values were used as initial guesses as indicated in Table 4.1.2. Degradation profiles were simulated applying all the three models using the estimated biokinetic parameters for different sets of initial guess values. The coefficient of determination (R^2) for each case was determined and summarized in Table 4.1.2. The sensitivity analysis (Table 4.1.2) shows that the Haldane model is the most consistent among the three models. Previously, El-Naas et al. (2009) also reported the successful fitting of Haldane model in describing the degradation kinetics of phenol by *P. putida* immobilized in poly-vinyl alcohol (PVA) gel. The higher K_I values of the immobilized cells as compared to corresponding free cells (Table 4.1.1), demonstrate the improved resistance to substrate inhibition in the immobilized cells. The Haldane model predicts the K_I values for the immobilized AKG1 and AKG2 cells as 6210 mg L^{-1} and 9108 mg L^{-1}, respectively.

Table 4.1.2. Initial guess values and the corresponding coefficient of determination (R^2)

Initial Value	R^2											
	Haldane Model				**Yano Model**				**Edward Model**			
	AKG1	*AKG2*	*Immo AKG1*	*Immo AKG2*	*AKG1*	*AKG2*	*Immo AKG1*	*Immo AKG2*	*AKG1*	*AKG2*	*Immo AKG1*	*Immo AKG2*
Case1: $q<1$, $K_S<1$, $K_I<1$	0.840	0.902	0.963	0.923	0.912	0.261	0.622	0.022	−2.941	0.277	0.202	0.653
Case 2: $q<1$, $K_S>1$, $K_I>1$	0.839	0.981	0.963	0.961	0.932	0.992	0.941	0.995	0.962	0.965	0.921	0.984
Case 3: $q=1$, $K_S>1$, $K_I>1$	0.770	0.872	0.843	0.937	0.858	0.992	0.874	0.986	0.952	0.741	0.601	0.655
Case 4: $q>1$, $K_S<1$, $K_I<1$	0.830	0.897	0.950	0.939	0.690	0.969	0.329	0.417	0.821	0.793	0.162	0.126

4.1.6. Conclusions

The degradation kinetics of phenol by free as well as immobilized *B. cereus* AKG1 MTCC9817 and AKG2 MTCC9818 were investigated and the optimum pH and alginate concentration for maximal degradation were determined. The enhanced tolerance of the immobilized cells to higher phenol level (up to 2000 mg L^{-1}) compared to free cells has been demonstrated. Moreover, the excellent storage stability of the immobilized strains and their potential application in repeated batch biodegradation have also been shown. The degradation kinetics could well be fitted by the Haldane model as well as Yano model. The insight gained in the present study for the potential of the immobilized *B. cereus* (AKG1 MTCC9817 and AKG2 MTCC9818) towards high phenol degradation can be extended for industrial effluent treatment.

4.2. BIODEGRADATION OF PETROLEUM WASTEWATER

4.2.1. Introduction

The high demand of petroleum and associated products during the last ten decades has made petroleum spills inevitable consequences of oil production and refining. As a result, the problem of pollution during production and transportation of refinery products would remain a major issue. Various organic compounds including phenol and other phenolics are the major components of refinery industrial effluents. Most of these compounds are also used in the preparation of antiseptics, dyes, synthetic resins, biocides, photographic chemicals, inks, and varnishes (Sittig, 1997; Patterson, 1985; Berkowitz, 1988). The toxic pollutants present in the petroleum wastewater pose serious environmental threats and critical health hazards even at low concentrations. The microbial treatment of petroleum wastewater for the reduction of pollutant level is one of the viable options to address this issue.

In this regard, as discussed in previous chapters, two phenol degrading bacterial strains (*Bacillus cereus* AKG1 MTCC9817 and *Bacillus cereus* AKG2 MTCC9818) have been isolated and demonstrated their excellent biodegradation efficacies for phenol as well as real petroleum wastewater samples in free cell based studies. Furthermore, the degradation of phenol by immobilized culture of these strains has also been investigated. Hence, in the present context, the microbial treatment of real petroleum wastewater samples by the immobilized AKG1 and AKG2 merits further investigation.

4.2.2. Literature Review

Various regulatory water authorities have imposed strict limits to refinery waste concentration in industrial discharge streams (Singleton, 1994). According to the United States Environmental Protection Agency (USEPA), a phenol concentration of 0.5 mg L^{-1} is the limit for wastewater that can be discharged into natural water bodies, land or municipal sewerage systems. For drinking waters, the limit is 1 µg L^{-1} (WHO, 1994). The permissible limit for oil and grease is 15 mg L^{-1} and for benzene and ethyl benzene are 5 µg L^{-1} and 0.7 mg L^{-1}, respectively.

The detailed information on microbial degradation behavior of real petroleum wastewater is limited. Tyagi et al. (1993) investigated the biodegradation of a

petroleum refinery wastewater in a modified rotating biological contactor (RBC), in which the removal efficiency of the total COD and oil were above 87 and 80%, respectively. A new fixed-film bioreactor system was constructed by Jou and Huang (2003) to investigate the biodegradation of industrial oil refinery wastewater. A consistent COD removal efficiency of more than 85% and nearly complete degradation of phenol from industrial oil refinery wastewater was reported by the authors. Nardi et al. (2005) investigated the biodegradability of gasoline contaminated wastewater in bench-scale horizontal-flow anaerobic immobilized biomass (HAIB) reactors and a COD removal efficiency of 99% was reported.

4.2.3. Outline of the Research Work

1) The degradation of real petroleum wastewater samples, collected from two different origins (Sample I from oil refinery site and Sample II from oil exploration site), by Ca-alginate immobilized *B. cereus* (AKG1 MTCC9817 and AKG2 MTCC9818) strains has been carried out in batch mode.
2) The degradation performances of the immobilized strains have been analyzed by measuring chemical oxygen demand (COD), total organic carbon (TOC), biological oxygen demand (BOD) and ammonium nitrogen (NH_4^+–N) level.
3) Finally, the biodegradation efficacies of the immobilized strains in treating petroleum wastewater samples have been compared with those of free cells.

4.2.4. Experimental Section

4.2.4.1. Chemicals and Culture Medium

The details of chemicals and culture medium have been described in *Section 2.4.1* in **Chapter 2**.

4.2.4.2. Microorganism and Culture Conditions

The isolated strains AKG1 and AKG2 (Banerjee and Ghoshal, 2010a) were grown in phenol containing MSM medium as discussed in *Section 3.1.4.2* of **Chapter 3**.

4.2.4.3. Immobilization of Bacterial Cell in Alginate Beads

The immobilization of bacterial cells was performed by the method described in *Section 4.1.4.2* (**Chapter 4**) with final alginate concentration of 3% (w/v).

4.2.4.4. Batch Biodegradation Study

To carry out the biodegradation of the petroleum wastewater, 100 mL of pre-autoclaved wastewater samples were incubated with 25 g (wet weight) of immobilized beads containing AKG1 or AKG2 in conical flasks at their optimum temperature 37 °C at 120 rpm for the desired period of time. During the experiment, 2 mL of samples were withdrawn at regular interval and analyzed for COD, TOC, BOD and NH_4^+–N, based on the standard methods (APHA, 1998). The detailed methods of measuring COD (*Section 3.2.4.4*), TOC (*Section 3.2.4.5*), BOD (*Section 3.2.4.6*) and NH_4^+–N (*Section 3.2.4.7*) have been described in **Chapter 3**.

4.2.5. Results and Discussion

4.2.5.1. Removal of COD from the Wastewater

Figure 4.2.1(a) and (b) show the percentage COD removal by the immobilized bacteria from influent wastewater samples, Sample I and Sample II, respectively. After 20 days of treatment, immobilized AKG1 and AKG2 reduced the COD level of Sample I by 24.32% and 10.81%, respectively. For Sample II, both the immobilized strain reduced COD by 10.25%, after 20 days. The COD removal by immobilized bacteria, even after 20 days, was substantially lower than the free cell or co-culture (Table 4.2.1). Table 4.2.1 shows that addition of external nitrogen, unlike the free cell system, did not have any significant effect on COD removal by immobilized system. As discussed in **Section 4.1**, the diffusion coefficient is the key parameter responsible for such slow rate of COD removal by the immobilized systems.

4.2.5.2. Removal of TOC from the Wastewater

The initial TOC content in the wastewater was 1550 and 1680 mg L^{-1} in Sample I and Sample II, respectively. The reduction in TOC level in wastewater sample during the microbial treatment by immobilized cells is shown in Figure 4.2.2. As evident from the figure, the TOC removal gradually increased with time in both the wastewater samples and immobilized AKG1 was better than immobilized AKG2 in this regard with 18.75% and 13.30% TOC removal from Sample I and Sample II, respectively. However, the immobilized strains were less effective than the free-cell systems in reducing the TOC level of the samples as shown in Table 4.2.2 which represent the comparative TOC

removal efficiencies of different systems after 20 days in the absence of any external nitrogen source.

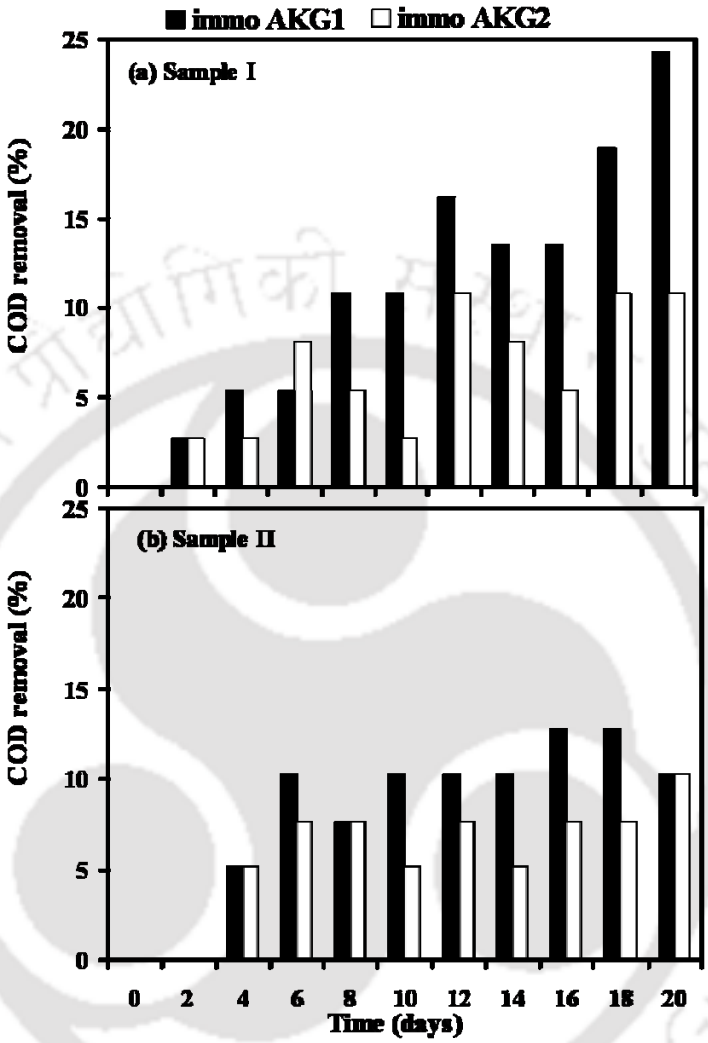

Figure 4.2.1. COD removal from wastewater samples (Sample I (a) and II (b)) by immobilized AKG1 and immobilized AKG2 in absence of external nitrogen source.

Table 4.2.1: Overall performance by various systems for COD removal after 20 days

	COD removal (%)					
	Without external nitrogen supplement		**Organic nitrogen supplement** (Yeast)		**Inorganic nitrogen supplement** (Ammonium Sulfate)	
	Sample I	*Sample II*	*Sample I*	*Sample II*	*Sample I*	*Sample II*
Free AKG1	61.11	34.14	69.44	51.21	66.66	41.46
Free AKG2	41.66	61.53	55.55	69.23	47.22	64.10
Co-culture	83.78	70	89.18	79.5	86.48	72.5
Immobilized AKG1	24.32	10.25	24.12	10.02	24.40	10.25
Immobilized AKG2	10.81	10.25	10.50	10.33	10.10	10.75

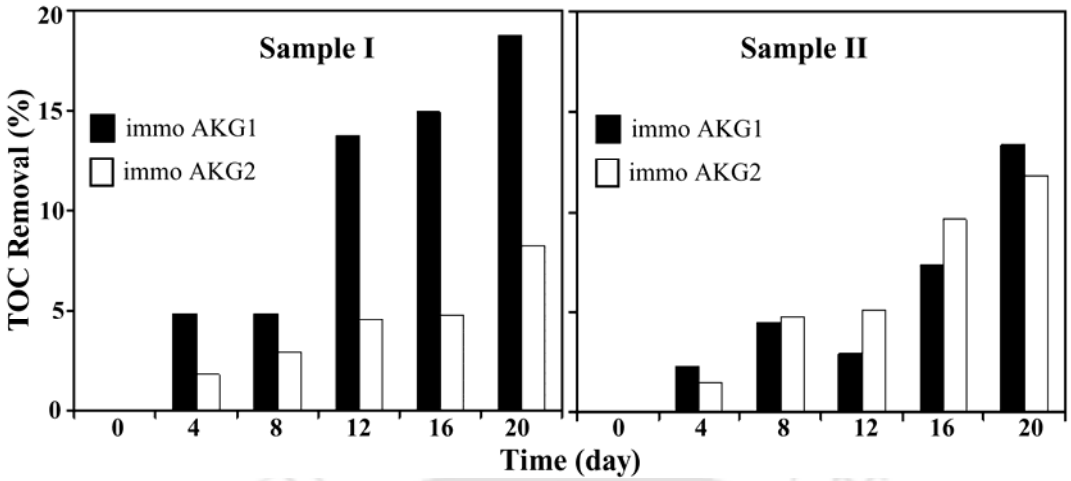

Figure 4.2.2. TOC removal from wastewater samples (Sample I and II) by immobilized AKG1 and immobilized AKG2 in absence of external nitrogen source.

Table 4.2.2: TOC removal (%) performance by various systems after 20 days

	Free AKG1	Free AKG2	Co-culture	Immo AKG1	Immo AKG2
Sample I	57.12	34.68	83.45	18.75	8.29
Sample II	30.00	41.59	54.00	13.30	11.80

4.2.5.3. Analysis of BOD in the Wastewater

Figure 4.2.3 shows the BOD level in the wastewater samples during the period of microbial treatment. The initial BOD of the wastewater was 180 mg L^{-1} and 420 mg L^{-1} in Sample I and Sample II, respectively. As evident from Figure 4.2.3, the BOD removal gradually increased with time in the wastewater samples. The immobilized AKG1 was better than immobilized AKG2 in increasing the BOD level in Sample I. On the other hand, immobilized AKG2 was more efficient in this regard for Sample II after 20 days of microbial treatment. On comparison with the performance of the free cells (Table 4.2.3), it was found that the immobilized bacteria were not as efficient as free cells in improving the BOD level of the petroleum wastewater sample.

As discussed earlier in **Section 3.2**, the index of biodegradability performance (Sun et al., 2008), defined as the BOD/COD ratio, was increased to 0.07 and 0.05 from as low as 0.03 in Sample I by the immobilized AKG1 and AKG2, respectively (Figure 4.2.4). The BOD/COD ratio in Sample II was increased from 0.065 to 0.12 and 0.15 by the immobilized AKG1 and AKG2, respectively (Figure 4.2.4). It may be mentioned hare that a BOD/COD ratio of 0.9~1.0 is generally considered as cut-off point for the

biodegradable wastewater (Contreras et. al., 2003; Gaetano J.C. 1999). However, as evident from Figure 4.2.4, the increase in the BOD/COD ratio was pronounced in Sample II as compared to Sample I. Moreover, the BOD/COD ratio was lower in microbial treatment by immobilized strains as compared to that of free cells.

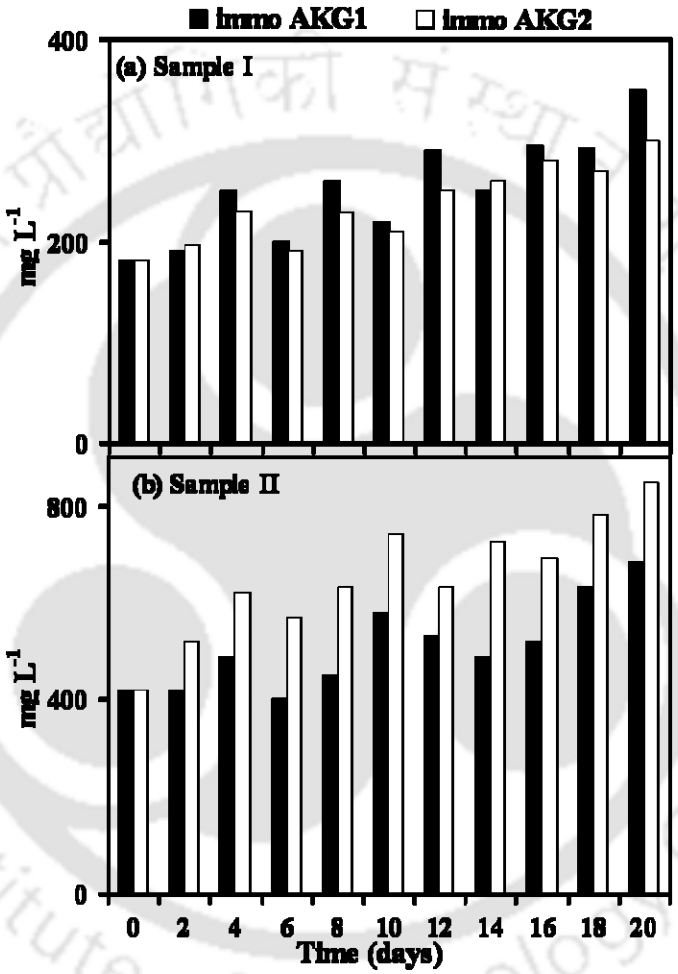

Figure 4.2.3. The BOD level in the wastewater samples during the microbial treatment by AKG1, AKG2 and the co-culture.

Table 4.2.3: BOD of the wastewater after microbial treatment by various systems for 20 days

	BOD (mg L^{-1})				
	Free AKG1	**Free AKG2**	**Co-culture**	**Immo AKG1**	**Immo AKG2**
Sample I	672	524	861	350	299
Sample II	997	1237	1532	685	846

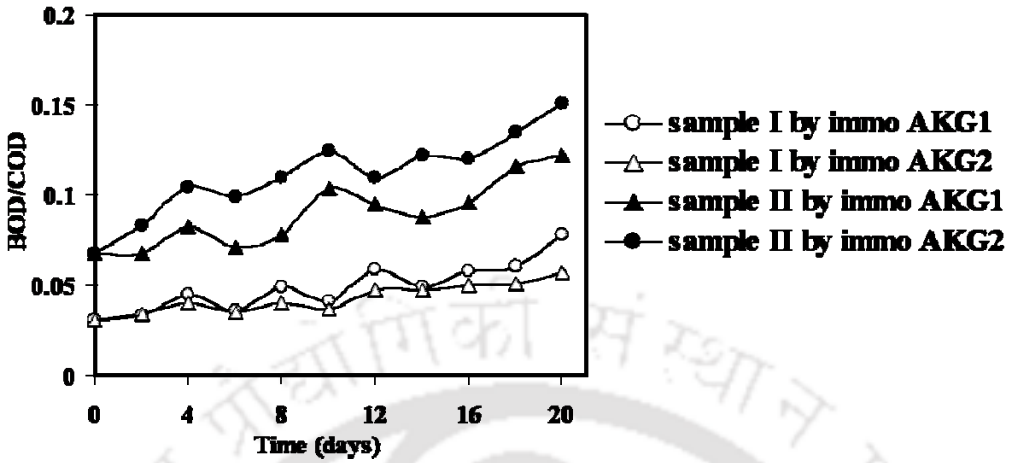

Figure 4.2.4. The BOD/COD ratio of the wastewater samples during the microbial treatment by the immobilized strains.

4.2.5.4. Removal of Ammonium Nitrogen (NH_4^+−N) from the Wastewater

Figures 4.2.5 shows the amount of NH_4^+−N in the wastewater samples I and II during the microbial treatment by the immobilized strains. It is clear from the figure that the treatment gradually reduced the NH_4^+−N level in the wastewater samples. The immobilized AKG2 was more efficient than immobilized AKG1 in removing the NH_4^+−N from both the wastewater samples. The NH_4^+−N content was reduced by 38.5% and 42.4% in Sample I and Sample II, respectively, by the immobilized AKG2. The amount of NH_4^+−N removal by different systems, namely free cells, co-culture and immobilized cells, is listed in Table 4.2.4. As evident from the table, the immobilized system was not as effective as the free cells in reducing the NH_4^+−N level from the wastewater.

It is worth mentioning here that the diffusion coefficient, as discussed earlier in **Section 4.1**, is the key responsible parameter for the observed lower performance of the immobilized system as compared to the free one in various wastewater treatment parameters such COD removal, TOC removal, improvement of BOD and ammonium nitrogen removal.

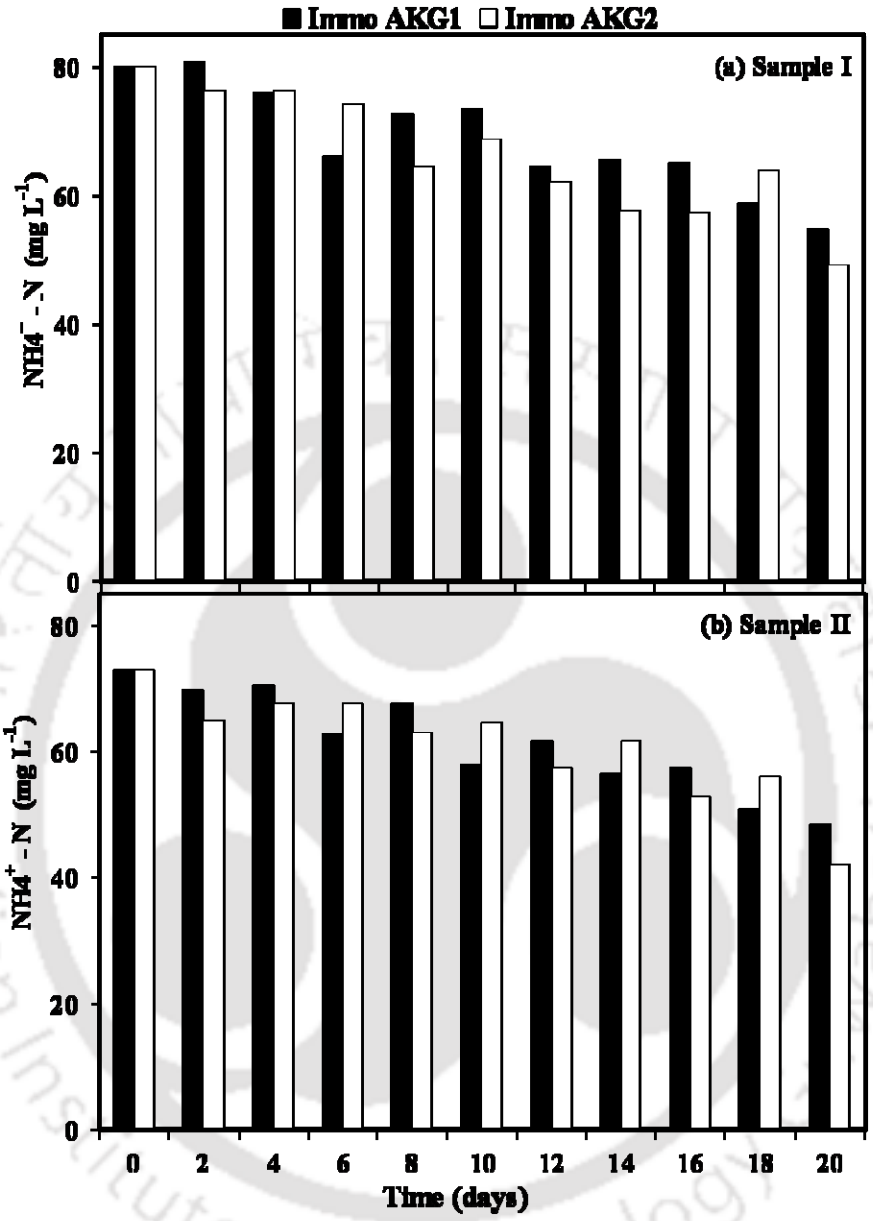

Figure 4.2.5. The ammonium nitrogen (NH_4^+–N) level in the wastewater samples during the microbial treatment by immobilized AKG1 and AKG2.

Table 4.2.4: Performance by various systems for ammonium- nitrogen (NH_4^+–N) reduction (%)

	Free AKG1	Free AKG2	Co-culture	Immo AKG1	Immo AKG2
Sample I	54	47.5	68.12	31.5	38.5
Sample II	55.34	82.46	69.45	33.83	42.46

4.2.6. Conclusions

The biodegradation of two real petroleum wastewater samples by immobilized AKG1 and AKG2 have been investigated and the concurrent changes in COD, TOC, BOD and NH_4^+− N contents have been evaluated. After 20 days of microbial treatment, COD removal was 24% and 10% in Sample I and Sample II, respectively, by immobilized AKG1. Immobilized AKG2 removed 10% of initial COD from both Sample I and Sample II. Addition of external nitrogen source, unlike the free cell systems, did not improve the biodegradation efficiencies of the immobilized strain significantly. Immobilized AKG1 reduced the TOC and NH_4^+−N level by 18% and 31% in Sample I, and 13% and 33% in Sample II, respectively. TOC and NH_4^+−N removal was 8% and 38% in Sample I, and 11% and 42% in Sample II, respectively, in case of immobilized AKG2. The BOD level of Sample I was increased by 1.9 and 1.6 times by immobilized AKG1 and immobilized AKG2, respectively. On the other hand, the same was increased by 1.6 and 2 times in Sample II by immobilized AKG1 and immobilized AKG2, respectively. However, when the biodegradation capabilities were compared, the immobilized cells were found to be less effective than the free cell systems in treating the petroleum wastewater samples.

CHAPTER 5

Degradation Study using Immobilized Cell Cultures

Chapter 5, divided into three parts, describes the implication of lab-scale bioreactor for wastewater treatment by immobilized B. cereus strains. The performance of immobilized strains for phenol degradation in a packed bed reactor and the combined effect of external mass transfer with biochemical reaction on the mass transfer correlation, determined in terms of Colburn factor (J_D) and Reynolds number (N_{Re}), has been reported in Section 5.1.

Section 5.2 presents biodegradation of petroleum wastewater in re-circulated packed bed reactor by the isolated strains immobilized in Ca-alginate beads and polyurethane foam cubes. The results demonstrated excellent efficacy of the immobilized strains in treating petroleum wastewater in packed bed reactor.

A preliminary study on the biodegradation of petroleum wastewater by immobilized bacterial strains in re-circulated fluidized bed reactors has also been included in Section 5.3.

Chapter 5

DEGRADATION STUDY USING IMMOBILIZED CELL CULTURES

5.1. PHENOL BIODEGRADATION IN PACKED BED REACTORS

5.1.1. Introduction

Among the hazardous pollutants present in the petroleum wastewater, phenol and other phenolic compounds pose serious environmental issues by contaminating nearby water sources (Naas et al., 2009; Mollaei et al., 2010). In addition to being lethal to fish at concentration as low as 5–25 ppm (Santos et al., 2009), human exposure to phenol causes critical health hazards and possible carcinogenesis (Naas et al., 2009). In this regard, biodegradation of phenol to reduce the phenol level in industrial effluents to environmentally acceptable limits has drawn considerable interest among the researchers (Cardoso et al., 2009; Banerjee and Ghoshal, 2010a; 2010b). To this end, the recycling mode of degrading toxic pollutants by the immobilized biomass, as compared to the batch mode, offers several advantages including the simplicity of automation and control resulting in a reduced operational cost and enhanced degradation (Tepe and Dursun, 2008; Sheeja and Murugesan, 2002). The packed bed reactor (PBR) is very convenient one among the wide range of reactor designs available for re-circulated operation with immobilized cells (Livingston and Chase, 1991; Quail and Hill, 1991).

Hence, it is intended to investigate the phenol biodegradation performance of the immobilized strains of isolated *B. cereus* AKG1 MTCC9817 and *B. cereus* AKG2 MTCC9818 in a packed bed reactor. The knowledge of the phenol biodegradation kinetics and the mass transfer correlations in the packed bed reactor is critical for the scale-up and successful application of these immobilized strains in the microbial treatment of real petroleum wastewater in the industrial scale.

5.1.2. Literature Review

The substrate inhibition of microbial growth at higher concentrations of toxic pollutants such as phenol remains a critical challenge in biodegradation of industrial wastewater (Wang and Loh, 1999). The immobilization of microorganisms on various supports has shown its potential for improving biodegradation efficiency in terms of sustainability as compared to free cells (Ehrhardt and Rehm, 1989). Whole cell entrapment in bio-polymeric beads (Mattiasson, 1983) is one of the most well established methods of cell immobilization where immobilized cells show improved cell viability and can tolerate higher concentrations of toxicants for longer duration (Patil et al., 2006; Ha et al., 2009). In this respect, Ca-alginate beads have been extensively studied for efficient entrapment of microbial cells owing to their low toxicity, ease of use and low cost (Gonzalez et al., 2001; Kathiravan et al., 2010).

The PBR, from the process–engineering perspective, has various advantages including high-yield operation, ease of scaling-up, possible automation of separation process leading to high degrees of purification, opportunity of treating large volume of wastewater treated by a specified quantity of immobilized cells, and reuse of biomass (Karel et al., 1985; Aksu and Bulbul, 1998; Tepe and Dursun, 2008). Although the successful biodegradation of various toxic materials by immobilized cells in PBRs have been widely reported (Zilouei et al., 2006; Waul et al., 2008; Kathiravan et al., 2010), there are only few reports on degradation of phenol in PBRs using cell-immobilized alginate beads as packing material and that too using *B. cereus* as the strain. In one of the early reports, Aksu and Bulbul (1998) investigated the combined effects of external mass transfer and biodegradation rates on phenol removal by immobilized *Pseudomonas putida* in a PBR. Later, Sheeja and Murugesan (2002) systematically studied the biodegradation of phenol and phenolic effluents by alginate immobilized *Pseudomonas pictorum* in an up-flow PBR. Apart from the extensively studied *Pseudomonas sp.*, recent attention has been drawn towards isolating and employing novel microorganisms for degrading phenol and phenolics more efficiently. To this end, the biodegradation of phenol by Ca-alginate immobilized *R. eutropha* in a PBR has been reported by Tepe and Dursun (2008). Furthermore, the parameters related to mass transfer are critical for the scale-up of PBR operation in recycle mode as the internal and external mass transfer resistances have been reported to limit the mass transfer effects on immobilized particles in PBR (Murty et al., 2005).

5.1.3. Outline of the Research Work

1) Biodegradation of phenol by immobilized *B. cereus* AKG1 MTCC9817 and *B. cereus* AKG2 MTCC9818 in a packed bed reactor has been performed.
2) The observed biodegradation rate constants have been calculated at various flow rates by assuming first-order biodegradation kinetics.
3) The effect of external mass transfer combined with intrinsic biodegradation reaction on the observed biodegradation was investigated by the correlation between the Colburn factor (J_D) and Reynolds number (N_{Re}) as $J_D = K\, N_{\mathrm{Re}}^{-(1-n)}$.

5.1.4. Theory

5.1.4.1. Biodegradation and Observed Rate Constant

The material balance for phenol (substrate) in the PBR at steady state, considering spherical immobilized beads, no axial dispersion and plug flow, can be established as (Smith, 1987; Tepe and Dursun, 2008):

$$\left(\frac{hQ}{W}\right)\frac{dC}{dz} = -r \qquad (5.1.1)$$

where h is the height of the column (cm), Q is the volumetric flow rate (L h^{-1}), W is the total amount of dried cells in the immobilized particles (g), dC/dz is the concentration gradient along the column length (mg L^{-1} cm^{-1}) and r is the biodegradation rate (mg g^{-1} h^{-1}).

Assuming first-order biodegradation (a valid assumption at low phenol concentrations (Dursun and Tepe 2005)), the relation between the observed biodegradation rate constant k_p (L g^{-1} h^{-1}) and phenol concentration C (mg L^{-1}) in PBR can be expressed as:

$$r = k_p C \qquad (5.1.2)$$

Combining Eq. (5.1.1) and Eq. (5.1.2), the following equation can be obtained:

$$\left(\frac{hQ}{W}\right)\frac{dC}{dz} = -k_p C \qquad (5.1.3)$$

Integrating Eq. (5.1.3) with boundary condition of $C = C_0$ at $z = 0$ and $C = C$ at $z = h$, Eq. (5.1.4) is obtained:

$$\ln\left(\frac{C_0}{C}\right) = \frac{W}{Q}k_p \qquad (5.1.4)$$

where, C and C_0 are the exit and inlet phenol concentrations (mg L^{-1}), respectively. Different values of k_p can be calculated by using Eq. (5.1.4) at different initial flow rates with constant dried biomass amount in the immobilized beads (Smith, 1987; Nath and Chand, 1996; Tepe and Dursun, 2008).

5.1.4.2. Mass Transfer and External Film Diffusion

As the fluid passes over the immobilized beads in a PBR, regions develop near the periphery of the beads where the velocity of the fluid is very low (Nath and Chand, 1996). A near-stagnant film of fluid exists in such regions around the surface of the beads. Now, the substrate (phenol in the present study) needs to be transported through this fluid film, primarily by molecular diffusion. The observed reaction rate, hence, can be significantly affected by this external film diffusion (Nath and Chand, 1996; Aksu and Bulbul, 1998).

The rate of film diffusion of the substrate (phenol) from the bulk fluid to the surface of the immobilized cells should be proportional to the area for mass transfer and the driving force for mass transfer which can be expressed by the concentration difference between the bulk and the external surface of the immobilized biomass. Hence, the following equation can be developed for the mass transfer:

$$r_m = k_m A_m (C - C_S) \tag{5.1.5}$$

where r_m is the mass transfer rate (mg g^{-1} h^{-1}), k_m is the external mass transfer coefficient (L cm^{-2} h^{-1}), A_m is the surface area per unit weight of immobilized beads for mass transfer (cm^2 g^{-1}), C is the phenol concentration in bulk liquid and C_S is the phenol concentration at the surface of immobilized cell (mg L^{-1}).

The value of A_m can be calculated by the following equation (Aksu and Bulbul, 1998):

$$A_m = \frac{6}{\rho_p d_p} \tag{5.1.6}$$

where d_p is the bead diameter (cm) and ρ_p is the density of the bead (g cm^{-3}).

5.1.4.3. Mass Transfer and Biodegradation: Combined Effect on Observed Degradation Rate

The first-order biodegradation rate of phenol by immobilized beads can be expressed as (Nath and Chand, 1996):

$$r = kA_m C_S \tag{5.1.7}$$

where r and k stand for phenol removal rate (mg g^{-1} h^{-1}) and intrinsic first-order biodegradation rate constant (L cm^{-2} h^{-1}), respectively.

Now, the rate of phenol removal and the rate of mass transfer will be same at steady state. Hence, equating Eq. (5.1.5) and (5.1.7), the unknown surface concentration (C_S) can be calculated as:

$$C_S = \frac{k_m C}{k + k_m} \tag{5.1.8}$$

From Eq. (5.1.2), (5.1.7) and (5.1.8), the observed biodegradation rate (k_p) can be expressed as:

$$k_p = \frac{k k_m A_m}{k + k_m} \tag{5.1.9}$$

or

$$\frac{1}{k_p} = \frac{1}{k_m A_m} + \frac{1}{k A_m} \tag{5.1.10}$$

Eq. (5.1.10) shows the combined effect of biodegradation and mass transfer rates on the observed rate of phenol biodegradation.

5.1.4.4. Determination of the Mass Transfer Correlation

Commonly, the mass transfer coefficient is correlated with the variables of flow rate, reactor diameter and fluid properties through the dimensionless group J_D, defined as (Levenspiel, 1972; Nath and Chand, 1996; Kathiravan et al., 2010; Dizge and Tansel, 2010):

$$J_D = \frac{k_m \rho}{G}\left(\frac{\mu}{\rho D_f}\right)^{2/3} = K\, N_{\mathrm{Re}}^{\text{-(1-}n)} \tag{5.1.11}$$

where J_D is the Colburn factor and defined in terms of Reynolds number (N_{Re}). In Eq. (5.1.10), D_f, ρ and μ represent the diffusivity, density and viscosity of feed fluid, respectively. G (g cm^{-2} h^{-1}) is the superficial mass velocity which can be calculated as:

$$G = \frac{Q\rho}{1000 \times A} \tag{5.1.12}$$

The external mass transfer coefficient can be affected depending on the different values of K and n. Various mass transfer correlations having different values of K and n have been reported in literature. The value of n, in these reports, varies from 0.1 to 1.0

(Bailey and Ollis, 1987; Nath and Chand, 1996; Kathiravan et al., 2010; Dizge and Tansel, 2010).

From Eq. (5.1.11), the mass transfer coefficient can be expressed as:

$$k_m = NG^n \tag{5.1.13}$$

where,

$$N = \frac{K}{\rho}\left(\frac{\mu}{\rho D_f}\right)^{-2/3}\left(\frac{d_p}{\mu}\right)^{-(1-n)} \tag{5.1.14}$$

Substituting Eq. (5.1.13) in Eq. (5.1.10), the following equation can be developed:

$$\frac{1}{k_p} = \left(\frac{1}{NA_m}\right)\left(\frac{1}{G^n}\right) + \frac{1}{kA_m} \tag{5.1.15}$$

Eq. (5.1.15) implies that the plot of $\frac{1}{k_p}$ vs. $\frac{1}{G^n}$, based on the experimentally measured values, will yield a straight line with slope of $\frac{1}{NA_m}$ and intercept of $\frac{1}{kA_m}$. Thus, by assuming different values of K and n, various A_m values can be calculated. Now, comparing these calculated values of A_m with the experimentally obtained A_m value, most suitable n and K values can be predicted to propose the best external mass transfer correlation for our present study of phenol biodegradation by immobilized cells in PBR.

5.1.5. Experimental Section

5.1.5.1. Microorganisms and Culture Medium

The details of microorganisms and culture medium have already been described in *Section 3.1.4.2* in **Chapter 3** and *Section 2.4.1* in **Chapter 2**, respectively.

5.1.5.2. Immobilization of Bacterial Cell in Alginate Beads

The phenol degrading bacteria (AKG1 MTCC9817 and AKG2 MTCC9818) were harvested after 12 h of growth by centrifugation at 5,000 rpm for 10 min. The cell pellet of AKG1 (12.03 g dry weight containing 1.029×10^{27} cfu) and AKG2 (13.39 g dry weight containing 1.050×10^{27} cfu) were collected together and subsequently resuspended in phosphate buffered saline (PBS). A stock of 5 % (w/v) sodium alginate

was prepared in the MSM medium and autoclaved at 121 °C for 15 min. Total bacterial cell suspension (25.42 g dry weight containing 2.07 $\times 10^{27}$ cfu) was added to 200 mL of sterilized alginate solution (3%, w/v) and mixed by stirring on a magnetic stirrer. The alginate–cell mixture was extruded drop by drop into a cold sterile 0.1 M calcium chloride solution ($CaCl_2$) using a peristaltic pump with 70 mL h^{-1} flow rate. The drops of alginate–cell solution were gelled to form uniform-sized (0.35 cm) sphere upon contact with $CaCl_2$ solution. The immobilized beads were kept in 0.2 M $CaCl_2$ solution at room temperature for 1 h to complete the gel formation. The beads were then rinsed with MSM followed by distilled water to remove residual $CaCl_2$. It may be mentioned here that AKG1 and AKG2 were immobilized together in the Ca-alginate beads for the biodegradation of phenolic wastewater in the PBR because co-culture of the isolated strains was found to be more efficient than individual free cultures in degrading petroleum wastewater, as already discussed in **Section 3.2**.

5.1.5.3. Packed Bed Reactor Setup

The PBR used for the biodegradation of phenol in the present study was a tubular system with an internal diameter of 5 cm and 100 cm in height as shown schematically in Figure 5.1.1(a). The picture of the experimental set-up is given in Figure 5.1.1(b). The reactor bed (54 cm high) was constructed by placing two circular discs, joined together with a cylindrical rod, inside the tubular system. The active bed volume was calculated to be 1017.9 cm^3 and packed with 0.35 cm immobilized alginate beads containing AKG1 and AKG2 equivalent to 25.42 g of dried microorganism. The average density of immobilized beads was measured to be 1.254 g cm^{-3}. The feed solution was prepared by diluting stock solution of phenol with MSM (without any Yeast extract) to desired concentration and fed to the reactor from the bottom in an up-flow mode of operation with recycling. Outlet was collected at regular intervals from the top of the reactor in order to measure the residual phenol concentration. All the biodegradation experiments were carried out at room temperature (~30 °C).

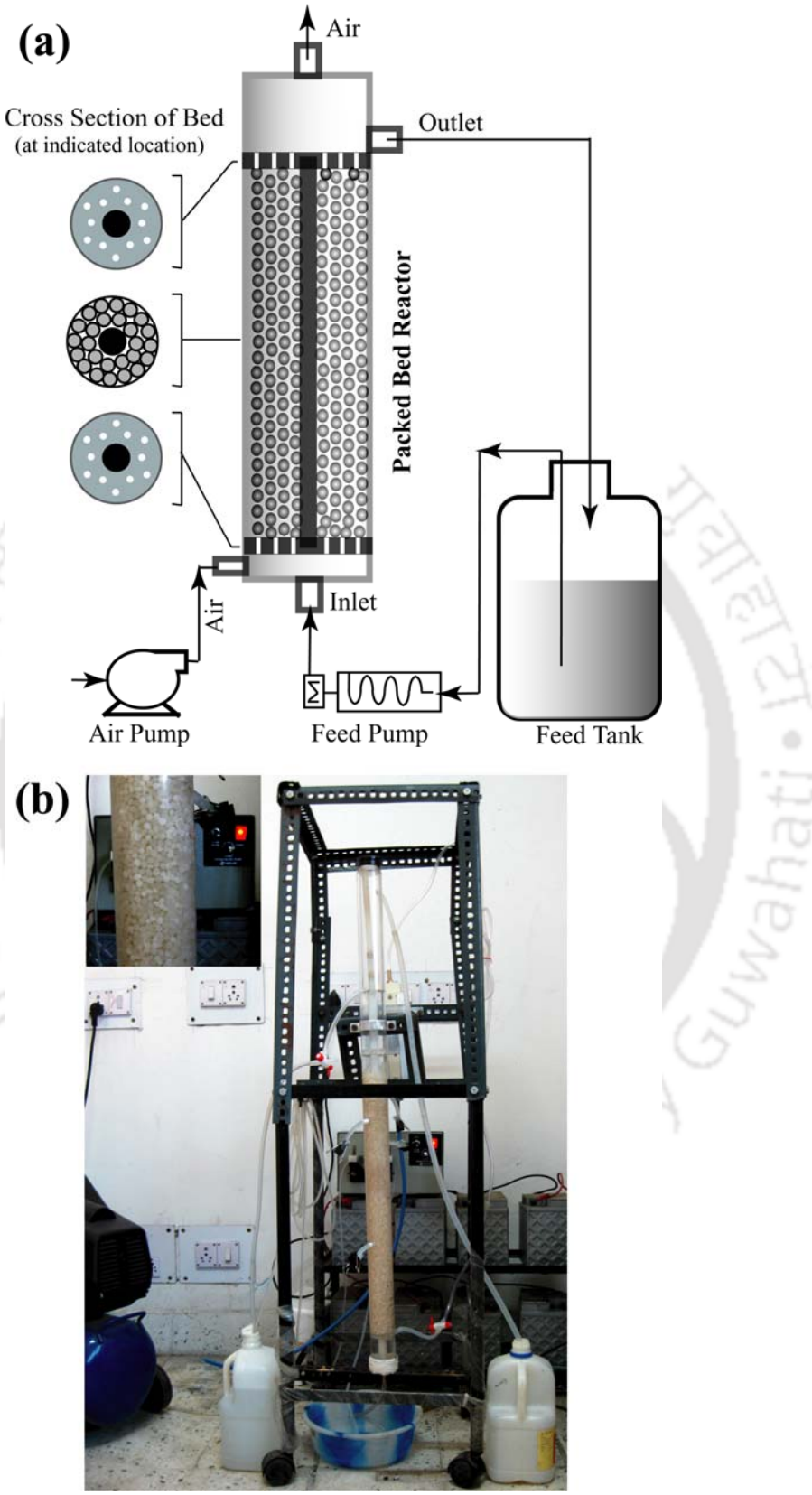

Figure 5.1.1. (a) Schematic representation of the re-circulated up-flow packed bed reactor (dimensions are not in scale). **(b)** Experimental set-up, (inset) Closer view of the reactor bed.

5.1.5.4. Analysis of Phenol Concentration

The concentration of residual phenol in the outlet solution was determined by spectrophotometric method (Eaton and Franson, 2005). In brief, 2.5 mL 0.5N NH_4OH solution was added to 100 mL of appropriately diluted sample and the pH was adjusted to 7.9 ±0.1 with phosphate buffer. Then, 1.0 mL 4-aminoantipyrine and 1.0 mL potassium ferricyanide solution were added sequentially and mixed well after each addition. After 15 min, absorbance of the colored antipyrine dye formed was recorded at 500 nm. Finally, the residual phenol concentration was determined from the calibration curve constructed from the phenol standards.

5.1.6. Results and Discussion

5.1.6.1. Effect of Initial Phenol Concentration and Flow Rate on Biodegradation

As predicted from the mass transfer considerations, operating parameters such as initial substrate concentration, flow rate, particle and column size and amount of biomass play crucial role in affecting the biodegradation rate observed in a re-circulated up-flow PBR (Sheeja and Murugesan, 2002). The influence of initial phenol concentration on the biodegradation was studied with a wide range of phenol concentration varying from 50 to 1500 mg L^{-1}. The phenol degradation profile of alginate immobilized *Bacillus sp.* in the PBR at various initial phenol concentrations is shown in Figure 5.1.2 (a). The figure reveals that the % phenol removal, after a specified time interval, gradually decreased with increasing initial phenol concentration. For example, complete degradation of phenol was observed after 20 h at initial concentration of 200 mg L^{-1} whereas about 170 h were required for complete phenol degradation at 1500 mg L^{-1} initial concentration. This is because of the fixed amount of biomass in the packed bed, which can degrade a certain amount of phenol in the feed. Anything more has to be treated for longer duration. This fact can further be evident from Figure 5.1.2 (b) which shows the variation of number of cycles, required for particular amount of phenol degradation (%), with varying concentration of phenol. It can be seen from Figure 5.1.2 (b) that there is a jump in the number of cycles as the initial phenol concentration is 750 mg L^{-1} or more. This phenomenon is also irrespective of the percentage removal. This behaviour corroborates the fact of biomass limiting phenomena in an immobilized bed and also the inhibition effect of phenol.

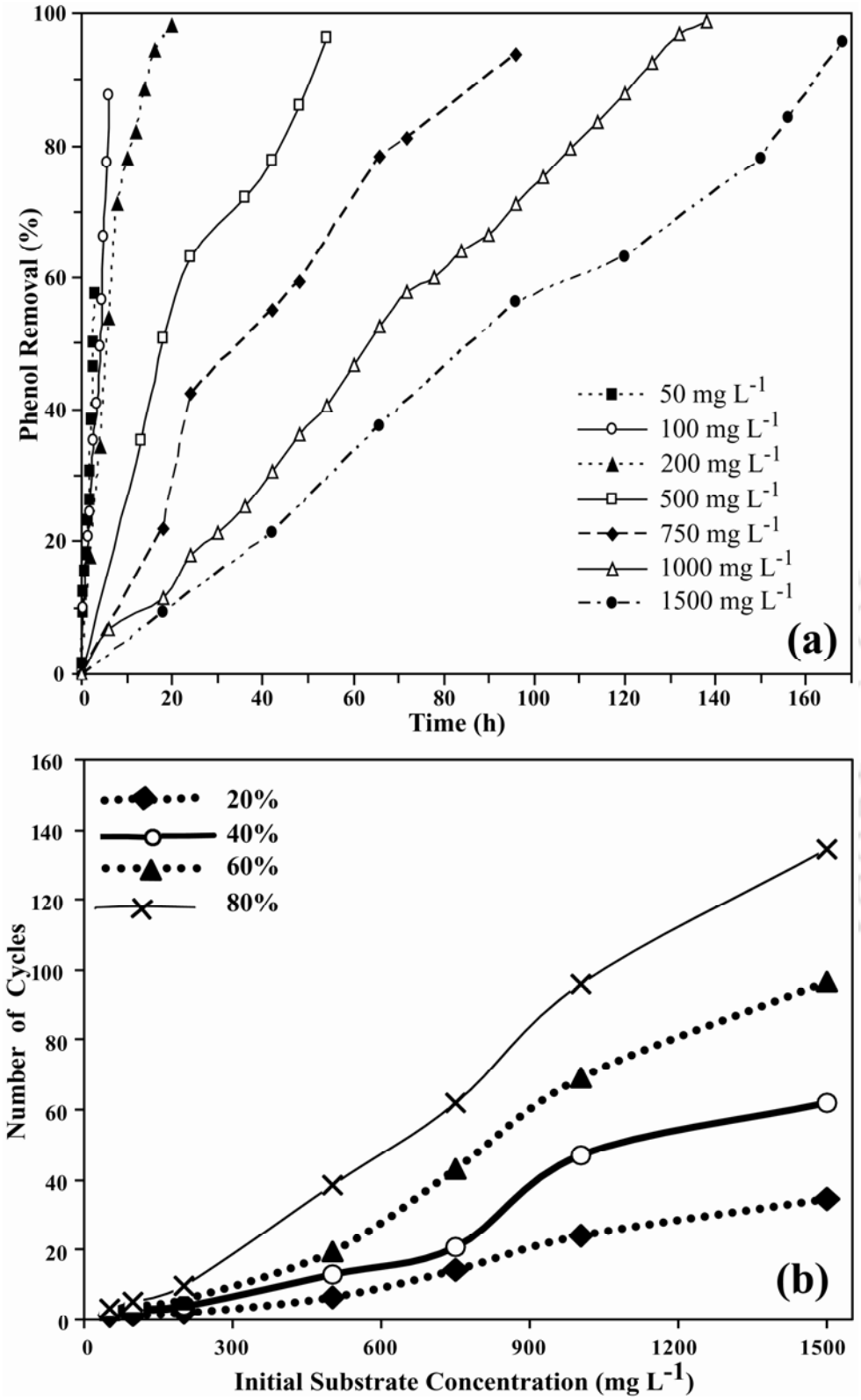

Figure 5.1.2. (a) Phenol removal (%) at various initial phenol concentrations (Q = 0.36 L h^{-1}). (b) Variation of number of cycles with respect to initial phenol concentration for various % phenol removal.

The effect of flow rate on the observed biodegradation rate in the present study was investigated by operating the PBR at different flow rate ranging from 0.36 L h^{-1} to 1.80 L h^{-1} with constant initial phenol concentration of 200 mg L^{-1}. The biodegradation rates were calculated from Eq. (5.1.1) and plotted against corresponding flow rates (Figure 5.1.3). As is evident from Figure 5.1.3, low rates of biodegradation were observed at low flow rates. This can be explained by the formation of mass transfer resistance at the liquid film layer around bead surface which could be reduced, in one way, by increasing the flow rate (Tepe and Dursun, 2008). The increase in the flow rate in the present study, indeed, resulted in the enhanced biodegradation rate due to the reduction of mass transfer resistance (Figure 5.1.3). Table 5.1.1 shows the experimental values of Q and corresponding k_p (calculated from Eq. (5.1.4)) at constant initial phenol concentration of 200 mg L^{-1}. It can be seen from Table 5.1.1 that the observed first-order biodegradation rate constant increases with increasing flow rates.

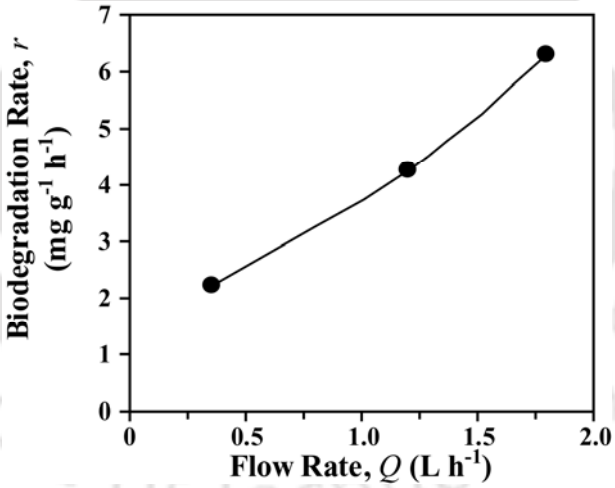

Figure 5.1.3. Effect of flow rate on the observed biodegradation rate (C_0 = 200 mg L^{-1}).

5.1.6.2. Effect of External Mass Transfer

The impact of the external mass transfer on the observed biodegradation rate was analyzed by calculating Reynolds numbers (N_{Re}) and mass fluxes (G) for different experimental flow rate using experimentally determined values of d_p = 0.35 cm, μ = 8.46×10^{-3} g cm^{-1} s^{-1}, ρ = 0.993 g cm^{-3}, ε = 0.401, $D_f = 5.78 \times 10^{-6}$ cm^2 s^{-1} (Aksu and Bulbul, 1999) and A = 18.85 cm^2. Table 5.1.1 presents the estimated values of G, N_{Re}, $1/k_p$ and $1/G^n$ for different values of n. According to Eq. (5.1.15), the plot of $1/k_p$ vs. $1/G^n$ yields a straight line. For different values of n, $1/k_p$ vs. $1/G^n$ was plotted and the values of corresponding slopes and intercepts measured from these plots are listed in Table 5.1.2. Figure 5.1.4 shows the representative plot of $1/k_p$ vs. $1/G^n$ for n = 0.1, 0.35 and 0.8. It was observed that the slope as well as intercept values increased with increasing n values. It may be mentioned here that negative intercepts were obtained for $n < 0.35$ and, hence, not considered for further analysis. Although all n values demonstrated reasonable straight line fit, not all those n values ultimately resulted in a satisfactory estimate for the experimentally calculated A_m value. Therefore, further analysis was carried out to calculate the value of N for various K values reported in previous literatures as summarized in Table 5.1.3. The values of N, calculated from Eq. (5.1.14), were then used to determine the values of A_m and k from the slope and intercept of the $1/k_p$ vs. $1/G^n$ plots, respectively. The calculated values of N, A_m and k for different values of K and n are listed in Table 5.1.4. Among several calculated values, the A_m obtained for K = 1.34 and n = 0.35 was closest to the experimental A_m value of 13.671 cm^2 g^{-1} as determined by Eq. (5.1.6).

Table 5.1.1. Experimentally determined values of k_p by Eq. (5.1.4) and calculated values of G, N_{Re}, $1/k_p$ and $1/G^n$ at various Q (C_0 = 200 mg L^{-1})

Q (L h^{-1})	$k_p \times 10^3$ (L g^{-1} h^{-1})	G (g cm^{-2} h^{-1})	N_{Re}	$1/k_p$ (g h L^{-1})	$1/G^n$									
					n = 0.1	n = 0.2	n = 0.35	n = 0.4	n = 0.5	n = 0.6	n = 0.7	n = 0.8	n = 0.9	n = 1
0.36	21.358	18.964	0.218	46.821	0.745	0.555	0.357	0.308	0.230	0.171	0.127	0.095	0.071	0.053
1.20	28.218	63.215	0.726	35.438	0.661	0.436	0.234	0.190	0.126	0.083	0.055	0.036	0.024	0.016
1.80	41.764	94.822	1.090	23.944	0.634	0.402	0.203	0.162	0.103	0.065	0.041	0.026	0.017	0.011

Table 5.1.2. Slope and intercept values obtained from the $1/k_p$ vs $1/G^n$ plots for different n values.

	n													
	0.1	*0.3*	*0.35*	*0.36*	*0.37*	*0.38*	*0.39*	*0.4*	*0.5*	*0.6*	*0.7*	*0.8*	*0.9*	*1*
Slope	–	–	132.86	133.87	134.98	136.21	137.54	138.97	158.63	188.24	229.34	284.71	358.43	456.14
Intercept	Negative	Negative	0.2129	1.2356	2.2021	3.1167	3.9834	4.8058	11.179	15.365	18.302	20.459	22.098	23.375

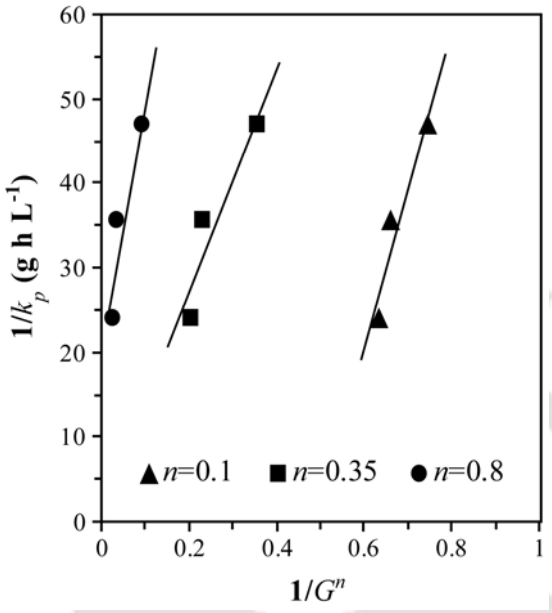

Figure 5.1.4. Representative plot showing relation of $1/k_p$ with $1/G^n$ for different values of n.

Table 5.1.3. Different values of K reported in previous studies.

Study	Mass transfer correlation	Value of K
Tepe and Dursun, 2008	$J_D = 1.34\ N_{Re}^{-0.35}$	1.34
Rovito and Kittrell, 1973	$J_D = 1.625\ N_{Re}^{-0.507}$	1.625
Aksu and Bulbul, 1998	$J_D = 1.625\ N_{Re}^{-0.507}$	
Wilson and Geankoplis, 1966	$J_D\varepsilon = 1.09\ N_{Re}^{-2/3}$	1.09/ε (= 2.718 for present study)
Nath and Chand, 1996	$J_D = 5.7\ N_{Re}^{-0.59}$	5.7
Kathiravan et al., 2010	$J_D = 5.7\ N_{Re}^{-0.70}$	
Dizge and Tansel, 2010	$J_D = 5.7\ N_{Re}^{-0.90}$	
	$J_D = 5.7\ N_{Re}^{-0.18}$	

Table 5.1.4. Calculated values of N, mass transfer area (A_m) and intrinsic first-order degradation rate constant (k) for various n and K.

	K = 1.34			**K = 1.625**			**K = 2.718**			**K = 5.7**		
n	$N \times 10^4$	A_m ($cm^2\ g^{-1}$)	k ($L\ cm^{-2}\ h^{-1}$)	$N \times 10^4$	A_m ($cm^2\ g^{-1}$)	k ($L\ cm^{-2}\ h^{-1}$)	$N \times 10^4$	A_m ($cm^2\ g^{-1}$)	k ($L\ cm^{-2}\ h^{-1}$)	$N \times 10^4$	A_m ($cm^2\ g^{-1}$)	k ($L\ cm^{-2}\ h^{-1}$)
0.35	9.268	8.121	0.578	11.239	6.697	0.701	18.798	4.004	1.173	39.422	1.909	2.460
0.36	9.619	7.766	0.104	11.665	6.404	0.126	19.511	3.829	0.211	40.918	1.826	0.443
0.37	9.984	7.420	0.061	12.108	6.119	0.074	20.251	3.659	0.124	42.470	1.744	0.260
0.38	10.362	7.085	0.045	12.567	5.842	0.055	21.019	3.493	0.092	44.080	1.666	0.193
0.39	10.756	6.760	0.037	13.043	5.574	0.045	21.817	3.333	0.075	45.752	1.589	0.158
0.40	11.162	6.446	0.032	13.538	5.315	0.039	22.644	3.178	0.065	47.487	1.515	0.137
0.50	16.199	3.895	0.023	19.644	3.209	0.028	32.857	1.919	0.047	68.905	0.915	0.098
0.60	23.504	2.260	0.029	28.503	1.864	0.035	47.675	1.114	0.058	99.981	0.531	0.122
0.70	34.105	1.279	0.043	41.359	1.054	0.052	69.177	0.630	0.087	145.073	0.301	0.182
0.80	49.487	0.710	0.069	60.012	0.585	0.084	100.376	0.350	0.140	210.503	0.167	0.293
0.90	71.805	0.389	0.116	87.077	0.320	0.141	145.647	0.192	0.236	305.441	0.091	0.495
1	104.190	0.210	0.203	126.350	0.173	0.247	211.335	0.104	0.412	443.197	0.050	0.865

In order to further verify the applicability of estimated values of n and K to the experimental data, the mass transfer coefficient (k_m) was determined from Eq. (5.1.10) by using experimental k_p, and A_m and k values obtained for $K = 1.34$ and $n = 0.35$. The k_m values calculated for different flow rates are shown in Table 5.1.5. Eq. (5.1.13) implies that the plot of ln k_m vs ln G yields an intercept of ln N and slope of n. The variation of k_m with respect to mass flux (G) in the present study is depicted in Figure 5.1.5; and the slope and the intercept of the ln k_m vs ln G plot were found to be 0.37 and −7.0796, respectively. From the intercept, the value of N was measured to be 8.42×10^{-4} which is closest to the N value determined at $K = 1.34$ and $n = 0.35$ (Table 5.1.4). Based on these results, hence, the mass transfer correlation which satisfactorily predicts the biodegradation of phenol in the present study can be proposed as:

$$J_D = 1.34\, N_{\mathrm{Re}}^{-0.65} \tag{5.1.16}$$

Finally, in order to validate the proposed mass transfer correlation more precisely, the k_p values were estimated by Eq. (5.1.9) for different n values and compared with experimental k_p values measured from Eq. (5.1.4) (Table 5.1.6). The difference between calculated and experimental value of k_p was measured in terms of normalized deviation (%Δ), defined as:

$$\%\Delta = \frac{\sum_{i=1}^{P} \left| \frac{k_{p_{\text{experimental}}} - k_{p_{\text{calculated}}}}{k_{p_{\text{experimental}}}} \right|}{P} \times 100 \tag{5.1.17}$$

where P is the number of data points. From Table 5.1.6, it can be observed that the normalized deviation for $n = 0.35$ is less than that of other n values and, hence, indicates the closest estimate of the experimental data. The proposed mass transfer correlation with the estimated values of $K = 1.34$ and $n = 0.35$, therefore, adequately predicts the present experimental data for the bio-degradation of phenol by immobilized *Bacillus sp.* in a re-circulated PBR.

Table 5.1.5. Estimated values of k_m at various mass fluxes (G) for $K = 1.34$ and $n = 0.35$

Q (L h^{-1})	G (g cm^{-2} h^{-1})	$k_m \times 10^3$ (L cm^{-2} h^{-1})
0.36	18.964	2.642
1.20	63.215	3.495
1.80	94.822	5.189

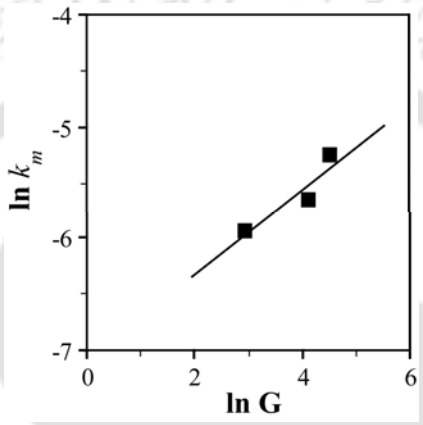

Figure 5.1.5. Plot of ln k_m vs ln G.

Table 5.1.6. Comparison of experimentally measured k_p values from Eq. (5.1.4) with those ones calculated by Eq. (5.1.9) at various n values.

Q (L h^{-1})	Experimental value of $k_p \times 10^3$ (L g^{-1} h^{-1})	Calculated value of k_p from Eq. (5.1.9)					
		n = 0.35		n =0.5		n =0.9	
		$k_p \times 10^3$ (L g^{-1} h^{-1})	%Δ	$k_p \times 10^3$ (L g^{-1} h^{-1})	%Δ	$k_p \times 10^3$ (L g^{-1} h^{-1})	%Δ
0.36	21.358	20.987		21.006		21.068	
1.20	28.218	31.910	8.95	32.123	9.44	32.592	10.51
1.80	41.764	36.738		36.404		35.642	

5.1.7. Conclusion

The biodegradation of phenol by Ca-alginate immobilized *Bacillus cereus* was carried out in a packed bed reactor with re-circulated mode of operation. The biodegradation rate of phenol was found to be dependent on the flow rate as well as the initial phenol concentration. The combined impact of external mass transfer with biochemical reaction on the phenol degradation was investigated and the mass transfer correlation developed, $J_D = 1.34\ N_{\mathrm{Re}}^{-0.65}$ satisfactorily predicted the present experimental data. The insight gained in the present study along with the proposed correlation could be helpful in designing and scale-up of up-flow packed bed reactor systems suitable for re-circulated biodegradation of phenol-containing wastewater.

Symbols

A : column cross sectional area (cm^2)	A_m : surface area per unit weight of immobilized bead ($cm^2\ g^{-1}$)
C : outlet phenol concentration ($mg\ L^{-1}$)	C_0 : inlet phenol concentration ($mg\ L^{-1}$)
C_S : phenol concentration at cell surface ($mg\ L^{-1}$)	d_p : immobilized bead diameter (cm)
D_f : phenol diffusivity ($cm\ s^{-1}$)	G : mass flux of phenol solution ($g\ cm^{-2}\ h^{-1}$)
h : height of the reactor bed (cm)	J_D : Colburn factor (dimensionless)
k : intrinsic first-order degradation rate constant ($L\ cm^{-2}\ h^{-1}$)	k_m : mass transfer coefficient ($L\ cm^{-2}\ h^{-1}$)
k_p : observed first-order biodegradation rate constant ($L\ g^{-1}\ h^{-1}$)	K : Constant in Eq. (5.1.11)
N : Parameter in Eq. (5.1.13)	N_{Re} : Reynolds number ($= d_pG/\mu$)
Q : volumetric flow rate ($L\ h^{-1}$)	r : phenol removal rate ($mg\ g^{-1}\ h^{-1}$)
r_m : mass transfer rate ($mg\ g^{-1}\ h^{-1}$)	W : dry weight of biomass (g)
dz : change in height of column (cm)	ε : void fraction in packed bed
μ : feed viscosity ($g\ cm^{-1}\ s^{-1}$)	ρ : feed density ($g\ cm^{-3}$)
ρ_p : bead density ($g\ cm^{-3}$)	

5.2. WASTEWATER DEGRADATION IN PACKED BED REACTOR

5.2.1. Introduction

Reduction of toxic pollutants level in petroleum wastewater by means of microbial biodegradation is a promising option. The microbial treatment of industrial wastewater in re-circulated mode, especially that of the packed bed reactor, has gained much attention due to easier automation and better control of the process parameters (Livingston and Chase, 1991; Quail and Hill, 1991; Tepe and Dursun, 2008; Sheeja and Murugesan, 2002). The utilization of immobilized cells has shown potential in biodegradation process including wastewater treatment. In industrial operations, immobilized microbial cell systems can provide additional advantages over freely suspended cells such as simple reuse of the biomass, easier liquid–solid separation and minimal clogging in re-circulated flow systems (Arica et al., 2001; Tieng and Sun, 2000). Hence, in this regard, the microbial treatment of real petroleum wastewater samples by the immobilized strains of isolated *B. cereus* AKG1 MTCC9817 and *B. cereus* AKG2 MTCC9818 in a packed bed reactor merits further investigation.

5.2.2. Literature Review

Cell immobilization can be achieved by different methods such as cell entrapment and cell attachment. In the entrapment process, microorganisms are trapped and physically restrained within the fibrous or porous materials. Various polymers such as alginate, chitosan, chitin and cellulose derivatives have been used as the matrix for cell entrapment method. On the other hand, microorganisms adhere to the surfaces of suitable materials by self adhesion in the attachment process. The materials commonly used for the cell attachment method include polyurethane foam, nylon sponge, synthetic foams, etc. (Nakamura et al., 1997). Both types of support materials have been shown to be appropriate for microbial treatment of wastewater (Guimaraes et al., 2002).

Among the wide range of bioreactor designs, packed bed reactor is the most convenient one (Beverly and Hill, 1991; Livingston and Chase, 1991) due to its various advantages including high-yield operation, ease of scaling-up, possible automation of

separation process leading to high degrees of purification, opportunity of treating large volume of wastewater re-circulated by a specified quantity of immobilized cells, reuse of biomass (Aksu and Bulbul, 1998; Tepe and Dursun, 2008). With respect to the continuous microbial treatment of petroleum wastewater, Pour et al. (2005) reported the biodegradation of petroleum hydrocarbons in an immobilized cell airlift bioreactor by using soil contaminated with petroleum hydrocarbons as the source of naturally occurring microorganisms. Lohi et al. (2008) treated diesel fuel contaminated wastewater aerobically in a three-phase fluidized bed reactor under unsteady and steady state. Attached biomass, in this regard, has been claimed to be more resistant towards toxicity than freely suspended ones (Pedersen and Arvin, 1995). On the other hand, biofilm based reactors using a wide range of packing materials such as granular activated carbon (GAC), polyurethane, kaolin, polystyrene, etc have been reported in the literature for successful biodegradation (Guerin, 2002; Pruden et al., 2003; Ohlen et al., 2005; Kermanshahi pour et al., 2005).

5.2.3. Outline of the Research Work

1) Biodegradation of real petroleum wastewater sample collected from oil refinery site has been carried out in a packed bed reactor by Ca-alginate immobilized *B. cereus* (AKG1 MTCC9817 and AKG2 MTCC9818) strains.
2) Biodegradation of petroleum wastewater samples in packed bed reactor has also been performed by biofilm of the isolated *B. cereus* strains grown on polyurethane foam (PUF).
3) The degradation performances of both the systems have been evaluated by measuring the chemical oxygen demand (COD), total organic carbon (TOC), total phosphate and ammonium nitrogen (NH_4^+–N) levels in the wastewater during the microbial treatment.

5.2.4. Experimental Section

5.2.4.1. Microorganisms and Culture Medium

The details of microorganisms and culture medium have already been described in *Section 3.1.4.2* in **Chapter 3** and *Section 2.4.1* in **Chapter 2**, respectively.

5.2.4.2. Immobilization of Biomass into Ca-alginate Beads

The bacterial cells of AKG1 MTCC9817 and AKG2 MTCC9818 were immobilized into Ca-alginate beads by following the same procedure as described in *Section 5.1.5.2* in **Chapter 5**.

5.2.4.3. Surface Immobilization of Biomass on PUF

For surface immobilization, polyurethane foam (PUF) cube (1 cm × 1 cm × 1 cm) was chosen as a biomass support material due to its high surface area available for high accumulation of biomass. AKG1 and AKG2 strains were grown in phenol containing MSM supplemented with Yeast extract (1 L culture medium for each strain) for 24 h as described in *Section 3.1.4.2* of **Chapter 3**. Subsequently, the bacterial cells were harvested by centrifugation at 5,000 rpm for 10 min. Bacterial cells of AKG1 (1.013×10^{27} cfu) and AKG2 (1.022×10^{27} cfu) were inoculated in phenol-containing fresh MSM media (1 L for each strain) together with the PUF cubes (300 cubes for each strain) and incubated overnight for the attachment of bacterial cells onto the PUF surface. A total number of 470 PUF cubes, taking 235 PUF cubes from each of AKG1 and AKG2 strains, were used in the column which resulted in 54 cm bed height. Details of the cube weights are listed in Table 5.2.1.

Table 5.2.1: Weight of a single PUF cube

	Weight (g)
Mean dry weight of a single PUF cube	0.049 ± 0.01
Mean wet weight of a single PUF cube after 24 h immersion in water	0.277 ± 0.02
Mean wet weight of a single PUF cube with attached biomass before experiment	1.060 ± 0.05
Mean wet weight of a single PUF cube with attached biomass after experiment	1.120 ± 0.08

5.2.4.4. Packed Bed Reactor Setup for Biodegradation

The reactor setup has been described in detail in *Section 5.1.5.3* and schematically shown in Figure 5.1.1 (**Section 5.1**). Photographs of the real experimental set-ups are shown in Figure 5.2.1. The active bed volume (1017.9 cm^3) was packed with either immobilized alginate beads (containing AKG1 and AKG2 equivalent to 25.42 g of

dried microorganism; diameter = 0.35 cm) or PUF cubes (with biofilm of AKG1 and AKG2 grown on the surface). The average density of immobilized beads and PUF cubes was measured to be 1.254 g cm^{-3} and 0.0488 g cm^{-3}, respectively. Pre-autoclaved refinery wastewater (1.2 L) was used as feed to the reactors from the bottom in an up-flow mode of operation. The flow rate of the feed was kept constant at 6.0 mL min^{-1} and an air-flow of 0.5 LPH was maintained during the entire period (10 days) of experiment. All the biodegradation experiments were carried out at room temperature (~ 30 °C). Feed samples were collected at regular intervals from the top of the reactor in order for further analysis.

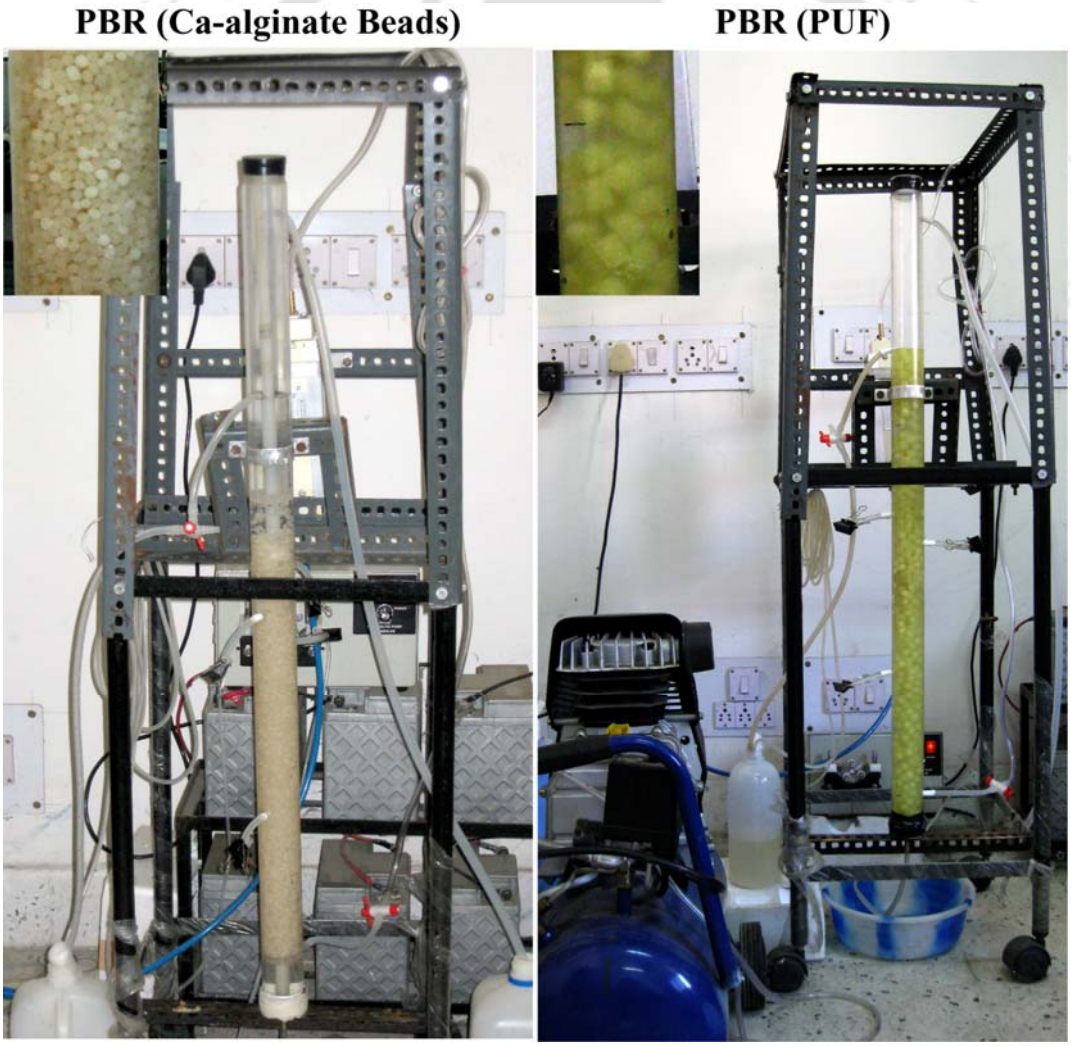

Figure 5.2.1. Photograph of the experimental set-ups used for the treatment of the petroleum wastewater, (inset) closer view of the corresponding reactor beds.

5.2.4.5. Analysis of COD

The COD of the samples was measured by following the method as described in *Section 3.1.4.4* in **Chapter 3**.

5.2.4.6. Analysis of TOC

TOC content of the samples was measured by following the method as described in *Section 3.2.4.5* in **Chapter 3**.

5.2.4.7. Analysis of Ammonium Nitrogen (NH_4^+−N)

NH_4^+−N content of the samples was measured by following the method as described in *Section 3.2.4.7* in **Chapter 3**.

5.2.4.8. Analysis of Phosphate (PO_4^{3-}−P) Content

PO_4^{3-}−P content of the samples was measured by the ascorbic acid method (4500-P E., APHA). In this method, ammonium molybdate and potassium antimonyl tartrate react in acid medium with orthophosphate to form a hetero-polyacid — phosphomolybdic acid — that is reduced to intensely colored molybdenum blue by ascorbic acid. In brief, one drop of phenolphthalein indicator was added to 50 mL sample. 5*N* H_2SO_4 solution was added dropwise, if a red color developed, just to discharge the color. Then, 8 mL of combined reagent (mixture of 5*N* H_2SO_4, potassium antimonyl tartrate solution, ammonium molybdate solution and ascorbic acid solution in 10:1:3:6 weight ratio) was added to the sample and mixed thoroughly. Finally the absorbance of the sample at 880 nm was recorded after 10–15 min.

5.2.4.9. Analysis of Phenolic Compounds

The concentration of phenolic compounds in the samples was determined by following the method described in *Section 5.1.5.4* in **Chapter 5**.

5.2.4.10. Multi-parametric Analysis

Other parameters of the wastewater sample such as conductivity, total dissolved solid (TDS), oxidation reduction potential (ORP) and chloride (Cl^-) were also analyzed with Multi Parameter Water Quality Sonde (Model: 6920-42, USA), at the start and completion of the microbial treatment.

5.2.5 Results and Discussion

5.2.5.1. Removal of COD from Wastewater

COD is a widely used parameter to assess the degree of pollution in a particular wastewater sample. The initial COD level of the refinery wastewater in the present study, before the microbial treatment, was measured to be 9200 mg L^{-1}. The percentage COD removal from the refinery wastewater by AKG1 and AKG2, immobilized in alginate beads as well as surface-attached to PUF cubes, is shown in Figure 5.2.2. From Figure 5.2.2, it is evident that the COD removal by the bacterial strains immobilized either in alginate beads or in PUF gradually increased as the microbial treatment progressed. However, an initial lag phase of about 20 h can be seen in PUF packed bioreactor, possibly due to the adjustment of the bacterial strains with the toxic environment of the wastewater sample. The lag phase is continued to be about 40 h possibly due to continuous exposure to such toxic environment when PUF is used as packing material. For 50% COD removal, the alginate beads took around 80 h while the same was ~120 h for PUF-based system. Furthermore, on the completion of the biodegradation experiment (~241 h), COD level of the wastewater was reduced by 99.24% and 90.97% by the Ca-alginate immobilized and PUF immobilized biomass, respectively. After 241 h of microbial treatment, the final COD level of the refinery wastewater reached a value of 70 mg L^{-1} and 830 mg L^{-1} in the alginate beads packed and PUF-packed bioreactors, respectively. The results essentially demonstrate that the high level of COD (9200 mg L^{-1}) in the refinery wastewater was successfully removed (>90% removal efficiency) by the immobilized AKG1 and AKG2.

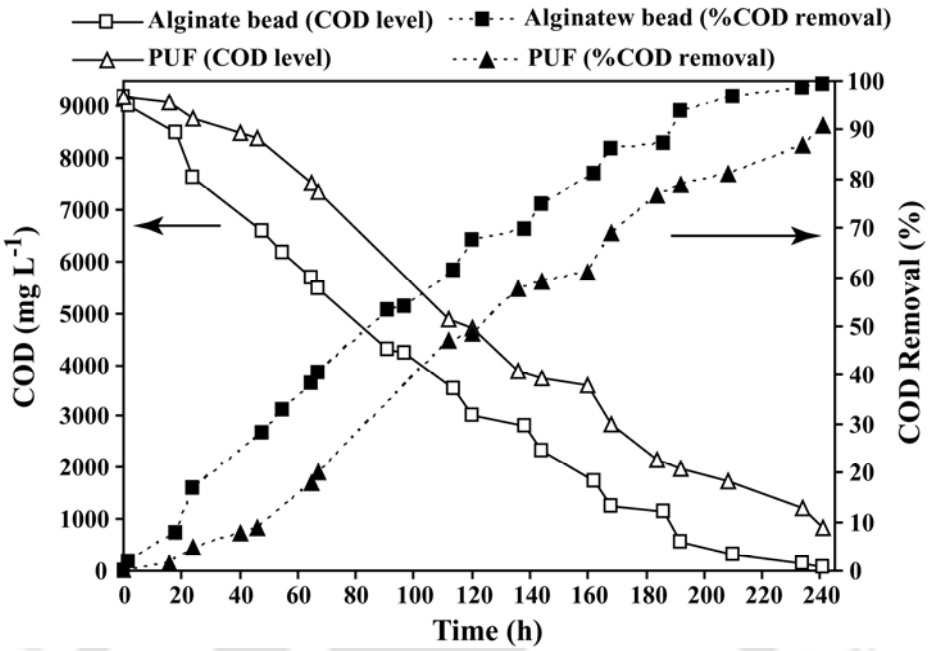

Figure 5.2.2. The COD level and the corresponding COD removal (%) in the refinery wastewater during the microbial treatment in packed bed reactors by Ca-alginate immobilized (*squares*) and PUF immobilized (*triangles*) AKG1 and AKG2, respectively.

5.2.5.2. Removal of TOC from the Wastewater

Figure 5.2.3 shows the TOC content of the refinery wastewater during the microbial degradation in the packed bed reactors. It can be seen from Figure 5.2.3 that the TOC level in the wastewater during the microbial treatment followed similar trend as that of COD and decreased gradually with time in both alginate and PUF immobilized systems. After 192 h (8 days) of microbial treatment, the percentage TOC removal in the alginate bead packed and PUF packed bioreactors was measured to be 93.42% and 87.20%, respectively; which did not increase significantly afterwards in either of the reactors. This indicates that the biodegradation of the refinery wastewater was completed during the 10 days (241 h) of biodegradation experiment resulting in the final TOC level of 184.97 mg L^{-1} and 545.64 mg L^{-1} in case of alginate bead and PUF-packed reactors, respectively, from an initial wastewater TOC of 4548 mg L^{-1}. Finally, the reduction of TOC content by 95.94% and 88%, after complete microbial treatment in the alginate bead and PUF based bioreactors for 10 days, demonstrates the potential of immobilized AKG1 and AKG2 for efficient removal of organic compounds from the refinery wastewaters.

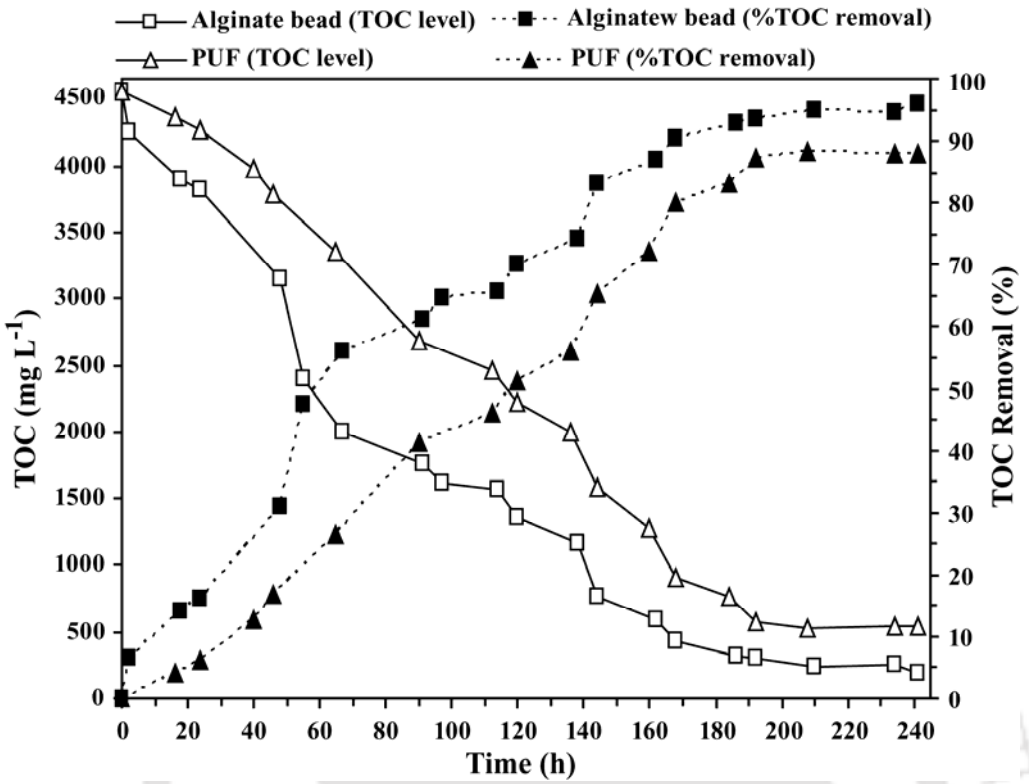

Figure 5.2.3. TOC content and the corresponding TOC removal (%) in the refinery wastewater during the microbial treatment in packed bed reactors by Ca-alginate immobilized (*squares*) and PUF immobilized (*triangles*) AKG1 and AKG2, respectively.

5.2.5.3. Removal of Phenolic Compounds from the Wastewater

Phenol and other phenol derivatives are the major organic compounds present in the refinery wastewater and have a direct relation with COD (1 mg phenol ≡ 2.38 mg COD) (Tyagi et al., 1993). Hence, the removal of phenolic compounds (%) by the immobilized systems as shown in Figure 5.2.4 increased gradually with time following the same trend as that of COD removal (Figure 5.2.2). In the bioreactor packed with Ca-alginate immobilized bacterial strains, the phenolic compounds were biodegraded almost linearly in the initial period of the microbial treatment up to 97 h (~ 4 days) resulting in 84.10% removal of the phenolics present in the refinery wastewater. Subsequently, the rate of phenolics removal decreased and the phenolic compounds of the wastewater were completely (99.80%) removed after 241 h (~10 days) of treatment. On the other hand, the level of phenolic compounds in the bioreactor packed with PUF-immobilized biomass, after an initial lag phase of ~ 40 h, decreased linearly up to 192 h with 91.47% removal of phenolics. The initial lag period observed during the phenolics

removal in PUF-based system could be due to the acclimatization of the biofilm to the toxic environment of the wastewater as the bacterial strains attached on the surface of the PUF, unlike the Ca-alginate immobilized strains, received the direct exposure of toxic pollutants present in the refinery wastewater.

It is interesting to note that the removal of phenolic compounds after 192 h (8 days) reached a value of 98.31% and 91.46% in alginate- and PUF-immobilized system, respectively, and remained almost constant subsequently. This observation further confirmed the inference drawn from the results of TOC removal (Figure 5.2.3) that the microbial degradation of the refinery wastewater in the packed bed reactor was completed after 8 days in both the immobilized systems. The result of the present study clearly demonstrated the excellent capacity of AKG1 and AKG2 strains for removing phenol and other phenolic compounds from the petroleum wastewater contaminated with as high as 3561 mg L^{-1} of phenolic compounds, resulting in phenolics level as low as 8 mg L^{-1} (alginate) and 303 mg L^{-1} (PUF) in the treated wastewater.

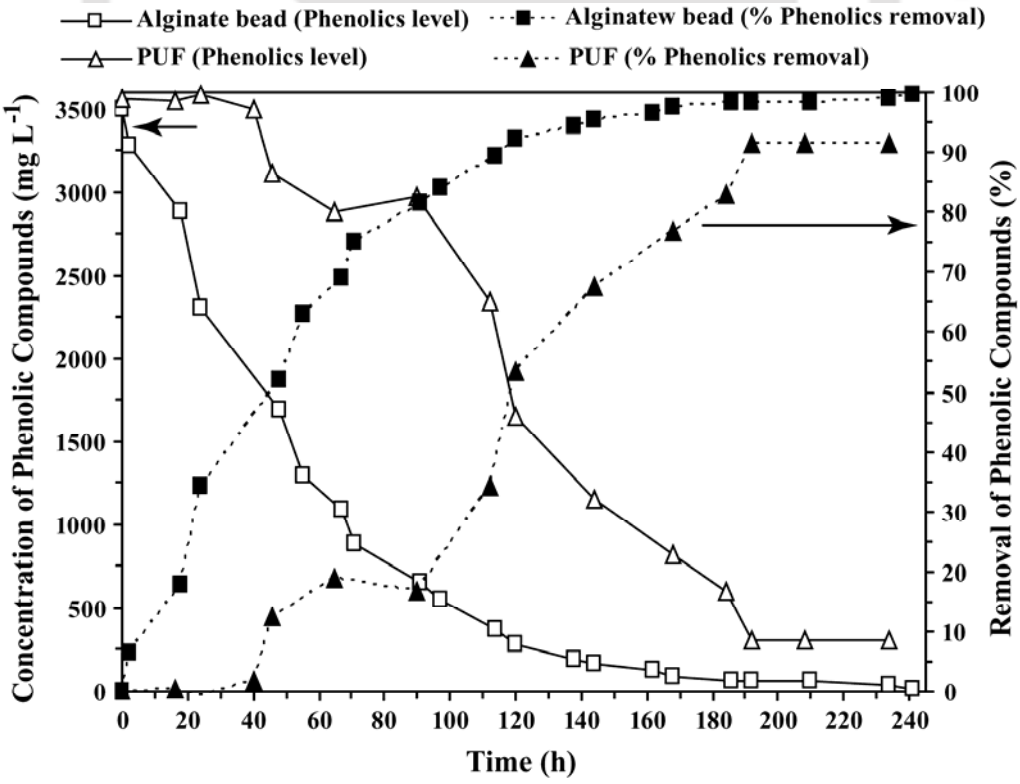

Figure 5.2.4. Concentration of phenolic compounds and the corresponding removal (%) in the refinery wastewater during the microbial treatment in packed bed reactors by Ca-alginate immobilized (*squares*) and PUF immobilized (*triangles*) AKG1 and AKG2, respectively.

5.2.5.4. Removal of Ammonium Nitrogen (NH_4^+−N) from Wastewater

The presence of ammonia (NH_3), mostly in the form of ammonium ions (NH_4^+), in the industrial wastewater is toxic to various aquatic organisms. In this regard, it is important for a successful microbial treatment process to reduce the ammonium level in the industrial effluents such as refinery wastewater. The NH_4^+−N content of the refinery wastewater used in the present study was measured to be 121.092 mg L^{-1}. Figure 5.2.5 shows the percentage removal of NH_4^+−N from the refinery wastewater by immobilized AKG1 and AKG2 in the packed bed reactor in the present study. As the microbial treatment progressed, in the bioreactor packed with Ca-alginate immobilized strains, the NH_4^+−N level decreased almost linearly up to ~120 h (5 days) resulting in ~48.94% NH_4^+−N removal. The NH_4^+−N level did not change significantly in the later stages of the treatment and reached a value of 61.262 mg.L^{-1} after 10 days (241 h) of microbial degradation. On the other hand, the PUF-immobilized bacterial strains reduced the NH_4^+−N level very rapidly up to 46 h (49.09% removal) and then started removing NH_4^+−N slowly to ultimately result in a final NH_4^+−N level of 69.291 mg L^{-1}. The results showed that the NH_4^+−N could efficiently be removed from the refinery wastewater by the microbial treatment in packed bed reactors using the immobilized AKG1 and AKG2 strains, with removal efficiency being ~50% and ~70% in case of Ca-alginate and PUF-immobilized system, respectively.

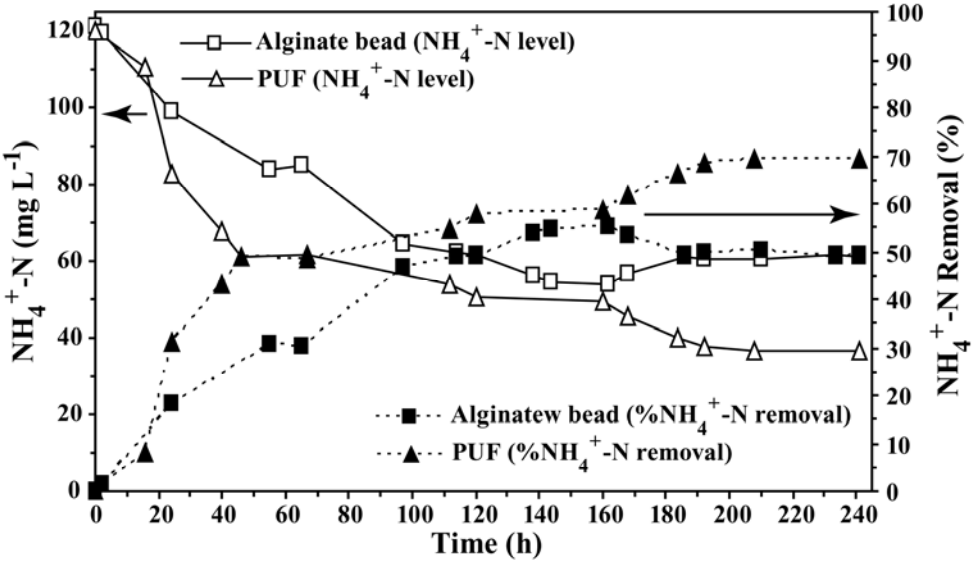

Figure 5.2.5. NH_4^+−N content and the corresponding NH_4^+−N removal (%) in the refinery wastewater during the microbial treatment in packed bed reactors by Ca-alginate immobilized (*squares*) and PUF immobilized (*triangles*) AKG1 and AKG2, respectively.

5.2.5.5. Removal of Phosphate Phosphorus (PO_4^{3-}–P) from Wastewater

The reduction of phosphate in the industrial wastewater is critical as the elevated level of phosphate results in the 'eutrophication' of natural waterbodies, a process in which the dissolved oxygen is greatly depleted exerting negative environmental effects on the aquatic life. The initial PO_4^{3-}–P content of the refinery wastewater before the microbial degradation was measured to be 121.092 mg L^{-1}. Figure 5.2.6 shows the PO_4^{3-}–P level in the refinery wastewater during the microbial treatment in the packed bed reactors by the immobilized strains of AKG1 and AKG2. It can be seen from the figure that the PO_4^{3-}–P level in the wastewater gradually decreased, although not in a linear fashion, during the treatment process. After 241 h of microbial treatment, the PO_4^{3-}–P level of the refinery wastewater in the alginate bead packed reactor reached a value of 67.308 mg L^{-1} which was equivalent to a removal efficiency of 42.62%. On the other hand, the final PO_4^{3-}–P level in the immobilized PUF packed bioreactor was measured to be 89.796 mg L^{-1}, equivalent to 24.14% removal efficiency, after 298 h of treatment.

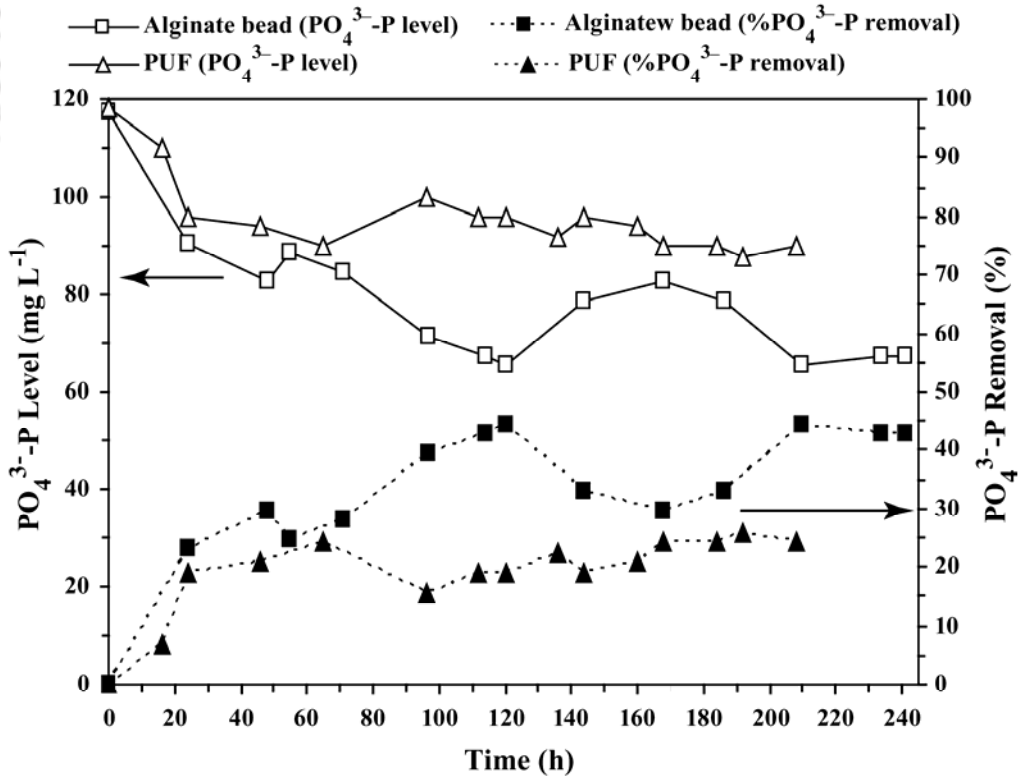

Figure 5.2.6. PO_4^{3-}–P content and the corresponding PO_4^{3-}–P removal (%) in the refinery wastewater during the microbial treatment in packed bed reactors by Ca-alginate immobilized (*squares*) and PUF immobilized (*triangles*) AKG1 and AKG2, respectively.

5.2.5.6. Multi-parametric Analysis

The result of multi-parametric analysis of the refinery wastewater before and after the microbial treatment (for 241 h), as probed by the Multi Parameter Water Quality Sonde, is shown in the Table 5.2.2. As evident from the table, the neutrality of the wastewater was improved from an acidic pH of 5.9 after the treatment. Also, the amount of dissolved solid materials (TDS) was reduced, which was further supported by the decrease in the turbidity of the wastewater as a result of treatment. It is interesting to note that the microbial treatment resulted in the increase of NO_3^- in the wastewater. This was due to the microbial oxidation of toxic NH_3 or NH_4^+ to NO_3^-, which was reflected in the reduction of NH_3 or NH_4^+ level. From Table 5.2.2 and Figure 5.2.2 – 5.2.6, it can be observed that the Ca-alginate immobilized strains were more efficient than the PUF-immobilized ones in removing the pollutants from the refinery wastewater. However, it should be mentioned here that it is difficult to draw a logical comparison between these two immobilized systems because of the difference in the number of immobilized cells, type of immobilization and the method of immobilization as well.

Table 5.2.2: Multi-parametric water quality analysis of the refinery wastewater after 241 h

Property/Analyte	**Before treatment**	**After treatment**	
		Alginate Bead	*PUF*
Conductivity (ms/cm)	0.525 ± 1.5	0.519	2.630
TDS (g L^{-1})	18	0.513	2.575
pH	5.9 ± 1.5	7.12	7.93
ORP (mV)	16.2 ± 1.5	123.8	152.9
NH_4^+ (mg L^{-1})	120 ± 1.5	61.26	36.77
NH_3 (mg L^{-1})	89	0.051	0.416
Cl^- (mg L^{-1})	48	9.34	2.565
NO_3^- (mg L^{-1})	12	489.5	627.4
Turbidity (NTU)	156	11.0	35.4
Phenolic compound (mg L^{-1})	3555	8.43	303.79
TOC (mg L^{-1})	4547	184.96	545.63
COD (mg L^{-1})	9200	70	830
PO_4^{3-}–P (mg L^{-1})	118	89.79	67.30

Measurements were carried out at 27.8 ±2.5 °C.

5.2.6. Conclusions

Biodegradation of the petroleum refinery wastewater in re-circulated packed bed reactors by the isolated strains of AKG1 and AKG2 immobilized in either Ca-alginate beads or PUF cubes was investigated. The biodegradation performances of both the immobilized systems were evaluated by determining the reduction in the COD, TOC, phenolic compounds, NH_4^+−N and PO_4^{3-}−P level in the wastewater sample. The microbial treatment reduced the initial COD level, TOC content and concentration of phenolic compounds by 90% or more demonstrating the excellent efficacy of the immobilized AKG1 and AKG2 strains in treating petroleum wastewater in re-circulated mode of operation. Moreover, the NH_4^+−N and PO_4^{3-}−P removal efficiency equivalent to 50 – 70% and 24 – 42%, respectively, was achieved in the microbial treatment. Overall, the results of the present study strongly show the successful implication of immobilized AKG1 and AKG2 in the treatment of petroleum wastewater in packed bed bioreactors.

5.3. WASTEWATER DEGRADATION IN FLUIDIZED BED REACTOR

5.3.1. Introduction

Several types of bioreactors have shown their potential for the microbial biodegradation of toxic pollutants, especially in the recirculated mode of operation. Among the different bioreactors, fluidized bed bioreactor (FBB) is one of the best and present many advantages related to hydrodynamics and mass transfer phenomena. The use of fluidization as a contact technique has gained considerable importance in the biochemical field (Reese et al., 1999; Schügerl, 1997) as the fluidized bed bioreactor gives intimate contact between the liquid and solid phases (Shieh et al., 1986; Worden et al., 1987). Various operational problems such as bed clogging and high pressure drop, which could be critical in case of high-surface-area media in a packed bed reactor, can easily be overcome by fluidization (Fernandez et al., 2008). Much attention has been directed to FBRs, in recent years, as an efficient technology to treat organic pollutants because FBR has been shown to be more effective than suspended-growth systems due to high biomass concentrations, low hydraulic residence times, small footprint requirements, and absence of mechanical moving parts (Lohi et al., 2008). Also, immobilized biomass has been preferred to free cells in the FBRs because of several advantages such as reduced mechanical stress, elimination of secondary clarifier and ease of sludge disposal (Fernandez et al., 2008).

Successful application of immobilized AKG1 and AKG2 in packed bed reactors for treating petroleum wastewater has already been discussed in the previous section (**Section 5.2**). Evaluation of the biodegradation performance of the isolated strains in a FBR, in this regard, will enrich our knowledge to asses the feasibility of using the strains in practical remediation applications. Hence, it would be interesting to investigate the microbial treatment of real petroleum wastewater by the immobilized strains of isolated *B. cereus* AKG1 MTCC9817 and *B. cereus* AKG2 MTCC9818 in a FBR in order to get a first hand information about the degradation behaviour of the strains in FBR.

5.3.2. Literature Review

Treatment of industrial wastewaters requires a great deal of space when using systems based on activated sludge or aerated lagoons in which the retention time can be many days (Huppe et al., 1990; Wu and Wisecarver,1990; Shieh and Keenan,1986). A fluidized bed bioreactor (FBB), on the other hand, is capable of achieving treatment in low retention time because of the high biomass concentration that can be attained in a bioreactor (Shieh and Keenan, 1986; Yoong et al., 1997). While similar in treatment concept to a trickling-filter (a packed-bed fixed-film bioreactor), the FBB offers distinct mechanical advantages which allow small and high surface area material to be used for biomass growth (Shieh and Keenan). Fluidization overcomes operating problems such as bed clogging and the high pressure drop which would occur if small and high surface area materials were employed in packed-bed operation. Rather than clog with new biomass growth, the FBB bed simply expands. Thus, for comparable treatment efficiency, the required bioreactor volume is greatly reduced (Shieh and Keenan). Hirata (1994) and Safferman (1996) reported that the fluidized bed reactor has active transfer phenomena accelerated by fluidizing materials, and the reactor retains 5–10 times higher biomass concentration than conventional activated sludge reactors. In these kinds of bioreactors, the solid particles covered by biofilm are fluidized by two ascending flows, air, and contaminated water.

With favourable operating conditions, from hydrodynamic and mass transfer point of view, the pollutant could be biologically degraded up to 90% (Livingston, 1991). Rusten et al. (1992) have applied a biomass support made of ethylene in an FBB used for treatment of wastewaters from dairy and food industry. With respect to the continuous microbial treatment of petroleum wastewater, Pour et al. (2005) reported the biodegradation of petroleum hydrocarbons in an immobilized cell airlift bioreactor by using soil contaminated with petroleum hydrocarbons as the source of naturally occurring microorganisms. Lohi et al. (2008) treated diesel fuel contaminated wastewater aerobically in a three-phase fluidized bed reactor under the unsteady and steady state conditions. Attached biomass, in this regard, has been claimed to be more resistant towards toxicity than freely suspended ones (Pedersen and Arvin, 1995).

5.3.3. Outline of the Research Work

1) Biodegradation of real petroleum wastewater sample collected from oil refinery site has been carried out in a fluidized reactor by Ca-alginate immobilized *B. cereus* (AKG1 MTCC9817 and AKG2 MTCC9818) strains.
2) The degradation performances of the systems have been evaluated by measuring the changes in chemical oxygen demand (COD) and level of phenolic compounds in the wastewater during the microbial treatment.

5.3.4. Experimental Section

5.3.4.1. Microorganisms and Culture Medium

The details of microorganisms and culture medium have already been described in *Section 3.1.4.2* of **Chapter 3** and *Section 2.4.1* of **Chapter 2**, respectively.

5.3.4.2. Immobilization of Biomass into Ca-alginate Beads

The bacterial cells of AKG1 MTCC9817 and AKG2 MTCC9818 were immobilized into Ca-alginate beads by following the same procedure as described in *Section 5.1.5.2* of **Chapter 5**.

5.3.4.3. Fluidized Bed Reactor Setup for Biodegradation

The FBR used for the biodegradation of petroleum wastewater in the present study was a tubular system with an internal diameter of 5 cm and 100 cm in height as shown schematically in Figure 5.3.1. The active bed volume (55 cm^3) was packed with immobilized alginate beads (containing AKG1 and AKG2 equivalent to 16.87 g of dried microorganism; diameter = 0.35 cm). The average density of immobilized beads was 1.254 g cm^{-3}. Pre-autoclaved refinery wastewater (1.2 L) was used as feed to the reactors from the bottom in an up-flow mode of operation. The flow rate of the feed was kept constant at 6.0 mL min^{-1} and an air-flow of 1 LPH was maintained during the entire period of experiment Total feed were fluidized by air circulation. The minimum air fluidization velocity was experimentally measured to be 0.306 LPH and elution velocity were 52.8 LPH. All the biodegradation experiments were carried out at room temperature of ca. 30 °C. Feed samples were collected at regular intervals from the top of the reactor in order for further analysis.

5.3.4.4. Analysis of COD

The COD of the samples was measured by following the method as described in *Section 3.1.4.4* of **Chapter 3**.

5.3.4.5. Analysis of Phenolic Compounds

The concentration of phenolic compounds in the samples was determined by following the method described in *Section 5.1.5.4* of **Chapter 5**.

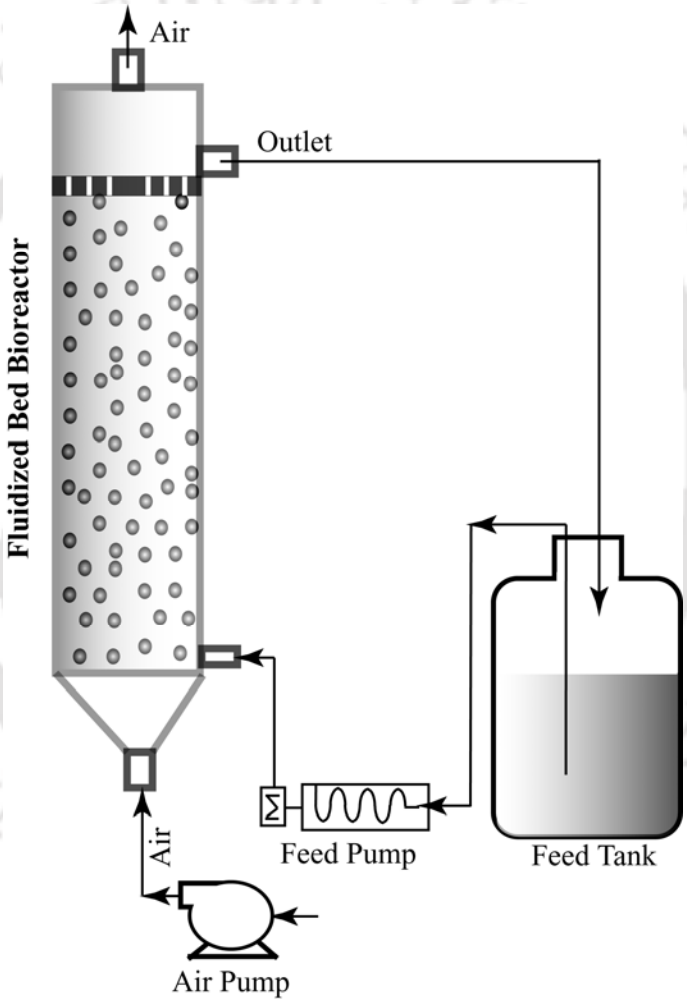

Figure 5.3.1. Schematic representation of the re-circulated up-flow fluidized bed bioreactor (dimensions are not in scale).

5.3.5 Results and Discussion

5.3.5.1. Removal of COD from the Wastewater

The initial COD level of the refinery wastewater in the present study, before the microbial treatment, was measured to be 5600 mg L^{-1}. The percentage COD removal from the refinery wastewater in the fluidized bed bioreactor by AKG1 and AKG2 immobilized in Ca-alginate beads is shown in Figure 5.3.2. From Figure 5.3.2, it is evident that the COD removal by the immobilized bacterial strains gradually increased as the microbial treatment progressed. For 50% COD removal, it took around 53 h. Furthermore, on the completion of the biodegradation experiment (~130 h), COD level of the wastewater was reduced by 97.86%. After 130 h of microbial treatment, the final COD level of the refinery wastewater reached a value of 50 mg L^{-1}. The results essentially demonstrate that the high level of COD (5600 mg L^{-1}) in the refinery wastewater was successfully removed by the immobilized AKG1 and AKG2 in the fluidized bed bioreactor.

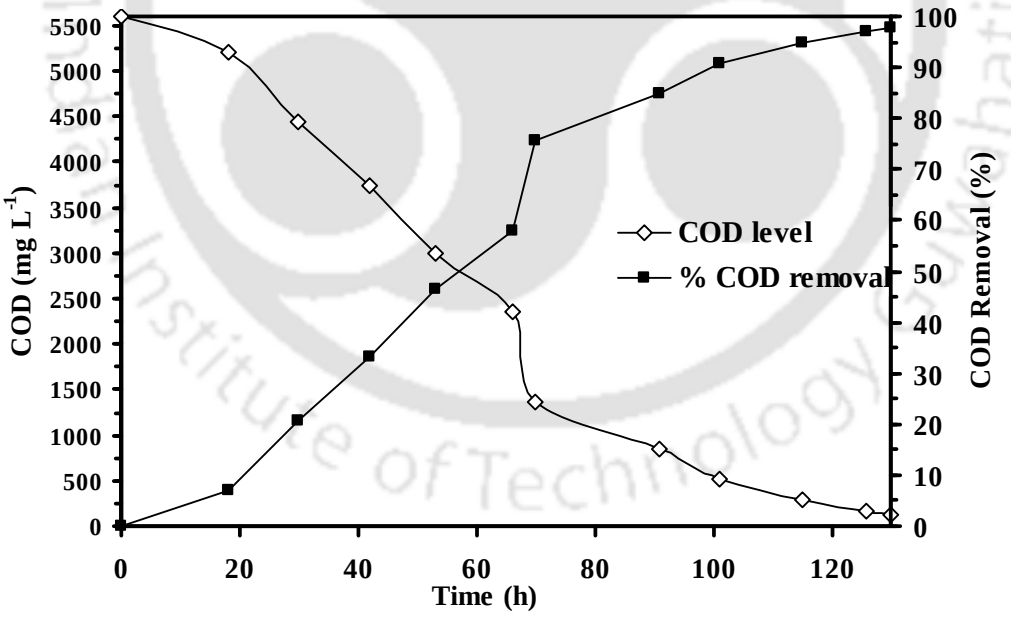

Figure 5.3.2. The COD level and the corresponding COD removal (%) in the refinery wastewater during the microbial treatment in fluidized bed reactors by Ca-alginate immobilized AKG1 and AKG2.

5.3.5.2. Removal of Phenolic Compounds from the Wastewater

Phenol and other phenol derivatives are the major organic compounds present in the refinery wastewater and have a direct relation with COD (1 mg phenol ≡ 2.38 mg COD) (Tyagi et al., 1993). The initial concentration of phenolic compounds in the petroleum wastewater at the beginning of the microbial treatment was measured to be as high as 2545 mg L^{-1}. Figure 5.3.3 shows the level of phenolic compounds in the petroleum wastewater and corresponding removal efficiency (%) during the microbial treatment in the fluidized bed bioreactor by immobilized bacterial strains. In the fluidized bed bioreactor, the phenolic compounds were biodegraded almost linearly in the initial period of the microbial treatment up to 70 h (~ 3 days) resulting in 75.63% removal of the phenolics present in the refinery wastewater. Subsequently, the rate of phenolics removal decreased and the phenolic compounds of the wastewater were completely (98.03%) removed after 130 h (~6 days) of treatment. As evident from Figure 5.3.3, the removal of phenolic compounds (%) by the immobilized systems followed the same trend as that of COD removal (Figure 5.3.2) demonstrating the relation of phenolic compounds with COD as discussed earlier.

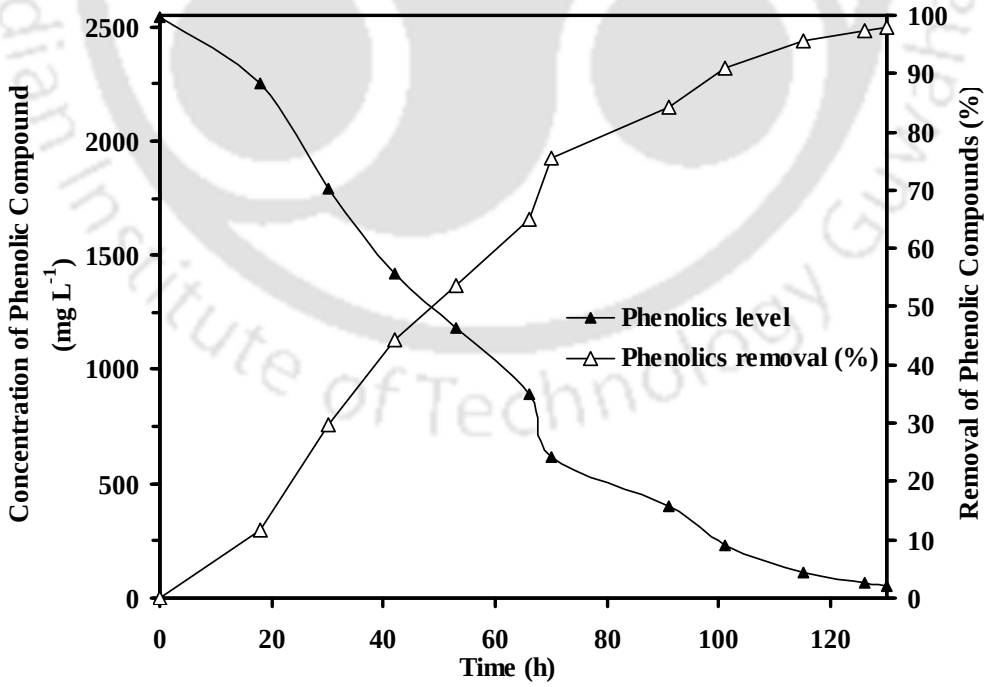

Figure 5.3.3. Concentration of phenolic compounds and the corresponding removal (%) in the refinery wastewater during the microbial treatment in fluidized bed reactors by Ca-alginate immobilized AKG1 and AKG2.

5.3.6. Conclusions

Biodegradation of the petroleum refinery wastewater in re-circulated fluidized bed reactors by the isolated strains of AKG1 and AKG2 immobilized in Ca-alginate beads was investigated. The biodegradation performance was evaluated by determining the reduction in the COD and phenolic compounds in the wastewater sample. The microbial treatment reduced the initial COD level and concentration of phenolic compounds by 95% or more demonstrating the excellent efficacy of the immobilized AKG1 and AKG2 strains in treating petroleum wastewater in re-circulated mode of operation. Overall, the results of the present study strongly show the successful implication of immobilized AKG1 and AKG2 in the treatment of petroleum wastewater in fluidized bed bioreactors.

CHAPTER 6

Conclusions and Scope for Future Work

Major inferences drawn from the present study and scopes for the future work are presented in this chapter.

Chapter 6

CONCLUSIONS AND SCOPE FOR FUTURE WORK

6.1. Conclusions

In the present thesis work, phenol-degrading bacteria were isolated from oil exploration and oil refinery site and their application in the biodegradation of phenolic and petroleum wastewaters has been investigated. The major inferences drawn from the present study are summarized below:

- The two phenol-degrading bacteria isolated from the oil refinery and exploration site are *Bacillus cereus* MTCC 9817 strain AKG1 and *Bacillus cereus* MTCC 9818 strain AKG2, respectively.
- The pH for optimum growth is 7.0 and 7.5 for AKG1 and AKG2, respectively; while a temperature of 37 °C is optimum for both the strains.
- Isolated strains can degrade phenol efficiently in the concentration range of 100 – 2000 mg L^{-1}. Biodegradation of phenol follows *meta*-cleavage pathway in both strains, while the degradation kinetics follows the Haldane model.
- Co-culture of free *B. cereus* AKG1 and *B. cereus* AKG2 is more efficient in biodegrading petroleum wastewater in batch mode as compared to individual strains.
- A mixture of 4-(phenylamino)-phenol and 2, 6-dichlorophenyl-1-acetonitrile is the probable end products of biodegradation of wastewater Sample I (collected from the refinery site) after 20 days of microbial treatment. On the other hand, 2-hydroxy-3-(3-methyl-2-butenyl) 1, 4-naphthalenedione is the predicted biodegradation product of the wastewater Sample II (collected from oil exploration site).
- The isolated bacterial strains adapt to the toxic environment of the petroleum wastewater by changing the polysaccharide and protein components of the bacterial membrane.
- Ca-alginate immobilized *B. cereus* AKG1 MTCC9817 and AKG2 MTCC9818 demonstrate enhanced tolerance to higher phenol concentration (up to 2000 mg

- L^{-1}) as compared to free cells. The optimum pH for maximal phenol degradationby immobilized strains is 6.7 and 6.9 for AKG1 and AKG2, respectively. An alginate concentration of 3% in immobilized beads is optimum for maximal phenol degradation.
- Immobilized strains are stable even after 60 days of storage at 4 °C and can be repeatedly used in batch degradation over a period of 80 days and 110 days in case of AKG1 and AKG2, respectively.
- Phenol degradation kinetics by the immobilized strains can be described well by the Haldane model.
- The petroleum wastewater samples can potentially be treated by immobilized AKG1 and AKG2 in batch culture. Though, the immobilized cells are less effective than the free cell systems in treating the petroleum wastewater samples.
- Biodegradation of phenol by Ca-alginate immobilized AKG1 and AKG2 in the laboratory scale packed bed reactor has been found efficient. The impact of external mass transfer combined with biochemical reaction on the phenol degradation is expressed by the mass transfer correlation as $J_D = 1.34\ N_{\mathrm{Re}}^{-0.65}$.
- The petroleum refinery wastewater can be treated efficiently in continuous re-circulated packed bed reactors by the isolated strains of AKG1 and AKG2 immobilized in either Ca-alginate beads or PUF cubes. The microbial treatment can reduce the initial COD level, TOC content and concentration of phenolic compounds by 90% or more after 10 days.
- Preliminary studies indicate that the petroleum wastewater can be treated successfully by immobilized AKG1 and AKG2 in fluidized bed bioreactors. The microbial treatment can reduce the COD level and phenolic compound of the wastewater by 98%.

The present work has shown the potential of strains Bacillus cereus towards degradation of phenol and other petroleum contaminants present in wastewater. Literature information on such performance by Bacillus cereus is scant. They degrade phenol via meta-cleavage pathway with the degradation kinetics following the Haldane model. Co-culture is more efficient than the individual strains. The isolated strains adapt to the toxic environment of the petroleum wastewater by changing the polysaccharide and protein components of the bacterial membrane. Phenol

degradation by Ca-alginate immobilized strains has been found efficient and the mass transfer correlation, $J_D = 1.34\, N_{\mathrm{Re}}^{-0.65}$ *is obeyed. The microbial treatment can reduce the initial COD level and phenolic compounds by 90 and 98% by packed bed and fluidized bed bioreactors respectively.*

6.2. Scope for Future Work

- The mechanism of phenol degradation by the AKG1 and AKG2 in the present work has been investigated at a preliminary level. Further investigation on the structural and functional characterization of the key enzymes involved in the degradation process is required in order to gain complete understanding of the biochemical pathway of phenol degradation. Also, the isolation and purification of the key degradation enzymes could provide the platform for successful immobilization of degradation enzymes and their application in enhanced phenol degradation. The present study focused mainly on phenol as a substrate. However, further studies could be carried out to examine the degradation capability of the isolated strains for other phenol derivatives and aromatic compounds considered as recalcitrant pollutants.
- The packed bed reactor system studied in the present work should be scaled up with real industrial wastewater in order to provide reactor optimized for field applications.
- Only preliminary studies on biodegradation of petroleum wastewater in the fluidized bed bioreactors have been carried out. Extended investigation on the optimization and kinetic study should be performed for better performance of the fluidized bed reactor.
- Mathematical modeling of the biodegradation of the phenolic and petroleum wastewater in continuous packed bed and fluidized bed bioreactors should be carried out for better understanding and prediction of the system performance.

REFERENCES

Abdelwahab, O., Amin, N.K., El-Ashtoukhy, E.S.Z., 2009. Electrochemical removal of phenol from oil refinery wastewater. J. Hazard. Mater. 163, 711–716.

Abuhamed, T., Bayraktar, E., Mehmetoglu, T., Mehmetoglu, U., 2004. Kinetics model for the growth of *Pseudomonas putida* F1 during benzene, toluene and phenol biodegradation. Process Biochem. 39, 983–988.

Adams, D., Ribbons, D.W., 1988. The metabolism of aromatic ring fission products by *Bacillus stearothermophilus* strain IC3. J. Gen. Microbiol. 134, 3179-3185.

Adjei, M.D., Ohta, Y., 2000. Factors affecting the biodegradation of cyanide by *Burkholderia* cepacia strain C-3. J. Biosci. Bioeng. 89, 274-277.

Agarry, S.E., Audu, T.O.K., Solomon, B.O.,2010. Kinetics of batch microbial degradation of phenols by indigenous binary mixed culture of *Pseudomonas aeruginosa* and *Pseudomonas fluorescens*. Int. J. Environ. Pollut. 43, 177 – 189.

Agarry, S.E., Durojaiye, A.O., Solomon A.B.O., 2008. Microbial degradation of phenols: a review. Int. J. Environ. Pollut. 32, 12 – 28.

Agarry, S.E., Durojaiye, A.O., Yusuf, R.O., Aremu, M.O., Solomon, B.O., Mojeed, O., 2008b. Biodegradation of phenol in refinery wastewater by pure cultures of *Pseudomonas aeruginosa* NCIB 950 and *Pseudomonas fluorescence* NCIB 3756. Int. J. Environ. Pollut. 32, 3 – 11.

Ahmaruzzaman, M., Sharma, D.K., 2005. Adsorption of phenols from wastewater. J. Colloid Interface Sci. 287, 14-24.

Ahmaruzzaman, Md., 2008. Adsorption of phenolic compounds on low-cost adsorbents: A review. Adv. Colloid Interface Sci. 143, 48–67.

Aiba, S., Shoda, M., Nagalani, M., 1968. Kinetics of product inhibition in alcohol fermentation. Biotechnol. Bioeng. 10, 845–864.

Akker, B.V.D., Holmes, M., Cromar, N., Fallowfield, H., 2008. Application of high rate nitrifying trickling filters for potable water treatment. Water Res. 42, 4514 – 4524.

Aksu Z., Bulbul, G., 1999. Determination of the effective diffusion coefficient of phenol in Ca-alginate-immobilized P. putida beads. Enzyme Microb. Technol. 25, 344 - 348.

Aksu, Z., Bulbul, G., 1998. Investigation of the combined effects of external mass transfer and biodegradation rates on phenol removal using immobilized *P. putida* in a packed-bed column reactor. Enzyme Microb. Technol. 22, 397–403.

Alagappan, G., Cowan, R.M., 2004. Effect of temperature and dissolved oxygen on the growth kinetics of *Pseudomonas putida* F1 growing on benzene and toluene. Chemosphere 54, 1255–1265.

Alberti, F., Bienati, B., Bottino, A., Capannelli, G., Comite, A., Ferrari, F., Firpo, R.,2007. Hydrocarbon removal from industrial wastewater by hollow-fibre membrane bioreactors. Desalination 204, 24-32.

Alcocer, A. S., Ordaz, N. R., Ramírez, C. J., Mayer, J. G., 2007. Continuous biodegradation of single and mixed chlorophenols by a mixed microbial culture constituted by *Burkholderia* sp., *Microbacterium phyllosphaerae* and *Candida tropicalis*. Biochem. Eng. J. 37, 201-211.

Ali, S., Lafuente, R. F., Cowan, D.A., 1998. Meta-pathway degradation of phenolics by thermophilic *Bacilli*. Enzyme Microb. Technol. 23, 462-468.

Allsop, P.J., Chisti, Y., Young, M.M., Sullivan, G.R., 1993. Dynamics of phenol degradation by *Pseudomonas putida*. Biotechnol. Bioeng. 41, 572– 580.

Altas, L., Büyükgüngör, H., 2008. Sulfide removal in petroleum refinery wastewater by chemical precipitation. J. Hazard. Mater. 153, 462–469.

Alva, V.A., Peyton, B. M., 2003. Phenol and Catechol Biodegradation by the haloalkaliphile *Halomonas campisalis*: influence of pH and salinity. Environ. Sci. Technol. 37, 4397–4402.

Alvaro, A.M.G., Rui, A.R., Alirio, E., 2000. Phenol biodegradation by *Pseudomonas putida* DSM548 in a batch reactor. Biochem. Eng. J. 6, 45-49.

Annadurai, G., Ling, L.Y., Lee, J.F., 2008. Statistical optimization of medium components and growth conditions by response surface methodology to enhance phenol degradation by *Pseudomonas putida*. J. Hazard. Mater. 151, 171-178.

APHA, 1998. Standard methods for the examination of water and wastewater, 20th Ed., American Public Health Association/American Water Works Association/Water Pollution Control Federation, Washington, DC.

Arica, M.Y., Kacar, Y., Genc, O.,2001. Entrapment of white-rot fungus *Trametes versicolor* in Ca–alginate beads: preparation and biosorption kinetic analysis for cadmium removal from an aqueous solution. Bioresour. Technol. 80,121–129.

Arutchelvan, V., Kanakasabai, V., Elangovan, R., Nagarajan, S., Muralikrishnan, V., 2006. Kinetics of high strength phenol degradation using *Bacillus brevis*, J. Hazard. Mater. B129, 216–222.

Attiogbe, F.K., Glover-Amengor, M., Nyadziehe, K.T., 2007. Correlating biochemical and chemical oxygen demand of effluents—a case study of selected industries in Kumasi, Ghana. W. Afr. J. Appl. Ecol. 11, 110–118.

Azbar, N., Tutuk, F., Keskin, T.,2009. Biodegradation performance of an anaerobic hybrid reactor treating olive mill effluent under various organic loading rates. Int. Biodeterio. Biodegrad. 63, 690-698.

Bai, J., Wen, J.P., Li, H.M., Jiang, Y., 2007. Kinetic modeling of growth and biodegradation of phenol and *m*-cresol using *Alcaligenes faecalis*. Process Biochem. 42, 510-517.

Bailey, J.E., Ollis, D.F., 1987. Biochemical engineering fundamentals. McGraw-Hill, Singapore, 432–449.

Bajaj, M., Gallert, C., Winter, J., 2009a. Phenol degradation kinetics of an aerobic mixed culture. Biochem. Eng. J. 46, 205-209.

Bajaj, M., Gallert, C., Winter, J., 2009b. Treatment of phenolic wastewater in an anaerobic fixed bed reactor (AFBR)—recovery after shock loading. J. Hazard. Mater. 162, 1330-1339.

Bajaj, M., Gallert, C., Winter, J.,2008. Biodegradation of high phenol containing synthetic wastewater by an aerobic fixed bed reactor. Bioresour. Technol. 99, 8376-8381.

Bandhyopadhyay, K., Das, D., Bhattacharyya, P., Maiti, B.R., 2001. Reaction engineering studies on biodegradation of phenol by *Pseudomonas putida* MTCC 1194 immobilized on calcium alginate. Biochem. Eng. J. 8, 179–186.

Bandhyopadhyay, K., Das, D., Maiti, B.R., 1999. Kinetics of phenol degradation using *Pseudomonas putida* MTCC 1194. Bioprocess Eng. 18, 373–377.

Bandyopadhyay, K., Das, D., Maiti, B.R., 1998. Kinetics of phenol degradation using *Pseudomonas putida* MTCC 1194. Bioprocess Eng. 18, 373 – 377.

Banerjee, A., Ghoshal, A.K., 2010a. Isolation and characterization of hyper phenol tolerant *Bacillus* sp. from oil refinery and exploration sites. J. Hazard. Mater. 176, 85-91.

Banerjee, A., Ghoshal, A.K., 2010b. Phenol degradation by Bacillus cereus: Pathway and kinetic modeling. Bioresour. Technol. 101, 5501-5507.

Banerjee, A., Ghoshal, A.K., 2011. Phenol degradation performance by isolated *Bacillus cereus* immobilized in alginate. Int. Biodeterio. Biodegra. Accepted Manuscript. 10.1016/j.ibiod.2011.04.011

Barbour, I., Brooks, H., Lakoff, S., Opie, J., 1982. Energy and american values, New York: Praeger Publishers.

Berkowitz, J.B., 1988. Standard handbook of hazardous water treatment and disposal — hazardous waste recovery processes, McGraw-Hill, New York.

Beverly, E.Q., Hill, G.A., 1991. A packed column bioreactor for phenol degradation: model and experimental verification. J. Chem. Technol. Biotechnol. 52, 545-557.

Bhatt, P., Kumar, M.S., Mudliar, S., Chakrabarti, T., 2007. Biodegradation of chlorinated compounds—a review. Crit. Rev. Environ. Sci. Technol. 37, 165 – 198.

Britto, J.M., Oliveira, S.B.D., Rabelo, D., Rangel, M.D.C., 2008. Catalytic wet peroxide oxidation of phenol from industrial wastewater on activated carbon, Catal. Today 133–135, 582–587.

Brown, D. W., Ramos, L. S., Fiedman, A. J., Macleod, W. D., 1969. Analysis of trace levels of petroleum hydrocarbons in marine sediments using a solvent-slurry extraction procedure, in: Trace organic analysis: a new frontier in analytical chemistry. Special publication no. 519. National Bureau of Standards, Washington, D.C., pp. 161-167.

Brown, V.M., Jordan, D. H. M., Tiller, B. A., 1967. The effect of temperature on the acute toxicity of phenol to rainbow trout in hard water. Water Res. 1, 587-594.

Caetano, M., Valderrama, C., Farran, A., Cortina, J.L., 2009. Phenol removal from aqueous solution by adsorption and ion exchange mechanisms onto polymeric resins. J. Colloid Interface Sci. 338, 402–409.

Cai, W., Li, J., Zhang, Z., 2007. The characteristics and mechanisms of phenol biodegradation by *Fusarium* sp. J. Hazard. Mater. 148, 38–42.

Calheiros, C. S.C., Rangel, A.O.S.S., Castro, P.M.L., 2009. Treatment of industrial wastewater with two-stage constructed wetlands planted with *Typha latifolia* and *Phragmites australis*. Bioresour. Technol. 100**,** 3205-3213.

Calvo, J.J.O., Lahlou, M., Jimenez, C.S., 1997. Effect of organic matter and clays on the biodegradation of phenanthrene in soils. Int. Biodeterio.Biodegra. 40, 101-106.

Cao, B., Loh, K. C., 2008. Catabolic pathways and cellular responses of *Pseudomonas putida* P8 during growth on benzoate with a proteomics approach. Biotechnol. Bioeng. 101, 1297 – 1312.

Cardoso, R.B., Texier, A.C., Solís, Á. A.. Gómez, J., Flores, E.R., 2009. Phenol and sulfide oxidation in a denitrifying biofilm reactor and its microbial community analysis. Process Biochem. 44**,** 23-28.

Carmona, M., Lucas, A.D., Valverde, J.L., Velasco, B., Rodriguez, J.F., 2006. Combined adsorption and ion exchange equilibrium of phenol on amberlite IRA-420. Chem. Eng. J. 117, 155-160.

Chakraborty, S., Bhattacharya, T., Patel, T.N., Tiwari, K.K., 2010. Biodegradation of phenol by native microorganisms isolated from coke processing wastewater. J. Environ. Biol. 31, 293-296.

Chang, H.N, Moon, R.K., Park, B.G., Lim, S., Choi, D.W., Lee, W.G., 2000. Simulation of SBR operation for simultaneous removal of nitrogen and phosphorus. Bioprocess Eng. 23, 513–521.

Chasanov, M.G., Icunin, R., Mcgarvey, F., 1956. Sorption of phenols by anion exchange resins, Ind. Eng. Chem. 48, 305-309.

Chen, C.Y., Chen, S.C., Fingas, M., Kao, C.M., 2010. Biodegradation of propionitrile by *Klebsiella oxytoca* immobilized in alginate and cellulose triacetate gel. J. Hazard. Mater. 177**,** 856-863.

Chen, G.Z., Huang, X.Z., Liu, W.Y., 1985. Ultraviolet visible spectrophotometry, Atomic Publisher, Beijing, pp. 25–26.

Chen, J.P., Lin, Y.S., 2007. Decolorization of azo dye by immobilized *Pseudomonas luteola* entrapped in alginate-silicate sol-gel beads. Process Biochem. 42**,** 934–942.

Chen, S., Sun, D., Chung, J.S., 2007. Anaerobic treatment of highly concentrated aniline wastewater using packed-bed biofilm reactor. Process Biochem. 42, 1666–1670.

Chen, Y.M., Lin, T.F., Huang, C., Lin, J.C., Hsieh, F.M., 2007b. Degradation of phenol and TCE using suspended and chitosan-bead immobilized *Pseudomonas putida*. J. Hazard. Mater. 148, 660–670.

Chitra, S., Sekaran, G., Padmavathi, S., Gowri, C., 1995. Removal of phenol from wastewater using a biocatalyst. Proceedings of the National Symposium Frontiers in Appl. Environ. Microbiol. 74–77.

Choi, Y., Jung, E., Kim, S., Jung, S.,2003. Membrane fluidity sensoring microbial fuel cell. Bioelectrochemistry 59,121–127.

Chung, T.P., Tseng, H.Y., Juang, R.S., 2003. Mass transfer and intermediate detection for phenol degradation in immobilized *Pseudomonas putida* systems. Process Biochem. 38,1497–1507.

Chung, T.P., Wu, P.C., Juang, R.S.,2005. Use of microporous hollow fibers for improved biodegradation of high-strength phenol solutions. J. Membr. Sci. 258, 55-63.

Chung, T.S., Loh, K.C., Tay, H.L., 1998. Development of polysulfone membranes for bacteria immobilization to remove phenol. J. Appl. Polym. Sci. 70, 2585–2594.

Coelho, A., Castro, A.V., Dezotti, M., Sant'Anna Jr., G.L., 2006. Treatment of petroleum refinery sourwater by advanced oxidation processes. J. Hazard. Mater. 137, 178–184.

Contreras, S., Rodriguez, M., Al Momani, F., Sans, C., Esplugas, S., 2003. Contribution of the ozonation pre-treatment to the biodegradation of aqueous solutions of 2, 4-dichlorophenol.Water Res. 37, 3164-3171.

Dereeper, A., Guignon, V., Blanc, G., Audic, S., Buffet, S., Chevenet, F., Dufayard, J.F., Guindon, S., Lefort, V., Lescot, M., 2008. Phyologeny.fr: robust phylogenetic analysis for the non-specialist. Nucleic Acids Res. 36, W465-459.

Devinny, J.S., Deshusses, M.A., Webstar, T.S.,1999. Biofiltration for air pollution control, CRC publishers Inc. Boca Raton, FL, USA.

Dizge, N., Tansel, B., 2010. External mass transfer analysis for simultaneous removal of carbohydrate and protein by immobilized activated sludge culture in a packed bed batch bioreactor. J. Hazard. Mater. 184, 671-677.

Doggett, T., Rascoe, A., 2009. Global Energy Demand Seen up 44 Percent by 2030. http://www.reuters.com/articles/GCAGreenBusiness/idUSN2719528620090527 (accessed 17.09.09).

Dong, F.M., Wang, L.L., Wang, C.M., Cheng, J.P., He, Z.Q., Sheng, Z. J., Shen, R.Q., 1992. Molecular cloning and mapping of phenol degradation genes from *Bacillus stearothermophilus* FDTP-3 and their expression in *Escherichia coli*. Appl. Environ. Microbiol. 58, 2531-2535.

Du, Z., Li, H., Gu, T., 2007. A state of the art review on microbial fuel cells: A promising technology for wastewater treatment and bioenergy. Biotechnol. Adv. 25, 464–482.

Dursun, A.Y., Tepe, O., 2005. Internal mass transfer effect on biodegradation of phenol by Ca-alginate immobilized *Ralstonia eutropha*. J. Hazard. Mater. 126, 105–111.

Edalatmanesh, M., Mehrvar, M., Dhib, R., 2008. Optimization of phenol degradation in a combined photochemical–biological wastewater treatment system. Chem. Eng. Res. Des. 86, 1243-1252.

Edwards, V.H., 1970. The influence of high substrate concentrations on microbial kinetics. Biotechnol. Bioeng. 12, 679–712.

Effluent standard for Oil refinery, Central Pollution Control Board, Ministry of Environment and Forest, Government of India (http://cpcb.nic.in/Industry-Specific-Standards/Effluent/Effluent-std-oil-refinery-2008.pdf)

Ehrhardt, H.M., Rehm, H.J., 1989. Semicontinuous and continuous degradation of phenol by *Pseudomonas putida* P8 adsorbed on activated carbon. Appl. Environ. Microbiol. 30**,** 312–317.

El-Naas, M.H., Al-Muhtaseb S.A., Makhlouf, S., 2009a. Biodegradation of phenol by *Pseudomonas putida* immobilized in polyvinyl alcohol (PVA) gel. J. Hazard. Mater. 164, 720-725.

El-Naas, M.H., Al-Zuhair, S., Alhaija, M.A., 2010a. Reduction of COD in refinery wastewater through adsorption on date-pit activated carbon. J. Hazard. Mater. 173, 750-757.

El-Naas, M.H., Al-Zuhair, S., Al-Lobaney, A., Makhlouf, S., 2009b. Assessment of electrocoagulation for the treatment of petroleum refinery wastewater. J. Environ. Manage. 91, 180–185.

El-Naas, M.H., Al-Zuhair, S., Makhlouf, S.,2010b. Batch degradation of phenol in a spouted bed bioreactor system. J. Ind. Eng. Chem.16, 267-272.

El-Naas, M.H., Al-Zuhair, S., Makhlouf, S.,2010c. Continuous biodegradation of phenol in a spouted bed bioreactor (SBBR). Chem. Eng. J. 160, 565-570.

Environmental Health Safety Guidelines, 2009. Petroleum Refining in Pollution Prevention and Abatement Handbook. http://www.ifc.org/ifcext/enviro.nsf/Content/Enviromental Guidelines (accessed 27.09.09).

Feng, Q., Yu, A., Chu, L., Xing, X.H., 2008. Performance study of the reduction of excess sludge and simultaneous removal of organic carbon and nitrogen by a combination of fluidized- and fixed-bed bioreactors with different structured macro-porous carriers. Biochem. Eng. J. 39, 344-352.

Feng, W., Wen, J., Liu, C., Yuan, Q., Jia, X., Sun, Y., 2007. Modeling of local dynamic behavior of phenol degradation in an internal loop airlift bioreactor by yeast *Candida tropicalis*. Biotechnol. Bioeng. 97, 251–264.

Fernández, N., Montalvo, S., Borja, R., Guerrero, L., Sánchez, E., Cortés, I., Colmenarejo, M.F., Travieso, L., Raposo, F., 2008. Performance evaluation of an anaerobic fluidized bed reactor with natural zeolite as support material when treating high-strength distillery wastewater. Renewable Energy 33, 2458-2466.

Gaetano, J.C. 1999. Industrial waste treatment process engineering: biological processes, Volume II, CRC Press.

Gander, M., Jefferson, B., Judd, S., 2000. Aerobic MBRs for domestic wastewater treatment: a review with cost considerations, Sep. Purif. Technol. 18, 119–130.

Gao, B., Zhu, X., Xu, C., Yue, Q., Li, W., Wei, J., 2008. Influence of extracellular polymeric substances on microbial activity and cell hydrophobicity in biofilms. J. Chem. Technol. Biotechnol. 83, 227– 232.

Gargouria, B., Karraya, F., Mhiria, N., Alouia, F., Sayadi, S., 2011. Application of a continuously stirred tank bioreactor (CSTR) for bioremediation of hydrocarbon-rich industrial wastewater effluents. J. Hazard. Mater. 189, 427-434.

Gerrard, A.M., Júnior, J.P., Kostecková, A., Páca, J., Stiborová, M., Soccol, C.R., 2006. Simple models for the continuous aerobic biodegradation of phenol in a packed bed reactor. Braz. Arch. Biol. Technol. 49, 669-676.

Gianfreda, L., Iamarino, G., Scelza, R., Rao, M.A., 2006. Oxidative catalysts for the transformation of phenolic pollutants: a brief review. Biocatal. Biotransform. 24,177–87.

Gil, G.C., Chang, I.S., Kim, B.H., Kim, M., Jang, J.Y., Park, H.S., 2003. Operational parameters affecting the performance of a mediatorless microbial fuel cell. Biosens. Bioelectron.18,327–334.

Gladyshev, M.I., Sushchik, N.N., Kalachova G.S., Shchur, L.A., 1998. The effect of algal blooms on the disappearance of phenol in a small forest pond. Water Res. 32, 2769-2775.

Godjevargova, T., Ivanova, D., Aleksieva, Z., Burdelova, G.,2006. Biodegradation of phenol by immobilized *Trichosporon cutaneum* R57 on modified polymer membranes. Process Biochem. 41, 2342-2346.

Goldsmith, J.C.D., Balderson, R.K., 1988. Biodegradation and growth kinetics of enrichment isolates on benzene, toluene and xylene. Water Sci. Technol. 20, 505–507.

Gonzalez, G, Herrera, G, Garcia, M.T., 2001a. Biodegradation of phenolic industrial wastewater in a fluidized bed bioreactor with immobilized cells of *Pseudomonas putida*. Bioresour. Technol. 80, 137-142.

González, G., Herrera, M. G., García, M. T., Peña, M. M., 2001b. Biodegradation of phenol in a continuous process: comparative study of stirred tank and fluidized-bed bioreactors. Bioresour. Technol. 76, 245-251.

Guerin, T.F., Horner, S., McGovern, T., Davey B., 2002.An application of permeable reactive barrier technology to petroleum hydrocarbon contaminated groundwater. Water Res. 36, 15-24.

Guimaraes, C., Matos, C., Azeredo, J., Mota, M., Oliveira, R., 2002. The importance of the morphology and hydrophobicity of different carriers on the immobilization and sugar refinery effluent degradation activity of Phanerochaete chrysosporium. Biotechnol. Lett. 24,795–800.

Gupta, V.K., Mohan, D., Sharma, S., Sharma, M., 2000. Removal of basic dyes (rhodamine B and methylene blue) from aqueous solutions using bagasse fly ash. Sep. Sci. Technol. 35, 2097-2113.

Gurujeyalakshmi, G., Oriel, P., 1989. Isolation of phenol-degrading *Bacillus stearothermophilus* and partial characterization of the phenol hydroxylase. Appl. Environ. Microbiol. 55, 500-502.

Ha, J., Engler, C.R., Wild, J.R., 2009. Biodegradation of coumaphos, chlorferon, and diethylthiophosphate using bacteria immobilized in Ca-alginate gel beads. Bioresour. Technol. 100**,** 1138–1142.

Haines, J. R., Alexander, M., 1974. Microbial degradation of high-molecular weight alkanes. Appl. Microbiol. 28, 1084-1085.

Haldane ,J.B.S., 1965. Enzymes, MIT Press, Cambridge, MA.

Hami, M.L., Al-Hashimib, M.A., Al-Dooric, M.M., 2007. Effect of activated carbon on BOD and COD removal in a dissolved air flotation unit treating refinery wastewater. Desalination 216, 116–122.

Hamoudi, S., Sayari, A., Belkacemi, K., Bonneviot, L., Larachi, F., 2000. Catalytic wet oxidation of phenol over $Pt_xAg_{1-x}MnO_2/CeO_2$ catalysts. Catal. Today 62, 379–388.

Harry, M.F., 1995. Industrial Pollution Handbook. McGraw Hill Inc., New York.

Hill, G.A., Robinson, C.W., 1975. Substrate inhibition kinetics: phenol degradation by *Pseudomonas putida*. Biotechnol. Bioeng. 17, 1599-1615.

Hilpert, L. R., May, W. E., Wise, S. A., Chesler, S. N., Hertz, H. S., 1978. Inter-laboratory comparison of determinations of trace level petroleum hydrocarbons in marine sediments. Anal. Chem. 50, 458–463.

Hirata, A., Takemoto, T., Ogawa, K., Auresenia, J., Tsuneda, S., 2000. Evaluation of kinetic parameters of biochemical reaction in three-phase fluidized bed biofilm reactor for wastewater treatment. Biochem. Eng. J. 5, 165–171.

Ho, K.L., Lin, B., Chen, Y.Y., 2009. Biodegradation of phenol using Corynebacterium sp DJ1 aerobic granules. Bioresour. Technol. 100, 5051-5055.

Hsieh, C.T., Teng, H., 2000. Liquid-phase adsorption of phenol onto activated carbons prepared with different activation levels. J. Colloid Interface Sci. 230, 171–175.

Hsieh, F.M., Huang, C., Lin, T.F., Chen, Y.M., Lin, J.C., 2008. Study of sodium tri polyphosphate-cross linked chitosan beads entrapped with *Pseudomonas putida* for phenol degradation. Process Biochem. 43, 83-92.

Huppe, P., Hoke, H., Hempel, D.C., 1990. Biological treatment of effluents forms a coal tar refinery using immobilized biomass. Chem. Eng. Technol. 13, 73–79.

Hussain, A., Kumar, P., Mehrotra, I., 2010. Nitrogen biotransformation in anaerobic treatment of phenolic wastewater. Desalination 250, 35-41.

Jadhav, N., Vanjara, A.K., 2004. Removal of phenol from wastewater using sawdust, polymerized sawdust and sawdust carbon. Ind. J. Chem. Technol.11, 35-41.

Ji, G.D., Sun, T.H., Ni, J.R., Tong, J.J., 2009. Anaerobic baffled reactor (ABR) for treating heavy oil produced water with high concentrations of salt and poor nutrient, Bioresour. Technol. 100, 1108-1114.

Jiang, H.L., Tay, J.H., Maszenan, A.M., Tay, S.T.L., 2006. Enhanced phenol biodegradation and aerobic granulation by two coaggregating bacterial strains. Environ. Sci. Technol**.** 40, 6137–6142.

Jiang, Y., Ren, N., Cai, X., Wu, D., Qiao, L., Lin S., 2008. Biodegradation of phenol and 4-chlorophenol by the mutant strain CTM 2. Chin. J. Chem. Eng. 16, 796-800.

Jiang, Y., Wen, J., Bai, J., Jia, X., Hu Z., 2007. Biodegradation of phenol at high initial concentration by *Alcaligenes faecalis*. J. Hazard. Mater. 147, 672-676.

Jianlong, W., Liping, H., Hanchang, S., Yi, Q., 2001. Biodegradation of quinoline by gel immobilized *Burkholderia sp.* Chemosphere 44, 1041-1046.

Jin, L., Wang, X.J., Gu, Z.L., Zhou, D.Z., Xie, S.Q., 2006. Biodegradation of lubricating oil in wastewater with *Zoogloea* sp. Pedosphere 16, 540-544.

Jou, C.J.G., Huang, G.C., 2003. A pilot study for oil refinery wastewater treatment using a fixed-film bioreactor. Adv. Environ. Res. 7, 463-469.

Juang, R.S., Huang, W.C., Hsu, Y.H., 2009. Treatment of phenol in synthetic saline wastewater by solvent extraction and two-phase membrane biodegradation. J. Hazard. Mater. 164, 46-52.

Juang, R.S., Tsai, S.Y., 2006. Growth kinetics of *Pseudomonas putida* in the biodegradation of single and mixed phenol and sodium salicylate. Biochem. Eng. J. 31, 133-140.

Juang, R.S., Wu, C.Y.,2007. Microbial degradation of phenol in high-salinity solutions in suspensions and hollow fiber membrane contactors. Chemosphere 66, 191-198.

Kanai, T., Uzumaki, T., Kawase, Y.,1996. Simulation of airlift bioreactors: Steady-state performance of continuous culture processes. Comput. Chem. Eng. 20, 1089-1099.

Karel, S.F., Libicki, S.B., Robertson, C.R., 1985. The immobilization of whole cells: Engineering principles. Chem. Eng. Sci. 40, 1321–1354.

Kathiravan, M.N., Rani, R.K., Karthick, R., Muthukumar, K., 2010. Mass transfer studies on the reduction of Cr (VI) using calcium alginate immobilized *Bacillus* sp. in packed bed reactor. Bioresour. Technol. 101, 853–858.

Kator, H., Oppenheimer, C.H., Miget, R.J., 1971. Microbial degradation of a Louisiana crude oil in closed flasks and under simulated field conditions, in: Joint Conference on Prevention and Control of Oil Spills. American Petroleum Institute, Washington, D.C., 287-296.

Keith, L., Telliard, W., 1979. Priority pollutants: I-a perspective view. Environ. Sci. Technol. 13, 416–423.

Khleifat, K.M., 2006. Biodegradation of phenol by *Ewingella americana*: Effect of carbon starvation and some growth conditions. Process Biochem. 41, 2010-2016.

Kılıç, N.K., 2009. Enhancement of phenol biodegradation by *Ochrobactrum* sp. isolated from industrial wastewaters, Int. Biodeterio. Biodegrad. 63, 778-781.

Kim, K., Logan, B.E., 2001. Microbial reduction of perchlorate in Pure and mixed culture packed-bed bioreactors. Water Res. 35, 3071–3076.

Kim, M.K., Singleton, I., Yin, C.R., Quan, Z.X., Lee, M., Lee, S.T., 2006. Influence of phenol on the biodegradation of pyridine by freely suspended and immobilized *Pseudomonas putida* MK1. 42, 495–500.

Kornaros, M., Lyberatos, G.,2006. Biological treatment of wastewaters from a dye manufacturing company using a trickling filter. J. Hazard. Mater. 136, 95–102.

Kozhevnikov, S.A., Motovilova, N.N., Sibarov, D.A., Vinogradov, M.V., 1985. Properties of zeolite catalysts and their effect on the formation of cresols from phenol and toluene. Russ. J Appl Chem USSR, 58, 1412-1415.

Ku, Y., Lee, K.C., 2000. Removal of phenols from aqueous solution by XAD-4 resin. J. Hazard. Mater. 80, 59-68.

Kujawski,W., Warszawski, A., Ratajczak, W., Porebski, T., Capała, W., Ostrowska, I., 2004. Application of pervaporation and adsorption to the phenol removal from wastewater. Sep. Purif. Technol. 40, 123-132.

Kuleyin, A., 2007. Removal of phenol and 4-chlorophenol by surfactant-modified natural zeolit. J. Hazard. Mater.144, 307-315.

Kulkarni, U.S., Dixit, S.G., 1991. Destruction of phenol from wastewater by oxidation with $S0_{32}$—0_2, Ind. Eng. Chem. Res. 30, 1916-1920.

Kumar, A., Kumar S., Kumar, S., 2005. Biodegradation kinetics of phenol and catechol using Pseudomonas putida MTCC 1194. Biochem. Eng. J. 22, 151-159.

Kumar, A., Kumar, S., Kumar, S., Gupta, D.V., 2007. Adsorption of phenol and 4-nitrophenol on granular activated carbon in basal salt medium: Equilibrium and kinetics. J. Hazard. Mater. 147, 155–166.

Kunin, R., Mcgarvey, F. X., 1949. Equilibrium and column behavior of exchange resins-strong base anion exchange resin, Ind. Eng. Chem., 41, 1265–1268.

Kwon, K.H., Yeom, S.H., 2009. Optimal microbial adaptation routes for the rapid degradation of high concentration of phenol. Bioprocess Biosyst. Eng. 32, 435-442.

Lalwani, M., Singh, M., 2010. Conventional and renewable energy scenario of India: Present and future. Can. J. Electri. Electron. Eng. 1, 122-140.

Lathasree, S., Rao, N., Sivashankar, B., Sadasivam, V., Rengaraj, K., 2004. Heterogeneous photo catalytic mineralization of phenols in aqueous solutions. J. Mol. Catal. A: Chem. 223, 101–105.

Lee, J., Shim, W., Ko J., Moon, H., 2004. Adsorption equilibria, kinetics, and column dynamics of chlorophenols on a nonionic polymeric sorbent, XAD-1600. Sep. Sci. Technol. 39, 2041–2065.

Lee, S.Y., Kim, B.N., Han, J.H., Chang, S.T., Choi, Y.W., Kim, Y.H., Min, J., 2010. Treatment of phenol-contaminated soil by *Corynebacterium glutamicum* and toxicity removal evaluation. J. Hazard. Mater. 182, 937-940.

Leung, K.T., Cassidy, M.B., Homes, S.B., Lee, H., Trevors, J.T., 1995. Survival of κ-carrageenan-encapsulated and unencapsulated Pseudomonas UG2Lr cells in forest soil monitored by polymerase chain reaction and spread plating. FEMS Microbiol. Ecol. 16, 71–78.

Levén, L., Nyberg, K., Korkeaaho, L., Schnürer, A.,2006. Phenols in anaerobic digestion processes and inhibition of ammonia oxidising bacteria (AOB) in soil. Sci.Total Environ. 364, 229-238.

Levenspiel, O. *Chemical Reaction Engineering.* Wiley and Sons, Singapore, 1972, 460–505.

Levin, L., Vialeb, A., Forchiassina, A., 2003. Degradation of organic pollutants by the white rot *basidiomycete Trametes trogii*, Int. Biodeterio.Biodegra. 52, 1-5.

Li, H.Q., Han, H.J., Du, M.A., Wang, W.,2011. Removal of phenols, thiocyanate and ammonium from coal gasification wastewater using moving bed biofilm reactor. Bioresour. Technol. 102, 4667-4673.

Li, Y., Li, J., Wang C., Wang, P., 2010. Growth kinetics and phenol biodegradation of psychrotrophic *Pseudomonas putida* LY1, Bioresour. Technol. 101, 6740-6744.

Li, Y., Loh, K.C.,2007. Continuous phenol biodegradation at high concentrations in an immobilized-cell hollow fiber membrane bioreactor. J. Appl. Polym. Sci. 105, 1732–1739.

Lide, D.R., 2004. CRC Handbook of Chemistry and Physics, 85th Ed., CRC Press,

Lika, K., Papadakis, I.A., 2009. Modeling the biodegradation of phenolic compounds by microalgae. J. Sea Res. 62, 135-146.

Liu, H., Ramnarayanan, R., Logan, B.E.,2004. Production of electricity during wastewater treatment using a single chamber microbial fuel cell. Environ. Sci. Technol. 28,2281–2285.

Liu, Y., Yang, C.H., Li, J., 2007. Adhesion and retention of a bacterial phytopathogen *Erwinia chrysanthemi* in biofilm-coated porous media. Environ. Sci. Technol. 42, 159–165.

Liu, Y.J., Zhang, A.N, Wang, X.C., 2009. Biodegradation of phenol by using free and immobilized cells of *Acinetobacter sp*. XA05 and *Sphingomonas* sp. FG03. Biochem. Eng. J. 44, 187-192.

Livingston A.G., Chase H.A., 1991. Development of a phenol degrading fluidized bed bioreactor for constant biomass holdup. Chem. Eng. J. 45, B35-B47.

Loh, K.C., Chua, S.S., 2002. Ortho pathway of benzoate degradation in *Pseudomonas putida*: induction of meta pathway at high substrate concentrations. Enzyme Microb. Technol. 30, 620-626.

Loh, K.C., Liu, J.,2001. External loop inversed fluidized bed airlift bioreactor (EIFBAB) for treating high strength phenolic wastewater. Chem. Eng. Sci. 56, 6171-6176.

Lohi, A., Cuenca, M. A., Anania, G., Upreti, S.R., Wan, L.,2008. Biodegradation of diesel fuel-contaminated wastewater using a three-phase fluidized bed reactor. J. Hazard. Mater.154, 105-111.

Luo, H., Liu, G., Zhang, R., Jin S., 2009. Phenol degradation in microbial fuel cells. Chem. Eng. J. 147, 259-264.

Ma, F., Guo, J.B., Zhao, L.J., Chang, C.C., Cui, D., 2009. Application of bioaugmentation to improve the activated sludge system into the contact oxidation system treating petrochemical wastewater. Bioresour. Technol. 100, 597–602.

Mahajan, S.P., 1989. Pollution control in process industries, McGraw-Hill, New Delhi.

Marcilly, C., 2003. Present status and future trends in catalysis for refining and petrochemicals. J. Catal. 216, 47–62.

Marrot, B., Martinez, A. B., Moulin, P., Roche, N., 2006. Biodegradation of high phenol concentration by activated sludge in an immersed membrane bioreactor. Biochem. Eng. J. 30, 174-183.

Martínez, D.A.B., Giraldo, L., Piraján, J.C.M., 2009. Effect of the pH in the adsorption and in the immersion enthalpy of monohydroxylated phenols from aqueous solutions on activated carbons. J. Hazard. Mater. 169, 291–296.

Masque, C., Nolla, M., Bordons, A., 1987. Selection and adaptation of a phenol degrading strain of *Pseudomonas*. Biotechnol. Lett. 9, 655–660.

Masters, G. M., 1998. Introduction to environmental engineering and science, Second edition, Prentice Hall Inc., NJ.

Mattiasson, B., 1983. Immobilized Cells and Organelles: Vol. II, First ed., CRC Press.

Mayer, J.G., Gallegos, J.R., Ordaz, N.R., Ramírez, C.J., Alcocer, A. S., Varaldo, H.M.P.,2008. Phenol and 4-chlorophenol biodegradation by yeast Candida tropicalis in a fluidized bed reactor. Biochem. Eng. J. 38, 147-157.

McKenna, E. J., Kallio, R. E., 1964. Hydrocarbon structure: its effect on bacterial utilization of alkanes, in: Heukelian, H., Dondero, N. C., (Eds.), Principles and applications in aquatic microbiology. John Wiley & Sons, Inc., New York, 1-14.

Melo, J.S., Kholi, S., Patwardhan, A.W., D'Souza, S.F., 2005. Effect of oxygen transfer limitations in phenol biodegradation. Process Biochem. 40, 625-628 .

Meyer, J.S., Marcus, M.D., Bergman, H.L., 1984. Inhibitory interactions of aromatic organics during microbial degradation. Enivron. Toxicol. Chem. 3, 583-587.

Min, B., Kim, J.R., Oh, S.E., Regan, J.M., Logan, B.E.,2005. Electricity generation from swine wastewater using microbial fuel cells. Water Res. 39,4961–4968.

Mitra, S., Kambiz, A. N., Hossein, S. Z., Tayebe, B., Gholamreza, K., Monir, M., Iman, R., Solmaz, A., Jamshid, R., Habib, A., 2009. Efficient phenol degradation by a newly characterized *Pseudomonas* sp. SA01 isolated from pharmaceutical wastewaters. Desalination 246, 577-594.

Mollaei, M., Abdollahpour, S., Atashgahi, S., Abbasi, H., Masoomi, F., Rad, I., Lotfi, A.S., Zahiri, H.S., Vali, H., Noghabi, K.A., 2010. Enhanced phenol degradation by *Pseudomonas* sp. SA01: gaining insight into the novel single and hybrid immobilizations. J. Hazard. Mater. 175, 284–292.

Monsalvo, V.M., Mohedano, A.F., Casas, J.A., Rodríguez, J.J., 2009. Cometabolic biodegradation of 4-chlorophenol by sequencing batch reactors at different temperatures. Bioresour. Technol. 100, 4572-4578.

Monteiro Á.A.M.G., Boaventura R.A.R., Rodrigues A.E., 2000. Phenol biodegradation by *Pseudomonas putida* DSM 548 in a batch reactor, Biochem. Eng. J. 6, 45-49.

Moon, H., Chang, I.S., Kim, B.H.,2006. Continuous electricity production from artificial wastewater using a mediator-less microbial fuel cell. Bioresour. Technol.97,621–627.

Mordocco, A., Kuek, C., Jenkins, R., 1999. Continuous degradation of phenol at low concentration using immobilized *Pseudomonas putida*. Enzyme Microb. Technol. 25, 530-536.

Mrayyana, B., Battikhi, M.N., 2005. Biodegradation of total organic carbons (TOC) in Jordanian petroleum sludge. J. Hazard. Mater. 120, 127–134.

Munoz, R., Jacinto, M., Guieysse, B., Mattiasson, B., 2005. Combined carbon and nitrogen removal from acetonitrile using algal-bacterial bioreactors. Appl. Microbiol. Biotechnol. 67, 699–707.

Murty, V.R.C., Bhat, J., Muniswaran, P.K.A., 2005. External mass transfer effects during the hydrolysis of rice bran oil in immobilized lipase packed bed reactor. Chem. Biochem. Eng. 19, 57–61.

Nakamura, Y., Sawada, T., Sungusi, M.G., Kobayashi, F., Kuwahara, M., Ito, H., 1997. Lignin peroxidase production by Phanerochaete chrysosporium. J. Chem. Eng. Japan 30, 1–6.

Namane, A., Hellal, A., 2006. The dynamic adsorption characteristics of phenol by granular activated carbon. J. Hazard. Mater. 137, 618-625.

Nardi, I.R., Ribeiro, R., Zaiat, M., Foresti, E., 2005. Anaerobic packed-bed reactor for bioremediation of gasoline-contaminated aquifers. Process Biochem. 40, 587-592.

Nath, S., Chand, S., 1996. Mass transfer and biochemical reaction in immobilized cell packed bed reactor: correlation of experiment with theory. J. Chem. Technol. Biotechnol. 66, 286–292.

Neumann, G., Teras, R., Monson, L., Kivisaar, M., Schauer, F., Heipieper, H.J., 2004. Simultaneous degradation of atrazine and phenol by *Pseudomonas* sp. strain ADP: effects of toxicity and adaptation. Appl. Environ. Microbiol. 70, 1907-1912.

Nuhoglu, A., Yalcin, B., 2005. Modeling of phenol removal in a batch reactor. Process Biochem. 40, 1233-1239.

Oh, C.G., Ahn, J.H., Ihm, S.K., 2003. Adsorptive removal of phenolic compounds by using hypercrosslinked polystyrenic beads with bimodal pore size distribution. React. Funct. Polym. 57, 103-111.

Oh, S.E., Logan, B.E.,2005. Hydrogen and electricity production from a food processing wastewater using fermentation and microbial fuel cell technologies. Water Res. 39, 4673–4682.

Ohlen, K., Chang, Y.K., Hegemann, W., Yin, C.R., Lee, S.T., 2005. Enhanced degradation of chlorinated ethylenes in groundwater from a paint contaminated site by two-stage fluidizedbed reactor. Chemosphere 58, 373–377.

Oliveira, S.V.W.B., Moraes, E.M., Adorno, M.A.T., Varesche, M.B.A., Foresti, E., Zaiat, M., 2004. Formaldehyde degradation in an anaerobic packed-bed bioreactor. Water Res. 38, 1685–1694.

Onysko, K.A., Budman, H.M., Robinson, C.W., 2000. Effect of temperature on the inhibition kinetics of phenol biodegradation by *Pseudomonas putida* Q5. Biotechnol. Bioeng. 70, 291–299.

Oswald, W., 1907. The modern theory of energetics. The Monist, 17, 510-511.

Ozkaya, B., 2006. Adsorption and desorption of phenol on activated carbon and a comparison of isotherm models. J. Hazard. Mater. B129, 158–163.

Pardeshi, S.K., Patil, A.B., 2008. A simple route for photocatalytic degradation of phenol in aqueous zinc oxide suspension using solar energy. Sol. Energy 82, 700–705.

Patil, N.K., Veeranagouda, Y., Vijaykumar, M.H., Nayak, S. A., Karegoudar, T.B., 2006. Enhanced and potential degradation of o-phthalate by *Bacillus sp.* immobilized cells in alginate and polyurethane. Int. Biodeterio. Biodegra. 57, 82–87.

Patterson, J.W., 1985. Industrial wastewater treatment technology, 2nd Edition, Butterworths, USA.

Pavlova, A., Ivanova, R., 2003. Determination of petroleum hydrocarbons and polycyclic aromatic hydrocarbons in sludge from wastewater treatment basins. J. Environ. Monit. 5, 319–323.

Pawlowsky, U., Howell, J.A., 1973. Mixed culture bio-oxidation of phenol I. Determination of kinetic parameters. Biotechnol. Bioeng. 15, 889–896.

Pedersen, A.R., Arvin, E., 1995. Removal of toluene in waste gases using a biological trickling filter. Biodegradation 6, 109–118.

Phan, T.N.T., Bacquet, M., Morcellet, M.J., 2000. Synthesis and characterization of silica gels functionalized with monochlorotriazinyl β-cyclodextrin and their sorption capacities towards organic compounds. Inclusion Phenom. Macrocyclic Chem. 38, 345-359.

Pinto1, G., Pollio, A., Previtera, L., Temussi, F., 2002. Biodegradation of phenols by microalgae. Biotechnol. Lett. 24,2047–2051.

Poulton, S.W., Krom, M.D., Rijn, J.V., Raiswell, R., 2002. The use of hydrous iron (III) oxides for the removal of hydrogen sulphide in aqueous systems. Water Res. 36, 825–834. **1**

Pour, A. K., Karamanev, D., Margaritis, A., 2005. Biodegradation of petroleum hydrocarbons in an immobilized cell airlift bioreactor, Water Res. 39, 3704–3714.

Pramanik, S., McEvoy, J., Siripattanakul, S., Khan E., 2011. Effects of cell entrapment on nucleic acid content and microbial diversity of mixed cultures in biological wastewater treatment. Bioresour. Technol. 102, 3176-3183.

Pruden, A., Sedran, M., Cuidan, M., Venosa, A., 2003. Biodegradation of MTBE and BTEX in an aerobic fluidized bed reactor. Water Sci. Technol. 47, 123–128.

Quail, B.E., Hill, G.A., 1991. A packed-column bioreactor for phenol degradation: Model and experimental verification. J. Chem. Technol. Biotechnol. 52, 545-557.

Quan, X., Shi, H., Zhang, Y., Wang, J., Qian, Y., 2004. Biodegradation of 2,4-dichlorophenol and phenol in an airlift inner-loop bioreactor immobilized with *Achromobacter* sp. Sep. Purif. Technol. 34, 97-103.

Ramos, J. L., Duque, E., Rodriguez-Herva, J.-J., Godoy, P., Haidour, A., Reyes, F., Fernandez-Barrero, A., 1997. Mechanisms for solvent tolerance in bacteria. J. Biol. Chem. 272, 3887-3890.

Rao, J.R., Viraraghavan, T., 2002. Biosorption of phenol from an aqueous solution by *Aspergillus niger* biomass. Bioresour. Technol. 85,165-171.

Rao, N.C., Mohan, S.V., Muralikrishna, P., Sarma, P.N., 2005. Treatment of composite chemical wastewater by aerobic GAC-biofilm sequencing batch reactor (SBGR). J. Hazard. Mater. B124, 59–67.

Reardon, K.F., Mosteller, D.C., Rogers, J.D.B., 2000. Biodegradation kinetics of benzene, toluene and phenol as single and mixed substrates for *Pseudomonas putida* F1. Biotechnol Bioeng. 69, 385–400.

Reda, A. B., Ashraf, T.A.H., 2010. Optimization of bacterial biodegradation of toluene and phenol under different nutritional and environmental conditions. J. Appl. Sci. Res. 6, 1086-1095.

Reese, J., Silva, E.M., Yang, S.T., Fan, L. S., 1999. Fluidization solids handling and processing.Siemens westinghouse power corporation, Pittsburgh, PA, USA, 582-682.

Ren, S., Frymier, P.D., 2003. Toxicity estimation of phenolic compounds by bioluminescent bacterium. J. Environ. Eng. ASCE 129, 328–335.

Rhee, J.S., Jung., M.W., Paeng, K.J., 1998. Evaluation of chitin and chitosan as a sorbent for the preconcentration of phenol and chlorophenols in water. Anal. Sci. 14, 1089-1092.

Rigo, M., Alegre, R.M., 2004. Isolation and selection of phenol-degrading microorganisms from industrial waste waters and kinetics of the biodegradation. Folia Microbiol. 49, 41–45.

Rodríguez, I., Llompart, M. P. Cela, R., 2000. Solid-phase extraction of phenols. J. Chromatogr. A 885, 291-304.

Rosvita, E. M., Fiona, M. D., Rudolf M., 1999. Catechol 2,3-dioxygenase from the thermophilic, phenol-degrading *Bacillus thermoleovorans* strain A2 has unexpected low thermal stability. Extremophiles 3, 185-190.

Rovito, B.J., Kittrell, J.R., 1973. Film and pore diffusion studies with immobilized glucose oxidase. Biotechnol. Bioeng. 15, 143–161.

Ruiz-Ordaz, N., Ruiz-Lagunez, J.C., Castañon-González, J.H., Hernández-Manzano, E., Cristiani-Urbina, E., Galíndez-Mayer, J., 2001. Phenol biodegradation using a repeated batch culture of Candida tropicalis in a multistage bubble column. Rev. Latinoam. Microbiol. 43, 19-25.

Rusten, B., Odegaard, H., Lundar, A., 1992. Treatment of dairy wastewater in a novel moving bed biofilm reactor. Wat. Sci. Technol. 26, 703–711.

Sá, C. S. A., Boaventura, R. A. R.,2001. Biodegradation of phenol by *Pseudomonas putida* DSM 548 in a trickling bed reactor. Biochem. Eng. J. 9, 211-219.

Safferman, S.L., Bishop, P.L., 1996. Aerobic fluidized bed reactor with internal media cleaning. J. Environ. Eng. 122, 284–291.

Salame I.I., Bandosz, T.J., 2003. Role of surface chemistry in adsorption of phenol on activated carbons, J. Colloid Interface Sci. 264, 307–312.

Santos, F.V., Azevedo, E.B., Sant'Anna Jr., G.L., Dezotti, M., 2006. Photocatalysis as a tertiary treatment for petroleum refinery wastewaters. Braz. J. Chem. Eng. 23, 450–460.

Santos, V.L., Linardi, V.R., 2004. Biodegradation of phenol by filamentous fungi isolated from industrial effluents– identification and degradation potential. Process Biochem. 39,1001–1006.

Santos, V.L.D., Monteiro, A.D.S., Telles Braga, D., Santoro, M.M., 2009. Phenol degradation by *Aureobasidium pullulans* FE13 isolated from industrial effluents. J. Hazard. Mater. 161, 1413–1420.

Saravanan, P., Pakshirajan, K., Saha P.K., 2008. Growth kinetics of an indigenous mixed microbial consortium during phenol degradation in a batch reactor. Bioresour. Technol. 99, 205-209.

Saravanan, P., Pakshirajan, K., Saha, P.K., 2009. Treatment of phenolics containing synthetic wastewater in an internal loop airlift bioreactor (ILALR) using indigenous mixed strain of *Pseudomonas* sp. under continuous mode of operation. Bioresour. Technol. 100, 4111-4116.

Sayler, G.S., Ripp, S., 2000. Field applications of genetically engineered microorganisms for bioremediation processes. Curr. Opin. Biotechnol. 11, 286-289.

Schmauder, H.P., 2004. Methods in biotechonology, Taylor & Francis, London, UK.

Schügerl, K., 1997. Three-phase-biofluidization—application of three-phase fluidization in the biotechnology—a review.Chem. Eng. Sci. 52, 3661-3668.

Semple, K.T., Cain R.B., 1996. Biodegradation of phenols by the alga *Ochromonas danica*. Appl. Environ. Microbiol. 62, 1265–1273.

Sen, S., Demirer, G. N., Anaerobic treatment of real textile wastewater with a fluidized bed reactor. Water Res. 37, 1868-1878.

Sheeja R.Y., Murugesan T., 2002, Mass transfer studies on the biodegradation of phenols in up-flow packed bed reactors, J. Hazard. Mater. 89, 287–301.

Sheng, G.P., Yu, H.Q., Wang, C.M., 2006. FTIR-spectral analysis of two photosynthetic H_2-producing strains and their extracellular polymeric substances, Appl. Microbiol. Biotechnol. 73, 204-210.

Shetty, K.V., Kalifathulla, I., Srinikethan, G., 2007. Performance of pulsed plate bioreactor for biodegradation of phenol. J. Hazard. Mater.140, 346-352.

Shieh, W.K., Keenan, J.D., 1986. Fluidized bed biofilm reactor for wastewater treatment. Adv. Biochem. Eng. Biotechnol. 33, New York, 131–169.

Shourian, M., Noghabi, K.A., Zahiri, H.S., Bagheri, T., Karballaei, G., Mollaei, M., Rad I., Ahadi, S., Raheb, J., Abbasi, H., 2009. Efficient phenol degradation by a newly characterized *Pseudomonas* sp. SA01 isolated from pharmaceutical wastewaters. Desalination 246, 577-594.

Shukla, P., Sun, H., Wang, S.H., Ang, H.M., Tadé, M.O., 2011. Co-SBA-15 for heterogeneous oxidation of phenol with sulfate radical for wastewater treatment, Catal. Today doi:10.1016/j.cattod.2011.03.005.

Silva, M.R., Coelho, M.A.Z., Araújo, O.Q.F., 2002. Minimization of phenol and ammoniacal nitrogen in refinery wastewater employing biological treatment, Engenharia Térmica, Edição Especial, 1, 33-37.

Simpson, C. D., Cullen, W. R., Quinlan K. B., Reimer, K. J., 1995. Methodology for the determination of priority pollutant polycyclic aromatic hydrocarbons in marine sediments. Chemosphere 31, 4143-4155.

Singleton, I., 1994. Microbial metabolism of xenobiotics: fundamental and applied research. J. Chem. Technol. Biotechnol. 59, 9–23.

Sittig, M., 1997. How to remove pollutants and toxic materials from air and water — a practical guide. Noyes Data Corporation, Park Ridge, NJ, USA.

Smith, A.J., Tobias, R.S., Cassidy, N., 1996. Influence of substrate nature and immobilization of implanted dentin matrix components during induction of reparative dentinogenesis. Connect. Tissue Res. 32, 291–296.

Smith, J.M. 1987. Chemical engineering kinetics, 3rd ed., McGraw Hill, New York.

Soda, S., Ike, M., Fujita, M., 1998. Effects of inoculation of a genetically engineered bacterium on performance and indigenous bacteria of a sequencing batch activated sludge process treating phenol. J. Fermen. Bioeng. 86**,** 90–96.

Stehlickova L., Svab, M., Wimmerova, L., Kozler, J., 2009. Intensification of phenol biodegradation by humic substances, Int. Biodeterio. Biodegrad. 63, 923-927.

Stoilova, I., Krastanov, A., Stanchev, V., Daniel, D., Gerginova, M., Alexieva, Z., 2006. Biodegradation of high amounts of phenol, catechol, 2,4-dichlorophenol and 2,6-dimethoxyphenol by *Aspergillus awamori* cells. Enzyme Microb. Technol. 39, 1036-1041.

Stoilova, I., Krastanov, A., Yanakieva, I., Kratchanova, M., Yemendjiev, H., 2007. Biodegradation of mixed phenolic compounds by *Aspergillus awamori* NRRL 3112. Int. Biodeterio. Biodegrad. 60, 342-346.

Sun, Y. S., Zhang, Y., Quan, X., 2008. Treatment of petroleum refinery wastewater by microwave-assisted catalytic wet air oxidation under low temperature and low pressure. Sep. Purif. Technol. 62, 565-570.

Sundstrom, D.W., Klei, H.E., 1979. Wastewater treatment, Second Edition. Prentice-Hall, New York.

Suzuki, S., Karube, I., Matsunaga, T.,1978. Application of a biochemical fuel cell to wastewater. Biotechnol. Bioeng. Symp. 8, 501–511.

Takako, M.N., Kohtaro, K., Kuniki, K., 2003. Degradation of dimethyl sulfoxide by the immobilized cells of *Hyphomicrobium denitrificans* WU-K217. Biochem. Eng. J. 15,199–204.

Tepe O.**,** Dursun A.Y., 2008. Combined effects of external mass transfer and biodegradation rates on removal of phenol by immobilized *Ralstonia eutropha* in a packed bed reactor. J. Hazard. Mater. 151, 9-16.

Terzyk, A.P., 2003. Further insights into the role of carbon surface functionalities in the mechanism of phenol adsorption. J. Colloid Interface Sci. 268, 301-329.

Tieng, Y.P., Sun, G., 2000. Use of polyvinyl alcohol as a cell entrapment matrix for copper biosorption by yeast cells. J. Chem. Technol. Biotechnol. 75,541–546.

Tor, A., Cengeloglu, Y., Aydin, M.E., Ersoz, M., 2006. Removal of phenol from aqueous phase by using neutralized red mud. J. Colloid Interface Sci. 15,498-503.

Trabelsi, F., Lyazidi, H.A., Ratsimba, B., Wilhelm, A.M., Delmas, H., Fabre, P.L., Berlan, J., 1996. Oxidation of phenol in wastewater by sonoelectrochemistry. Chem. Eng. Sci. 51, 1857-1865.

Treccani, V., 1964. Microbial degradation of hydrocarbons. Prog. Ind. Microbiol. 4, 3-33.

Trevors, J.T., Elsas, J.D., Lee, H., Wolters, A.C., 1993. Survival of alginate encapsulated *Pseudomonas fluorescens* cells in soil. Appl. Microbiol. Biotechnol. 39, 637–643.

Trigo, A., Valencia, A., 2009. Ildefonso Cases. Syst. Approach. Biodegrad. 33, 98–108.

Tsai, S.C., Tsai, L.D., Li, Y.K., 2005. An isolated *Candida albicans* TL3 capable of degrading phenol at large concentration. Biosci. Biotechnol. Biochem. 69, 2358–2367.

Tsai, S.Y., Juang, R.S., 2006. Biodegradation of phenol and sodium salicylate mixtures by suspended *Pseudomonas putida* CCRC 14365. J. Hazard. Mater. 138, 125-132.

Tumbasa, I.I., Trickovic, J., Karlovic, E., Tamas, Z., Roncevic, S., Dalmacija, B., Petrovic, O., Klasnja, M., 2004. GC/MS-SCAN to follow the fate of crude oil components in bioreactors set to remediate contaminated soil. Int. Biodeterio. Biodegra. 54, 311 – 318.

Tyagi, R.D., Tran, F.T., Chowdhury, A.K.M.M., 1993a. A pilot study of biodegradation of petroleum refinery wastewater in a polyurethane-attached RBC. Process Biochem. 28, 75-82.

Tyagi, R.D., Tran, F.T., Chowdhury, A.K.M.M., 1993b. Biodegradation of petroleum refinery wastewater in a modified rotating biological contactor with polyurethane foam attached to the disks. Water Res. 27, 91-99.

Tziotzios, G., Teliou, M., Kaltsouni, V., Lyberatos, G., Vayenas, D.V., Biological phenol removal using suspended growth and packed bed reactors. Biochem. Eng. J. 26, 65-71.

Ucun H., Yildiz, E., Nuhoglu, A., 2010. Phenol biodegradation in a batch jet loop bioreactor (JLB): Kinetics study and pH variation. Bioresour. Technol. 101, 2965-2971.

Varma, R.J., Gaikwad, B.G., 2008. Rapid and high biodegradation of phenols catalyzed by *Candida tropicalis* NCIM 3556 cells. Enzyme Microb. Technol. 43, 431-435.

Varma, R.J., Gaikwad, B.G., 2009. Biodegradation and phenol tolerance by recycled cells of *Candida tropicalis* NCIM 3556. Int. Biodeterio. Biodegrad. 63, 539-542.

Venkataraman, J., Kaul, S. N., Satyanarayan, S., 1992. Determination of kinetic constants for a two-stage anaerobic upflow packed-bed reactor for dairy wastewater. Bioresour. Technol. 40, 253-261.

Venu Vinod, G., Reddy, V.,enkat, 2006. Mass transfer correlation for phenol biodegradation in a fluidized bed bioreactor. J. Hazard. Mater. 136, 727-734.

Verner, L., Ludmila, L., Jan, A., Franch, B., 2000. Identification of compounds and specific functional groups in the wavelength region 168–330 nm using gas chromatography with UV detection. J. Chromatogr.,A 867**,** 187–206.

Vijayagopal, V., Viruthagiri, T., 2005. Kinetics of biodegradation of phenol using mixed culture isolated from mangrove soil. Pollut. Res. 24, 157–162.

Vinod, V.A., Reddy, G.V., 2005. Simulation of biodegradation process of phenolic wastewater at higher concentrations in a fluidized-bed bioreactor. Biochem. Eng. J. 24, 1–10.

Wake, H., 2005. Oil refineries: a review of their ecological impacts on the aquatic environment. Estuar. Coast Shelf Sci. 62, 131–140.

Wang Y., Tian, Y., Han, B., Zhao, H.B., Bi, J.N., Cai, B.L., 2007. Biodegradation of phenol by free and immobilized *Acinetobacter* sp. strain PD12, J. Environ. Sci.19, 222-225.

Wang, D.I.C., Cooney, C.L., Demain, A.L., Dunhill, P., Humphrey, A.E., Lilly, M.D., 1979. Fermentation and enzyme technology, John Wiley & Sons, New York.

Wang, L., Li, Y., Yu, P., Xie, Z., Luo, Y., Lin, Y., 2010. Biodegradation of phenol at high concentration by a novel fungal strain *Paecilomyces variotii* JH6, J. Hazard. Mater. 183, 366-371.

Wang, M.L., Hu, K.H., 1994. Extraction of phenol using sulfuric acid salts of trioctylamine in a supported liquid membrane. Ind. Eng. Chem. Res. 33, 914–921.

Wang, S.J., Loh, K.C., 1999. Modeling the role of metabolic intermediates in kinetics of phenol biodegradation. Enzyme Microb. Technol. 25, 177-184.

Wang, Y., Tian, Y., Han, B., Zhao, H. B., Bi J.B., CAI, B.l., Biodegradation of phenol by free and immobilized *Acinetobacter* sp. strain PD12. J. Environ. Sci. 19, 222-225.

Wang, Y.C., Riess, R., Nemati, M., 2008. Scale-up impacts on mass transfer and bioremediation of suspended naphthalene particles in bead mill bioreactors. Bioresour. Technol. 99, 8143-8150.

Wang, L., Barringtonb, S., Kimb, J.W., 2007. Biodegradation of pentyl amine and aniline from petrochemical wastewater. J. Environ. Manage. 83, 191–197.

Waul, C., Arvin, E., Schmidt, J.E., 2008. Model description and kinetic parameter analysis of MTBE biodegradation in a packed bed reactor. Water Res. 42, 3122-3134.

Webb, J.L., 1963. Enzyme and metabolic inhibitors, Academic Press, Boston, USA.

Wei, G., Yu, J., Zhu, Y., Chen, W., Wang, L., 2008. Characterization of phenol degradation by *Rhizobium* sp. CCNWTB 701 isolated from *Astragalus chrysopteru* in mining tailing region. J. Hazard. Mater. 151, 111–117.

WHO, 1994. Phenol, Environmental Health Criteria—EHC 161, World Health Organization, Geneva.

Wilderer, P.A., Irvine, R.L., Goronszy, M.C., 2001. Sequencing batch reactor technology, Scientific and technical report, IWA Publishing, London, UK.

Wilson, E.J., Geankoplis, C.J., 1966. Liquid mass transfer at very low Reynolds numbers in packed beds. Ind. Eng. Chem. Fundam. 5, 9–14.

Worden, R.M., Donaldson, T.L., 1987. Dynamics of a biological fixed film for phenol degradation in a fluidized-bed bioreactor. Biotechnol. Bioeng. 30, 398–412.

Wu, K.Y.A., Wisecarver, K.D., 1992. Cell immobilization using PVA crosslinked with boric acid. Biotech. Bioeng. 39, 447–449.

Xu, J.Q., Duan, W.H., Zhou, X.Z., Zhou, J.Z., 2006. Extraction of phenol in wastewater with annular centrifugal contactors. J. Hazard. Mater. 131, 98-102.

Xu, M.C., Zhoua, Y., Huang, J.H., 2008. Adsorption behaviors of three polymeric adsorbents with amide groups for phenol in aqueous solution. J. Colloid Interface Sci. 327, 9-14.

Yang, R.D., Humphrey, A.E., 1975. Dynamic and steady state studies of phenol biodegradation in pure and mixed cultures. Biotechnol. Bioeng. 17, 1211–1235.

Yano, T., Nakahara, T., Kamiyama, S., Yamada, K., 1966. Kinetic studies on microbial activities in concentrated solutions. I. Effect of excess sugars on oxygen uptake rate of a cell-free respiratory system. Agric. Biol. Chem. 30, 42–48.

Yapar, S., Yilmaz, M., 2004. Removal of phenol by using montmorillonite, clinoptilolite and hydrotalcite. Adsorption 10, 287-298.

Yoong, E.T., Lant, P.A., Greenfield, P.F., 1997. The influence of high phenol concentration on microbial growth.Water Sci. Technol. 36, 75-79.

Yu, G.H., He, P.J., Shao, L.M., Zhu, Y.S., 2007. Extracellular proteins, polysaccharides and enzymes impact on sludge aerobic digestion after ultrasonic pretreatment. Water Res. 42, 1925–1934.

Zhao, Xin, Wan,g Y., Ye, Z., Borthwick, A.G.L., Ni, J., 2006. Oil field wastewater treatment in Biological Aerated Filter by immobilized microorganisms, Process Biochem. 41, 1475–1483.

Zilouei, H., Guieysse, B., Mattiasson, B., 2006. Biological degradation of chlorophenols in packed-bed bioreactors using mixed bacterial consortia. Process Biochem. 41, 1083-1089.

Zuo, Y., Maness, P.C., Logan, B.E.,2006. Electricity production from steamexploded corn stover biomass. Energ Fuel 20, 1716–1721.

LIST OF PUBLICATIONS

Publication in Peer-Reviewed Journal

1) Aditi Banerjee, Aloke K. Ghoshal, Isolation and characterization of hyper phenol tolerant *Bacillus* sp. from oil refinery and exploration sites. *Journal of Hazardous Materials* 176 (**2010**) 85-91.
2) Aditi Banerjee, Aloke K. Ghoshal, Phenol degradation by *Bacillus cereus*: Pathway and kinetic modeling. *Bioresource Technology* 101(**2010**) 5501-5507.
3) Aditi Banerjee, Aloke K. Ghoshal, Phenol degradation performance by isolated *Bacillus cereus* immobilized in alginate. *International Biodeterioration & Biodegradation* (**2011**). *Accepted, doi:10.1016/j.ibiod.2011.04.011.*

Publication in Peer-Reviewed Conference

1) Aditi Banerjee, Aloke K. Ghoshal, **2010**. Biodegradation of phenol by isolated *Bacillus cereus* immobilized in alginate. Oral Presentation: *2010 AIChE Annual Meeting*, Salt Lake City, UT.
2) Aditi Banerjee, Aloke K. Ghoshal, **2010**. Biodegradation of refinery wastewater by free and immobilized *Bacillus cereus*. Oral Presentation: *2010 AIChE Annual Meeting*, Salt Lake City, UT.

Manuscript under Communication/ Preparation

1) Aditi Banerjee, Aloke K. Ghoshal, Degradation of petroleum wastewater by *Bacillus cereus*. (Communicated)
2) Aditi Banerjee, Aloke K. Ghoshal, Biodegradation of phenol by calcium-alginate immobilized *Bacillus cereus* in a packed bed reactor and determination of the mass transfer correlation (Under preparation)
3) Aditi Banerjee, Aloke K. Ghoshal, Degradation of petroleum wastewater in packed bed reactor by immobilized *Bacillus cereus* (Under preparation).